Role of chromatin regulators AtRING1 and AtZRF1 in Arabidopsis growth and development

Qiannan Wang

UNIVERSITÉ DE STRASBOURG

ÉCOLE DOCTORALE DES SCIENCES DE LA VIE ET DE LA SANTÉ

[Institut de Biologie Moléculaire des Plantes, UPR2357 CNRS]

THÈSE

présentée par :

[Qiannan WANG]

soutenue le : **14 Décembre 2018**

pour obtenir le grade de : **Docteur de l'université de Strasbourg**

Discipline/ Spécialité : Aspects Moléculaires et Cellulaires de la Biologie

Investigation du mécanisme fonctionnel des gènes *AtRING1* et *AtZRF1* dans la régulation de la croissance et du développement chez les plantes

THÈSE dirigée par :

[M. SHEN Wen-Hui] Directeur de Recherche CNRS, Université de Strasbourg

RAPPORTEURS :

[Mme. PROBST Aline] Directeur de Recherche CNRS, Université Clermont Auvergne

[Mme. DELARUE Marianne] Professeur, Université Paris-Sud, Université Evry et, Université Paris-Saclay

AUTRES MEMBRES DU JURY :

[M. OTTEN Léon] Professeur, Université de Strasbourg

ACKNOWLEDGMENTS

First, I would like to express my sincere gratitude to my supervisor, Dr. Wen-Hui Shen, for the scientific supervision during the thesis.

I am also grateful to Dr. Alexandre Berr and Dr. Donghong Chen, for their valuable advice on the experiments and the constant encouragements throughout my PhD studies.

I also owe a special debt of gratitude to all the jury members, Dr. Aline Probst, Dr. Marianne Delarue, Dr. Léon Otten, who kindly accepted to evaluate my work.

I am also grateful for lab members in Shen's group. Moreover, I am especially grateful for my former colleagues in China for their instructions in experiment design and data analysis, even though their research field is not epigenetics.

Many thanks to my roommates, my friends and my parents for the continuous encouragements and understandings during my PhD.

I acknowledge Chinese Scholarship Council (CSC) for supporting my PhD program.

RESUME DE THESE

INTRODUCTION

Chez les plantes comme chez les animaux, les protéines du groupe Polycomb (PcG) jouent des rôles essentiels dans les processus développement aux par la répression de l'expression des gènes. Ces protéines fonctionnent en complexes multi-protéiques; dont les mieux caractérisés sont Polycomb Repressive Complex 1 (PRC1) et PRC2. Classiquement, PRC2 catalyse le trimethylation de l'histone H3 lysine 27 (H3K27me3), et PRC1 lit H3K27me3 et catalyse la monoubiquitination de l'histone H2A (H2Aub1). Les composants et les fonctions moléculaires de PRC2 sont conservés au cours de l'évolution et sont bien caractérisés chez les animaux et chez les plantes. Ce pendant, ce n'est que récemment que des composants de PRC1 ont été étudiés chez les plantes (revue dans (Yang et al. 2017b; Wang and Shen 2018). Chez Arabidopsis, la protéine LIKE HETEROCHROMATIN PROTEIN 1 (LHP1) fonctionne comme lecteur de H3K27me3, un rôle équivalant à Pc/Cbx du PRC1 chez les animaux. EMBRYONIC FLOWER 1 (EMF1) est un composant plante-spécifique et joue peut-être un rôle partiellement équivalent à Ph du PRC1 chez les animaux. Les composants du PRC1 les plus conservés entre plantes et animaux se trouvent chez les protéines à domaine RING. Les protéines d'Arabidopsis AtRING1A et AtRING1B appartiennent à la sous-famille de RING1, et celles AtBMI1A, AtBMI1B et AtBMI1C appartiennent à la sous-famille de BMI1. Ces protéines à domaine RING possèdent une activité E3-ligase leur permettant de catalyser H2Aub1. En lien avec la répression de PRC1, ZUOTIN-RELATED FACTOR 1 (ZRF1) est proposé comme lecteur de H2Aub1. Chez les mammifères, ZRF1 se lie spécifiquement à H2Aub1 et dissocie le PRC1 de la chromatine, ce qui engendre ensuite la dissociation du PRC2 et par conséquence la levé de la répression (Richly et al. 2010). Cependant, chez Arabidopsis, les deux homologues AtZRF1A et AtZRF1B jouent des rôles en partie similaires à AtRING1 et AtBMI1 dans

la répression des gènes (Feng et al. 2016).

L'objectif de ma thèse était d'approfondir nos connaissances sur les rôles biologiques et les mécanismes fonctionnels des gènes *AtRING1A/AtRING1B* et *AtZRF1A/AtZRF1B* chez Arabidopsis.

RESULTATS et DISCUTION

Génération des mutants en ciblant différentes régions de AtRING1A par CRISPR/Cas9

Le mutant *Atring1ab* manifeste beaucoup de défauts développementaux (Xu and Shen 2008; Chen et al. 2010; Chen et al. 2016), et la protéine recombinante de AtRING1 est capable de catalyser H2Aub1 *in vitro* (Bratzel et al. 2010). Cependant, le rôle de H2Aub1 dans le fonctionnement biologique de AtRING1 n'avait pas été examiné jusqu'à ce jour. La partie major de mes travaux de thèse s'est donc concentrée sur la caractérisation moléculaire de la fonction de AtRING1.

Les mutants disponibles à ce jour (y compris *Atring1ab*) sont obtenus par l'approche de l'insertion d'un T-DNA dans le gène *AtRING1A* ou *AtRING1B*, une mutagénèse qui modifie l'activité du gène mais qui ne permet pas de recueillir les fonctions spécifiques des différentes régions de la protéine codée par le gène. Dans mes travaux de thèse, j'ai exploité l'utilisation du système CRISPR/Cas9 pour muter une région spécifique du gène *AtRING1A* dans le fond *Atring1b* dont la fonction AtRING1B est déjà perdue. J'ai déssiné neuf sgRNAs couvrant les régions codant les domaines RING (proche de la partie N-terminale) et RAWUL (du coté C-terminal) et aussi la région inter-domaine et N-terminale de la protéine AtRING1A (522 aa en longueur totale). Basé sur mes analyses d'un nombre allant de dix à une centaine de transformants pour chaque construction sgRNA, un taux de mutation a été observé et s'est avéré plus faible pour les quatre sgRNAs visant le domaine RING (0% à 55.5%) que pour les deux sgRNAs visant

le domaine RAWUL (54.3%~71.4%). J'ai ensuite analysé de 3 à 4 générations de ségrégants et j'ai pu obtenir des mutants exempts de la construction de mutagénèse sgRNA et Cas9. Au final, quatre lignées de mutants ont été sélectionnées pour la suite de monétude:

-*mut1*, portant l'insertion d'un nucléotide A à la position précédant la région codant le domaine RING;

-*mut2*, portant l'insertion d'un nucléotide A à la position précédant la région codant le domaine RAWUL;

-*mut3*, portant une délétion de 43 nucléotides au niveau dela région codant le domaine RAWUL;

-*mut4*, portant une conversion de C en T à l'origine d'une substitution dela leucine-429 en une phénylalanine (L429F) à l'intérieur du domaine RAWUL.

Les mutants *mut1* à *mut4* manifestent divers défauts phénotypiques

Le mutant *mut1* ne peut être maintenu qu'à l'état hétérozygote. Un faible pourcentage (≈10%) degraines pour le mutant *mut1* à l'état homozygotea été obtenu à partir de l'autofécondation d'une plante mère hétérozygote. Après germination en culture *in vitro*, ces graines une masse de cellules non différenciées (callus). Le phénotype du *mut1* est le plus sévère observé chez tous les mutants *Atring1* connus à ce jour. La mutation dans le mutant *mut1* prédit un codon stop en amont du domaine RING, correspondant ainsi à une perte-de-fonction totale du gène *AtRING1A*. Mes résultats montrent que AtRING1 est nécessaire à la différenciation cellulaire pendant le développement embryonnaire et post-embryonnaire des plantes; ceci est en accords avec le rôle général connu pour PcG chez les plantes.

A l'inverse de *mut1*, les mutants *mut2* et *mut3* présentent des phénotypes beaucoup moins sévères. Néanmoins, des multiples défauts existent chez ces mutants et j'ai pu les caractériser avec des données quantitatives. Ainsi, j'ai mesuré le taux de germination des

graines, la croissance de la rosette, le temps de floraison, le nombre d'organes floraux, et la productivité de graine. Mes résultats montrent que les plantes mutantes *mut2* et *mut3* ont des défauts similaires, *e.g.* une inhibition de l'expansion de largeur des feuilles, un retard de floraison, et une augmentation de variabilité du nombre de graines produites par silique. Le mutant *mut4* a été analysé en même temps, et mes résultats montrent que ce mutant ressemble au témoin sauvage et au mutant simple *Atring1b*.

Ensuite j'ai analysé par RT-PCR quantitative chez mes mutants l'expression d'un certain nombre de gènes qui ont été antérieurement décrits comme cibles, montrant une levée de répression chez le double mutant *Atring1ab*. Mes résultats montrent que chez le mutant *mut2,* mais pas *mut4,* le niveau d'expression est plus élevé par rapport au témoin sauvage ou à *Atring1b* pour le gène *KNAT2* de la famille des gènes à homéoboîte *KNOX*, des gènes *CUC1/2* fonctionnant dans l'établissement des frontières entre organes, et des gènes *MAF4/5* codant pour des répresseurs de la transition florale. En accords avec la sévérité de son phénotype, le mutant *mut1* montre des nivaux d'expression de ces gènes beaucoup plus élevés.

A ce stade, mes résultats indiquent que la substitution L429F dans *mut4* n'affecte pas la fonction biologique de AtRING1A, et que les mutations plus conséquentes du domaine RAWUL chez *mut2* et *mut3* affaiblissent sans abolir complétement la fonction de AtRING1A, expliquant les phénotypes beaucoup moins sévères observé chez *mut2* et *mut3* par rapport à *mut1*.

Les analyses moléculaires révèlent une fonction importante du domaine RAWUL dans la monoubiquitinationde H2A

Au cours de mon étude des mutants *atzrf1a;b* et *Atring1ab*, l'analyse en Western-blot a révélé que le niveau global de H2Aub1 est maintenu chez ces mutants. Si ce résultat est attendu pour *atzrf1a;b* parce que ZRF1 fonctionne comme un lecteur de H2Aub1, il intérogele mécanisme fonctionnel de AtRING1 comme dépendant ou indépendant de

H2Aub1.

Afin de vérifier si le gène *AtRING1A* est activement exprimé dans les mutants *mut1* à *mut4*, j'ai tout d'abord analysé le niveau de transcrit du gène par RT-PCR quantitative. Par rapport au témoin sauvage ou *Atring1b*, j'ai trouvé que *AtRING1A* est exprimé à un niveau similaire chez *mut4*, légèrement supérieur (<2 fois) chez *mut2* et *mut3*, et nettement supérieur (>4 fois) chez *mut1*. Ensuite, j'ai amplifié et séquencé les cDNAs complets du gène *AtRING1A* à partir des RNA extraits des plantes mutantes *mut1 à mut4*. Mes résultats confirment que le gène *AtRING1A* est transcritint égralement et que le cDNA porte un codon stop prématuré en N-terminal du domaine RING chez *mut1*, du côté C-terminal avant le domaine RAWUL chez *mut2* ou *mut3*, et une substitution L429F chez *mut4*. On peut conclure que les mutations portées par *mut1 à mut4* n'affectent pas la transcription du gène *AtRING1A* mais interférent plutôt avec sa traduction, ou encore au niveau post-traductionnelle très probablement sur la protéine AtRING1A elle-même.

Ensuite, j'ai analysé le niveau H2Aub1 et H3K27me3 chez les mutants *mut1 à mut4.* Dans un premier temps, les extraits nucléaires de protéines et les extraits enrichis d'histone ont été préparés à partir des jeunes plantes. L'analyse en Western avec un anticorps anti-H2Aub1 a révélé que la quantité de H2Aub1 est fortement diminuée chez *mut2* et *mut3* comme chez le mutant *atbmi1ab*, et est indétectable chez *mut1*. D'une manière surprenante, malgré son absence de phénotype évident, le mutant *mut4* montre une diminution plus faible mais significative de la quantité de H2Aub1. Cependant, l'analyse avec l'anticorps anti-H3K27me3 n'a pas permis de détecter de changement de quantité chez les mutants *mut1 à mut4*. L'activité E3-ligase de AtRING1 et AtBMI1 est prédite comme étant portée par la partie N-terminale du domaine RING. Mes résultats montrent clairement que le domaine RAWUL du coté C-terminal est également essentiel à cette activité. Chez les animaux, il a été montré que le domaine RAWUL fonctionne dans l'interaction protéine-protéine. Il est possible que la mise en place de H2Aub1 se fasse *in vivo* par PRC1 au sein d'uncomplexe multi-protéique. Malgré tout, AtBMI1 ou

AtRING1 seule sont capables de catalyser la monoubiquitination de H2A *in vitro*.

Enfin, j'ai utilisé la technique d'immunoprécipitation de la chromatine (ChIP) pour adresser la question de l'état chromatinien desgènes de floraison (*FLC*, *MAF4*, *MAF5*) à l'aide d'anticorps anti-H2Aub1 et anti-H3K27me3. Mes résultats montrent que H2Aub1 sur *FLC*, *MAF4* et *MAF5* est réduit chez les mutants *atbmi1ab*, *mut3*, et beaucoup plus légèrement chez *mut4*, mais pas significativement chez le mutant *Atring1b*. Un profile de réduction largement similaire à celui de H2Aub1 a été observé pour H3K27me3, sauf que H3K27me3 sur *FLC* a été détectée à des niveaux similaires au témoins sauvage et à *Atring1b* chez les mutants *mut3* et *mut4*. Cette dernière observation est en accords avec mon observation en RT-qPCR montrant que l'expression de *MAF4* et de *MAF5*, mais pas de *FLC*, est fortement augmentée chez le mutant *mut3*. L'ensemble de mes données ChIP confirme l'importance du domaine RAWUL dans la mise en place de H2Aub1 *in vivo* ainsi quele rôle répressif de H2Aub1 et H3K27me3 dans la transcription. Toutefois, une corrélation stricte du niveau de H2Aub1 et de répression des gènes cibles n'a pas pu être établie.

AtZRF1A/AtZRF1B joue des rôles cruciaux dans le développement embryonnaire et post-embryonnaire de la racine

L'étude précédente a montré qu'une perte de fonction des gènes *AtZRF1A* et *AtZRF1B* perturbe des processus multiples de croissance et de développement chez Arabidopsis. Pourtant, les bases cellulaires et les mécanismes moléculaires sous-jacents demeurent en grande partie peu claire. La racine d'Arabidopsis a une structure bien-organisée, avec une organisation longitudinale simple et des cellules souches bien définies. C'est donc un excellent modèle pour l'étude de la division et de la différentiation cellulaire. Nous avons montré que chez le double mutant *atzrf1a;b* le taux de croissance racinaire est fortement réduit par rapport au témoin sauvage, menant ainsi à un phénotype de racine courte chez le mutant. Nos observations en microscopie confocale indiquent que les

cellules souches de RAM (Root Apical Meristem) subissaient une différentiation prématurée. Ensuite nous avons utilisé plusieurs gènes rapporteurs afin de caractériser les défauts du développement racinaire chez le double mutant *atzrf1a;b.* En utilisant le rapporteur *CYCB1;1:Dbox-GUS* qui marque les cellules à la transition G2-to-M du cycle cellulaire, nous avons montré que la capacité mitotique est diminuée et l'index d'endoréduplication est augmenté chez le mutant. En utilisant les rapporteurs *WOX5:erGFP, SCR:SCR-YFP*, *CO2:H2B-YFP*, et les lignées 'enhancer trap' GFP *J1092* et *J2341*, qui marquent spécifiquement l'identité des différents types de cellules dans la racine, nous avons pu déterminer avec précision les défauts cellulaires du développement embryonnaire et post-embryonnaire de la racine chez le mutant. Enfin, en utilisant le rapporteur *DR5rev:GFP* qui est activé en réponse à l'auxine, nous avons montré que le mutant *atzrf1a;b* subissait des défauts dans la signalisation, le transport et/ou la distribution cellule-spécifique de la phytohormone auxine. En outre, notre analyse temporelle de l'expression des gènes indique que plusieurs régulateurs importants du développement de la racine sont dérégulés chez le mutant. Dans son ensemble, cette première partie de mes travaux de thèse a permis de découvrir des fonctions cruciales de AtZRF1 dans le maintien de l'activité des cellules souches, de l'identité cellulaire, et de l'organisation spatiale des cellules pendant le développement embryonnaire et post-embryonnaire de la racine.

CONCLUSIONS et PERSPECTIVES

Les résultats de mon travail de thèse ont permis de réaliser des progrès significatifs dans notre compréhension des rôles et des mécanismes moléculaires de AtZRF1 et AtRING1 lors de la transcription et de la régulation du développement des plantes. En mettant l'accent sur AtRING1, mon travail a également permis de démontrerune fonction essentielle du domaine RAWUL dans la monoubiquitination de H2A *in vivo*. Les lignées de mutants générées durant ma thèse permettront d'éluciderpar une future approche génomique/épigénomiquele rôle global de H2Aub1 dans la structuration chromatinienne

et dans la régulation de la transcription du génome. A l'avenir, une caractérisation des protéines associées à AtRING1 *in vivo* pourrait permettre demieux comprendre la fonction et la composition biochimique du complexe PRC1, ainsi que la base moléculaire du mécanisme de ciblage de AtRING1 sur des sites spécifiques de la chromatine au sein dugénome.

Chapter I GENERAL INTRODUCTION

Chapter III - RESULTS Part II

Arabidopsis ZUOTIN RELATED FACTOR 1 Chromatin regulators Are Required for Proper Embryonic and Post-Embryonic Root Development

Chapter I

GENERAL INTRODUCTION

I.1. Chromatin structure and remodeling

As the physiological template carrying genetic information, chromatin contains genomic DNA packaged by evolutionarily conserved proteins: histones H1, H2A, H2B, H3, H4. Nucleosome is the fundamental repeating unit of chromatin, comprising 147 bp of DNA wrapping around a histone octamer, which is formed by two copies of each of the core histones H2A, H2B, H3 and H4 (Luger et al. 1997; Zhu and Li 2016) (**Figure I-1**). Inter-nucleosome DNA (linker DNA) is bound by H1, which further organizes nucleosomes into higher order chromatin structures (Fyodorov et al. 2018). The nucleosome organization and the chromatin condensation are not uniform (Misteli 2007). Specific regions termed euchromatin are relatively open and transcriptionally active, whereas regions termed heterochomatin are highly condensed and transcriptionally silent (Misteli 2007). The chromatin dynamics is regulated *via* diverse mechanisms including nucleosome assembly, ATP-dependent chromatin remodeling and covalent modifications of histones.

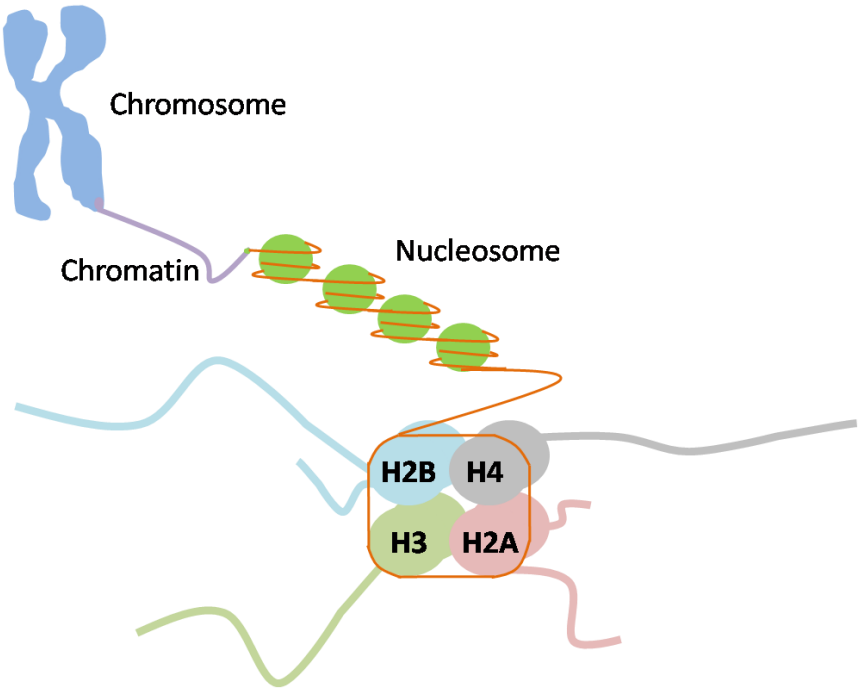

Figure I-1. Schematic representation of the organization and packaging of chromatin.

I.1.1. Nucleosome assembly

Nucleosome assembly occurs during DNA replication, gene transcription and DNA damage repair (**Figure I-2**). Nucleosome is structured by the $(H3\text{-}H4)_2$ tetramer at the center and the two H2A-H2B dimers attached symmetrically on either side (Luger et al. 1997). Thus, nucleosome assembly is a two-step process started by the deposition of a histone $(H3\text{-}H4)_2$ tetramer on DNA, followed by the addition of two H2A-H2B dimers. This ordered process is reversed in nucleosome disassembly, by first eviction of H2A-H2B and then dissociation of H3-H4 from DNA (Dahlin et al. 2015). The strong electrostatic interactions between DNA and histones preclude the efficient spontaneous assembly/disassembly of nucleosomes at physiological ionic strength in the nucleus. Histone chaperones bind histones and play a crucial role in shielding histone surfaces for proper nucleosome assembly/disassembly (Hammond et al. 2017). Most histone chaperones are conserved in yeast, plants and animals; they can be classified as either a H3/H4-type or a H2A/H2B-type histone chaperone (Zhu et al. 2011a). In plants, the best-studied histone chaperones are the H3/H4-type chaperones CHROMATIN ASSEMBLY FACTOR-1 (CAF-1), HISTONE REGULATORY HOMOLOG A (HIRA) and ANTI-SILENCING FUNCTION1 (ASF1), and the H2A/H2B-type chaperones NUCLEOSOME ASSEMBLY PROTEIN1 (NAP1) and NAP1-RELATED PROTEINS (NRPs), and FACILITATES CHROMATIN TRANSCRIPTION (FACT) (DUC ET AL. 2015; ZHOU ET AL. 2016A). More recently, ATRX (Alpha Thalassemia-mental Retardation X-linked) was reported to act together with HIRA in regulating deposition of the variant histone H3.3 in Arabidopsis (Duc et al. 2017).

During DNA replication, nucleosomes located ahead of replication fork need to be disassembled to allow access of DNA by the replication machinery. Once the DNA is replicated, it needs to be packaged into nucleosomes by using the parental and the newly synthesized histones, a process called ‘DNA replication-coupled nucleosome assembly’ (RCNA, **Figure I-2**) (McKnight and Miller 1977; Sogo et al. 1986; Kaufman et al. 1995; Dahlin et al. 2015). In yeast, ASF1 binds the newly synthesized H3-H4 forming the

substrate for Rtt109, which catalyzes H3K56 acetylation (H3K56ac), and H3K56ac facilitates the interaction with the E3 ubiquitin ligase $Rtt101^{Mms1}$ to promote the ubiquitination at H3K122 (H3K122ub) (English et al. 2006; Masumoto et al. 2005; Driscoll et al. 2007; Han et al. 2013). Subsequently, the H3K122ub formation promotes the hand-off of H3K56ac-H4 from ASF1 to CAF-1 and other chaperones to deposit H3-H4 onto nascent DNA (Su et al. 2012; Yang et al. 2016). After the deposition of H3-H4, the H2A/H2B chaperones such as FACT carry out the deposition of H2A-H2B (Belotserkovskaya et al. 2003). Compared to the newly synthesized H3-H4, how the parental H3-H4 is reassembled with DNA remains currently more elusive. In human cells, ASF1 and FACT are proposed to act together with the MCM helicase to deposit parental histones (Foltman et al. 2013; Tan et al. 2006; Gambus et al. 2006). The parental H3-H4 is conservatively propagated as tetramers in proliferating cultured cells (Prior et al. 1980; Jackson 1987). In Arabidopsis, loss-of-function of either CAF1, ASF1 or FACT drastically impairs cell proliferation and cell cycle (Zhou et al. 2015; Zhu et al. 2011b; Chen et al. 2008; Lolas et al. 2010), which is in agreement with their key functions in nucleosome assembly.

During gene transcription, replication-independent nucleosome assembly (RINA) occurs (Dahlin et al. 2015) (**Figure I-2**). Nucleosome assembly not only is important for maintenance of chromatin structure but also provides opportunity to change nucleosome composition, *e.g.* by incorporation of variant histones such as H3.3, CenH3, H2A.Z, H2A.X and H2A.W (Mattiroli et al. 2015; Yelagandula et al. 2014). Due to the peripheral position within the nucleosome, H2A-H2B is exchanged more actively than H3-H4 (Kimura and Cook 2001; Thiriet and Hayes 2005). The FACT and NAP1 chaperones as well as the H2A.Z-specific chaperone CHZ1 all play important roles in regulation of H2A-H2B dynamics and exchange with variants (Zhou et al. 2015; Dronamraju et al. 2017). In Arabidopsis, loss of NAP1 barely affects plant cell proliferation but significantly perturbs transcription of a good number of genes (Zhou et al. 2016a), suggesting important function of NAP1 in RINA. In addition to transcription, RINA also occurs during DNA damage repair (**Figure I-2**). Consistently, the

Arabidopsis *nap1* mutants are hypersensitive to genotoxic stress and display defects in nucleotide excision repair and in homologous DNA recombination (Zhou et al. 2015). Both H2A.Z and H2A.X are involved in DNA damage repair, which also implicates ATP-dependent chromatin-remodeling factors (Lukas et al. 2011; Turinetto and Giachino 2015; Piquet et al. 2018).

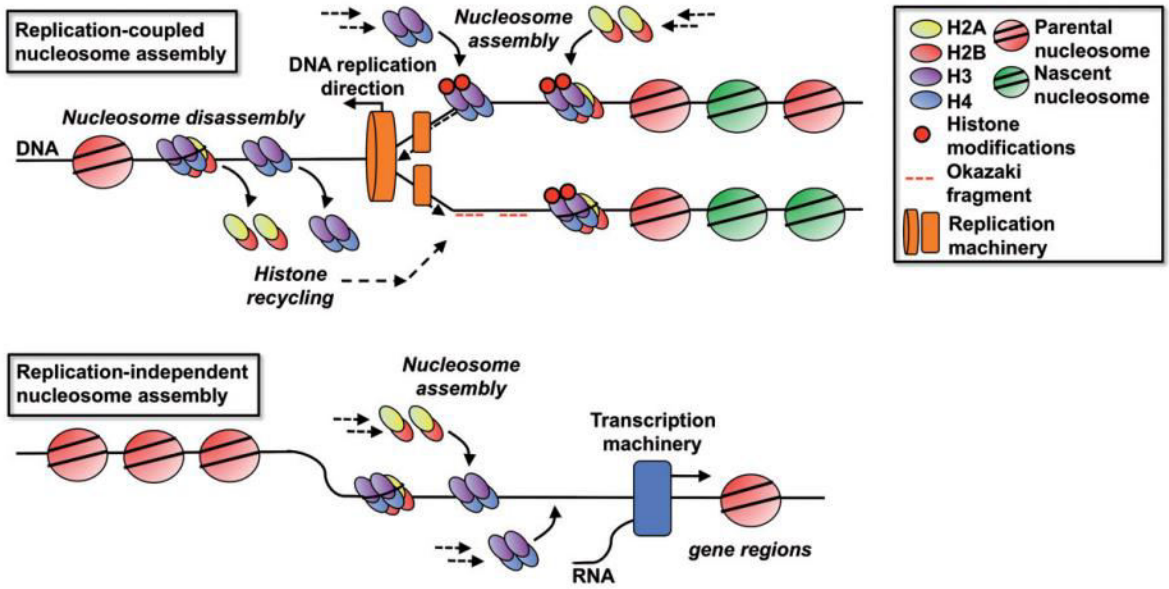

Figure I-2. General schematic of RCNA and RINA (adapted from (Dahlin et al. 2015)).

(**Top**) RCNA. The nucleosomes are disassembled to make the DNA accessible for the DNA replication machinery. Following the DNA replication, nucleosomes are reassembled to the lagging and leading strands.

(**Bottom**) RINA. Nucleosomes disassembly and assembly for replication-independent events like transcription.

I.1.2. ATP-dependent chromatin remodeling

Distinct from histone chaperones that do not consume ATP, chromatin-remodeling factors/complexes contain an ATPase domain and use ATP as source of energy to remodel chromatin structure. ATP-dependent chromatin-remodeling factors are proposed to change chromatin structure by nucleosome sliding, histone exchange, nucleosome eviction and/or alteration of contact between DNA and nucleosomal histones (**Figure I-3**). The chromatin remodeling factors fall into four families: Inositol requiring 80 (Ino80), Chromodomain Helicase DNA-binding (CHD), Switch/Sucrose

Non-Fermentable (Swi/SNF), and Imitationswitch (ISWI) (Clapier et al. 2017). The CHD family remodelers could function by spacing nucleosomes to expose gene promoters and by incorporating the histone variant H3.3 (Lusser et al. 2005; Murawska and Brehm 2011; Konev et al. 2007). The ISWI family remodelers mainly function by limiting chromatin accessibility and regulating gene expression by mediating the complexes assembly and nucleosomes spacing (Grune et al. 2003; Whitehouse and Tsukiyama 2006; Gangaraju and Bartholomew 2007; Tirosh et al. 2010; Bartholomew 2014). The SWI/SNF family remodelers mainly function to activate or repress gene expression by sliding and/or eviction of nucleosomes (Hohmann and Vakoc 2014). Furthermore, SWI/SNF was also reported to recruit Mre-Rad50-Xrs2 (MRX) to regulate homologous recombination in DNA repair (Wiest et al. 2017). The Ino80 family comprises two subfamilies, namely the INO80 and SWR1 subfamilies. Both INO80 and SWR1 function as large multiprotein complexes containing 15 and 14 subunits, respectively (Morrison and Shen 2009; Bao and Shen 2011). Among these subunits, INO80 and SWR1 share four common ones, namely Act1, Arp4, Rvb1 and Rvb2. The Ino80 family remodelers plays a broad range of functions in gene transcription, DNA replication and repair, by regulating nucleosome spacing, H2A.Z localization and nucleosome positioning at gene promoters (Papamichos-Chronakis et al. 2011; Udugama et al. 2011; Krietenstein et al. 2016; Brahma et al. 2017; Eustermann et al. 2018).

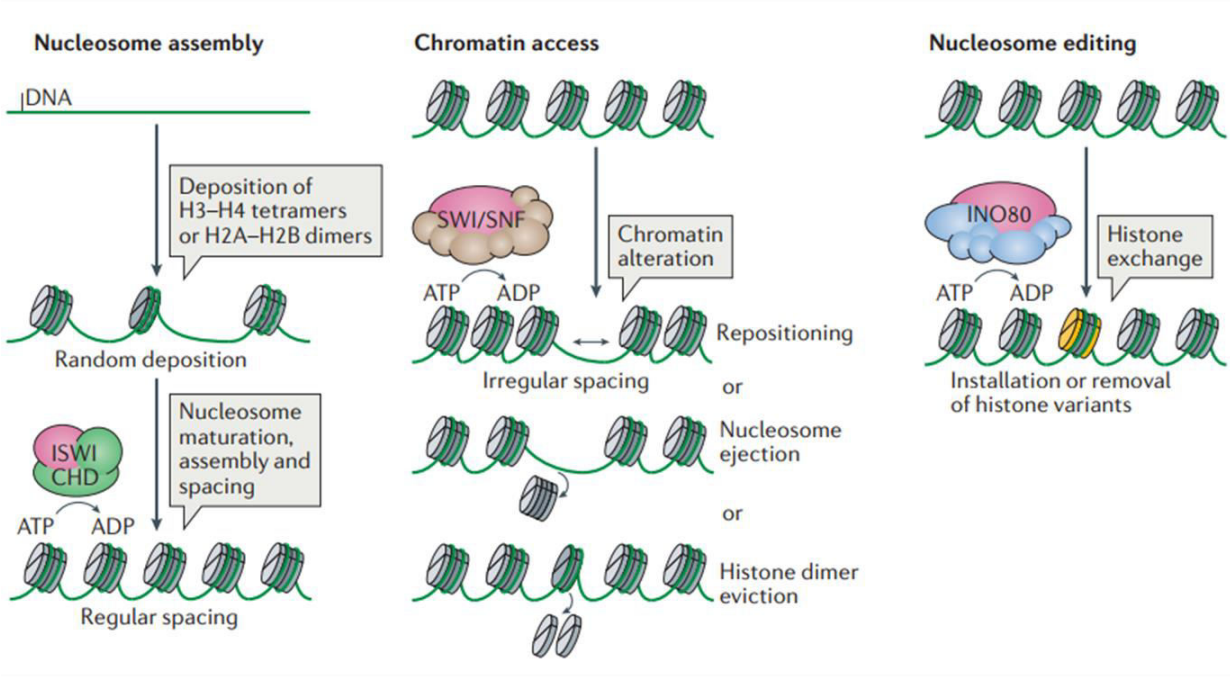

Figure I-3. Simplified function classification of chromatin remodelers (adapted from (Clapier et al. 2017)).

The ATPase-translocase subunit of all remodellers is depicted in pink; additional subunits of ISWI and CHD, SWI/SNF and INO80 are depicted in green, brown and blue.

ISWI and CHD subfamily remodelers are involved in nucleosome assembly: the random deposition of histones, the maturation of nucleosomes and their spacing.

SWI/SNF subfamily remodellers primarily participate in chromatin access: altering chromatin by repositioning nucleosomes, ejecting octamers or evicting histone dimers.

INO80 subfamily remodellers function in nucleosome editing: changing nucleosome composition though exchanging canonical and variant histones, for example, and installing H2A.Z variants (yellow).

The different families of chromatin-remodeling factors are also identified in plants and shown to play many different functions in regulating plant growth and development as well as plant response to environmental cues (Han et al. 2015). Three core components (PIE1, ARP6, SEF) of SWR1 were characterized and shown as required for H2A.Z incorporation into chromatin (March-Diaz and Reyes 2009). Arabidopsis SWR1 is required for regulation of proper mitotic and meiotic homologous recombination (Choi et al. 2013; Rosa et al. 2013). It contributes also to salicylic acid dependent natural

immunity in Arabidopsis (March-Diaz et al. 2008). Three core components of INO80, AtINO80 (Fritsch et al. 2004a; Zhang et al. 2015; Fritsch et al. 2004b), AtARP4 and AtARP5 (Kandasamy et al. 2009), were characterized in Arabidopsis. The *atarp4* and *atarp5* mutant plants are hypersensitive to DNA damaging reagents, including HU (Hydroxyurea), MMS, and bleocin, indicating that they may play a conserved role as its yeast homolog in DNA repair (Kandasamy et al. 2009). As compared to the wild-type control plants, the *Atino80* mutant plants showed a reduction of homologous recombination in normal growth conditions but an increase of homologous recombination in genotoxin-challenged plant growth conditions (Zhou et al. 2016a). Interestingly, the *Atino80* mutant showed a hypostatic genetic interaction with a NAP1-loss-of-function mutant (Zhou et al. 2016a), suggesting that INO80 may regulate DNA repair *via* a covalent modification of histones, such as H2A.X phosphorylation.

I.1.3. Covalent modifications of histones

The nucleosome core histones and their variants are organized by a central structured globular part together with two flexible protruding tails. Both the N-terminal and the C-terminal tails are subjected to diverse post-translational modifications (PTMs), *e.g.* phosphorylation, acetylation, methylation, and ubiquitination (Cosgrove et al. 2004; Cosgrove and Wolberger 2005; Zhang et al. 2003) (**Figure I-4**). These different PTMs index nucleosomes, affect chromatin compaction, and epigenetically regulate genome activities including gene transcription, DNA replication and repair (Hauer and Gasser 2017; Tessarz and Kouzarides 2014; Latrasse et al. 2016).

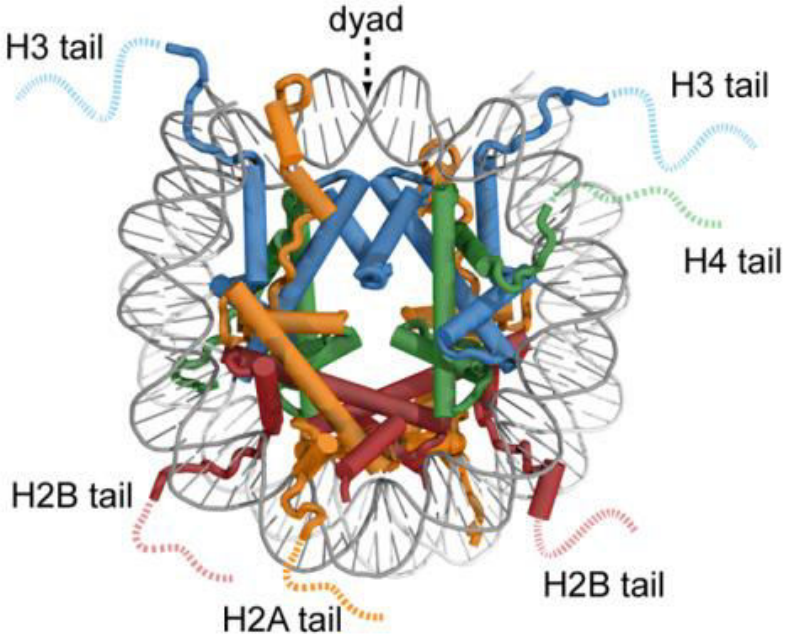

Figure I-4. The face view of the nucleosome structure (adapted from (Bowman and Poirier 2015)).

I.1.3.1. Histone phosphorylation

Histone phosphorylation is a transient and highly dynamic modification occurring at all five types of histones. Specific serine (S), threonine (T) and tyrosine (Y) residues can be phosphorylated by kinases and dephosphorylated by phosphatases (Rossetto et al. 2012). Serine is the major phosphorylation residue. During phosphorylation, a phosphate group from ATP is transferred to the hydroxyl group on the target residues on histones. Histone phosphorylation is associated with chromosome condensation and segregation in the progress of mitosis and meiosis as well as in transcription regulation and DNA damage repair (Rossetto et al. 2012; Zhang et al. 2014). H2A.X phosphorylation (γ-H2A.X) occurs early upon DNA damage and is the most extensively characterized histone modification in DNA damage repair (van Attikum and Gasser 2005; Rossetto et al. 2010). It is involved together with ATP-dependent chromatin remodelers such as INO80 in double-strand-break DNA repair (Rossetto et al. 2012). The phosphorylations on H3S28 (Lau and Cheung 2011; Gehani et al. 2010), H3S10 (Chadee et al. 1999; Cheung

et al. 2000; Clayton et al. 2000; Lo et al. 2000), H3Y41 (Dawson et al. 2009), H2BS32 (Lau et al. 2011; Chadee et al. 1999; Choi et al. 2005), H2BS36 (Bungard et al. 2010), H2BY37 (Mahajan et al. 2012), H4S1 (Utley et al. 2005) are related to transcription regulation. A same modification, such as H4S1 phosphorylation, could be involved in not only transcription regulation but also DNA damage repair and chromatin compaction (Rossetto et al. 2012).

Some 14-3-3 or BRCT domains containing proteins are identified to recognize the phophorylated histone and to induce downstream events (Yun et al. 2011). Strikingly, little is known about enzymes catalysing phosphorylation/dephosphorylation of the different specific residues of histones. In Arabidopsis, AURORA-like kinases were characterized and shown as responsible for H3S10 phosphorylation at centromeres during mitosis in Arabidopsis (Demidov et al. 2005). AtHaspin was shown to be able to phosphorylate H3T3 and H3T11 *in vitro* (Kurihara et al. 2011), and plays a role in embryonic patterning (Ashtiyani et al. 2011). The rice BRK1, a H2A-kinase BUB1-related protein, is required for maintenance of proper tension between the homologous kinetochores to facilitate the accurate segregation of homologous chromosomes during meiosis (Wang et al. 2012). Histone dephosphorylation was studied essentially by using phosphatase inhibitors. As an example, a high level of H3S10 phosphorylation along the chromosome arms during mitosis was observed after plant treatment using cantharidin, an inhibitor of both PP2A and PP1 phosphatases (Manzanero et al. 2002).

I.1.3.2. Histone acetylation

Acetylation was the first type of histone modifications discovered (Phillips 1963), and acetylation sites were found abundantly on the tails and less abundant in the globular domains of all types of histones, including H1 (Tweedie-Cullen et al. 2012). Acetylation neutralizes the positive charge of histone lysine (K) residues by transferring of an acetyl group from acetyl-CoA to K and therefore relieves histone interaction with the negatively charged DNA (Yang and Seto 2007). Thus, histone acetylation forms an open

chromatin state (Lee et al. 2007). It makes DNA accessible to transcription machinery by disrupting the interaction between K-rich nucleosome and DNA phosphodiester backbones. Therefore, histone acetylation is linked to transcriptional activation in euchromain (Yang and Seto 2007).

Histone acetylation levels are regulated by histone acetyltransferases (HATs) and histone deacetylases (HDACs),which catalyze the deposition and remove of acetyl group from K residues of histones, respectively (Ali et al. 2018). Histones H3 (K4, K9, K14, K18, K23, K27, K36) and H4 (K5, K8, K12, K16, K20) are found as acetylated in Arabidopsis as well as in some other organisms (Shahbazian and Grunstein 2007).

Based on the sequence conservation and biochemical properties, plant HATs are grouped in four families, namely the GCN5-related N-acetyltransferases (GNAT), the MOZ, Ybf2, Sas2, and Tip60 (MYST), the p300/CREB-binding protein (p300/CBP) and the TATA binding protein associated factor (TAFII250) families (Ali et al. 2018). In Arabidopsis, 12 HAT genes have been identified: 3 ones belong to the GNAT family (*HAG1/AtGCN5*, *HAG2*, and *HAG3*), 2 ones belong to the MYST family (*HAG4/HAM1* and *HAG5/HAM2*), 5 ones belong to the p300/CBP family (*HAC1*, *HAC2*, *HAC4*, *HAC5*, and *HAC12*), and 2 ones belong to the TAFII250 family (*HAF1* and *HAF2*) (Pandey et al. 2002). A majority of these genes had been characterized and they are found to play many roles spanning diverse processes of plant growth and development as well as signaling of plant response to light and temperature (Boycheva et al. 2014; Chen and Tian 2007). In contrast to the function of HATs in transcriptional activation, HDACs are involved in transcriptional repression. Plant HDACs are grouped into three families, namely the RPD1/HDA1 (homologous to the Reduced Potassium Deficiency 3 in yeast and animals), the SIR2 (Silent Information Regulator 2) and the HD2 (a HDAC first identified in maize) families (Pandey et al. 2002). The HD2 family is plant-specific and is absent from animals (Wu et al. 2000). In Arabidopsis, a total of 16 HDACs genes have been identified, of which 10 belong to the RPD1/HDA1 family that can be further divided into class-I (*HDA1/HDA19/HD1*, *HDA6/AXE1*, *HDA7* and *HDA9*), class-II (*HDA5*, *HDA15* and *HDA18*), class-III (*HDA2*) and unclassified ones (*HDA8* and

HDA14), 2 belong to the SIR2 family (*SRT1* and *SRT2*), and 4 belong to the HD2 family (*HDT1/AtHD2A*, *HDT2/AtHD2B*, *HDT3/AtHD2C* and *HDT4/AtHD2D*) (Pandey et al. 2002). Similar to HATs, HDACs also play important roles in many processes of plant growth and development as well as in plant response to light signaling, cold, and to pathogens (Hollender and Liu 2008; Liu et al. 2014a). In addition to a direct effect interfering histone-DNA interaction, histone acetylation can also provide a mark in recruiting other factors. Some proteins containing a bromodomain (Dhalluin et al. 1999) and/or a tandem PHD (Plant Homeobox Domain) domain (Zeng et al. 2010) could bind acetylated histone and function as a reader to link with other function regulators.

I.1.3.3. Histone methylation

Histone methylation is one of the most extensively studied modifications, which plays important roles in transcription regulation, genome management, organism development, response to environmental signals and biotic stress (Liu et al. 2010; Ramirez-Prado et al. 2018; Black et al. 2012).

Histone methylation was predominantly occurring at lysine (K) and arginine (R) residues of histone tails or globular domains and existing in multivalent (mono-, di-, or trivalent at lysine; mono-, asymmetrically di-, symmetrivalent at arginine) states (Bannister and Kouzarides 2011). In Arabidopsis, the reported lysine methylation sites are located at K4, K9, K23, K27 and K36 of H3. Amongst them, the di/tri-methylation at K4 and K36 on H3 is associated with transcription activation, while methylations at K9, K27 on H3 are related to repression of transcription (Johnson et al. 2004; Martin and Zhang 2005). H3K23me1 is associated with CG DNA methylation (Trejo-Arellano et al. 2017).

The lysine methylation is catalyzed by histone lysine methyltransferases (HKMTs). In human, HKMTs are categorized to be two classes based on the analysis of the conserved catalytic domains, the SET domain containing HKMTs which generally catalyze lysine methylation at histone tails (Jenuwein et al. 1998; Dillon et al. 2005) and DOT1L which

catalyzes H3K79 methylation in the globular domain (Singer et al. 1998; Feng et al. 2002). The SET domain is named with the first letter of three HKMTs identified in fly (*Drosophila melanogaster*): SU(VAR)3–9, Enhancer of zeste [E(z)], and Trithorax (Trx) (Jenuwein 2006). In Arabidopsis, there are 47 genes encoding SET-domain proteins (Thorstensen et al. 2011) but no DOT1L homologs exist. Based on the sequence analysis, the functionally characterized SET-domain HKMTs in Arabidopsis are categorized into four groups: the SU(VAR)3–9 group members (*e.g.* KYP (kryptonite)/SUVH4/SDG33, SUVH5/SDG9, SUVH6/SDG23, SUVH2/SDG3, and SUVR4/SDG31) involved in H3K9 methylation, the E(z) homologs (CLF, SWN, and MEA) involved in H3K27 methylation, the Trithorax (Trx) group (ATXs and ATXRs) and the ASH1 group (*e.g.* SDG8/EFS, SDG26 and SDG4/ASHR3) involved in catalyzing H3K4 or/and H3K36 methylation (Liu et al. 2010; Yu et al. 2009). The E(z) homologs, CLF, SWN and MEA, are subunits of Arabidopsis polycomb repressive complex 2 (PRC2), which together with other PRC2 subunits to silence target genes and regulate female gametophyte, endosperm and vegetative development and floral transition (Xiao et al. 2016; Mozgova et al. 2015; Huo et al. 2016). The activity of PcG proteins can be counteracted by TrxG factors, which function as the positive regulators of gene expression in animals and plants (Sanchez et al. 2015; Pu and Sung 2015; Schuettengruber et al. 2017). The transcription activation related modification, H3K36 methylation and H3K4 methylation are catalyzed by the ASH1 protein in mammals and fly and TrxG proteins in fly and yeast, respectively (Berger 2007; Li et al. 2007; Schuettengruber et al. 2017). In Arabidopsis, ASH1 protein SDG8 participates in H3K36 di- and trimethylation and play roles in regulating plant size, flowering and fertility (Zhao et al. 2005; Xu et al. 2008; Kim et al. 2005b). The ATX1, ATX2, ATXR3/SDG2, ATXR7/SDG25 have H3K4 HMTase activity (de la Paz Sanchez et al. 2015) and involved in mediating floral organ development and floral transition. SDG4 and SDG26 are involved in methylating both H3K36 and H3K4 and regulated flower development (Cartagena et al. 2008; Thorstensen et al. 2008; Xu et al. 2008).

The lysine methylation is removed by histone lysine demethylases (KDMs). KDMs are

composed of two families, the larger subfamily JmjC KDMs (Tsukada et al. 2006; Klose et al. 2006) and the smaller subfamily KDM1 (KDM1A, KDM1B) (Shi et al. 2004; Liu et al. 2010; Black et al. 2012). In Arabidopsis, 21 JmjC domain containing KDMs and 4 KDM1 homologs were identified. JmjC KDMs can be classified into five groups on the basis of phylogenetic analysis, 6 members belonging to KDM5/JARID1 group (AtJMJ14, AtJMJ15, AtJMJ16, AtJMJ17, AtJMJ18, AtJMJ19), 3 members belonging to KDM4/JHDM3 group (AtJMJ11, AtJMJ12, AtJMJ13), 6 members belonging to KDM3/JHDM2 group (AtJMJ24, AtJMJ25, AtJMJ26, AtJMJ27, AtJMJ28, AtJMJ29), 2 members belonging to JMJD6 group (AtJMJ21, AtJMJ22), and 4 members belonging to JmjC domain–only group (AtJMJ20, AtJMJ30, AtJMJ31, AtJMJ32), while the KDM1s homologs are FLOWERING LOCUS D (FLD), LSD1-LIKE 1 (LDL1), LDL2, and LDL3 (Lu et al. 2008; Spedaletti et al. 2008). KDMs and KMTs co-ordinately mediate histone methylation levels so as to regulate gene expression. Amongst them, LDL1, LDL2, FLD, JMJ14 (He et al. 2003; Jiang et al. 2007; Shafiq et al. 2014b; Zhao et al. 2015; Lu et al. 2010) and JMJ15 (Yang et al. 2012b; Shen et al. 2014b; Lu et al. 2008; Yang et al. 2012a) have H3K4 demethylase activity and participate in regulating plant development and flowering, while REF6 (JMJ12) (Noh et al. 2004; Lu et al. 2011) and ELF6 (JMJ11) (Crevillen et al. 2014) can remove H3K27 methylation from *FLC* and involved in flowering photoperiod pathway and vernalization pathway. As the only H3K36 demethylase, JMJ30 also functions with JMJ32 as a potential H3K27me2/3 demethylase to regulate flowering (Yan et al. 2014; Gan et al. 2014).

Histone methylation doesn't change the histone charge but increases the lysine hydrophobicity, which recruits specific effector proteins to regulate downstream nuclear processes (Liu et al. 2010; Bannister and Kouzarides 2011). The histone methylation readers are identified with conserved functional domains, such as chromodomain, tudor domain, malignant brain tumor (MBT), Pro-Trp-Trp-Pro (PWWP), the plant homeodomain finger (PHD) superfamily, Morf Related Gene (MRG), WD40 repeat and Bromo adjacent homology (BAH) domain (Ruthenburg et al. 2007; Taverna et al. 2007; Li et al. 2018; Liu et al. 2010). In Arabidopsis, the PHD-containing proteins ORC1a,

ORC1b (Sanchez and Gutierrez 2009), AtING1/2, Alfin1-like (AL 1-7) (Lee et al. 2009), the WD40 repeat containing protein WDR5a (Jiang et al. 2009) are shown to recognize H3K4 methylation; MRG containing MRG1 and MRG2 can bind both H3K4me3 and H3K36me3 to mediate floral transition (Bu et al. 2014; Xu et al. 2014); chromodomain containing protein LHP1 and BAH-domain containing protein SHL, EBS are able to recognize H3K27me3 to fulfill PRC1-like function (Zhang et al. 2007c; Turck et al. 2007b; Li et al. 2018).

I.1.3.4. Histone mono-ubiquitination

Ubiquitin (Ub) is a small protein of 76 amino acids and was first discovered in 1975 (Goldstein et al. 1975). Ubiquitination is the process of depositing ubiquitin to a lysine (K) residue of substrate proteins. This process comprises three major steps: activating Ub by an E1 enzyme, conjugating Ub from E1 to an E2 enzyme, and transferring Ub by an E3 ligase to the target protein (Komander and Rape 2012; McDowell and Philpott 2013; Pickart and Eddins 2004). Substrate specificity is primarily determined by specific E2 and/or E3 enzymes used in the process. The resulted product could be a monoubiquitinated or polyubiquitinated form of the protein. Polyubiquitination frequently results in proteasome-mediated degradation of the target protein (Glickman and Ciechanover 2002), whereas monoqubiquitination (ub1) frequently modifies the target protein property and subcellular localization (Nakagawa and Nakayama 2015). While all the five types of histones can be ubiquitinated, the best-characterized ones are H2Aub1 and H2Bub1 (Feng and Shen 2014).

H2Bub1 is an epigenetic mark associated with transcriptional activation. The K residue is conserved as H2BK123 in budding yeast, H2BK119 in fission yeast, H2BK120 in human, and H2BK143 in Arabidopsis (Feng and Shen 2014). In yeast, the Rad6 (radiation sensitivity proteins 6) and Bre1 (Brefeldin-A sensitivity protein 1) are the E2 and E3 enzymes responsible for catalysing H2Bub1 formation, respectively (Robzyk et al. 2000; Wood et al. 2003). In Arabidopsis, homologues of both Rad6 (AtUBC1 and AtUBC2) and Bre1 (HUB1 and HUB2) have been characterized and they were shown to

play important roles in plant flowering time control, pathogen resistance, and several other process (Feng and Shen 2014). Deubiquitination of H2Bub1 is carried out by Ubp8 and Ubp10 in yeast (Henry et al. 2003; Emre et al. 2005). In Arabidopsis, UBP26 plays a role in flowering time control likely through H2Bub1 deubiquitination at flowering time gene locus (Schmitz et al. 2009). Interestingly, a recent study demonstrated that the SAGA-like complex containing UBP22 is a major player in H2Bub1 deubiquitination in Arabidopsis (Nassrallah et al. 2018). Several H2Bub1-binding proteins were identified in yeast and other organisms (Fuchs and Oren 2014), but how they may function as readers of H2Bub1 remains to be studied.

H2Aub1 is an important epigenetic mark associated with gene repression and DNA damage response (Feng and Shen 2014; Sobhian et al. 2007). H2Aub1 is catalyzed at K119 in human, at K118 in fly and at K121 in Arabidopsis (Lagarou et al. 2008; Wang et al. 2004; Zhou et al. 2017a). The fly dRING1 and Psc as well as the mammalian RING1B and BMI1 function as a heterodimer in H2A monoubiquitination (Wang et al. 2004). In Arabidopsis, each of the homologs of RING1 (AtRING1A, AtRING1B) and BMI1 (AtBMI1A, AtBMI1B, AtBMI1C) alone has an E3-ligase activity in *in vitro* H2A ubiquitination assay (Bratzel et al. 2010; Bratzel et al. 2012). They play important roles in germination, cell fate determination, vegetative development, juvenile-to-adult transition and flowering. H2A deubiquitination is performed by Ubp-M, 2A-DUB and USP21 in animals (Nakagawa et al. 2008) and UBP12 and UBP13 in Arabidopsis. UBP12 and UBP13 participate in PcG gene silencing and fertilization-independent endosperm development (Derkacheva et al. 2016).

H2AK119ub1 provides binding platform for its reader: ZUOTIN-RELATED FACTOR 1 (ZRF1), which evicts PRC1 from chromatin and facilitates transcription activation (Richly et al. 2010). The ZRF1 homologs in Arabidopsis, AtZRF1A and AtZRF1B were identified and involved in germination, flower development, male and female transmission as well as embryogenesis (Guzman-Lopez et al. 2016; Feng et al. 2016). Furthermore, AtZRF1 was shown to potentially recognize H2Aub1 and increase the level of H2Aub1 and H3K27me3 at seed development genes (Feng et al. 2016).

I.2. Polycomb Group (PcG) proteins

Polycomb Group (PcG) proteins act in the transcriptional repression of a broad range of genes including those playing crucial roles in various key developmental processes in both animals and plants (Mozgova and Hennig 2015; Xiao and Wagner 2015; Kassis et al. 2017; Schuettengruber et al. 2017; Fletcher 2017).

I.2.1. Discovery of PcG in animals

The founding member of the PcG family is Polycomb (Pc), which was first discovered in fruit fly as a repressor of homeotic (*Hox*) genes (Lewis 1978; Jurgens 1985). Nowadays, four types of multimeric PcG complexes have been identified in fly: Pho-Repressive Complex (PhoRC) involved in PcG recruitment, Polycomb Repressive Complex 2 (PRC2) catalyzing trimethylation on histone 3 lysine 27(H3K27me3), Polycomb Repressive Complex 1 (PRC1) and related PRC1-type complexes that all mediate monoubiquitination of histone H2A (H2Aub1), and Polycomb Repressive Deubiquitinase complexes (PR-DUB) that participate in H2A deubiquitination (Lanzuolo and Orlando 2012; Kassis et al. 2017; Schuettengruber et al. 2017). So far, the most extensively studied complexes are PRC2 and PRC1. The fly PRC2 is composed of four core subunits: Enhancer of zeste (E[z]), Suppressor of zeste 12 (Su[z]12), Extra sex combs (Esc), and the nucleosome-remodeling factor Nurf55 (Lanzuolo and Orlando 2012; Kassis et al. 2017; Schuettengruber et al. 2017) (**Figure I-5A**). The fly PRC1 also contains four core subunits: Polycomb (Pc), which recognizes and binds H3K27me3; Posterior sexcombs (Psc) and dRING/Sex combs extra (Sce), which form a ubiquitin-ligase module to catalyze H2Aub1 formation; and Polyhomeotic (Ph), which likely participates in directing PRC1 assemblies (Connelly and Dykhuizen 2017; Kassis et al. 2017; Schuettengruber et al. 2017) (**Figure I-5B**). In vertebrate, multiplication occurs for most subunits of PRC2 and PRC1 (**Figure I-5**). For PRC1, the chromodomain proteins CBX2, CBX4, CBX6, CBX7 and CBX8 play a role as Pc in H3K27me3 binding. The RING1A and RING1B proteins are functional equivalent to

dRing; and the

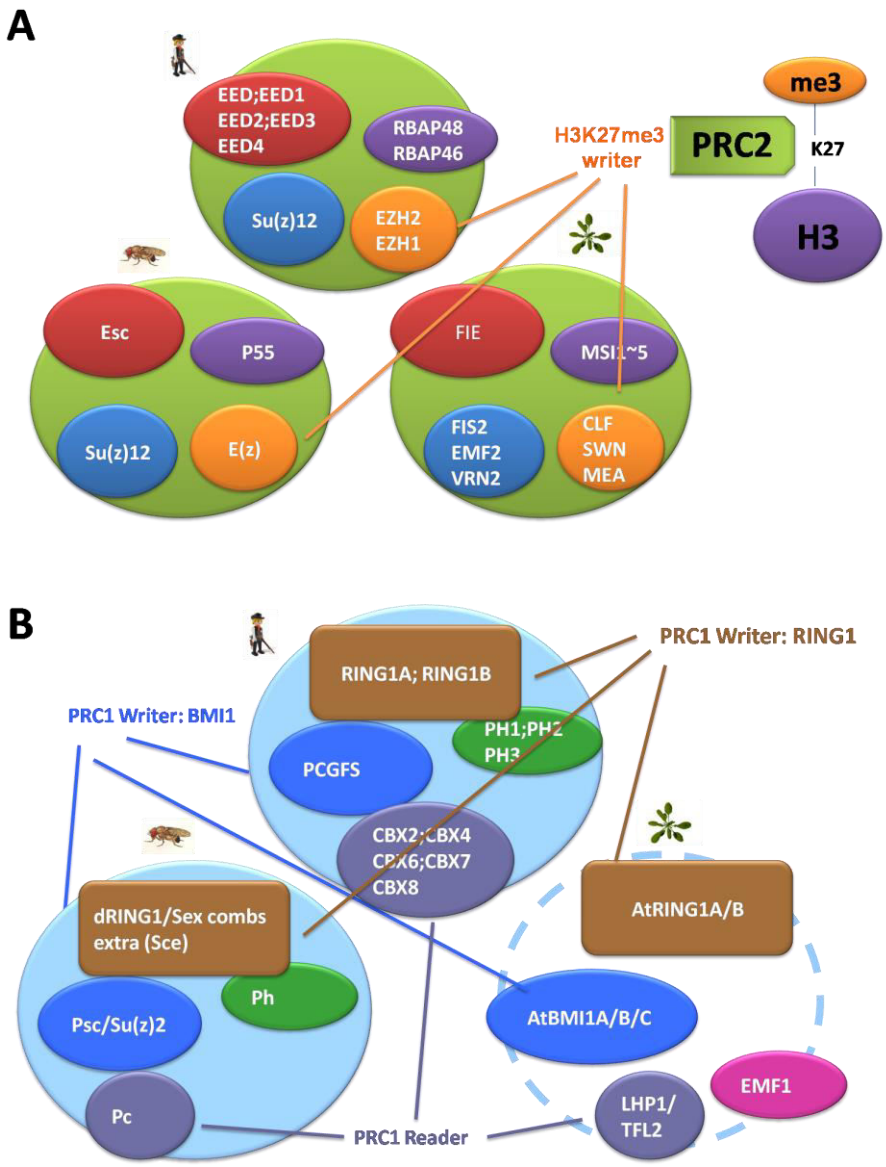

Figure I-5. Conserved components of PRC2 and PRC1 in fly, vertebrate, and Arabidopsis.

Core components of PRC2 (**A**) and PRC1 (**B**) are listed for vertebrate (upper circle), fly (bottom and left circle), and Arabidopsis (bottom and right circle). The homologs in different species are indicated in a same color. The components directly involved in catalyzing histone modifications (Writer) as well as those involved in binding modified histone (Reader) are indicated.

BMI1, NSPC1,MEL18, PCGF3, PCGF5 and MBLR proteins, which are collectively named PcG RING fingers (PCGFs), play an analogous role equivalent to Psc. The PH1, PH2, and PH3 proteins are functional counterparts of Ph. In addition, more diverged

PRC1-type complexes exist and share a similar biochemical activity in catalysis of H2A monoubiquitination (Connelly and Dykhuizen 2017; Bajusz et al. 2018; Schuettengruber et al. 2017).

I.2.2. PcG in plants

I.2.2.1. PRC2 in Arabidopsis

In *Arabidopsis thaliana* as well as in several other Magnoliophyta plants, homologs of all the four PRC2 subunits have also been identified and most of them show multiplication (Huang et al. 2017) (**Figure I-5**). The Arabidopsis CURLY LEAF (CLF) (Goodrich et al. 1997), MEDEA (MEA) (Grossniklaus et al. 1998), FERTILIZATION INDEPENDENT SEED 1 (FIS1) and SWINGER (SWN) (Chanvivattana et al. 2004) are homologs of E(z); EMBRYONIC FLOWER 2 (EMF2), VERNALIZATION 2 (VRN2) and FIS2 are homologs of Su(z)12 (Yoshida et al. 2001; Gendall et al. 2001; Luo et al. 1999); MULTIPLE SUPPRESSOR OF IRA 1–5 (MSI1–MSI5) are homologs of Nurf55/p55 (albeit only MSI1 is currently known as a *bona fide* PRC2 subunit) (Kohler et al. 2003; De Lucia et al. 2008; Derkacheva et al. 2013). The only exception in Arabidopsis is FERTILIZATION INDEPENDENT ENDOSPERM (FIE) (Ohad et al. 1999), which is the unique Esc homolog. So far, molecular and biochemical characterization has unraveled that Arabidopsis has at least three different *bona fide* PRC2 complexes: VRN2–PRC2 (composed of VRN2, CLF/SWN, FIE, MSI1), EMF2–PRC2 (composed of EMF2, CLF/SWN, FIE, MSI1) and FIS2–PRC2 (composed of FIS2, MEA, FIE, MSI1) (Mozgova and Hennig 2015; Xiao and Wagner 2015). VRN2-PRC2 is implicated in vernalization pathway of flowering, and EMF2-PRC2 complex regulate development of flower organ and transition from vegetative to reproductive development. FIS-PRC2 complex is involved in female gametophyte and seed development (Butenko and Ohad 2011; Mozgova et al. 2015).

I.2.2.2. PRC1 in Arabidopsis

Compared to the extensive characterization of plant PRC2, studies of plant PRC1 were more recent (Molitor and Shen 2013; Feng and Shen 2014; Merini and Calonje 2015; Yang et al. 2017b). During the past few years, great progress had been made in characterization of composition, biological roles and molecular mechanisms of function of the plant PRC1 complexes.

I.2.2.2.1. LHP1

The Arabidopsis LIKE HETEROCHROMATIN PROTEIN 1 (LHP1) was first identified as a homolog of the animal Heterochromatin Protein1 (HP1) (Gaudin et al. 2001), a protein acting in heterochromatin maintenance in animals. LHP1 contains three characteristic regions: a chromodomain (CD) that binds methylated H3, a chromo-shadow domain (CSD) involved in protein–protein interaction, and an intrinsically disordered 'Hinge' region (**Figure I-6A**). In contrast to the animal HP1 that binds the heterochromatin mark H3K9me2, LHP1 is located in euchromatin (Libault et al. 2005) and is co-associated with H3K27me3-enriched chromatin regions in genome-wide profiling analyses (Turck et al. 2007a; Zhang et al. 2007b). The N-terminal CD is responsible for LHP1 binding to H3K27me3, which is important for its biological function (Exner et al. 2009). A more recent study showed that the RNA-binding 'Hinge region' and to a much lesser degree the H3K27me3-binding CD are crucial for Polycomb-body-reminiscent punctate nuclear distribution of LHP1 (Berry et al. 2017). These studies together have firmly established LHP1 as a reader of H3K27me3 and as a key factor in plant PcG silencing. The idea that LHP1 might play an analogous role as the fly Pc in a PRC1-like complex has been gained supports through the findings of Arabidopsis RING-finger proteins as partners of LHP1 (Xu and Shen 2008; Bratzel et al. 2010; Chen et al. 2010).

I.2.2.2.2. RING finger proteins

Five PRC1 RING-finger proteins are present in Arabidopsis: AtRING1A and AtRING1B belonging to the RING1 subfamily (**Figure I-6B**), and AtBMI1A, AtBMI1B and AtBMI1C belonging to the BMI1 subfamily (**Figure I-6C**). The RING-finger domain is the enzyme core catalyzing monoubiquitination on H2A. The fly dRING1 and Psc as well as the mammalian RING1B and BMI1 function as a heterodimer in H2A monoubiquitination (Wang et al. 2004). In contrast, each of the five Arabidopsis PRC1 RING-finger proteins alone has an E3-ligase activity in *in vitro* H2A ubiquitination assay (Bratzel et al. 2010; Bratzel et al. 2012). Nevertheless, AtRING1A and AtRING1B can self-interact, cross-interact, as well as bind each with AtBMI1A, AtBMI1B or AtBMI1C (Xu and Shen 2008; Bratzel et al. 2010; Chen et al. 2010). Loss of either AtRING1A/B or AtBMI1A/B/C causes reduction of H2Aub1 in the Arabidopsis mutant plants (Bratzel et al. 2010; Yang et al. 2013a; Li et al. 2017). So far, however, it remains unclear whether or not heterodimerization between AtRING1A/B and AtBMI1A/B/C enhances their E3-ligase activity in H2A monoubiquitination *in vivo*. The N-terminus of AtRING1A comprising RING-finger was shown to bind AtRING1A and AtBMI1B (Molitor et al. 2014).

Based on the protein sequence analysis of the PRC1 RING finger proteins, the RAWUL domain is defined. The subsequent research showed that RAWUL domain is involved in the interaction with both the PRC1 partners, such as RYBP, CBX, and BCOR, BCORL1, PHC1/2/3 (Wang et al. 2010; Blackledge et al. 2015; Junco et al. 2013; Alkema et al. 1997; Gunster et al. 1997; Bezsonova et al. 2009), and transcription factors, such as E4F4 (Chagraoui et al. 2006), Zrp277 (Negishi et al. 2010), and PLZF-RARA fusion proteins (Boukarabila et al. 2009) in animal (Gray et al. 2016). Further, the interaction between PCGF1 and BCORL1 *via* RAWUL domain creates the platform for interacting with KDM2B so as to mediate the H2Aub1 activity (Wong et al. 2016). The BMI1 homodimer and the BMI1-PHCs formed *via* the RAWUL domain are essential for the H2Aub1 (Gray et al. 2016). In Arabidopsis, C terminal region containing RAWUL

domain of AtRING1 interacts with AL2 or AL6 (Peng et al. 2018; Molitor et al. 2014).

Both AtRING1A/B and AtBMI1A/B/C can bind LHP1 (Xu and Shen 2008; Bratzel et al. 2010; Chen et al. 2010). Yet, *in planta* H2A monoubiquitination was reported to be generally independent of LHP1 (Zhou et al. 2017a). *AtRING1A/B* and *AtBMI1A/B/C* are required for proper plant growth and development through different stages. The AtRING1A and AtRING1B proteins, the AtBMI1A and AtBMI1B share a high sequence homology and their genes are expressed broadly in different plant organs/tissues, whereas AtBMI1C is more diverged and its gene is specifically expressed in endosperm, pollen and root (Chen et al. 2010; Bratzel et al. 2010; Bratzel et al. 2012; Chen et al. 2016). The *AtBMI1A* and *AtBMI1B* genes have redundant functions.

I.2.2.2.3. EMF1

Arabidopsis does not contain a homolog of Ph. Instead, the plant-specific protein EMF1 is proposed to be a component of Arabidopsis PRC1 complexes. The *emf1* mutant displays similar phenotypes as the mutants lacking EMF2-PRC2, attributed majorly to ectopic expression of some MADS-box transcription factor genes such as *AGAMOUS* (*AG*), *PISTILATA* (*PI*), *APETALA1* (*AP1*) and *AP3* (Moon et al. 2003b; Kim et al. 2010; Calonje et al. 2008). The EMF1 protein interacts with AtRING1A/B and AtBMI1A/AtBMI1B as well as with LHP1, and the H2Aub1 level is reduced in *emf1* (Bratzel et al. 2010; Yang et al. 2013a; Wang et al. 2014). Very importantly, genome-wide mapping revealed that majority of genes occupied by EMF1 is also marked with H3K27me3 (Kim et al. 2012; Wang et al. 2016). Recently, EMF1 has been reported to function as either H3K27me3 or H3K4me3 reader *via* interacting with the (bromo-adjacent homology) BAH-plant homeodomain (PHD) containing protein EBS, SHL. During green lineage evolution, EMF1 is originated late, coinciding with seed plant appearance, whereas RING1 and BMI1 are found early from chlorophytes and LHP1 from mosses (Berke and Snel 2015).

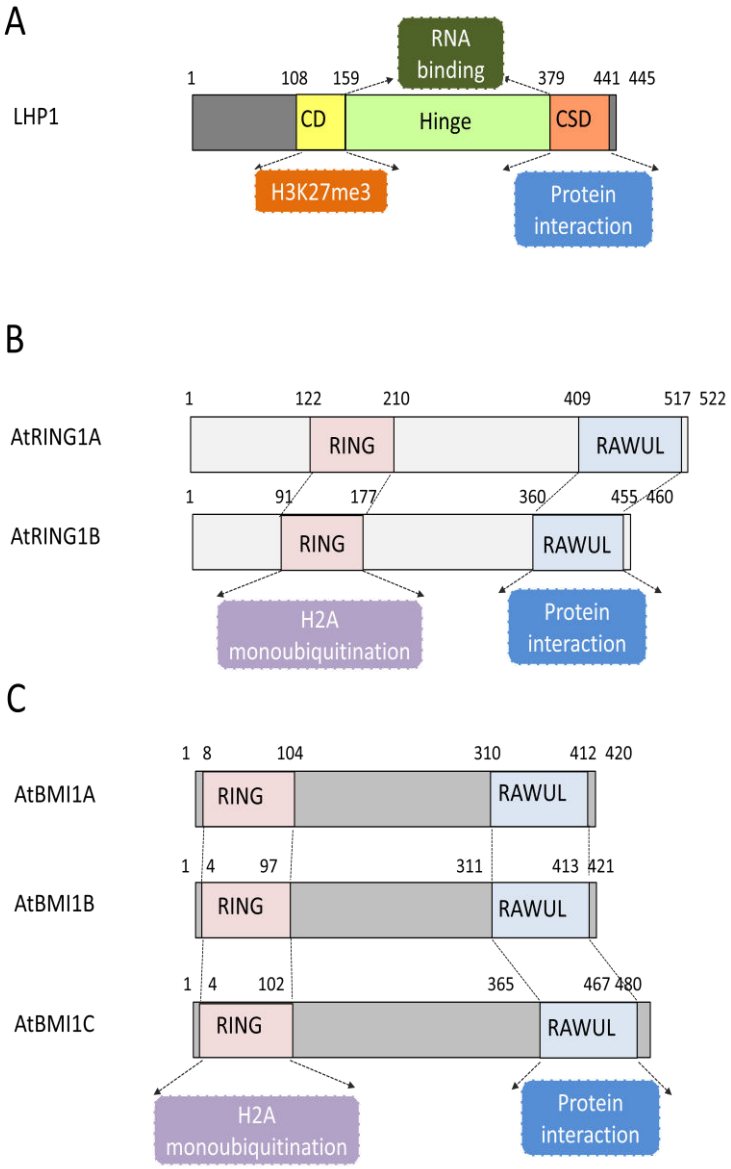

Figure I-6. Schematic presentation of Arabidopsis PRC1 core components for conserved functional domain organization.
(**A**) LHP1, analog of Pc.

(**B**) AtRING1A/B, homologs of dRING1.

(**C**) AtBMI1A/B/C, homologs of BMI1.

I.2.2.3. PcG in other plant species

Understanding of PcG functions in animal and Arabidopsis has been made largely progress in recent years, whereas the PcG function in other plant species is less advanced.

I.2.2.3.1. PRC2 in other plant species

The identification of PRC2 proteins in moss *Physcomitrella patens*, the basal embryo-phyte lineage, demonstrates that the PRC2 proteins evolved early and was maintained along the evolution (Butenko and Ohad 2011). Moss has four PRC2 components: PpEMF2_1, PpEMF2_2, PpEMF2_3) are homologous of Su(z)12 (Chen et al. 2009), while PpFIE, PpCLF and PpMSI1 were identified to be the othologs of ESC, E(z) and Nurf55, respectively (Mosquna et al. 2009; Okano et al. 2009; Shaver et al. 2010). PpFIE and PpCLF interact *in vivo* and both of the loss-of-function mutants showed gametophores development defects, indicating the regulatory roles in gametophyte stem cells proliferation and differentiation (Mosquna et al. 2009; Okano et al. 2009). The misregulated genes in mutants are related to H3K27me3 modification (Widiez et al. 2014). And it is the set domain that performed the methyltransferase activity of PpCLF (Pereman et al. 2016).

In rice, several PRC2 subunits are identified, while FIS2 and MEA/FIS1 which are critical for the endosperm and seed development in Arabidopsis are absent. Rice has two homologs of E[z] (OsiEZ1/SDG718 and OsCLF/SDG711), two homologs of Su[z]12 (OsEMF2a and OsEMF2b), three homologs of Nurf55 (OsRBAP1, OsRBAP2 and OsRBAP3) and two homologs of FIE (OsFIE1 and OsFIE2) (Hennig et al. 2005; Luo et al. 2009; Mukherjee and P. Khurana 2018). A series of researches have gradually characterized the function of some PRC2 components. Similar to the H3K27 methyltransferase activity of E(z), OsFIE2 together with OsCLF, OsiEZ1 and OsEMF2b forming complex owns the H3K27 methyltransferase activity in *in vitro* assay (Li et al. 2014; Nallamilli et al. 2013; Liu et al. 2014b). The PRC2 components also play important roles in rice development. OsiEZ1/SDG718 and OsCLF/SDG711 are involved in promoting flowering under short day and repressing flowering under long day, respectively (Liu et al. 2014b). OsEMF2b implicates in inducing flowering (Yang et al. 2013b) and determining floral meristem as well as regulating floral organ specification (Luo et al. 2009; Huang et al. 2016). The maternal imprinted OsFIE1 is involved in

mediating nutrient metabolism and H3K27me3 level during seed development (Luo et al. 2009; Huang et al. 2016). OsFIE2 participates in regulating seed, root and leaf development and affecting rice grain yield (Li et al. 2014; Nallamilli et al. 2013; Liu et al. 2016c). Moreover, the OsEMF2b, OsCLF and OsFIE2 are proposed to function as OsEMF2b-PRC2 to mediate flowering under long day (Yang et al. 2013b; Liu et al. 2014b) and regulate rice height (Zhong et al. 2018).

In tomato, SlEZ1,SlEZ2 and SlEZ3 are the three homologs of E(z); SlMSI1, SlEMF2p are the homolog to Nurf55 and Su(z)12, respectively (Butenko and Ohad 2011). Functional analysis shows that SlEZ1 is involved in flower development but not implicated in floral organ identity, which is different to the function of EMF2-PRC2 in Arabidopsis (How Kit et al. 2010). SlEZ2 is implicated in H3K27me3 levels and participate in vegetative development, which resembles the function of Arabidopsis CLF. In addition, SlEZ2 plays roles in fruit development but not in flowering time regulation and floral organ determination, indicating that the function of CLF is not conserved during evolution (Boureau et al. 2016). Similarly, the function of SlMSI1 also shows diversification to the MSI1 in Arabidopsis. MSI1 mainly functions in vegetative development, floral transition and seed development, but SlMSI1 is reported to be involved in fruit ripening (Liu et al. 2016a).

I.2.2.3.2. PRC1 in other plant species

The phylogenetic analysis shows that homologs of Arabidopsis PRC1 core components AtRING1, AtBMI1 and LHP1 occur in multiple plant species. In rice, the EMF1 homolog is CURVED CHIMERIC PALEA1 (CCP), and it participates in regulating palea development by mediating H3K27me3 level at *OsMADS58*, a carpel morphogenesis related gene (Yan et al. 2015a). Recently, CCP1 was reported to interact with *Oryza sativa* SHL1 to form BAH-EMF1c complex, which is identified to be the H3K27me3 reader to regulate genome wide transcription repression (Bajusz et al. 2018). The function mechanisms of the PRC-like components in other plant remain to be clarified.

I.3. PcG silencing mechanism in plants

I.3.1. PcG recruitment

Existence of direct recruitment of PRC1 by DNA-binding proteins, transcription or replication factors points to possibility of PRC1 action independent of PRC2 (**Figure I-7**). Additionally, cross component-interactions between PRC1 and PRC2 exist, *e.g.* AtRING1A with CLF, LHP1 with EMF2, MSI1 and VRN2, and EMF1 with MSI1 (**Table I-1**), suggesting intertwined roles of PRC1 and PRC2 in chromatin modulation. Together, these observations question about the order of recruitment and nuance the boundary of separate actions between PRC1 and PRC2 in PcG silencing. Classically, PRC2 catalyzes H3K27me3 deposition, and then PRC1 binds/reads H3K27me3 *via* Pc/LHP1 and further catalyzes H2Aub1 deposition (**Figure I-7A**). In contrast to this hierarchical mode of PRC2 and then PRC1 action, more recent studies have placed PRC1 upstream of PRC2 in repression of diverse plant developmental genes (recently reviewed in (Yang et al. 2017b) (**Figure I-7B**). Also genome-wide profiling analysis revealed involvement of LHP1, EMF1, AtRING1A/B and AtBMI1A/AtBMI1B in maintaining H3K27me3 throughout the genome (Kim et al. 2012; Veluchamy et al. 2016; Wang et al. 2016; Merini et al. 2017; Zhou et al. 2017a). Interestingly, different PRC1 components associate with PRC2 in preferential repression of distinct developmental program genes, *e.g.* LHP1 with CLF in repression of flower development genes whereas AtBMI1A/AtBMI1B and AtRING1A/B in repression of embryo development genes in Arabidopsis seedlings (Wang et al. 2016). Nevertheless, the H2Aub1 level as well as its genome-wide distribution is roughly unaffected in *lhp1* (Zhou et al. 2017a). It is currently unknown to which extent PRC1 action before PRC2 is H2Aub1-dependent. The ZUOTIN-RELATED FACTOR 1 (ZRF1) protein binds H2Aub1 and the *atzrf1ab* mutant plants display some defects similar to *Atbmi1ab* and *Atring1ab* (Feng et al. 2016). It remains to be investigated whether ZRF1 associates with PRC2, which may provide a mechanism for PRC2 reading of H2Aub1 after PRC1 deposition. Finally, PRC2 and PRC1 may also act independently (**Figure I-7C** and **I-7D**).

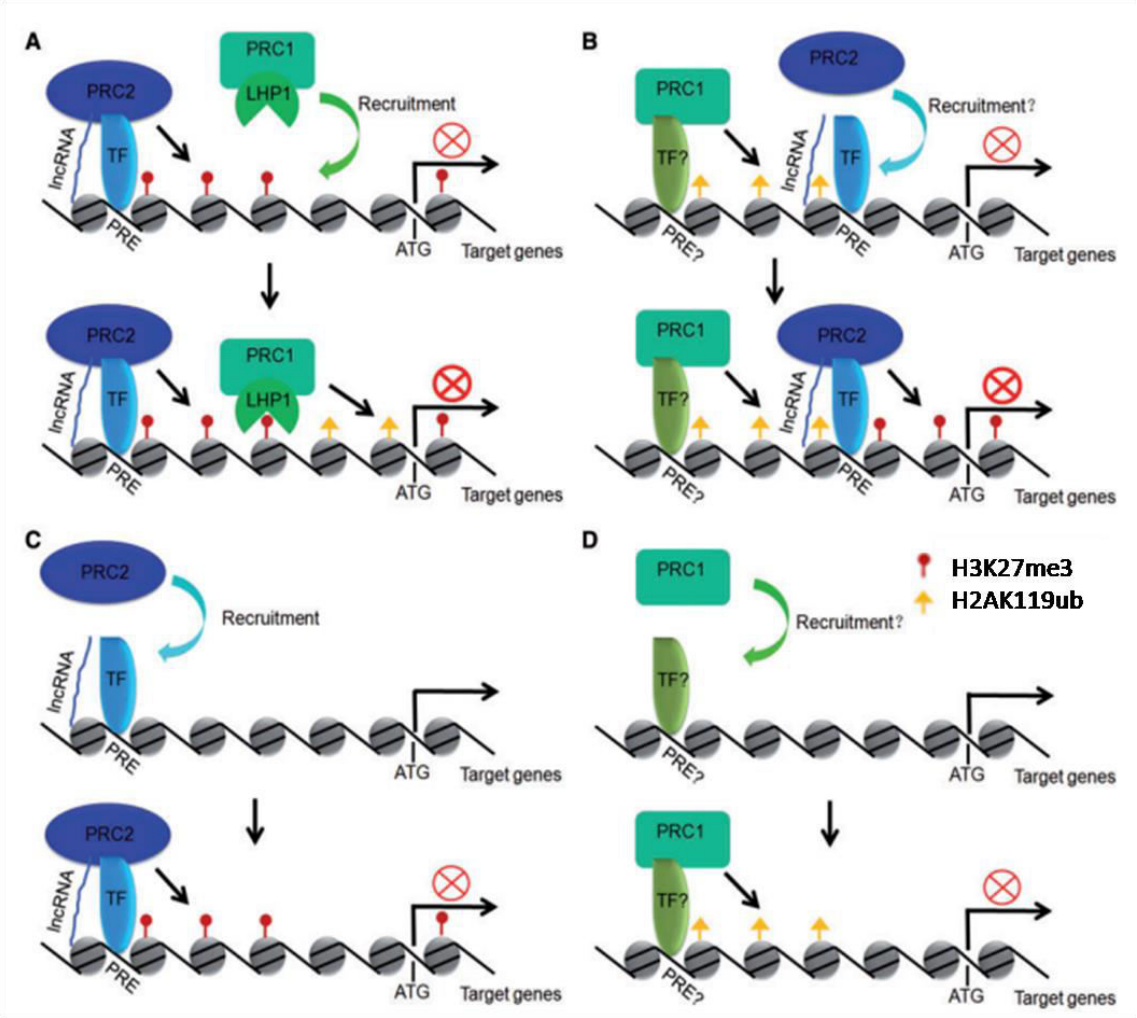

Figure I-7. The models of PRC1 and PRC2 recruitment mechanisms in Arabidopsis (adapted from(Yang et al. 2017b)).

(**A**) PRC2 acts upstream of PRC1. PRC2s are recruited by PREs, TFs or lncRNAs to target chromatin, which establishes H3K27me3 on target genes. H3K27me3 is recognized by LHP1 and PRC1 is recruited to the target sites to incorporate H2AK119ub1 to silence their expression.

(**B**) PRC1 acts upstream of PRC2. PRC1 is recruited first to target genes to establish H2Aub1. Next, PRC2 is recruited by PRC1 to the target genes and catalyzes H3K27me3 to silence the expression.

(**C**) The PRC2 alone model. PRC2s, recruited to generate H3K27me3 mark to silence the target genes.

(**D**) The PRC1 alone model. PRC1 is recruited to catalyze H2AK119ub1 mark to silence the target genes.

I.3.2. PcG-mediated gene repression

I.3.2.1. PRC2-mediated gene repression

PRC2 proteins deposit the repressive mark H3K27me3 to silencing gene expression, The EED subunits of PRC2 in animal and ESC in fly PRC2 could bind to H3K27me3 and pre-existing H3K27me3 enhance the enzyme activity of PRC2 to deposit H3K27me3, by which mechanism PRC2 maintain the H3K27me3 level (Margueron et al. 2009; Xu et al. 2010; Hansen et al. 2008). In addition, PRC2 has the preference in methylating dense polynucleosome arrays, by which PRC2 establish *de novo* K27me3 (Yuan et al. 2012; Hojfeldt et al. 2018). But the silencing mechanism of H3K27me3 is not clear. The previous prevailed explanation for the silencing mechanism is that H3K27me3 is read by LHP1 or BAH-EMF1 to recruits PRC1 complex to mediate the transcriptional repression (Turck et al. 2007a; Zhang et al. 2007b; Bajusz et al. 2018). The other explanation is the PRC2 or H3K27me3 could hinder the recruitment of Pol II to the gene promoters (Chopra et al. 2011). But the detailed mechanism needs further clarification.

I.3.2.2. PRC1-mediated gene repression

PRC1 repress gene expression by depositing H2Aubiquitination. As mentioned above, the RING-finger domain is the enzyme core catalyzing monoubiquitination on H2A. The fly dRING1 and Psc as well as the mammalian RING1B and BMI1 function as a heterodimer in H2A monoubiquitination (Wang et al. 2004). Notable, KDM2 is also required for the ubiquitination in mammal (Farcas et al. 2012; Wu et al. 2013; Lagarou et al. 2008). But the silencing mechanism of H2Aub1 is not clear. There are several possible explanations. H2Aub1 at bivalent promoters is proposed to limit the activity of RNA Pol II, which prevents the transcription elongation (Stock et al. 2007; Zhou et al. 2008). In addition, the modification of H2AK119ub1 is able to prevent H3K4 methylation (Nakagawa et al. 2008). It is also reported that a specific form of PRC2 can bind to H2Aub1 and catalyze H3K27me3 *in vitro* (Kalb et al. 2014).

Chromatin compaction contributes to the PRC1 mediated silencing independent of H2Aub1. The CBX and RING1B in vertebrates were shown to be related to compaction (Francis et al. 2001; King et al. 2002; Eskeland et al. 2010). Similarly, PSC, Ph and Pc in fly were reported to fold the chromatin, and the depression of Hox is correlated to the structure constraints imposed by the PRC1 components (Grau et al. 2011; Cheutin and Cavalli 2018; Kundu et al. 2017). In plants, EMF1 is proposed to be the function analog of PSC-CTR and mediate chromatin compaction (Beh et al. 2012; Kim et al. 2012). The CBX2 related compaction is even proposed to be the major gene silencing mechanism during mouse development (Lau et al. 2017). More recently, it is reported that PRC1 affects the nucleosome landscape but not influence the chromatin accessibility (King et al. 2018).

I.3.3. Association of PcG with other factors

Given the fact that Arabidopsis mutant phenotypes of different PRC1 components varied considerably, PRC1 functions might depend on formation of distinct multiple complexes. Indeed, a number of protein factors have been identified as associated with the Arabidopsis PRC1 core components (**Table I-1**).

The PHD-domain H3K4me2/3-reader AL6 physically interacts with AtRING1A and AtBMI1A/AtBMI1B and the AL PHD-PRC1 complexes have been shown to promote seed germination *via* chromatin state switch from an H3K4me3-associated activation to the H3K27me3-associated repression of seed developmental genes (Molitor et al. 2014). Recently, the proximal site and distal site on AtRING1A are shown to be responsible for the AL-PRC1 complexes based on the crystal structure analysis of AL2-PAL-AtRING1A complexes (Peng et al. 2018). During seedling growth, the B3-domain VP1/ABI3-LIKE (VAL) family transcription factors recruit PRC1 *via* interaction with AtBMI1A/AtBMI1B to repress seed maturation-related genes to initiate the switch from embryonic to post-germinative plant growth (Yang et al. 2013a). Furthermore, the H3K4-demethylase JMJ14 (also known as PKDM7B) interacts with several PRC1 components (AtBMI1A/AtBMI1B, LHP1, EMF1), which is proposed to form a distinct

PcG complex in regulating the FLC-mediated *FT* suppression (Wang et al. 2014). The Bromo adjacent homology (BAH) domain-containing proteins EARLY BOLTING IN SHORT DAYS (EBS) and SHORT LIFE (SHL) interact with EMF1 and AtBMI1A to form a BAH-EMF1c, which binds H3K27me3 and function in PRC1-like way (Bajusz et al. 2018).

LHP1 plays an important function to link PcG complexes to chromatin mediating plant developmental programs. Firstly, the plant chromatin remodeler ATRX is reported to regulate floral transition by repressing *FLC* in a LHP1/PRC2-dependent manner (Wang et al. 2018). Secondly, LHP1 interacts with a number of DNA-binding proteins. The SCARECROW (SCR) and SHORT VEGETATIVE PHASE (SVP) transcription factors are among the first reported LHP1-interacting proteins (Cui and Benfey 2009; Liu et al. 2009). LHP1 also interacts with the ASYMMETRIC LEAVE 1 (AS1)–AS2 complex to recruit PRC2 to *cis*-acting elements in the promoter regions of some *KNOX* genes (Li et al. 2016). More recently, it was found that AG and LHP1 physically interact and form a chromatin loop in repressing *WUSCHEL* (*WUS*) expression in the regulation of floral meristem determinacy (Guo et al. 2018). Interestingly, the *GAGA*-binding factor BASIC PENTACYSTEINE 6 (BPC6) recruits LHP1 to Polycomb Responsive Element (PRE)-like *GAGA*-motifs, which may subsequently recruit PRC2 (Hecker et al. 2015). The RNA-binding protein LHP1-INTERACTING FACTOR2 (LIF2) interacts with LHP1 in regulating cell fate and plant stress responses (Latrasse et al. 2011; Molitor et al. 2016). LIF2 and LHP1 can operate both antagonistically and synergistically and their targeted regions contain the *GAGA*-like and *telobox*-like motifs (Molitor et al. 2016). Loss of the Myb-family transcription factors TELOMERE REPEAT BINDING PROTEIN 1 (TRB1) and TRB3 enhances the *lhp1* mutant phenotype, and LHP1 likely prevents binding of TRB1 at many target sites within the Arabidopsis genome (Zhou et al. 2016b). More additional PREs and potential transcription factors are identified to be involved in Arabidopsis PcG silencing (Xiao et al. 2017). Further characterization will likely provide an ample knowledge of DNA-binding proteins in the recruitment and function of plant PRC1 and PRC2 complexes.

In addition, the PWWP-DOMAIN INTERACTOR OF POLYCOMBS1 (PWO1) protein was identified as a novel type of H3 reader *via* PWWP domain, and PWO1-PWO3 were proposed to recruit PcG proteins to sub nuclear domains and to participate in chromatin compaction (Hohenstatt et al. 2018). Another subgroup of PWWP domain proteins PDP1-PDP3 function together with PRC1/PRC2 to repress *FLC*, *MADS AFFECTING FLOWERING4* (*MAF4*) and *MAF5* expression in Arabidopsis flowering time control (Zhou et al. 2018).

Lastly, LHP1 was previously shown to interact with CYCLOPHILIN 71 (CYP71) and with the DNA polymerase subunits EARLY IN SHORT DAYS 7 (ESD7) and INCURVATA 2 (ICU2) (Li and Luan 2011; del Olmo et al. 2010; Barrero et al. 2007), implying a function in re-establishing/maintaining repressive chromatin state during DNA replication. Forward genetic screen for enhancers of *lhp1* has identified *enhancer of lhp1* (*eol1*) and the EOL1 protein physically interacts with LHP1, CLF and SWN in maintenance of H3K27me3 at target genes (Zhou et al. 2017b). Since the yeast EOL1-homolog Ctf4 (Chromosome transmission fidelity 4) forms a trimeric complex with the DNA polymerase α and the CMG DNA helicase (Simon et al. 2014), it was proposed that EOL1 recruits LHP1-PRC2 to ensure faithful inheritance of H3K27me3 at target chromatin during replication (Zhou et al. 2017b). More globally, the DNA-replication-fork-associated protein PROLIFERATING CELL NUCLEAR ANTIGEN (PCNA) binds LHP1, and the CAF1 histone chaperone subunit FASCIATA 1 (FAS1) binds LHP1, AtRING1A, CLF as well as PCNA, likely together constituting a mechanism responsible for transmission of the epigenetic mark H3K27me3 through cell divisions (Jiang and Berger 2017).

Table I-1. List of protein factors reported to associate together with PRC1 core subunits.

PRC1 subunit	Associated factor	Function	Interaction assay	Reference
AtRING1A	AL6	H3K4me3-binding ALFIN1-like PHD-domain protein	Y2H, pulldown, CoIP, FLIM	(Molitor et al. 2014)
	AL2	H3K4me3-binding ALFIN1-like PHD-domain protein	pulldown	(Peng et al. 2018)
	FAS1	Chromatin Assembly Factor-1 (CAF-1) subunit	pulldown, CoIP, Y2H	(Jiang and Berger 2017)
	CLF	PRC2 component	Y2H, pulldown	(Xu and Shen 2008)
AtBMI1A	AL6	H3K4me3-binding ALFIN1-like PHD-domain protein	pulldown	(Molitor et al. 2014)
	VAL1	B3 domain-containing transcription repressor	pulldown	(Yang et al. 2013a)
	JMJ14	Histone H3K4 demethylase containing JmjC domain	Y2H, pulldown	(Wang et al. 2014)
	SHL	H3K27me3 and H3K4me3 binding BAH and PHD domain- containing proteins	Y2H, pulldown, CoIP	(Bajusz et al. 2018)
	EBS	chromatin remodeling factor	Y2H	(Bajusz et al. 2018)
AtBMI1B	AL6	H3K4me3-binding ALFIN1-likePHD-domain protein	Y2H, pulldown, FLIM	(Molitor et al. 2014)
	VAL1	B3 domain-containing transcription repressor	pulldown	(Yang et al. 2013a)
	JMJ14	Histone H3K4 demethylase containing JmjC domain	Y2H, pulldown	(Wang et al. 2014)
LHP1	JMJ14	Histone H3K4 demethylase containing JmjC domain	Y2H, pulldown	(Wang et al. 2014)
	SCR	GRAS family transcription factor	Y2H	(Cui and Benfey 2009)
	SVP	K-box region and MADS-box transcription factor family protein	Y2H, pulldown, BiFC	(Liu et al. 2009)
	AS1	myb-like HTH transcriptional regulator family protein involved in specification of the leaf proximodistal axis	Y2H, pulldown, BiFC	(Li et al. 2016)

	AS2	Lateral organ boundaries (LOB) domain family protein required for formation of a symmetric flat leaf lamina	Y2H, pulldown, BiFC	(Li et al. 2016)
	AG	MADS-domain transcription factor	Y2H, pulldown, CoIP	(Guo et al. 2018)
	BPC6	GAGA-motif binding BASIC PENTACYSTEINE (BPC) protein	Y2H, FLIM,BiFC	(Hecker et al. 2015)
	LIF2	RNA-binding hnRNP protein	Y2H, pulldown, BiFC	(Latrasse et al. 2011)
	PDP3	Tudor/PWWP/MBT superfamily protein	AP-MS	(Zhou et al. 2018)
	CYP71	WD40 domain cyclophilin	Y2H, pulldown, BiFC	(Li and Luan 2011)
	ESD7	DNA polymerase epsilon catalytic subunit.	pulldown	(del Olmo et al. 2010)
	ICU2	DNA-directed DNA polymerase	pulldown	(Barrero et al. 2007)
	EOL1	Transducin family protein / WD-40 repeat family protein	CoIP, pulldown, BiFC	(Merini et al. 2017)
	PCNA	proliferating cellular nuclear antigen	CoIP	(Jiang and Berger 2017)
	FAS1	Chromatin Assembly Factor-1 (CAF-1) subunit	pulldown, CoIP, Y2H	(Jiang and Berger 2017)
	ATRX	ADD and SNF helicase domain containing protein	CoIP, Y2H	(Wang et al. 2018)
	EMF2	PRC2 component	CoIP	(Derkacheva et al. 2013)
	MSI1	PRC2 component	pulldown, CoIP	(Derkacheva et al. 2013)
	VRN2	PRC2 component	FLIM, BiFC	(Hecker et al. 2015)
EMF1	JMJ14	Histone H3K4 demethylasecontaining JmjC domain	Y2H, pull down assay, CoIP	(Wang et al. 2014)
	MSI1	PRC2 component	pull down assay	(Calonje et al. 2008)
	ULT1	SAND domain-containing trxG factor	Y2H, LCI, BiFC, CoIP	(Xu et al. 2018b)
	SHL	H3K27me3 and H3K4me3 binding BAH and PHD domain- containing proteins	Y2H, BiFC, CoIP	(Bajusz et al. 2018)

EBS	chromatin remodeling factor	Y2H, BiFC,	(Bajusz et al. 2018)

Abbreviations:
Y2H, yeast-two-hybrid; CoIP, co-immunoprecipitation; BiFC, bimolecular fluorescence complementation;
FLIM, fluorescent lifetimeimaging microscopy; LCI, luciferase (LUC) complementation imaging; AP-MS, affinity purification and mass spectrometric analysis;
LOB, lateralorgan boundaries; BPC, BASIC PENTACYSTEINE; CAF-1, chromatin assembly factor-1.

I.3.4. Interplay of PcG with other epigenetic pathways

In general, TrxG proteins act antagonistically to PcG in transcriptional activation of genes during animal and plant development (Schuettengruber et al. 2017; Fletcher 2017).Accordingly, loss of Arabidopsis TRITHORAX1 (ATX1) counteracts *clf*, leading to the restoration of the single mutant phenotypes such that the *atx1clf* double mutant appears phenotypically similar to the wild-type control (Saleh et al. 2007). Analysis of several combined double mutants as well as study of histone methylation patterns at *FLC* during vernalization clearly establish antagonistic interplay between the TrxG-mediated H3K4me3/H3K36me3 and the PcG-mediated H3K27me3 deposition (Shafiq et al. 2014a; Yang et al. 2014). Physical interactions of the H3K4-demethylase JMJ14 with different PRC1 components implicate a PRC1 function associated with removal of H3K4me2/3 (Wang et al. 2014).Strikingly, ULTRAPETALA1 (ULT1), a SAND-domain protein bound with ATX1 and considered as a member of the TrxG family (Carles and Fletcher 2009), was found to interact physically with EMF1 (Xu et al. 2018b). The *atx1* and *ult1* alone cannot counteract the phenotype of *emf1*, but the triple mutant *emf1atx1ult1* showed H3K27me3-related derepression of masses of genes, including seed master regulatory genes. Moreover, EMF1, ATX1 and ULT1 bind chromatin of seed genes, indicating that ATX1-ULT1 and EMF1 cooperate to repress target gene expression (Xu et al. 2018b). This differs from the classical antagonistic roles between PcG and TrxG regulators.

The facts that LHP1 itself binds RNA (Ariel et al. 2014; Berry et al. 2017) and it also associates with the RNA-binding protein LIF2 (Latrasse et al. 2011; Molitor et al. 2016) implicate PRC1 function in RNA processes and/or in association with RNA in chromatin remodeling. Indeed, it was found that LHP1 bound the noncoding *APOLO* RNA, playing a key role *via* chromatin loop formation in fine-tuning expression of its neighboring gene *PINOID* involved in polar auxin transport regulation (Ariel et al. 2014). Since the RNA-binding activity of LHP1 and also possibly LIF2 is not RNA

sequence specific (thus not limited to specific RNA molecules), a broad range of interplays between LHP1/PRC1 and RNAs could be expected.

I.4. PcG repression in regulation of plant development

I.4.1. PcG in cell differentiation

Pluripotent stem cells are critical for morphogenesis in multicellular organism. In plant, the stem cells reside in microenvironments called meristem. There are two main meristems, the root apical meristem (RAM) and the shoot apical meristem (SAM), which are located at the tip of the root and shoot, respectively. The stem cells not only produce cells remain to be stem cell, but also derive cells giving rise to lateral organs (Laux 2003). The SAM controls the aerial growth and development. Mature plant organ also maintain amount of undifferentiated cells, which regenerate new tissues and organs under mechanical injuries or hormonal stimuli. The coordinated and precise cell differentiation and cell reprogramming require intricate regulation. PcG play important roles in the regulation.

In SAM, the identity of stem cell is specified by signaling from the organizing center (OC), which is located underneath the stem cell region. The OC cells express *WUS*, which plays critical roles in maintaining the stem cell identity (Mayer et al. 1998). The *WUS* loss-of-function mutants showed premature termination of the SAM, while the ectopic expression induces ectopic cell fate. PRC-mediated H3K27me3 repressed *WUS* in earlier leaf axil and differentiated tissues (Wang et al. 2017). In floral development, PcG factors are involved in repressing *WUS* expression after flower organs are formed. Firstly, PcG factors such as CLF, EMF2 and LHP1, which are recruited by AG at the *WUS* locus to repress its expression (Liu et al. 2011; Barrero et al. 2007). Later, AG evicts PcG from *KNUCKLES* (*KNU*) promoter and activates *KNU* expression to repress *WUS* expression (Sun et al. 2009; Sun et al. 2014). Recently, AG was found to physically interact with LHP1 forming a chromatin loop to repress *WUS* expression

(Guo et al. 2018). In addition, *WUS* is reported to be regulated by AtBMI1 (Merini et al. 2017).

The class I *KNOX* genes, such as *STM*, *BP*, *KNAT2* and *KNAT6*, are crucial for proper vegetative stem cell maintenance and for floral stem cell determinacy in the establishment of carpel cell fate identities (Xu and Shen 2008; Chen et al. 2016). In leaves, H3K27me3 is established at class I *KNOX* genes (Lafos et al. 2011) and the genes expression upregulated in PRC2 mutants (Katz et al. 2004; Schubert et al. 2006; Xu and Shen 2008). Furthermore, it has been shown that PRC2 subunits and LHP1 were recruited by *AS1* and *2* to the promoters of *BP* and *KNAT2* to repress their expression outside the meristem (Lodha et al. 2013; Li et al. 2016). In addition, PRC1 components AtRING1A/B are also involved in *KNOX* repression. The loss of function mutants *Atring1ab* showed misexpressed class I *KNOX* genes and ectopic SAM in leaves (Xu and Shen 2008; Lodha et al. 2013; Schubert et al. 2006) Similarly, the seedlings *Atbmi1ab* also exhibit ectopic embryonic traits associated with derepression of embryo developmental genes (Chen et al. 2010; Bratzel et al. 2010)

CUP-SHAPED COTYLEDON genes (*CUC1*, *CUC2*, and *CUC3*) play critical roles in establishing organ boundaries through repressing the cell proliferation. *CUC*s encode NAC domain transcription factors, and the loss-of-function of two of the three *CUC* genes impairs the boundary formation and exhibits a fused cotyledon phenotype (Aida et al. 1997; Takada et al. 2001; Vroemen et al. 2003; Kwon et al. 2006). Overexpression of *CUC1* was able to induce ectopic expression of class *I KNOX* genes in the cotyledon, resulting in ectopic meristem formation on the cotyledon (Hibara et al. 2003). But whether the expression of *CUC* genes is regulated by PcG proteins remain unclear.

I.4.2. PcG in seed germination

As sessile organism, plants have to adapt to the environment. It is extremely important for the plants to time the germination at their favorable season. Before germination, the

correct seed development is the prerequisite, which is composed of two major phases, morphogenesis and seed maturation (West and Harada 1993; Gutierrez et al. 2007). The morphogenesis starts from forming a single cell zygote and ends with arrests of cell division in the embryo (Raz et al. 2001). Following the morphogenesis, the seed goes through a series of stages to finish the maturation: embryo growth and filling, storage compounds accumulation, water content decrease, ABA level increase, desiccation tolerance and primary dormancy establishment (Holdsworth et al. 2008). The dormancy status increases as seed maturate and appears to be at the maximum in harvest-ripen seeds (Karssen et al. 1983; Ooms et al. 1993). After the seeds ripening, the seed dormancy status decreases until the seed is competent to germinate under imbibition at favorable environmental growth conditions (Holdsworth et al. 2008).

During the transition from a tiny seed to a normal seedling, drastic morphological changes take place and the expression of a large number of genes is altered. A few genes have been characterized to mediate seed maturation, dormancy and germination. Four major genes, *LEC2*, *ABI3*, *FUS3*, and *LEC1* (*LAFL*), organize a complex network and are shown to be partially functional redundant in seed maturation (Raz et al. 2001; Jia et al. 2014). Mutants of these four genes all show impaired seed maturation (Meinke 1992; Keith et al. 1994; Meinke et al. 1994; Parcy et al. 1997; Parcy et al. 1994; West et al. 1994; Lotan et al. 1998; Luerssen et al. 1998; Vicient et al. 2000; Raz et al. 2001; Stone et al. 2001; Kroj et al. 2003). *ABI3*, *FUS3* and *LEC2* (AFL) encode B3-domain transcription factors. ABI3 is shown to bind the 12S seed storage protein encoding genes *CRUCIFERIN1* (*CRU1/CRA1*), *CRU2* and *CRU3/CRC* (Monke et al. 2012). *LEC2* is required for seed maturation phase, which activity is to rapidly accumulate RNA during seed maturation. *LEC1* encodes a HAP3 subunit of the CCAAT-binding transcription factor, which controls the early and late phases of embryogenesis. The loss-of-function mutant exhibits precocious germination, which is similar to that of *lec2* and *fus3* (Lotan et al. 1998). *DOG1* is identified as a quantitative trait locus involved in enhancing dormancy under low temperature during seed maturation (Chiang et al. 2011; Kendall et

al. 2011; Nakabayashi et al. 2012). The VP1/ABI3-LIKE (VAL) family of B3-domain transcription factors represses *AFL* action to initiate germination (Suzuki et al. 2007; Suzuki and McCarty 2008). *PICKLE* (*PKL*) encodes a CHD3 chromatin-remodeling factor to suppress genes which promote embryonic identity (Dean Rider et al. 2003; Eshed et al. 1999; Ogas et al. 1999).

In Arabidopsis, PcG proteins are required for the normal seed development and germination. Both the PRC2 (FIS2, MEA) and PRC1 components (AtRING1B, AtBMI1C) were shown as maternally imprinted (Bratzel et al. 2012; Chen et al. 2016). During morphogenesis, the FIS-PRC2 complex functions in preventing the formation of endosperm before fertilization (Chaudhury et al. 1997; Sorensen et al. 2001). CLF may regulate molecular modules specifying seed size and lipid biosynthesis during post-fertilization development (Liu et al. 2016b). In seed development, the EMF2-PRC2 complex is involved in repressing seed maturation genes during germination (Bouyer et al. 2011; Tang et al. 2012). Consistently, there is H3K27me3 at *LAFL* loci in vegetative tissues and *FUS3* is identified to be the MEA target (Kim et al. 2012; Zhang et al. 2007a; Makarevich et al. 2006).

Furthermore, PRC1 is reported to participate in repressing seed development related genes. H2Aub1 levels were found reduced in chromatin at seed developmental genes, *e.g*. *ABI3*, *FUS3* and *LEC1* in the *Atbmi1* mutant seedlings (Yang et al. 2013a; Zhou et al. 2017a). AtBMI1A/B and AtRING1A/B are recruited by VALs and ALFIN1-like proteins (ALs) to seed maturation genes to repress the expression *via* switching the chromatin state from an H3K4me3-associated activation to the H3K27me3-associated repression of seed developmental genes (Molitor et al. 2014; Yang et al. 2013a). In addition, *AFL* were identified as direct targets of EMF1 (Kim et al. 2012). More recently, EMF1 is shown to work with ATX1, ULT1 to maintain gene repression at germination (Xu et al. 2018a).

I.4.3. PcG in vegetative growth

After germination, plants develop through different phases: a juvenile vegetative phase, an adult vegetative phase and a reproductive phase (Poethig 1990; Kerstetter and Poethig 1998). In juvenile phase, the plants are insensitive to environmental influence of the photoperiod, which prevents the precociously flowering when the plants are too small (Thomas and Vince-Prue 1997). The transition from juvenile vegetative phase to the adult vegetative phase is defined as the vegetative transition. In Arabidopsis, plant vegetative transition is characterized by the appearance of oval leaves, the progressively formation of the leaf abaxial trichcomes and the leaf serrations, and smaller cell size (Telfer et al. 1997; Tsukaya et al. 2000; Usami et al. 2009).

Molecular and genetic analysis has greatly advanced our understanding on the vegetative transition in Arabidopsis. Two major pathways participate in regulating the juvenile-to-adult phase transition. In the AGO7-miR390-TAS3 pathway, *TAS3* ta-siRNA targets *AUXIN RESPONSE FACTOR3* (*ARF3*) mRNA, which is involved in miR390-guided processing of primary transcripts in an ARGONAUTE 7 (AGO7)-dependent manner (Allen et al. 2005; Williams et al. 2005; Hunter et al. 2003; Hunter et al. 2006; Peragine et al. 2004; Adenot et al. 2006; Fahlgren et al. 2006). In the miR156/157-SPL pathway, miR156/157 targets on *SPL* genes and repress its expression by transcript cleavage or translational inhibition (Wu et al. 2009). Arabidopsis contains 8 *MIR156* genes (A~H) and 4 *MIR157* genes (A~D), which function redundantly. *MIR156A* and *MIR156C*, *MIR157A* and *MIR157C* are mainly responsible for the level of miR156 and miR157, respectively (Xu et al. 2018b; Yang et al. 2013c; Yu et al. 2013). miR157 is more abundant but plays a redundant but less important role in *SPL* repression than miR156 does. The Arabidopsis genome encodes 16 *SPL* genes and miR156/157 target on 10 of them (Xie et al. 2006; Riese et al. 2007; Preston and Hileman 2013). *SPL9*/*SPL13*/*SPL15* are reported to be more important in the vegetative transition (Xu et al. 2016a). The expression of miR156/157 is high in seedlings and

decreases gradually as the plants growing, and *SPL* shows the opposite trend (Wu and Poethig 2006; Wang et al. 2009) (**Figure I-8**). The overexpression of miR156 is capable of extending the juvenile phase. In the downstream of miR156/157-SPL pathway, another class of miRNA, miR172 exhibits increased expression during shoot development, and it targets a class of AP2-like transcription factors (Wu and Poethig 2006; Wu et al. 2009; Xu et al. 2018b). The high abundance of miR172 can suppress the late abaxial trichomes phenotype of the miR156 overexpression lines (Wu et al. 2009).

The vegetative transition is regulated by many other mechanisms, for example, the sugar signaling, starch anabolism, catabolism and so on (Matsoukas et al. 2013). The PcG proteins are involved in regulating the juvenile-to-adult transition (**Figure I-8**). PRC2 complex deposits the repressive mark H3K27me3 at *MIR156*/*157* loci but not at *SPL* loci targeted by miR156/157 (Lafos et al. 2011), suggesting that PRC2 repress the *MIR156*/*157* loci transcription to enhance the *SPL* transcription. Furthermore, the binding of PRC2 complex as well as the H3K27me3 deposition at *MIR156A* and *MIR156C* was found elevated during the vegetative transition, which accounts for the decreased transcription of these two loci (Xu et al. 2016b; Xu et al. 2016c). The PRC2 mutant *swn* showed delayed vegetative transition, and the H3K27me3 mark at *MIR156A/MIR156C* loci was significantly reduced in the *clf* mutants (Xu et al. 2016c; Xu et al. 2016b). PRC1 is also involved in the juvenile-to-adult transition. The PRC1 component AtRING1A/B plays an additive role with the AGO7-miR390-TAS3 pathway in regulating the vegetative phase transition (Li et al. 2017). AtBMI1-PRC1 represses *MIR156* to accelerate the vegetative transition. In *Atbmi1ab* double mutant, the H2Aub1 and H3K27me3 marks decrease at the TSS region of *MIR156A/MIR156C*, leading to the upregulation of *MIR156A/MIR156C* and prolonged juvenile phase (Pico et al. 2015). RING1-PRC1 and EMF1-PRC1 maintains the repression of *SPL*s and delay vegetative transition. In *Atring1ab*, the H2Aub1 mark at the promoter and coding regions of *SPL3*/*9*/*10* was downregulated, leading to a shortened juvenile phase(Li et al. 2017). In *emf1*, *SPL3*/*9* and miR172 were found upregulated, leading to early flowering phenotype

(Pico et al. 2015).

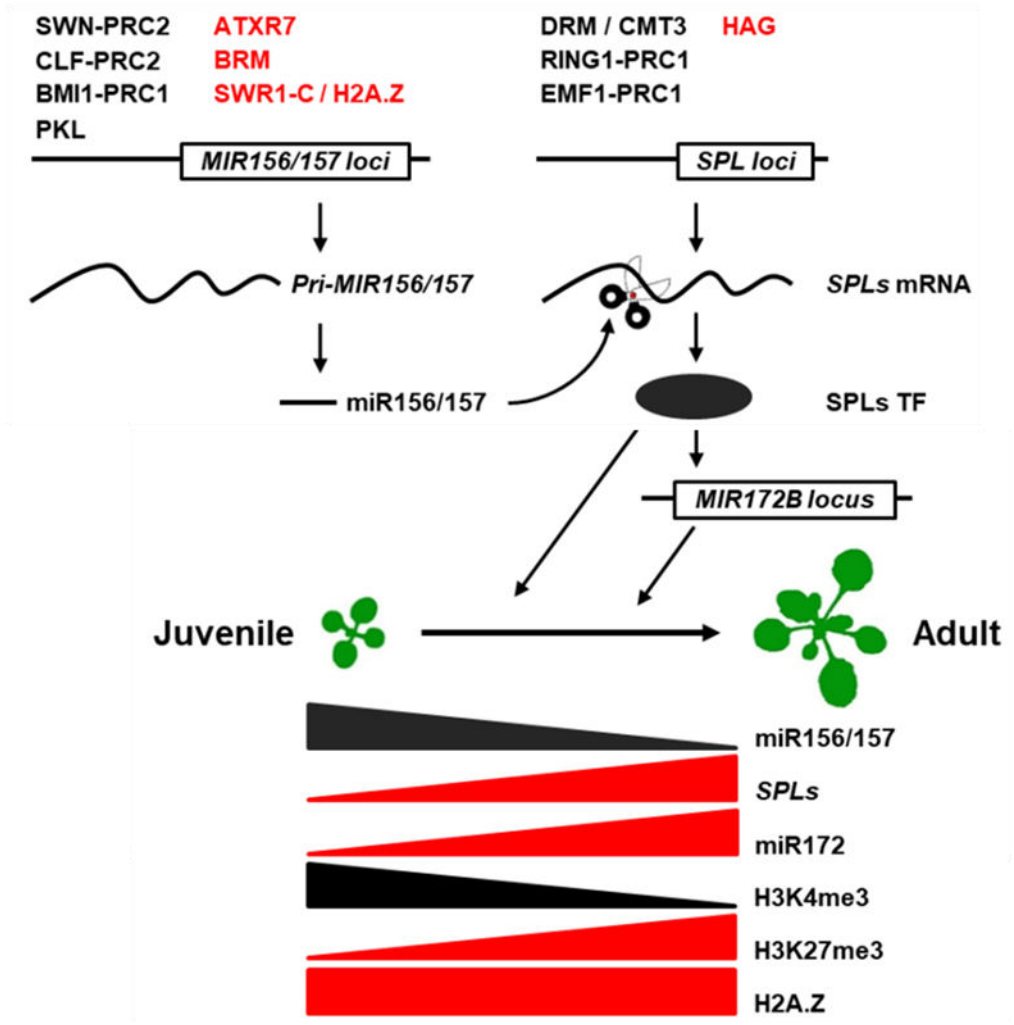

Figure I-8. Epigenetic regulation of the vegetative transition in Arabidopsis (adapted from (Xu et al. 2018c)).

The epigenetic regulators in red or black represents establishing active or repressive mark at *MIR156/157*and *SPL* loci, respectively. Triangle indicates gradual increase or decrease in the epigenetic modification levels of *MIR156* loci.

I.4.4. PcG in floral transition

To guarantee the reproductive success, the timing of transition from the vegetative phase to the reproductive phase is tightly regulated through the integration of environment inputs together with endogenous cues during plant growth. In Arabidopsis, five flowering time regulatory pathways are identified, namely the photoperiod, the vernalization, the autonomous, the age and the gibberellin pathways. PcG proteins are

involved in silencing key floral regulatory genes (**Figure I-9**).

Long-day plants such as Arabidopsis flowers earlier when the days become longer. The zinc finger transcription factor CONSTANS (CO) is responsible for measuring the day length change (Putterill et al. 1995). *CO* is mainly expressed in leaf vascular tissues and its expression follows the rhythmic cycling and coincides with light in long-day condition, while *CO* expression peaks after dusk in short day (An et al. 2004). GIGANTEA (GI)–F-BOX 1 (FKF1) regulatory complex and CONSTITUTIVE PHOTOMORPHOGENIC 1 (COP1) regulate *CO* at transcriptional and post-transcriptional level, respectively (Imaizumi et al. 2005; Fornara et al. 2009; Sawa et al. 2007; Song et al. 2012)). The accumulation of CO directly activates the *FT* expression (An et al. 2004). FT proteins act as a mobile signal, which is transported from the leaves to the shoot apex (Corbesier et al. 2007; Jaeger and Wigge 2007; Lin et al. 2007; Liu et al. 2012; Mathieu et al. 2007). In the SAM, a b-ZIP transcription factor FD forms a complex with FT to activate the expression of *LFY* and some MADS-box genes, such as *AP1* and *SOC1*, and subsequently induces flowering (Abe et al. 2005; Kobayashi and Weigel 2007; Wigge et al. 2005). Under non-inductive condition, the repression of *FT* requires PcG proteins. The PRC1-like EMF1c complex is recruited to *FT* by EMF1 to initiate *FT* silencing. The repression of *FT* is maintained by H3K27me3 deposited by PRC2 complex, which is recruited by interaction with LHP1 (Wang et al. 2014). When the plants are exposed to the inductive condition, EMF-PRC2 and VRN-PRC2 participate in silencing the *FT*-repressor genes *FLC* and *SVP* to prevent floral reversion (Muller-Xing et al. 2014).

In addition to photoperiod, temperature is also a key determinant for flowering time. Some Arabidopsis accessions require a prolonged exposure to low temperatures before flowering (a process known as vernalization). Molecular and genetic studies on these winter annual accessions have identified FRIGIDA (FRI) and FLC as major regulators in vernalization (Ream et al. 2012). FRI upregulates *FLC* and maintains its high expression level in the developing embryo and during vegetative plant growth (Choi et

al. 2011). FLC inhibits flowering by repressing floral integrator loci, including *FT*, *SOC1*, *LFY*, *AP1* (Boss et al. 2004; Kobayashi and Weigel 2007; Michaels 2009; Pazhouhandeh et al. 2011). *FLC* has 5 paralogs, *MAF1* to *MAF5*, all of which are involved in repressing flowering (Ratcliffe et al. 2001; Scortecci et al. 2003; Gu et al. 2013). During the vernalizaiton, the continuous low temperature represses *FLC* expression quantitatively. The PcG proteins are pivotal for this quantitative repression of *FLC*. At the early stage of cold temperature exposure, large amount of *COOLAIR*, a long noncoding RNA (lncRNA) generated from *FLC*, attributes to the downregulation of *FLC* (Rosa et al. 2016). Also at early stage, *VERNALIZATION INSENSITIVE 3* (*VIN3*) encoding a PHD-domain protein is induced by cold. The VIN3 and its homolog VIN3-LIKE 1 (VIL1)/VERNALIZATION5 (VRN5), VIL2/VIN3-LIKE1 (VEL1) proteins act as PHD-PRC2 complexes in targeting the nucleation region of *FLC* (Wood et al. 2006; De Lucia et al. 2008). The other two lncRNAs, *COLD ASSISTED INTRONIC NONCODING RNA* (*COLDAIR)* and *COLD OF WINTER-INDUCED NONCODING RNA FROM THE PROMOTER* (*COLDWRAP*), have been suggested to recruit PHD–PRC2 to the *FLC* locus by interacting with CLF (Heo and Sung 2011; Kim et al. 2017; Kim and Sung 2017). VAL1, which reads the *cis*-regulatory DNA element in the nucleation region of *FLC*, also helps in recruitment of PHD-PRC2 through the interaction with LHP1 to establish H3K27me3 in the nucleation region at *FLC* during vernalization (Yuan et al. 2016). A more recent study showed that ‘Hinge region’ and CD of LHP1 are crucial for LHP1-mediated repression of *FLC* in flowering time control (Berry et al. 2017). When the plants return to warm, the H3K27me3 deposited by PRC2 spreads across *FLC* and stabilize the silencing (Yang et al. 2017a). During DNA replication, CLF and LHP1 interact with proliferating cell nuclear antigen (PCNA) and FASCIATA1 (FAS1) of CAF-1 to transmit H3K27me3 to daughter cells (Jiang and Berger 2017). The PRC1 RING-finger proteins seem to be also involved in flowering time control. Overexpression of *AtBMI1C* accelerates flowering (Li et al. 2011), and AtRING1A was reported to suppress the expression of *MAF4* and *MAF5* by affecting

H3K27me3 at these loci (Shen et al. 2014a).

The autonomous pathway is constituted by a group of genes, such as *AGL28*, *CK2*, *DBP1*, *DRM1*, *DRM2*, *ESD4*, *FCA*, *FLD*, *FLK*, *FPA*, *FVE*, *FY*, *HDA5*, *HDA6*, *LD*, *PCFS4*, *PEP*, *PP2A-B'c*, *PRMT5*, *PRMT10*, *PRP39-1*, *REF6*, *SYP22*, all of which promote flowering by suppressing *FLC* (Cheng et al. 2017). The flowering promotion effect is independently of day length but the related mutants phenotypes can be recovered by treatment with vernalization (Abou-Elwafa et al. 2011). miR156-SPL and miR172 have also been shown to be involved in floral transition by activating downstream target or repressing negative regulators of flowering, which termed as age pathway (Aukerman and Sakai 2003). *SPL3* and *SPL9* promote flowering by activating *AP1*, *LFY*, *FUL* and *SOC1* in the shoot apex (Wang et al. 2009; Yamaguchi et al. 2009). The transcription factors TOE1 and AP2 repress the expression of *FT* in leaves and other flowering time regulators acting downstream of *FT* in the shoot apex (Mathieu et al. 2009). The phytohormone gibberellin (GA) also plays important roles in flowering time control. The negative role of GA on flowering time is performed through regulating expression of *SOC1* by transcriptional repressors DELLAs such as GA INSENSITIVE (GAI) and REPRESSOR OF GA1-3 (RGA) (Moon et al. 2003a).

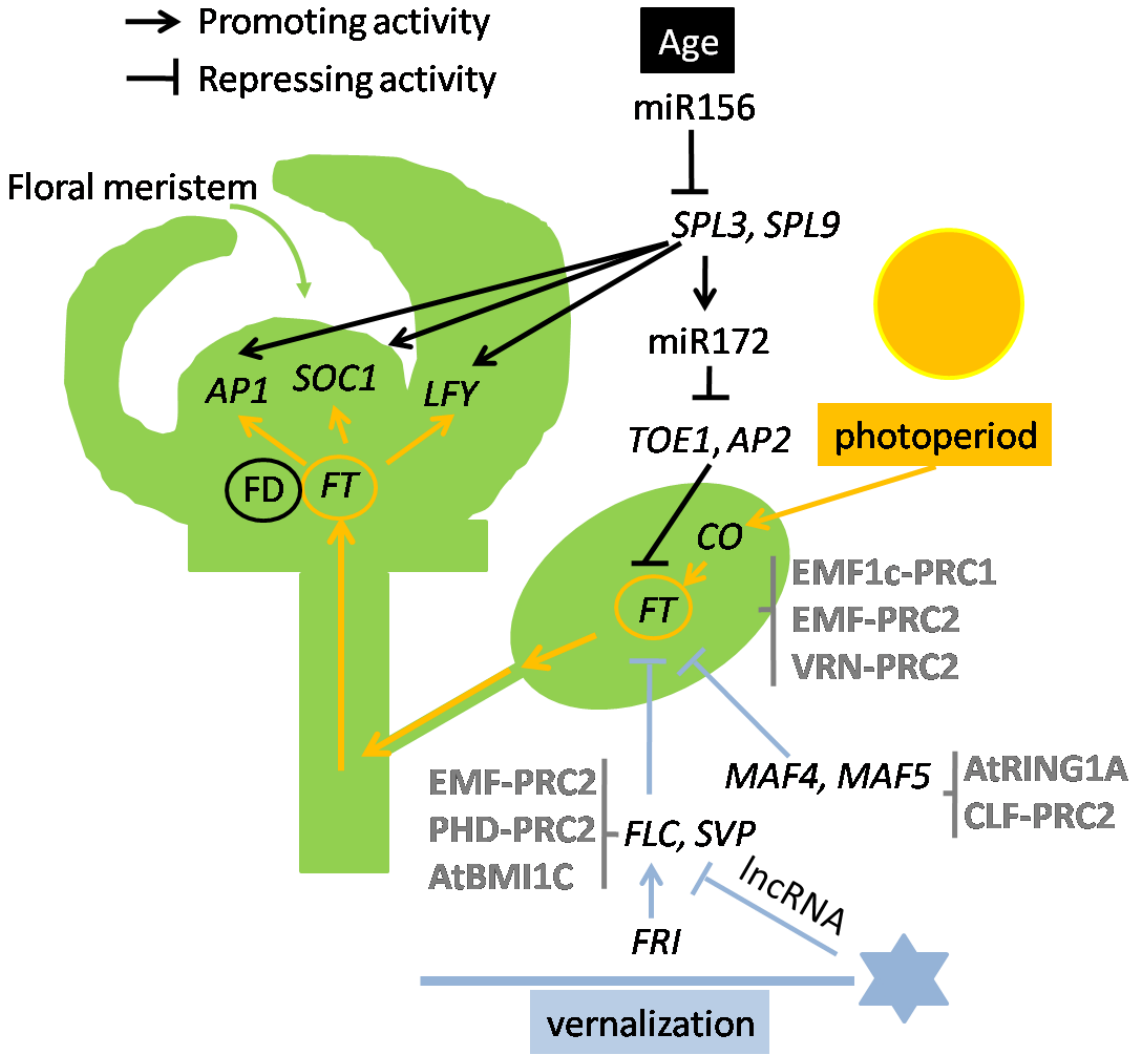

Figure I-9. Outline and the PcG regulation of the photoperiod, vernalization and age pathway in Arabidopsis (Based on (Khan et al. 2014)) .

The photoperiod, vernalization and age pathway are indicated by yellow, blue and black, respectively. The PRC complex involved in the epigenetic regulation are marked in grey.

THESIS OBJECTIVES

AtRING1A and AtRING1B, which are identified as homologs of dRING1 in fly and RING1A/RING1B in mammals, play redundant and pleiotropic roles in diverse developmental stages during the plant life cycle. AtRING1 is also reported to have an E3-ligase activity in *in vitro* H2A ubiquitination assay. However, little is currently known about the function of the RING domain and the RAWUL domain in H2A ubiquitination and regulation of plant growth and development. It is also unknown to which degree AtRING1 functions *via* H2Aub1 deposition. In my PhD thesis work, a specific region of AtRING1A was mutated in a *Atring1b* mutant background, and phenotypic and molecular analysis was conducted on the new AtRING1 mutants to unravel the functional role of protein domain in different processes. The related results will be described in **Chapter II**.

Understanding how H2Aub1 exerts downstream physiological functions is also of great interest in current research. J-domain-containing ZUO1/ZRF proteins had been shown to bind H2Aub1 involved in chromatin state switch in activation of PcG-repressed genes, and their orthologs AtZRF1A and AtZRF1B are present in Arabidopsis. AtZRF1A/B have been reported to play key roles in multiple processes of plant growth and development. But the cellular and molecular mechanisms underlying the mutant phenotype remain largely elusive. In **Chapter III**, I will provide insightful information about the functions of AtZRF1A/B in embryonic and post-embryonic root development at developmental and cellular levels.

The general aim of my thesis is thus to deepen our knowledge of the biological roles and functional mechanisms of the *AtRING1A/B* and *AtZRF1A/B* genes in Arabidopsis.

Chapter II

RESULTS – Part I

Investigation of Polycomb RING1 function in *Arabidopsis thaliana*

Qiannan WANG *et al*

II.1. Introduction

In plants and metazoans, Polycomb Group (PcG) proteins play key roles in regulating developmental processes by repression of gene expression (Mozgova and Hennig 2015; Xiao and Wagner 2015; Kassis et al. 2017; Schuettengruber et al. 2017; Fletcher 2017). PcG proteins function as multi-protein complexes; among them the best characterized ones are Polycomb Repressive Complex 1 (PRC1) and PRC2. Classically, PRC2 catalyzes histone H3 lysine 27 trimethylation (H3K27me3), and PRC1 can bind H3K27me3 and catalyzes H2A monoubiquitination (H2Aub1) (Wang and Shen 2018). The components and molecular functions of PRC2 are evolutionarily conserved and extensive characterized, while the repressive functional mechanism of PRC1 complexes is more recent and shows high divergences between animals and plants (Molitor and Shen 2013; Feng and Shen 2014; Merini and Calonje 2015; Yang et al. 2017b). In Arabidopsis, the LIKE HETEROCHROMATIN PROTEIN 1 (LHP1) was first identified as a PRC1 component, which functions as a reader of H3K27me3. EMF1 is proposed to be a plant-specific PRC1 component. Five PRC1 RING-finger proteins are present in Arabidopsis: AtRING1A and AtRING1B belonging to the RING1 subfamily, and AtBMI1A, AtBMI1B and AtBMI1C belonging to the BMI1 subfamily, all of which show an E3-ligase activity in *in vitro* H2A ubiquitination assays (Wang and Shen 2018). Loss of either AtRING1A/B or AtBMI1A/B/C causes reduction in H2Aub1 in the Arabidopsis mutant plants (Bratzel et al. 2010; Yang et al. 2013a; Li et al. 2017). Strikingly, the mutants of different PRC1 components share only limited similarities but show many phenotypic differences. The underlying mechanisms of PRC1 repression and functional diversity remain to be elucidated. Investigation of AtRING1 function is expected to provide some useful insights.

AtRING1A and AtRING1B are homologs of dRING1 in fly and RING1A/RING1B in mammals (Xu and Shen 2008). They have redundant functions, thus the *Atring1a* or

Atring1b single gene mutant exhibits relatively normal plant growth and development. In contrast, the *Atring1ab* double mutant displays severe phenotypic defects during different developmental stages of the plant life cycle, such as meristem formation (Xu and Shen 2008), embryonic development (Chen et al. 2010), seed germination (Molitor and Shen 2013), growth phase transitions (Li et al. 2017; Shen et al. 2014a), and floral organ development (Chen et al. 2016). AtRING1A or AtRING1B contain a N-terminal RING-domain and a C-terminal ubiquitin-like domain named RAWUL. In general, the RING-domain is considered to be a signature of E3 ligase activity and thus may be responsible for AtRING1 in catalyzing H2A monoubiquitination. The C-terminal RAWUL (Ring-finger and WD40-associated Ubiquitin-Like) domain is involved in binding to PRC1 partners and several transcription factors (Wang et al. 2010; Blackledge et al. 2015; Junco et al. 2013; Alkema et al. 1997; Gunster et al. 1997; Bezsonova et al. 2009; Chagraoui et al. 2006; Negishi et al. 2010; Boukarabila et al. 2009; Gray et al. 2016). In Arabidopsis, little is currently known about the role of the RING-domain in H2A ubiquitination and the RAWUL domain function. It is also unknown to which degree AtRING1 functions *via* H2Aub1 deposition. In-depth functional analysis is complicated by the fact that *Atring1ab* has severe pleotropic phenotypic defects.

Here, the CRISPR/Cas9 gene technology (Adli 2018) was used to mutagenize different regions of *AtRING1A* in the *Atring1b* mutant background. Four different mutants were obtained and their phenotypes were rigorously analyzed. The N-terminal region of AtRING1A containing the RING domain was found to be mainly required for plant growth and development, while RAWUL is also involved. Furthermore, RAWUL is demonstrated to be also involved in H2Aub1 deposition. Chromatin enrichment of H3K27me3 at some specific genes was found also affected.

II.2. Results

II.2.1. Mutagenesis of *AtRING1A* using CRISPR/Cas9 gene editing

II.2.1.1. Design of sgRNAs

We used the CRISPR/Cas9 vector in which *HspCas9* is driven by the promoter of *Yao*, an Arabidopsis genes highly expressed in embryo sac, embryo and endosperm as well as in pollen (Li et al., 2010), and the sgRNA cloning cassette is under the control of the *AtU6-26* small nuclear RNA gene promoter (**Figure II-1A**). This vector system had been previously constructed in Xie's Lab and reported as highly efficient in gene editing in Arabidopsis (Yan et al. 2015b). We used CRISPR-PLANT (https://www.genome.arizona.edu/crispr/) in sgRNA design and we selected 9 different sgRNAs to cover the *AtRING1A* gene (**Figure II-1B**). Both sgRNA1 and sgRNA2 are located to the 5'-end of the first exon and thus are aimed to create mutations preceding the RING-domain at the N-terminus of the AtRING1A protein. The next four sgRNAs (sgRNA3, sgRNA4, sgRNA5 and sgRNA6), located within exon 3 and/or 4, are aimed to directly mutagenize the RING domain of AtRING1A. The following sgRNAs, sgRNA7, located at the end of exon 7 coding a region between the RING and the RAWUL domains, and sgRNA8 and sgRNA9, located around the Tyr428-coding region of exon 8, are aimed to assess function of the RAWUL domain of AtRING1A. Tyr428 is a conserved amino acid equivalent to Tyr247, the CBX7 cbox loop binding site on RING1B in mammals (Wang et al. 2010).

It was reported that a sgRNA with a multi-site design could increase editing efficiency and cause different types of mutations, such as fragment deletion or inversion among different sites of double strand break (DSB), or simultaneous mutations of multiple homologous genes (Moreno-Mateos et al. 2015; Sander and Joung 2014). In our study, sgRNA1, sgRNA3 and sgRNA7 were designed to be double-target-site sgRNAs to

increase the mutation efficiency. All of our sgRNAs were cloned into the final binary vector and introduced in the *Agrobacterium tumefaciens* strain GV3101, and the resulting strains were used to transform the *Atring1b* plants using the floral dip method (Zhang et al. 2006).

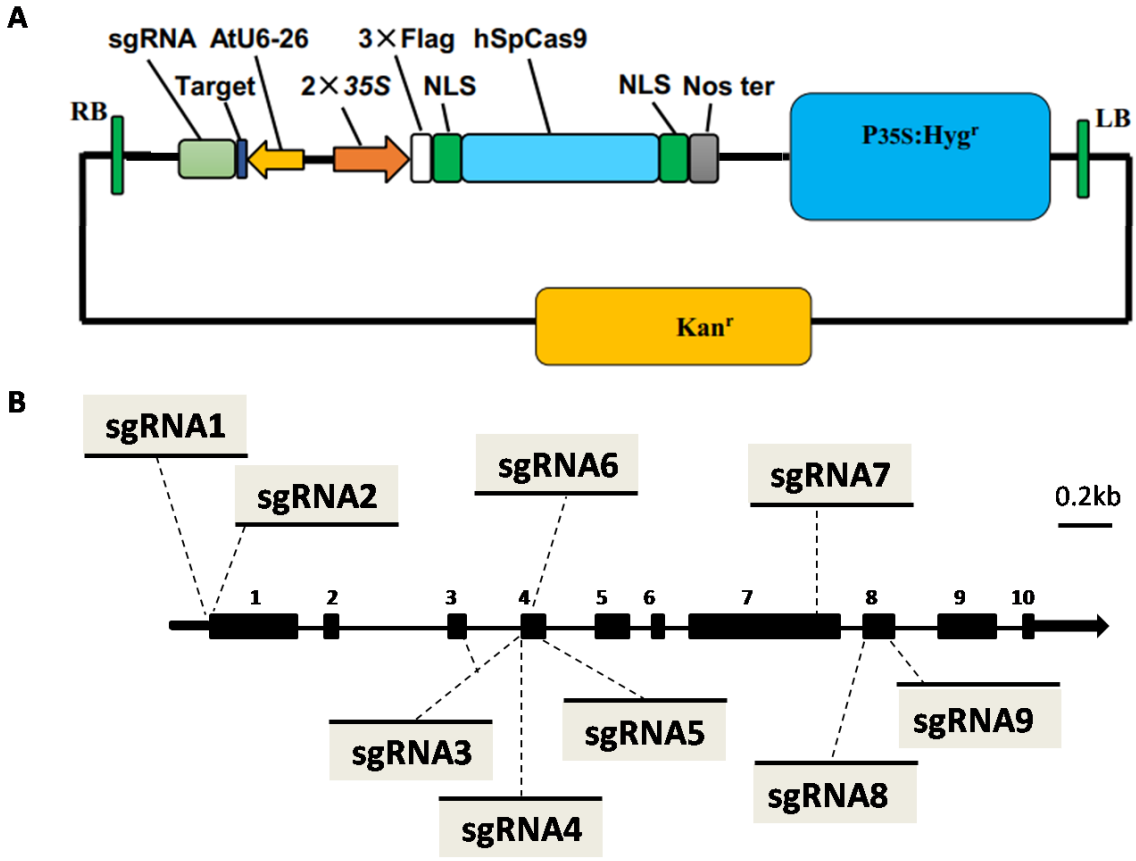

Figure II-1. Mutagenesis of *AtRING1A* using CRISPR/Cas9 gene editing technology.

(**A**) Structure of the CRISPR/Cas9 binary vectors for Arabidopsis transformation by floral dip. The *hSpCas9* gene is driven by the *YAO* promoter. The sgRNA containing target sequence is under the control of the *AtU6-26* promoter. NLS, nuclear localization sequence (adapted from (Yan et al. 2015b)).

(**B**) Nine different sgRNAs are designed to target different regions of *AtRING1A* to create diverse mutations.

II.2.1.2. Different sgRNAs cause varied mutation efficiencies

Seeds (T1 generation) were harvested from *Agrobacterium*-infiltrated plants (T0), and

screened for transformants by antibiotic resistance selection. A range of different numbers of transformants were obtained for different sgRNA constructs (**Table II-1**). These transgenic plants were grown in greenhouse and scored for leaf curling, a phenotype frequently manifested by PcG-loss-of-function mutant Arabidopsis plants (Xu and Shen 2008; Bratzel et al. 2010; Yoshida et al. 2001; Goodrich et al. 1997), and analyzed using PCR amplification and sequencing at predicted regions of the *AtRING1A* gene. A mutagenesis frequency was defined as the number of plants carrying mutations over the total number of the transformed plants. The 9 sgRNAs constructs showed drastically varied mutation efficiencies (**Table II-1**). Both sgRNA1 and sgRNA2 target a region at the N terminus of AtRING1A, but sgRNA1 showed a far more higher efficiency than sgRNA2 did, which is consistent with a double target-site design (sgRNA1) being more efficient than a single target-site design (sgRNA2). In contrast, sgRNA3 is also a double-target site design comprising sgRNA6, but its efficiency is only about half of that of sgRNA6, indicating that more factors could impact on editing efficiency and need to be considered in sgRNA design. Several factors, such as the GC content, the secondary structure, the spacer between the double-target site design of sgRNA as well as the chromatin accessibility of the targeted gene, all could influence editing efficiency (Yang et al. 2017c). The estimated free energy of sgRNA2 is much lower than that of sgRNA1 (**Table II-2**), which might also explain its lower efficiency than that of sgRNA1. Yet, a general co-relationship could not be established for all of our sgRNAs between their mutation efficiencies (**Table II-1**) and their GC contents or free energies (**Table II-2**). We noticed that the mutation rates of sgRNAs targeting regions of the RING domain ranged lower (0% to 55.5%) than those of sgRNAs targeting regions of the RAWUL domain (54.3%~71.4%). It is possible that N-terminal mutations cause more deleterious effects on AtRING1A function and an embryo lethality masks finding of mutations at post-embryonic stage.

Table II-1. Screen of T1 transgenic plants for edited mutation.

sgRNA	No. of T1 transgenic plants examined	No. of transgenic plants exhibited downward curling leaves phenotypes	No. of plants with the mutations	Mutation rate (%)
sgRNA1	115	84	86	74.8%
sgRNA2	13	0	0	0.0%
sgRNA3	26	9	9	34.6%
sgRNA4	49	0	1	2.0%
sgRNA5	37	0	0	0.0%
sgRNA6	9	2	5	55.5%
sgRNA7	102	10	26	25.5%
sgRNA8	149	23	81	54.3%
sgRNA9	140	54	100	71.4%
Average	71.1	20.2	34.2	35.4%

Table II-2. Summary of the GC content and free energy of sgRNAs.

sgRNA	GC content/%	ΔG/kcal/mol
sgRNA1-1	35.0	-1.10
sgRNA1-2	60.0	-4.50/ -4.80
sgRNA2	60.0	-7.10
sgRNA3-1	50.0	-2.20
sgRNA3-2	55.0	-0.30/-1.10
sgRNA4	25.0	-1.00
sgRNA5	50.0	-0.30/-0.70
sgRNA6	55.0	-0.30/-1.10
sgRNA7-1	40.0	1.60-2.50
sgRNA7-2	40.0	-2.60~ -1.60
sgRNA8	55.0	-1.60
sgRNA9	55.0	-3.30/-3.10

II.2.1.3. Establishment of stable mutant lines

To obtain the heritable CRISPR/Cas9-mediated gene-editing mutants, our mutant lines generated by sgRNA1, sgRNA7, sgRNA8 and sgRNA9 were passed to next step analysis. In the T2 generation, Cas9-free and homozygote or heterozygote for the target *Atring1a* mutation were obtained in our screening by PCR and sequencing. As shown in

Table II-3, Cas9-free homozygotes and heterozygotes of *Atring1* were obtained from mutants generated by sgRNA7 or sgRNA9, and heterozygotes but not homozygotes were obtained for mutants generated by sgRNA1 or sgRNA8.

Table II-3. Analysis of mutant plants at T2 generation.

sgRNA	line	Number of T2 plants screened	Number of Cas9-free plants	Number of WT	Number of heterozyote/ biallele/chimera	Number of homozygote	% of mutant Plant
sgRNA1	sgRNA1-1	48	14	12	2	0	14.29%
	sgRNA1-2	48	17	9	8	0	47.06%
sgRNA7	sgRNA7-1	48	10	9	1	0	10.00%
	sgRNA7-2	48	12	12	0	0	0.00%
	sgRNA7-3	48	2	0	1	1	100.00%
sgRNA8	sgRNA8-1	48	14	8	6	0	42.86%
	sgRNA8-2	48	15	12	3	0	20.00%
	sgRNA8-3	48	9	6	3	0	33.33%
sgRNA9	sgRNA9-1	48	7	3	2	2	57.14%
	sgRNA9-2	48	11	3	8	0	72.73%
	sgRNA9-3	48	15	8	5	2	46.67%

Target sites of sgRNA1, sgRNA7, sgRNA8, sgRNA9 were examined to screen for the AtRING1A mutants without CRISPR-Cas9 T-DNA insertion. Homozygotes of AtRING1A-sgRNA7, AtRING1A-sgRNA9 were found in T2 generation, indicating the stable transmission of Cas9-induced mutations

WT, wild-type sequence with no mutation detected.

Heterozygous/biallele/chimera, sequencing profile showed multiple peaks in target region.

Homozygote, sequence with mutation with single peak in target region.

I further screened the next T3 generation plants, confirmed the homozygous mutants originated from sgRNA7 or sgRNA9 gene editing, and obtained a mutant originated from sgRNA1 gene editing, which displays a pattern of single gene segregation ratio according to the Mendel's law (**Table II-4**). The mutant generated from sgRNA8

showed a complexity of more than a single allele mutation, and subsequently was not further used in our study. At the end, four *Atring1* mutants were established for further use in our work (**Figure II-2**). Both the *mut1* and *mut2* mutants contain an insertion of one nucleotide A, whereas *mut3* has a deletion of 43 bp and *mut4* has a C-to-T substitution, located at different positions along the *AtRING1A* gene.

Table II-4. Analysis of mutant plants at T3 generation.

sgRNA	**line**	**T2**			**T3**	
		zygosity	**genotype**	**Cas9**	**segregation ratio**	**Cas9**
sgRNA1	sgRNA1-2-1	Heterozygote	i1WT	-	31WT:45i1WT:8i1i1	-
sgRNA7	sgRNA7-3-1	Homozygote	i1i1	-	24i1i1	-
sgRNA8	sgRNA8-2-1	Bi-allele	i1i1’	-	2i1i1:4i1i1:3i1’i1’	-
sgRNA9	sgRNA9-1-2	Homozygote	r1r1	-	24r1r1	-
	sgRNA9-1-3	Homozygote	r1r1	-	24r1r1	-
	sgRNA9-3-1	Homozygote	d43d43	-	24d43d43	-
	sgRNA9-3-2	Homozygote	d43d43	-	10d43d43	-

i#, # of bp inserted at target site;

i#‘,# of bp insertion at the target site but with another nucleotide.

r#, # of bp replaced at target site.

d#, # of bp deleted from target site.

T2 homozygotes sgRNA7-3-1, sgRNA9-1-2, sgRNA9-1-3, sgRNA9-3-1, sgRNA9-3-2 faithfully passed the same mutation from T2 to T3. Both i1and WT in sgRNA1-2-1, i1 and i1’ mutations from sgRNA8-2-1 passed from T2 to T3 generation. sgRNA8-2-1 followed the classic Mendel’s law, while sgRNA1-2-1 not.

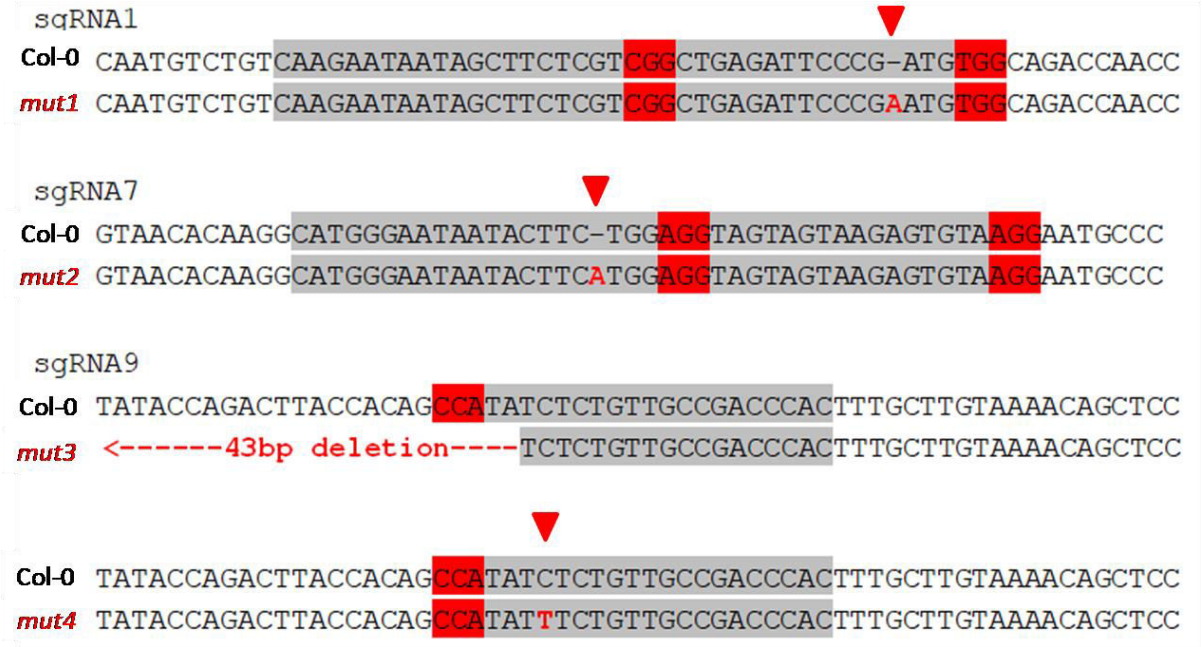

Figure II-2. Alignment of wild-type Col-0 and T3 mutant sequences surrounding the mutation target sequences.

The target sequences and tandem guanosine nucleotides (PAM) are in grey and red highlight, respectively. Insertions and replacement are in red font and indicated by red triangles, while deletion is represented by red hyphens and red arrowheads indicate the direction of the deletions.

II.2.1.4. Brief assessment of mutation effects

Effects of *Atring1* mutations were briefly assessed by observation of global phenotype of plants. *mut1* could be maintained only in the heterozygous state. A small percentage ($\approx$10%) of seeds were segregated to be homozygous from the offspring of the heterozygous parents. After germination in *in vitro* culture, the aerial part became transformed into an amorphous mass of callus-like, embryo-like structure (**Figure II-3A, B, C**). The phenotype of *mut1* is the most severe *Atring1* mutant known up to now. It is much stronger than the T-DNA insertion double mutant *Atring1ab*, in which only roughly 17% grow to form embryonic calli (Chen et al. 2010). It suggests that the T-DNA insertion does not represent a completely loss-of-function of *AtRING1A*. In

contrast to *mut1*, the mutations in *mut2* and *mut3* led to less severe growth phenotypes. Nevertheless, multiple defects exist in these mutants. Compared to Col-0, *mut2* and *mut3* had slightly smaller rosette width, wider leaves with slightly serration and lobe (**Figure II-3D, E, F, G**). The orders of leaf emergence were also disturbed. The *mut4* mutate was analyzed at the same time, and the results showed that this mutant resembles the wild-type Col-0 and the single mutant *Atring1b*.

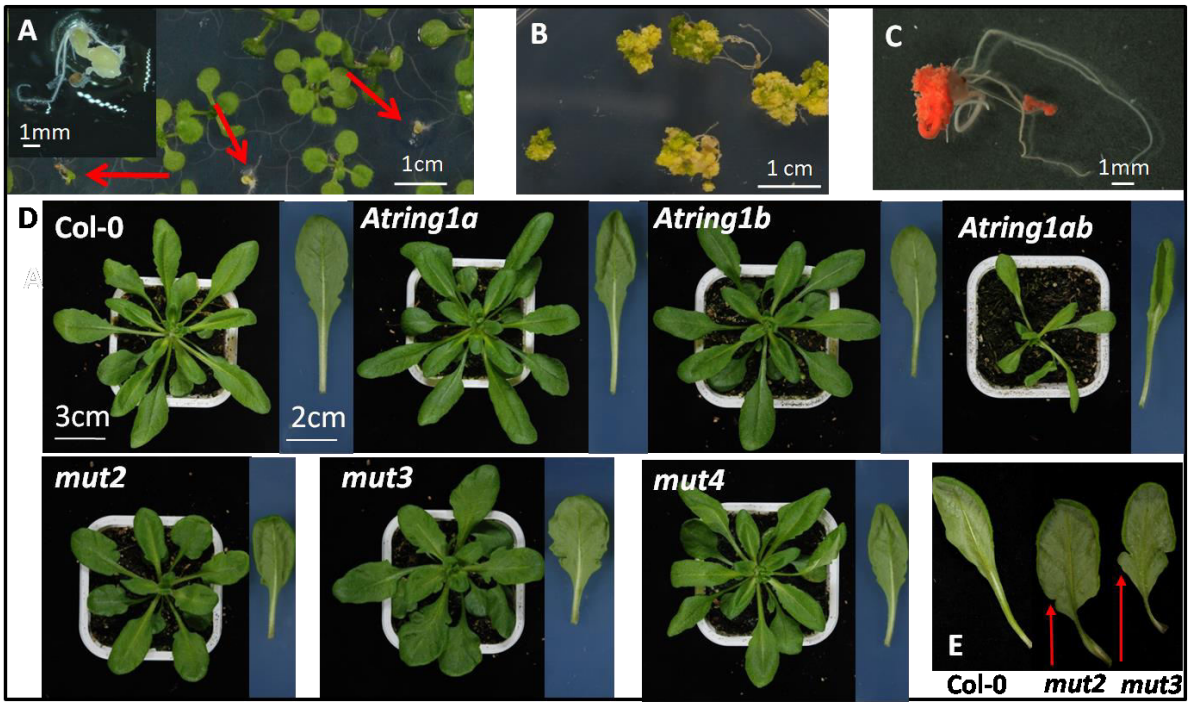

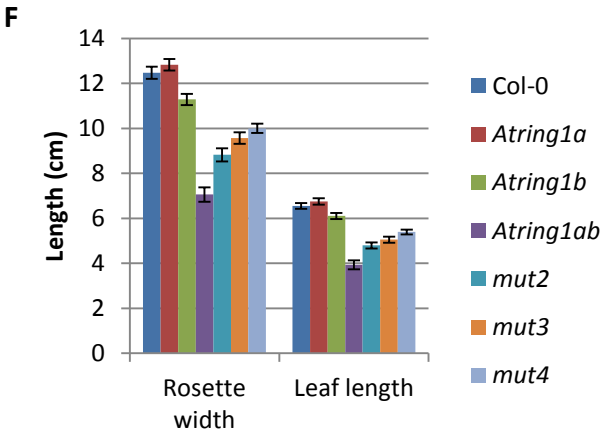

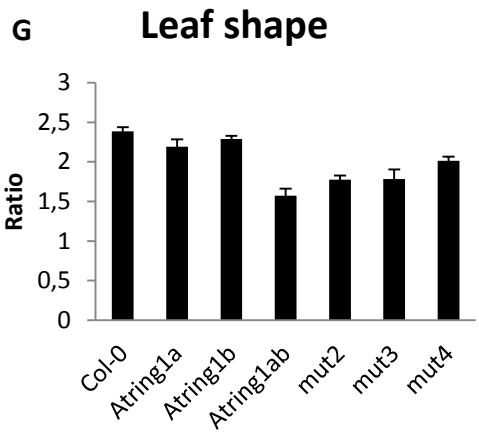

Figure II-3. Phenotype of the four mutants generated using CRISPR/Cas9 technology.

(**A**) Phenotype of ten-day-old *mut1* (red arrows). Scale bar represents 1 cm.

(**B**) Phenotype of seventy-day-old *mut1*. Scale bar represents 1 cm.

(**C**) Fat red staining thirty-day-old *mut1*. Scale bar represents 1 mm.

(**D**) The representative plants and the eighth leaves of thirty-day-old *Atring1* mutants and wild type grown under LD conditions. Scale bars represent 3cm and 2 cm, respectively.

(**E**) The eighth leaf of forty-day-old Col-0, *mut2* and *mut3* grown under LDs.

(**F-G**) The statistical data of rosette width, the leaf length (**F**) and the leaf shape (**G**) of *Atring1* mutants and Col-0 grown under LD conditions. Values were scored from 20 one-month-old plants of each genotype. Rosette width was measured as the maximum diameter of rosette in one plant; leaf length was the maximum vertical diameter from leaf tip to the center of the rosette in one plant; petiole length was the distance from the stem to the base of the blade; leaf width and petiole length were recorded for the same leaf which was measured for the leaf length; leaf width was the widest cross diameter; Leaf shape: (leaf length-petiole length)/leaf width.

II.2.2. Molecular characterization of mutations and their effects on global levels of H2Aub1 and H3K27me3 in *Atring1* mutants

II.2.2.1. Molecular characterization of mutations

To check whether the mutations in *mut1*, *mut2*, *mut3* and *mut4* affect *AtRING1A* transcription, the expression level of *AtRING1A* was analyzed by using quantitative RT-PCR. Compared to Col-0 and *Atring1b*, *mut1* showed a highest increase (roughly 4 folds) of *AtRING1A* expression, *mut2* and *mut3* showed a slight increase (less than 2 folds) of *AtRING1A* expression, whereas *mut4* showed an unchanged level of *AtRING1A* expression (**Figure II-4A**). It has been previously shown that *AtRING1A* as well as other Arabidopsis PcG RING-domain genes are themselves repressed by PcG silencing (Chen et al., 2010). The increase of *AtRING1A* transcription in *mut1*, *mut2* and *mut3* likely reflects an impaired PRC1 function because of AtRING1A mutations. Then, the

full-length cDNAs of the mutated *AtRING1A* genes in *mut1*, *mut2*, *mut3* and *mut4* were

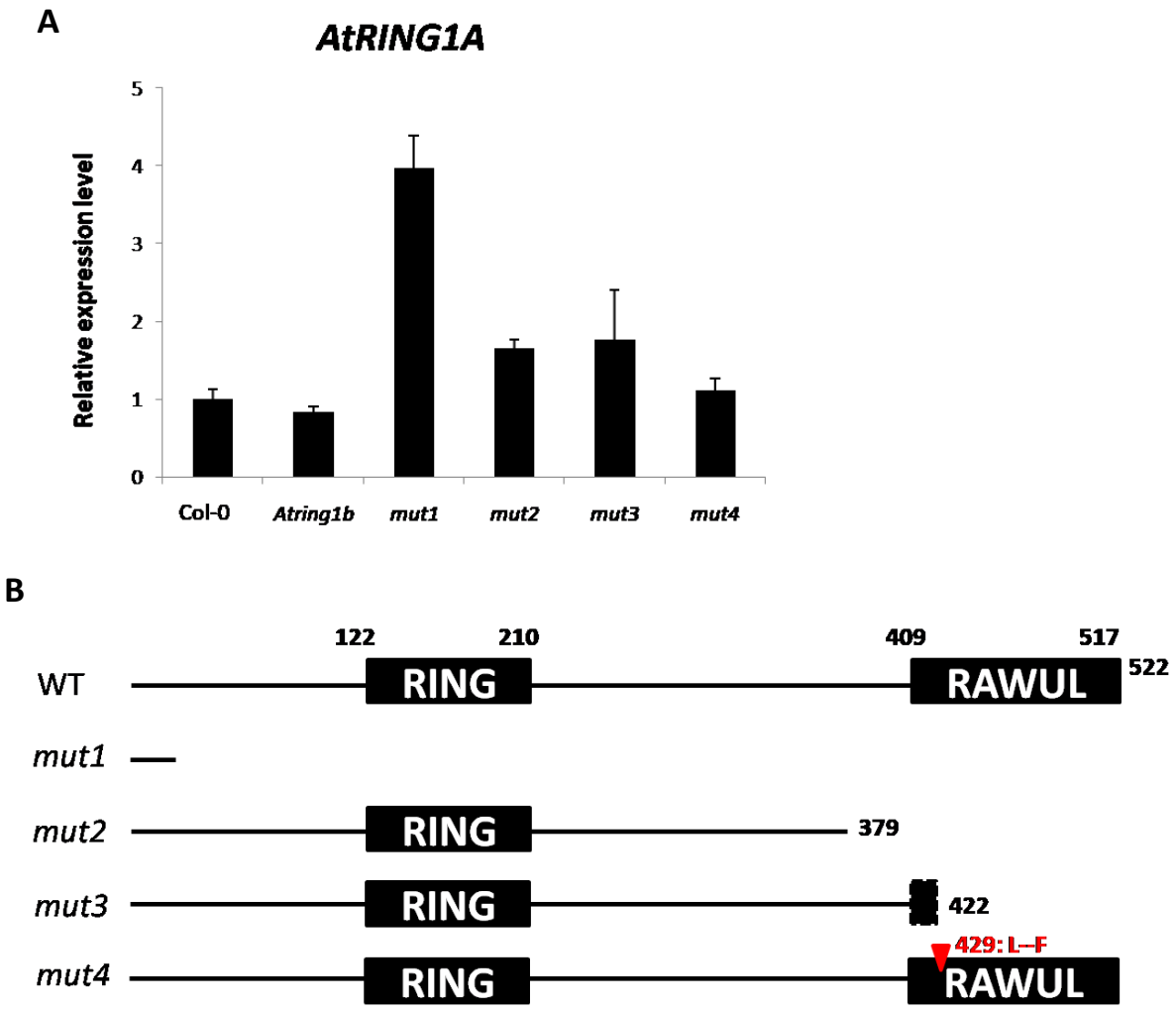

Figure II-4. The expression and coding capacity of AtRING1A in the *mut1*, *mut2*, *mut3* and *mut4* mutants.

(A) Expression of *AtRING1A* was determined by quantitative RT-PCR in 12-day-old seedlings of wild type Col-0 and Atring1 mutants. The expression levels were normalized to reference genes *GAPDH*, *EXP* and *Tip41* and relative to wild type. Data was shown as mean ± SD. Similar results were obtained in three independent biological repeats.

(B) The *in silico* analysis of coding capacity of *AtRING1A* in *mut1*, *mut2*, *mut3* and *mut4* mutants by ORF finder.

analyzed by RNAs extraction from these mutant seedlings followed by RT-PCR amplification and sequencing. Our results confirmed that *AtRING1A* is transcribed

integrally and cDNAs contain the designed mutations. Thus, *mut1* has an A-insertion at 44bp downstream of ATG, which creates a premature stop codon before RING-domain. *mut2* has a 43bp-deletion from 1245bp to 1287bp and *mut3* has an A-insertion at 1131bp, which create frame-shift and premature stop codon leading to a likely production of truncated proteins without RAWUL-domain (**Figure II-4B**). *mut4* has a C-to-T substitution, which changes the Leu429 (L)-codon CTC to a Phe (F)-codon TTC (**Figure II-4B**). Taken together, we conclude that the *mut1, mut2*, *mut3* and *mut4* mutations do not impede *AtRING1A* transcription but alter the gene product (protein) and functionality.

II.2.2.2. Analysis of global levels of H2Aub1 and H3K27me3 in *Atring1* mutants

To assess function of different *Atring1a* mutations on chromatin modifications, I analyzed the global level of H2Aub1 and H3K27me3 in the *mut1*, *mut2*, *mut3* and *mut4* plants. At first, nuclear protein extracts from 12-day-old seedlings were prepared. Immunoblotting analysis with the H2Aub1 antibody on the nuclear protein extract showed that the amount of H2Aub1 in *Atbmi1ab* was drastically decreased compared to that of Col-0 (**Figure II-5A, B**), which is consistent with previously published data (Bratzel et al. 2010; Yang et al. 2013a). There was barely difference at H2Aub1 level among *Atring1a*, *Atring1b*, *Atring1ab* and Col-0 seedlings. The amount of H2Aub1 was greatly decreased in *mut2* and *mut3*, and was barely detected in *mut1* (**Figure II-5A, B**). Surprisingly, in spite of a lack of obvious mutant plant phenotype, *mut4* showed a mild but significant decrease of H2Aub1 (**Figure II-5A, B**). In contrast to effects observed on H2Aub1, the analysis with anti-H3K27me3 antibody failed to detect any significant level change in *mut2*, *mut3* and *mut4* as compared to Col-0 (**Figure II-5A, B**). In this latter analysis, because of limited material quantity of *mut1*, H3K27me3 in this mutant has not been evaluated. We further performed western blot on protein extracts enriched

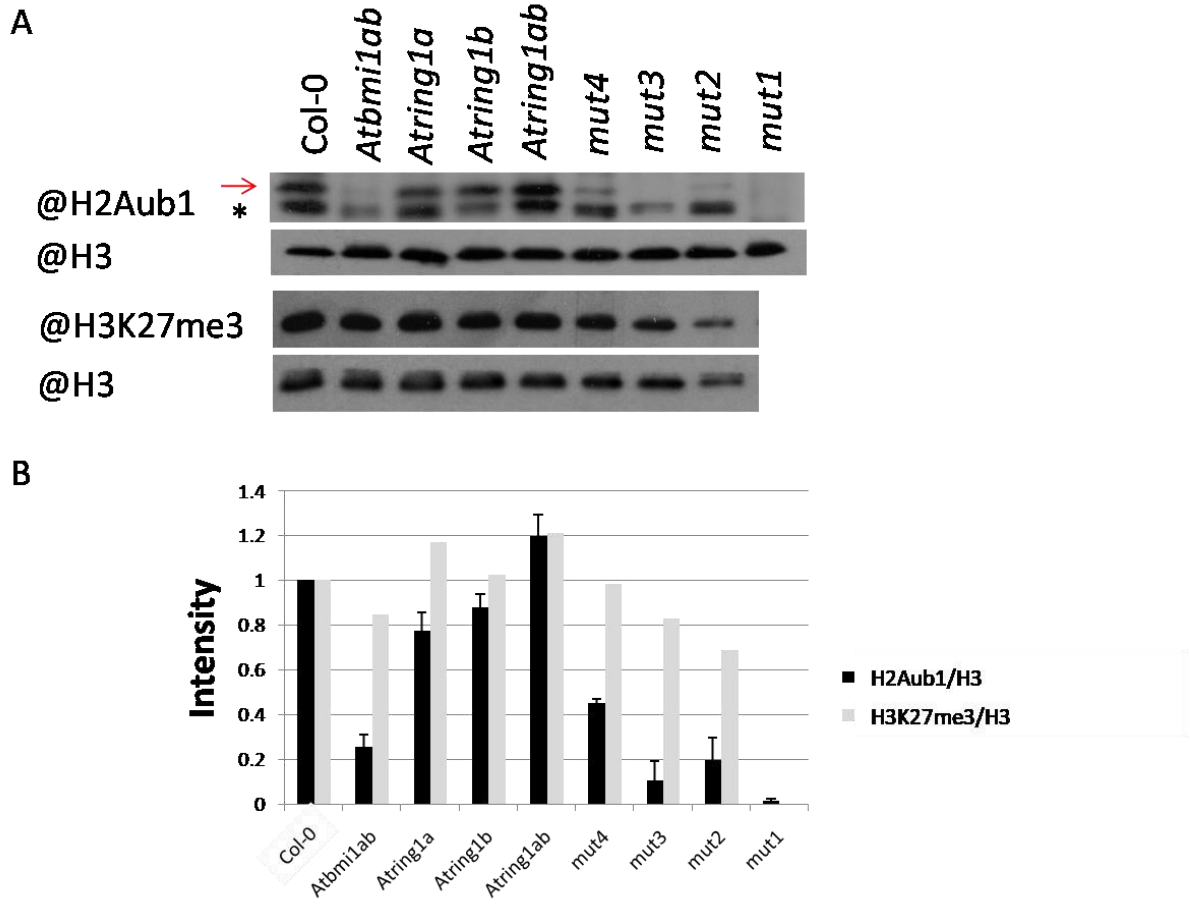

Figure II-5. Western blot analysis for H2Aub1 and H3K27me3 levels in nuclear extracts of the different mutants as compared to that of the wild-type control Col-0.

(**A**) The nuclear protein extracts of 12-day-old Col-0, *Atbmi1ab*, and *Atring1* mutants grown under LDs probed with H2Aub1 antibody (the candidate band is marked with a red arrow) or H3K27me3 antibody. H3 was used as the loading control. Star indicates a unspecific band.

(**B**) Quantification of western blot signals from (**A**) for H2Aub1 (in black) or H3K27me3 (in grey) by Image J software is normalized to H3 and conducted as mean ratio relative to Col. Error bars indicate SD for two independent biological repeats.

for histones according to a previous described method (Yu et al. 2004). In this case, anti-H2Aub1 lighted up more specifically the H2Aub1 band (**Figure II-6A**). Again, reductions of H2Aub1 levels were detected in *mut2*, *mut3* and to a lesser extent in *mut4* but not in *Atring1a*, *Atring1b* and *Atring1ab* as compared to Col-0 (**Figure II-6A, B**).

And H3K27me3 levels showed no significant change in the mutants (**Figure II-6A, B**). Taken together, my results indicate that the RAWUL domain on the C-terminal part is also essential for the activity.

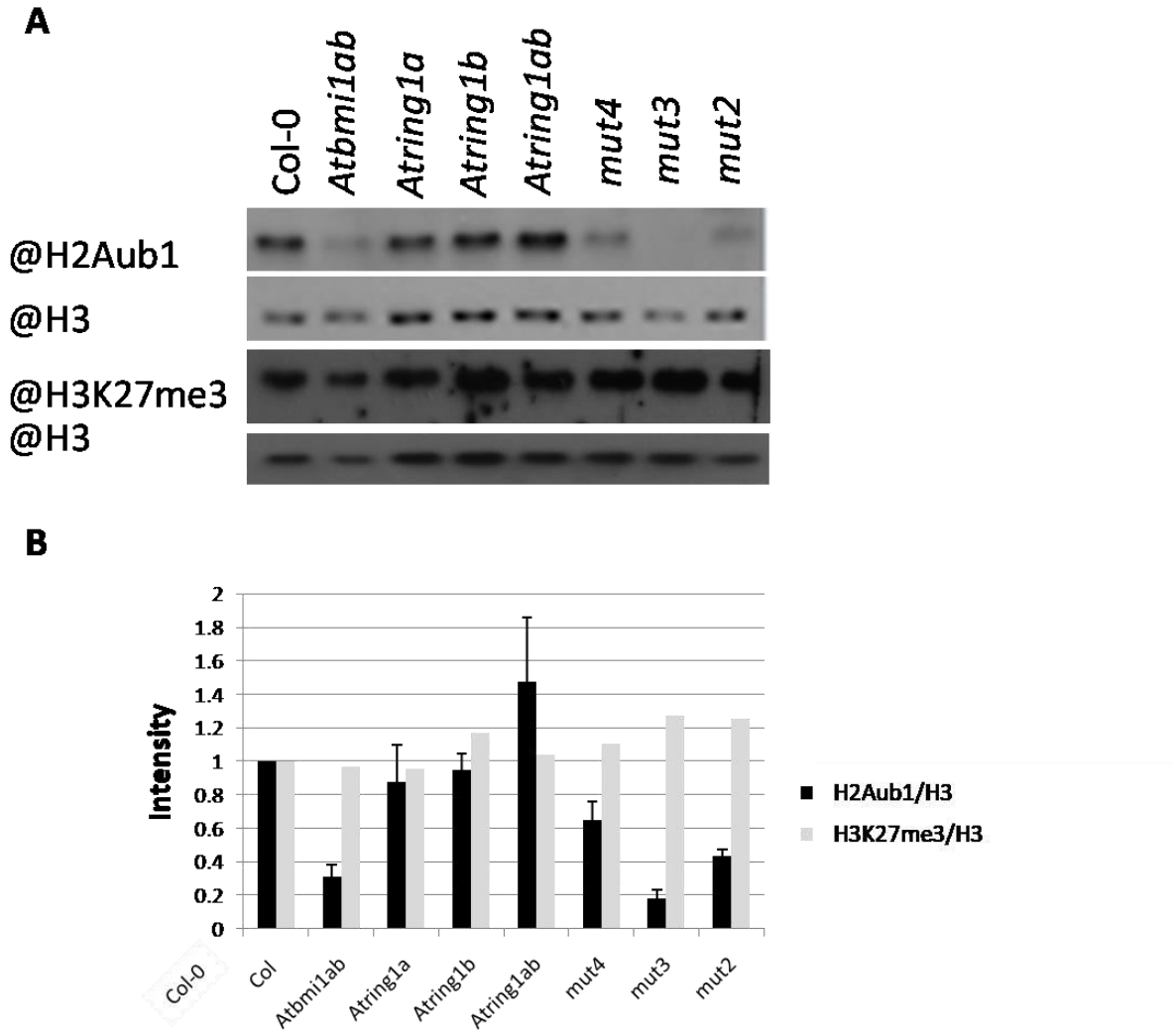

Figure II-6. Western blot analysis for H2Aub1 and H3K27me3 levels in histone-enriched nuclear extracts of the different mutants as compared to that of the wild-type control Col-0.

(**A**) The histone extracts of 12-day-old Col-0, *Atbmi1ab*, and *Atring1* mutants grown under LD conditions probed with H2Aub1 antibody or H3K27me3 antibody. H3 was used as the loading control.

(**B**) Quantification of western blot signals from (**A**) for H2Aub1 (in black) or H3K27me3 (in grey) by Image J software is normalized to H3 and conducted as mean ratio relative to Col. Error bars indicate SD for two independent biological repeats.

II.2.3. Characterization of plant developmental defects in different *Atring1* mutants

II.2.3.1. Seedling growth

To examine the function of RAWUL domain in plant growth and development, I characterized the phenotype of *mut2*, *mut3* and *mut4*. In vegetative development stage, *mut4* grew to be wild type like (**Figure II-7A, D**). In contrast to the consensus phenotype in the progeny of Col-0, the seedlings of *mut2* and *mut3* showed variability in leaf development (**Figure II-7B, D**). Different from a certain percentage of T-DNA insertion double mutant *Atring1ab* plants failing to produce rosette (Chen et al. 2010), all of *mut2* and *mut3* developed true leaves, while they were retarded than Col. We found seedlings with severe twisted and downward leaves, and some of them had tiny and sessile cotyledons (strong), some plants had relatively well expanded cotyledons (intermediate); and seedlings with slightly twisted- and downward-leaf phenotype (weak). The percentages of intermediate and strong mutants in *mut2* and *mut3* are smaller than those in *Atring1ab* (**Figure II-7D**). All of *mut1* grow to be embryonic calli (**Figure II-7C, D**). In total, the integrity of RAWUL domain in AtRING1 is important for plant growth.

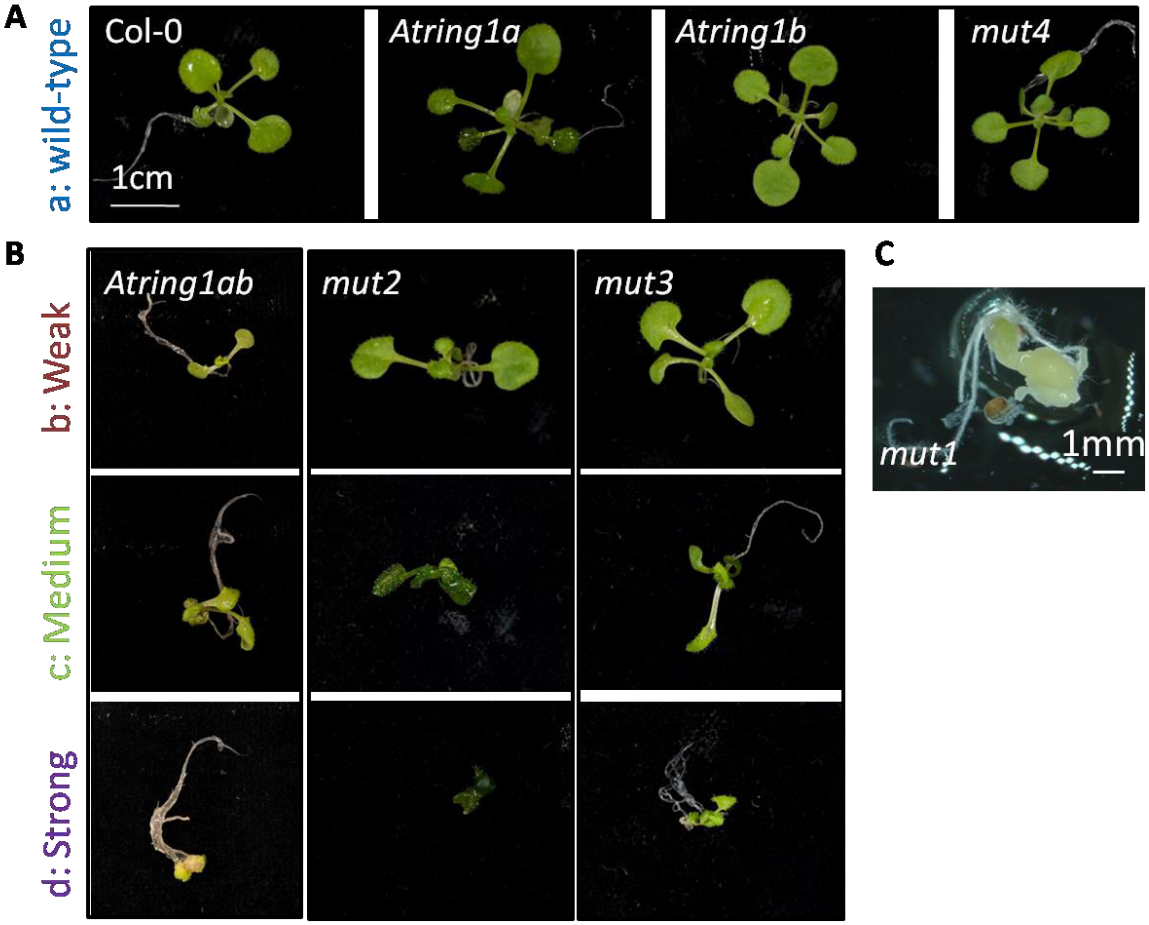
A
a: wild-type
Col-0
1cm
Atring1a
Atring1b
mut4
B
b: Weak
c: Medium
d: Strong
Atring1ab
mut2
mut3
C
mut1
1mm

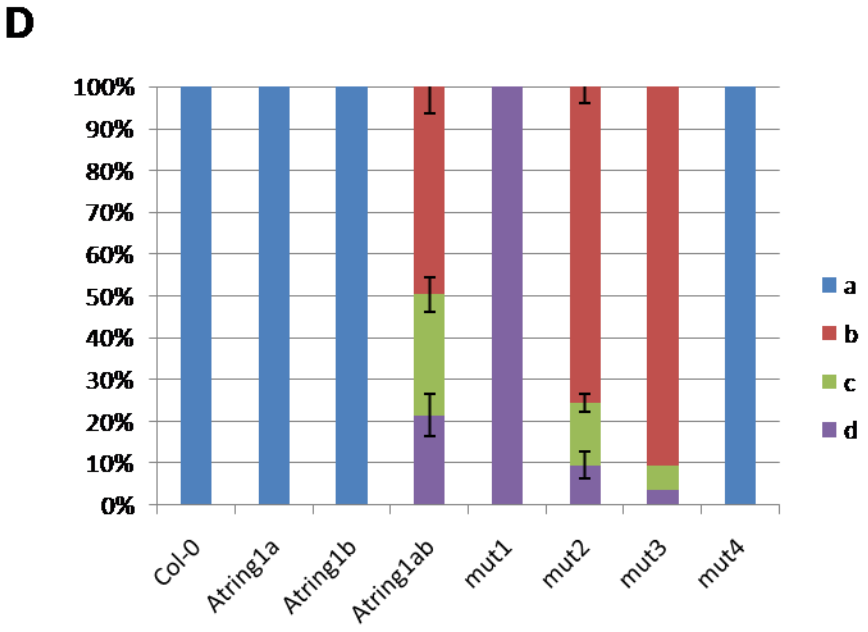
D
100%
90%
80%
70%
60%
50%
40%
30%
20%
10%
0%
Col-0
Atring1a
Atring1b
Atring1ab
mut1
mut2
mut3
mut4
a
b
c
d

Figure II-7. Seedling growth phenotypes of the different *Atring1* mutants.

(**A**) Twelve-day-old *Atring1a*, *Atring1b* and *mut4* were wild-type-like (represented by type a), Scale bar represents 1 cm.

(**B**) Twelve-day-old *Atring1ab*, *mut2*, *mut3* and *mut4* showed variation, which were classified as weak (represented by type b), medium (represented by type c) and strong (represented by type d) phenotype; Scale bars represents 1 cm.

(**C**) *mut1* displaying callus-like phenotype. Scale bar represents 1 mm.

(**D**) Quantitative analysis of the percentages of wild-type like (a), weak (b), medium (c) and strong (d) phenotype in each line. Data was shown as mean±SD. Similar results were obtained in three independent biological repeats.

II.2.3.2. Flower development

AtRING1 is reported to be important for gynoecium and carpel development (Chen et al. 2016). In my observation, there was no abnormality in flower development of *mut4*, while *mut2* and *mut3* showed a mild variation of flower morphology. The sizes of the flower organs were slightly larger (**Figure II-8A**). The statistical analysis of flower organs revealed that the mutant flowers contained about one more sepals and petals than those in wild type (**Figure II-8C**), which was much less than that of the *Atring1ab* (Xu and Shen 2008). There was no variation in the number of stamens, while the gynoecium phenotypes displayed diversified modifications but less severe than those in *Atring1ab*, such as the bulged and increased number of carpels, stigma papilla-like structure or outgrowth grown outside the replum or shorter stigmatic papillae and style (**Figure II-8B**). In total, during floral development, loss of RAWUL domain leads to increased flower organ number.

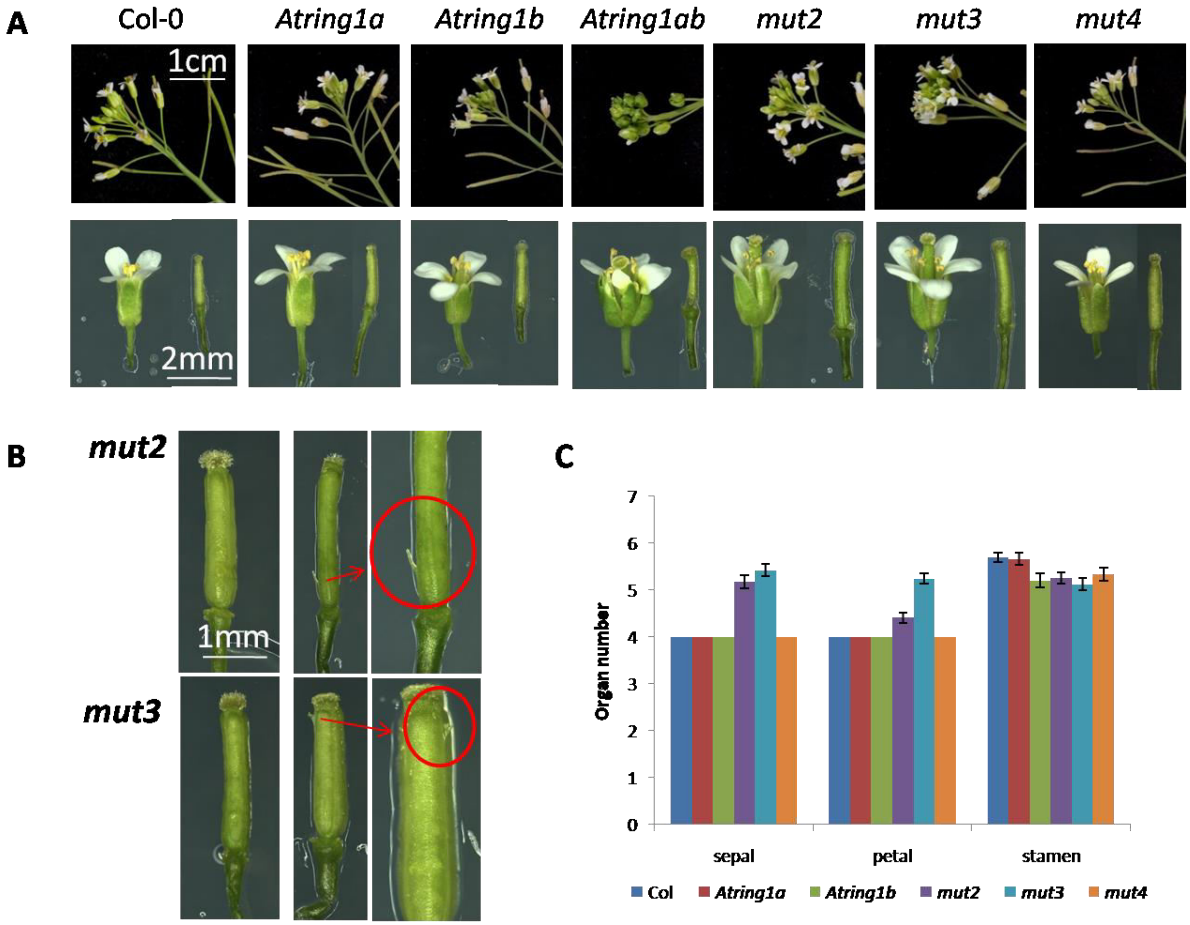

Figure II-8. Flower phenotypes of the different *Atring1* mutants.

(**A**) Representative primary inflorescence (upper panel), single flower (bottom panel, left) and gynoecium (bottom panel, right) of Col-0 and *Atring1* mutants.

(**B**) Gynoeciums of *mut2* (top) and *mut3* (bottom) with three caples (left) or outgrowth from the replum and shortened stigmatic papillae and style (middle and right).

(**C**) The quantitative analysis of the floral organ numbers of wild type and *Atring1* mutants. At least fifty flowers were measured randomly from top half of 5 plants per lines. Data was shown as mean ± SD. Similar results were obtained in three independent biological repeats.

II.2.3.3. Seed production

AtRING1 is also important for the normal ovule and embryo sac development (Chen et al. 2016), which are closely associated with the seed viability and seed production. Our data showed that the development of silique in *mut4* was not altered. In contrast, *mut2* and *mut3* exhibited silique developmental defects. Compared to Col, the replums are shortened and the tips of their valves were bulged, which changed the silique shape (**Figure II-9A-9E**). A small proportion of silique (~12% and ~16%) had 3 carpels, which is much lower than that in *Atring1ab* (~70%) (**Figure II-9C, 9E**). The central seplums in the siliques with 3 carpels were not complete formed (**Figure II-9F**). Different from the regular and compact seeds arrangement in Col, *mut2* and *mut3* siliques showed less ordered seeds arrangement, several empty spaces, shriveled white structures resembling degraded unfertilized ovules and shriveled brown seeds (**Figure II-9F**). The statistical analysis of the seeds per silique showed that *mut2* and *mut3* can produce more seeds than Col-0 (**Figure II-9H, 9I**). Manipulation of the RAWUL domain to increase the economic yield could be a feasible way to improve yield in crops. Moreover, previously research reported that the *Atring1ab* is completely sterile (Xu and Shen 2008); however, the weaker mutants which are able to produce a small quantity of seeds were screened in our subsequent studies, whereas the amount of seeds was extremely tiny (**Figure II-9H, 9I**).

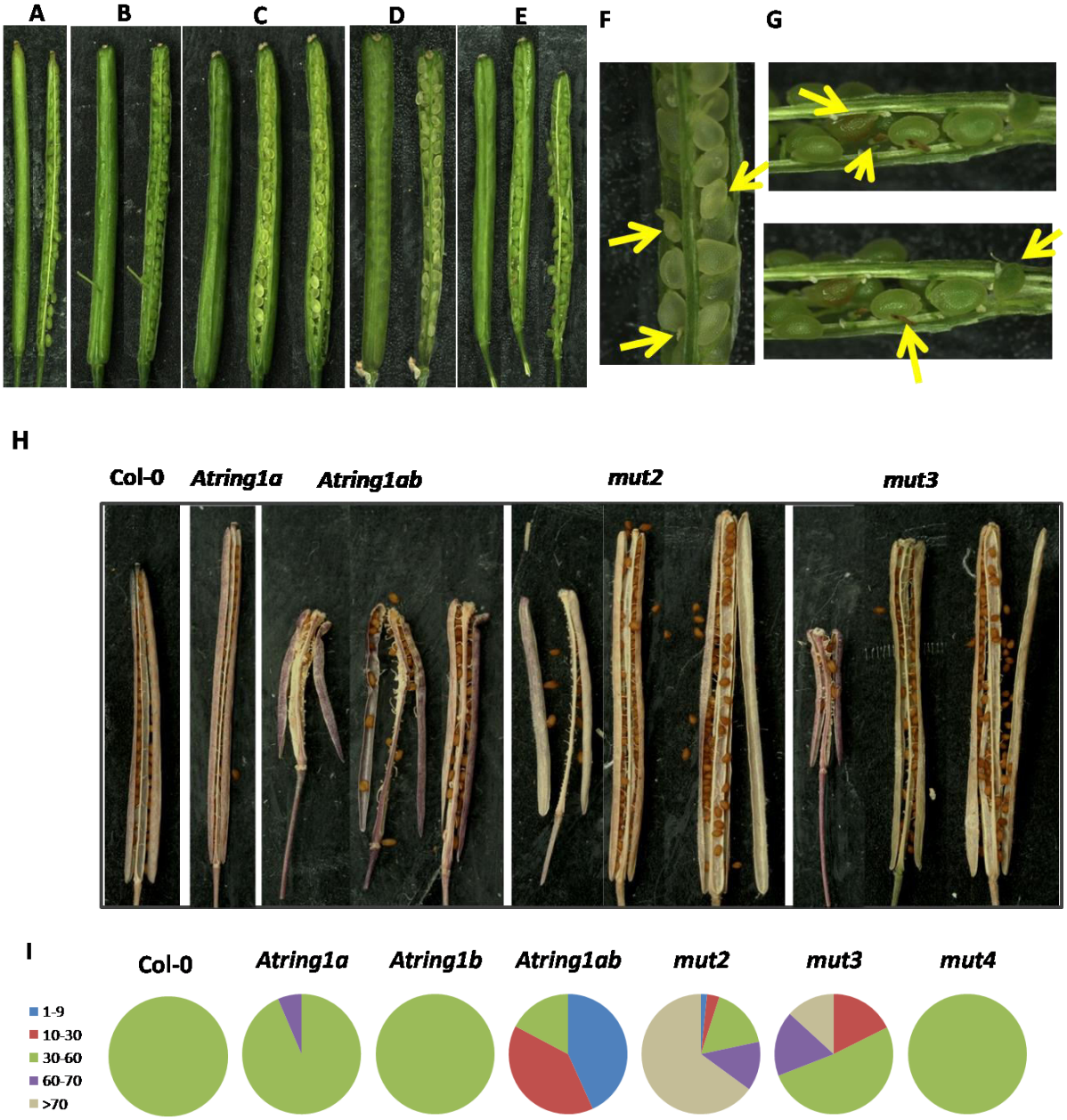

Figure II-9. Silique phenotype and seed production in the different *Atring1* mutants.

(**A-E**) Siliques of wild type (**A**), 2-carpel *mut2* (**B**), 3-carpel *mut2* (**C**), 2-carpel *mut3* (**D**), 3-carpel *mut3* (**E**) were displayed as complete and opened. The representative siliques were taken from the similar position of the 50-day-old plants grown under LDs.

(**F-G**) Representative 2-carpel silique (**F**) and 3-carpel silique (**G**) from *mut3*. These siliques contained a percentage of arrested ovules (indicated by arrows).

(**H**) The dissected mature siliques from 70-day-old wild type and *Atring1* mutants.

(**I**) Quantitative analysis on the average number of seeds per silique. At least fifty siliques were measured randomly from top half of 5 plants per lines.

II.2.3.4. Expression of some key developmental genes

These observations together reveal that the L429F substitution in *mut4* does not affect the biological function of AtRING1A, and the disruption of C-terminal in *mut2* and *mut3* weakens but not completely abolishes AtRING1A function. To investigate the mechanism under the less severe phenotype in *mut2* and *mut3*, the expression level of several genes involved in meristem maintenance (Class I *KNOX* genes) (**Figure II-10A**) and organ boundary establishment (*CUC1/2/3*) (**Figure II-10B**) was examined by quantitative RT-qPCR. *mut3* was chosen to be the representative line for the weak mutants.

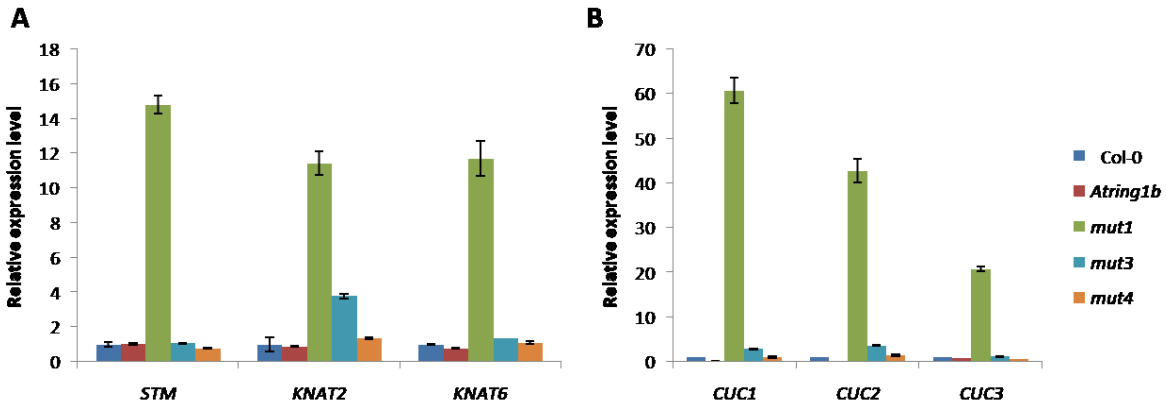

Figure II-10. Quantitative RT-PCR analysis of gene expression in the different *Atring1* mutants as compared to the wild-type control Col-0.

Relative mRNA levels of class I *KNOX* genes (*STM*, *KNAT2* and *KNAT6*) (**A**) and *CUC* genes (*CUC1*, *CUC2* and *CUC3*) (**B**) were determined by qRT-PCR in twelve-day-old seedlings. The expression levels were normalized to reference genes *GAPDH*, *EXP* and *Tip41* and relative to wild type. Data was shown as mean±SD. Similar results were obtained in three independent biological repeats.

As expected, the class I *KNOX* genes and *CUC* genes remained unchanged in *Atring1b* and *mut4* compared to Col, while all the genes examined above were drastically upregulated in *mut1*, which was consistent with the wild-type like phenotype in *mut4*

and callus-like phenotype in *mut1*. In *mut3*, no misexpression in the *STM*, *KNAT6* and *CUC3* transcripts was detected, whereas *KNAT2*, *CUC1* and *CUC2* were upregulated. These data indicate again that the loss of RAWUL domain partially disturbed the shoot apical meristem activity by upregulating *KNAT2*, *CUC1* and *CUC2* expression, which is in line with the medium severity of phenotype. It is in agreement with the known general role for PcG in plants (Mozgova et al. 2015; Wang and Shen 2018).

II.2.3.5. Histone modifications at some developmental genes

AtRING1 showed E3 H2Aub1 ligase activity *in vivo* (**Figure II-5, 6**) (Li et al. 2017), but whether AtRING1 mediates the expression of class I *KNOX* and *CUC* genes by incorporating H2Aub1 mark remains unknown. Therefore, the level of H2Aub1 at *KNAT2*, *CUC1* and *CUC2* was examined. My data showed that the H2Aub1 mark is clearly higher enriched at *CUC1* loci and the enrichment of H2Aub1 mark on these 3 genes in different plants followed the same rules. *Atring1b* and *mut4* showed unaffected or slightly reduced level of mark on *KNAT2*, *CUC1* and *CUC2*, while *Atring1ab*, *Atbmi1ab* and *mut3* had strongly decreased enrichment (**Figure II-11B**). It suggests that *KNAT2*, *CUC1* and *CUC2* are the H2Aub1 target and both AtRING1 and AtBMI1 participate in the H2Aub1 depositing. The disruption of RAWUL domain impaired the E3 ligase activity of AtRING1. Since AtBMI1 has been reported to affect the H3K27me3 at specific genes (Yang et al. 2013a) and the repression of class I *KNOX* genes by AtRING1 does not depend on H3K27me3 (Xu and Shen 2008), I further detected the H3K27me3 mark on *CUC1* and *CUC2* in *Atbmi1ab*, *Atring1ab*, *mut3* and *mut4* (**Figure II-11C**). I found that the levels of H3K27me3 at *CUC1* and *CUC2* loci were unaffected in *Atring1b* and *mut4*, but drastically decreased in *Atbmi1ab* and *Atring1ab*, indicating that AtRING1 and AtBMI1 are also implicated in depositing H3K27me3 mark at *CUC1* and *CUC2*. It is noteworthy that, in *mut3*, the level of H3K27me3 at *CUC2* was not affected but was dramatically reduced at *CUC1*. It

indicates the loss of RAWUL domain in AtRING1A impedes the H3K27me3 deposition at *CUC1* loci but not at *CUC2* loci. In summary, the performance of AtBMI1 and AtRING1 in depositing H2Aub1 and H3K27me3 mark on *KNAT2*, *CUC1* and *CUC2* suggests that the AtRING1-AtBMI1 containing PRC1 complex does not function in the downstream of PRC2 at the chromatin of *KNAT2*, *CUC1* and *CUC2*. The RAWUL domain might be involved in the recruitment of PRC2 to *CUC1*.

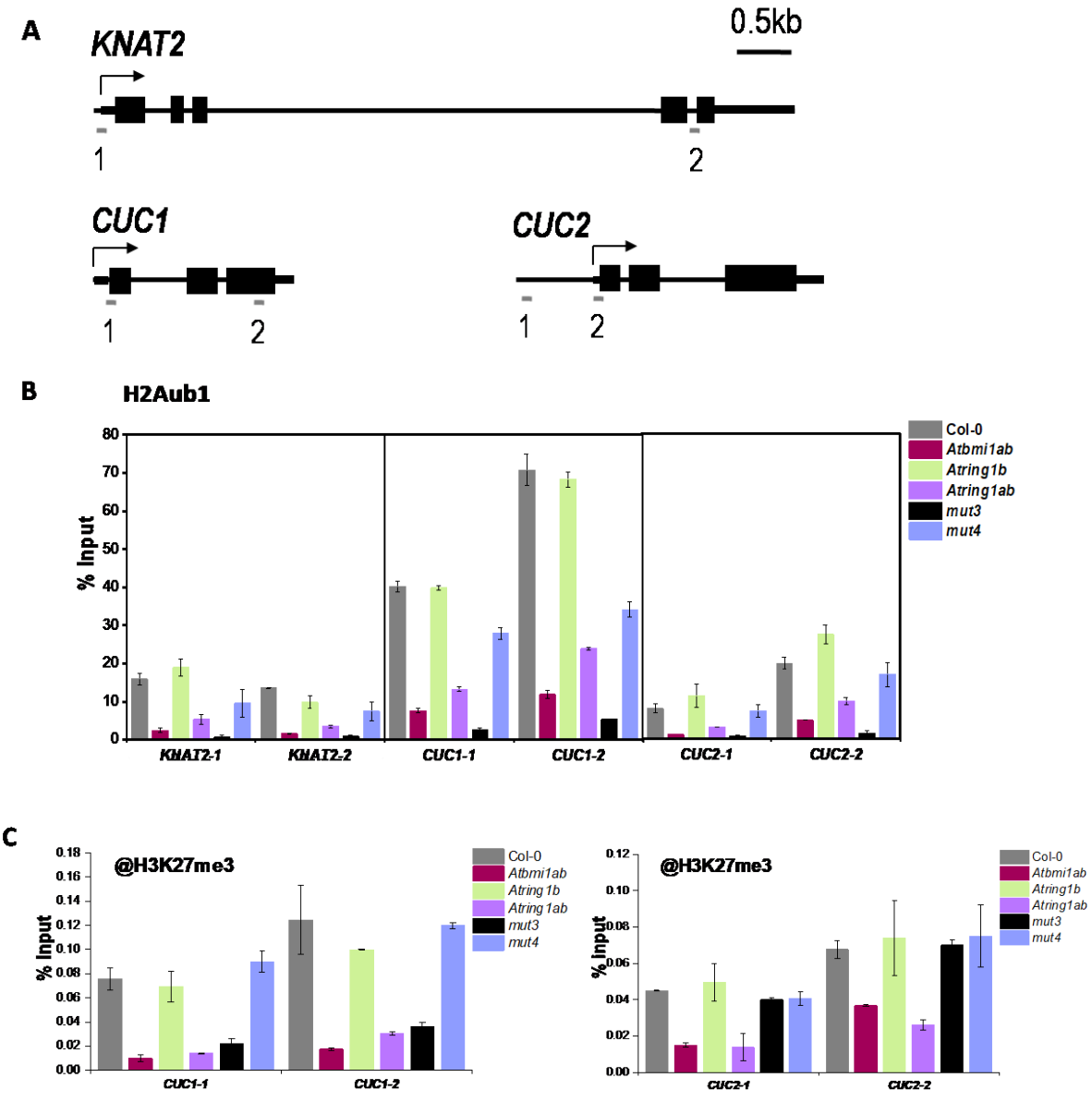

Figure II-11. ChIP analysis of H2Aub1 and H3K27me3 levels at specific gene regions in the different *Atring1* mutants as compared to the wild-type control Col-0.

(**A**) Gene structures of *KNAT2*, *CUC1* and *CUC2* are schematically represented by narrow boxes for untranslated regions, wide boxes for exons, black lines for introns, arrow for transcription start site. DNA regions analyzed by ChIP assay are indicated by the grey lines beneath the gene structure.

(**B-C**) H2Aub1 enrichment at *KNAT2*, *CUC1* and *CUC2* (**B**) and H3K27me3 enrichment at *CUC1* and *CUC2* (**C**) were analyzed by ChIP in twelve-day-old seedlings grown under long-day (LD) conditions. Data was normalized to the input and shown as mean ± SD. Similar results were obtained in three independent biological repeats.

II.2.4. Effects of different *Atring1* mutants on seed germination and regulation of seed developmental genes

II.2.4.1. Seed germination

Seed development and germination are key developmental programs in plant life cycle, which means the transformation from a seed to a seedling. Several key genes have been characterized to mediate the seed maturation, dormancy and germination, such as *ABI3*, *DOG1* (Raz et al. 2001; Jia et al. 2014; Chiang et al. 2011; Kendall et al. 2011; Nakabayashi et al. 2012). Previous research has reported the involvement of PRC2 in silencing the seed development and germination related genes by catalyzing H3K27me3 (Mozgova et al. 2015). The PRC1 components AtBMI1 and EMF1 were also implicated in repressing the seed developmental genes in a H2Aub1-dependent or H2Aub1-independent manner (Wang and Shen 2018). However, whether AtRING1 participate in regulating the seed development and germination is far from clear.

In the germination test, wild type Col-0, single mutant *Atring1a*, *Atring1b* and double mutant *Atring1ab* and *mut4* showed normal seed germination phenotype under standard growth conditions, whereas *mut2* and *mut3* displayed slightly delayed seed germination (**Figure II-12**). Compared to *mut2* and *mut3*, the germination progress of *mut1* was

more severely impaired. The germination defects in *mut1* suggest that AtRING1 participates in the germination regulation. The germination progress difference observed between *mut2*, *mut3* and *mut1* indicates the N-terminal portion containing RING domain is mainly responsible for normal germination (**Figure II-12**).

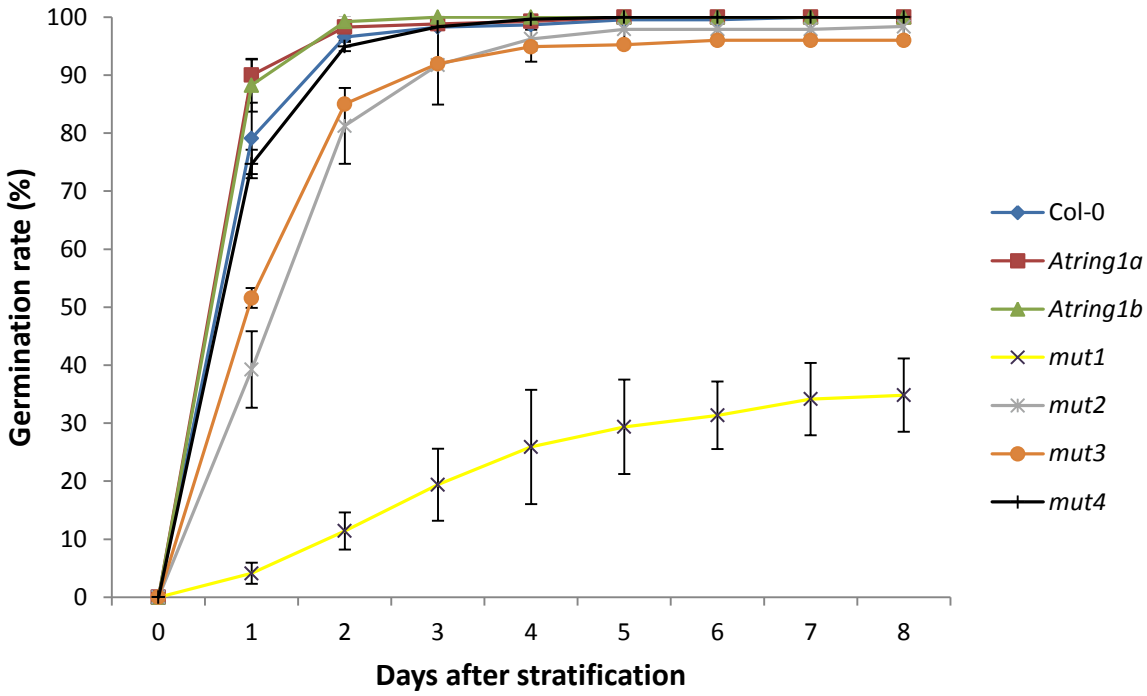

Figure II-12. Analysis of seed germination of the different *Atring1* mutants as compared to the wild-type control Col-0.

The percentage of germinated seeds (radicle emergence) of Col-0 and *Atring1* mutants were scored on 1/2 strength Murashige and Skoog (1/2 MS) for 8 days after stratification (DAS). Data was shown as mean ± SD. Similar results were obtained in three independent biological repeats. At least 80 seeds were sown on each plate.

II.2.4.2. Expression of seed developmental genes

Next, I investigated the expression of four seed development genes (*ABI3*, *DOG1*, *CRU1* and *CRU3*) using 12-day-old seedlings (**Figure II-13A**). *mut3* was selected as the representative line of the RAWUL disrupted plants. As expected, all these four genes displayed largely increased in *mut1* and slightly higher expression level in *mut3* as

compared to Col, and there was no difference between *mut4*, *Atring1b* and Col-0. The same tendency of the genes expression appeared at 72 hours after stratification (HAS) for *ABI3*, or even as earlier as 24 HAS for *DOG1*, *CRU1* and *CRU3* (**Figure II-13B**). It demonstrates that AtRING1 represses seed developmental genes during germination and early seedling growth, and C terminal part of AtRING1A containing RAWUL domain is involved in the repression.

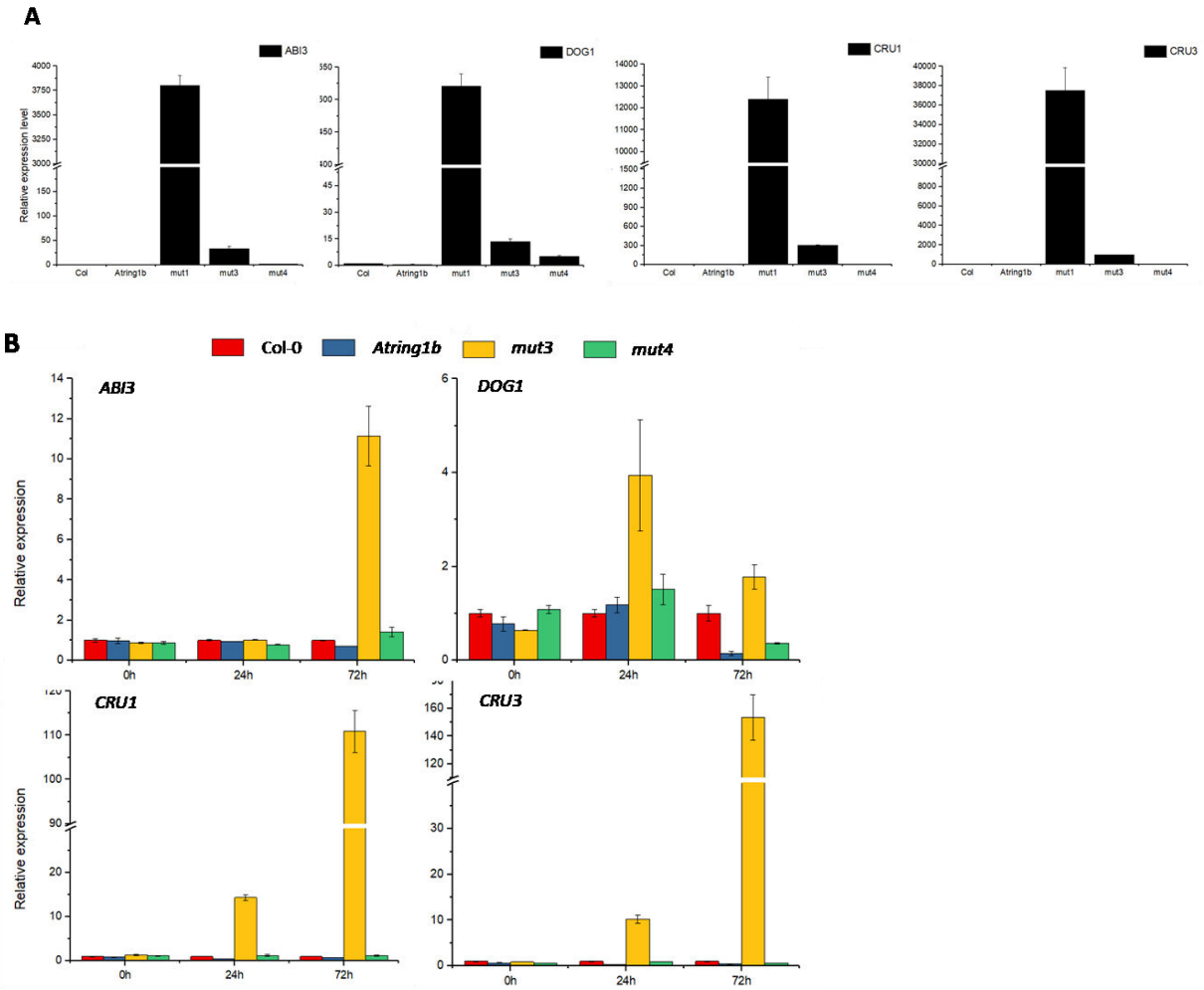

Figure II-13. Quantitative RT-PCR analysis of seed developmental gene expression in the different *Atring1* mutants as compared to the wild-type control Col-0.

Relative mRNA levels of *ABI3*, *DOG1*, *CRU1*, *CRU3* in twelve-day-old seedlings (**A**), seeds or seedlings at 0h, 24h, 72h after stratification (**B**). The expression levels were normalized to reference genes *GAPDH*, *EXP* and *Tip41* and relative to wild type. Data was shown as mean ± SD. Similar results were obtained in three independent biological repeats.

II.2.4.3. Histone modifications at seed developmental gene

To examine whether the gene repressing function of AtRING1 in seed germination is realized through affecting histone modification, I measured the H2Aub1 and H3K27me3 at the *ABI3* and *DOG1* loci by ChIP assay with 12-day-old seedlings (**Figure II-14B, 14C**). Compared to Col-0, the enrichment level of both the H2Aub1 and H3K27me3 mark at ABI3 and DOG1 in *Atbmi1*, *Atring1* and *mut3* were dramatically reduced, while *Atring1b* and *mut4* showed no substantial change (**Figure II-14B, 14C**). It indicates that the repression of *ABI3* and *DOG1* are related to the incorporation of H2Aub1 and H3K27me3, and the establishment of the repressive histone mark involves AtBMI1, AtRING1 and even the C terminal part of AtRING1.

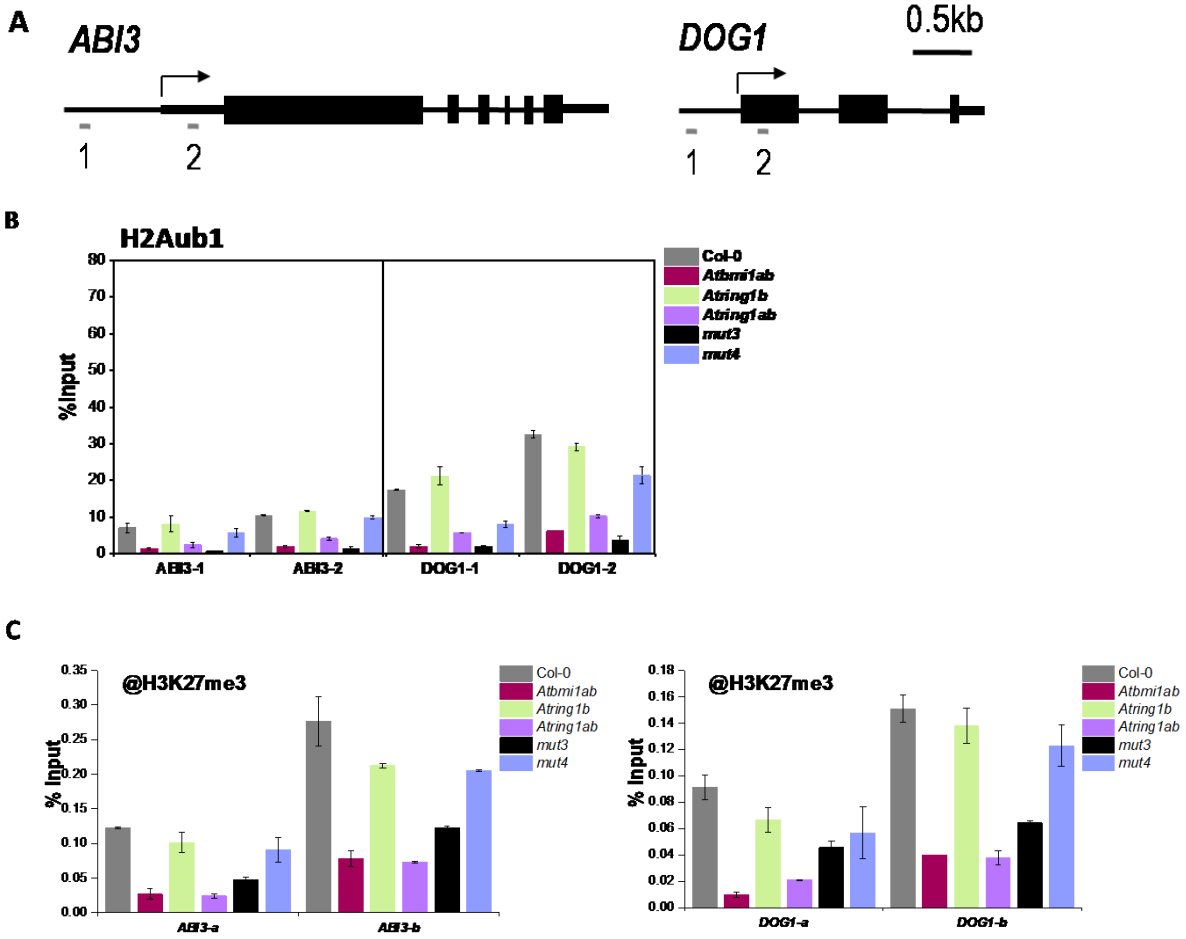

Figure II-14. ChIP analysis of H2Aub1 and H3K27me3 levels at specific regions of seed developmental genes.

(**A**) Gene structures of *ABI3* and *DOG1* are schematically represented by narrow boxes for untranslated regions, wide boxes for exons, black lines for introns, arrow for transcription start site. DNA regions analyzed by ChIP assay are indicated by the grey lines beneath the gene structure. Scale bar represents 0.5kb.

(**B-C**) ChIP analyses of H2Aub1 (**B**) and H3K27me3 (**C**) enrichment at *ABI3* and *DOG1* in wild type Col-0 and *Atring1* mutants. Chromatin was prepared from twelve-day-old seedlings grown under LD condition. Data was normalized to input and shown as mean ±SD. Similar results were obtained in three independent biological repeats.

II.2.5. Effects of different *Atring1* mutants on plant vegetative transition and expression of key regulatory gene

II.2.5.1. Vegetative transition

During the transition from juvenile to adult phase, plants undergo phenotypic changes in a series of indexes, such as the leaf morphology and the competence to flowering. To the best of our knowledge, both the miR156/157-SPL pathway and AGO-miR390-TAS3 pathway are involved in regulating the vegetative phase transition in Arabidopsis (Allen et al. 2005; Williams et al. 2005; Hunter et al. 2003; Hunter et al. 2006; Peragine et al. 2004; Adenot et al. 2006; Fahlgren et al. 2006; Wu et al. 2009). Both PRC2 and PRC1 core components are involved in repressing miR156 or SPL genes by influencing H3K27me3 enrichment (Lafos et al. 2011; Pico et al. 2015). In particularly, AtRING1 regulates *SPL* genes expression through depositing H2Aub1 mark (Li et al. 2017).

To investigate the effects of different mutations of AtRING1A on vegetative transition regulation, 20 plants of each line grown under short-day (SD) conditions were evaluated for the number of leaves without abaxial trichomes, which is the key trait of the juvenile leaves (**Figure II-15**). There was no difference among the number of leaves without trichomes in *mut4*, *Atring1b* and Col-0, indicating that the mutation in *mut4* doesn't

influence the vegetative transition. Consistent with the performance of *Atring1ab* in the previously published data (Li et al. 2017), *mut2* and *mut3* owned less juvenile leaves than that in Col-0. It suggested that the disruption of RAWUL domain in AtRING1A results in the precocious vegetative transition.

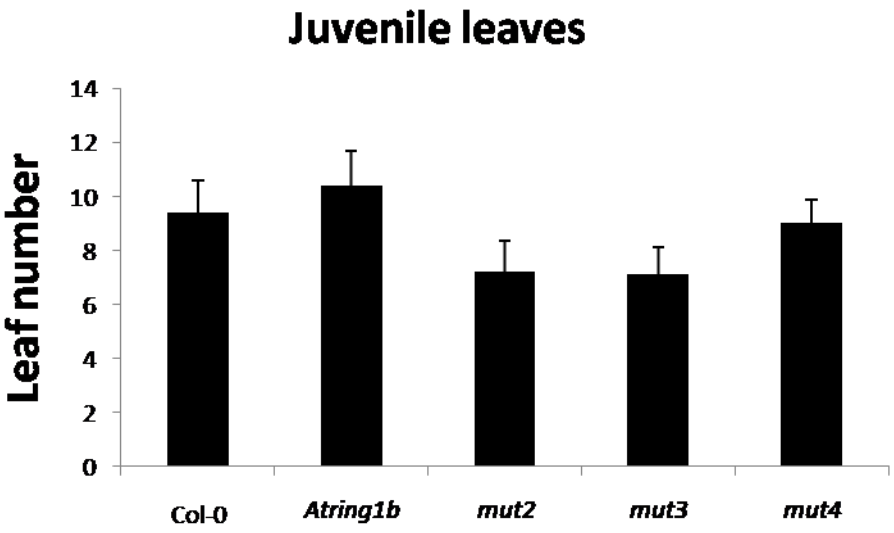

Figure II-15. Vegetative phase transition in different *Atring1* mutants and wild-type control Col-0.

The number of juvenile leaves in 30-day-old wild type and *Atring1* mutants under SDs. At least 15 plants were examined for the leaf number. Data was shown as mean ± SD.

II.2.5.2. Expression of vegetative transition related gene

The expression of *SPL3* was examined in 12-day-old *Atring1* mutants and Col-0 (**Figure II-16.A**). *mut4* and *Atring1b* showed no difference to that of Col-0. Surprisingly, the *SPL3* was downregulated in *mut1* and *mut3*, which is contradictory with the upregulated *SPL* family genes in 7-day-old *Atring1a-2Atring1b-3* (another T-DNA insertion loss-of-function AtRING1 mutant reported in 2017) grown under SD conditions (Li et al. 2017). Subsequently, I checked the *SPL3* expression in 12-day-old *Atring1ab* (described in (Xu and Shen 2008)) and it showed to be decreased, which is consistent with increased miR156 level in 14-day-old *Atring1ab* grown under LD condition (Pico et al.

2015) (**Figure II-16.B**). It suggests that AtRING1 might play different roles in regulating vegetative transition of different stage during plant growth. Furthermore, RAWUL domain is crucial for the function of AtRING1 in regulating *SPL* genes. More unknown mechanism might be involved in regulating the vegetative transition.

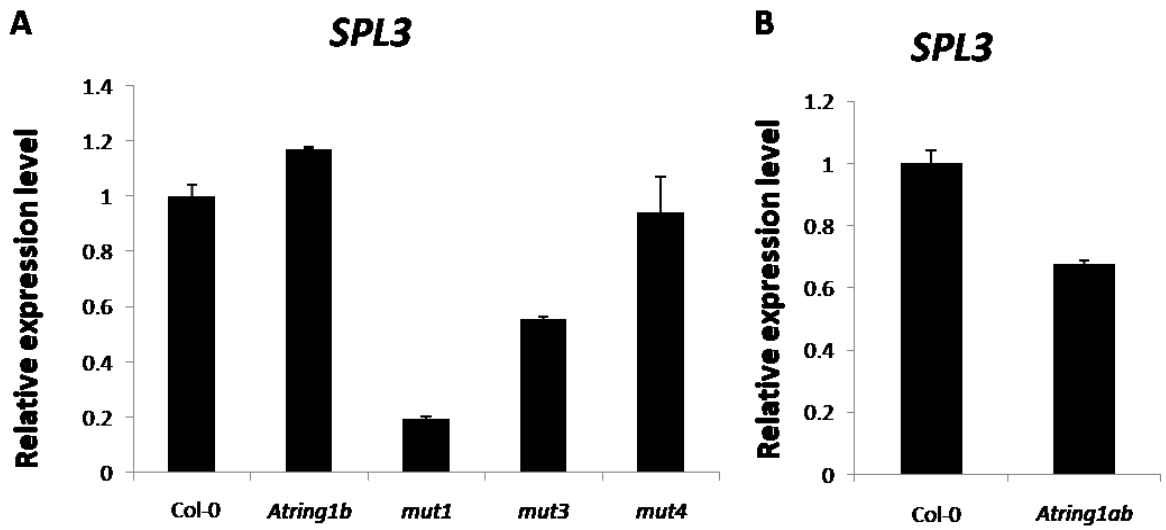

Figure II-16. Quantitative RT-PCR analysis of *SPL3* expression in different *Atring1* mutants as compared to wild-type control Col-0.

Quantitative real-time PCR analysis of *SPL3* in twelve-day-old seedlings grown under LDs. The expression levels were normalized to reference genes *GAPDH*, *EXP* and *Tip41* and relative to wild type. Data was shown as mean ± SD. Similar results were obtained in three independent biological repeats.

II.2.6. Effects of different *Atring1* mutants on plant flowering time and expression of key regulatory genes

II.2.6.1. Floral transition

Flowering is an important agronomic trait in crop requiring coordinated regulation to ensure the plants competitive to high seed production. Five major floral pathways are involved in the flowering regulation, which converges to several key floral regulators (Bloomer and Dean 2017). The regulation of these floral integrators involves multiple

chromatin modifications. EMF-PRC2, VRN-PRC2, PHD-PRC2, AtBMI1 are involved in repression *FLC* in different flowering regulatory pathways (Deng et al. 2018; Sharif and Koseki 2017; Yang et al. 2017a); EMF1 collaborates with PRC2 to silencing *FT*;

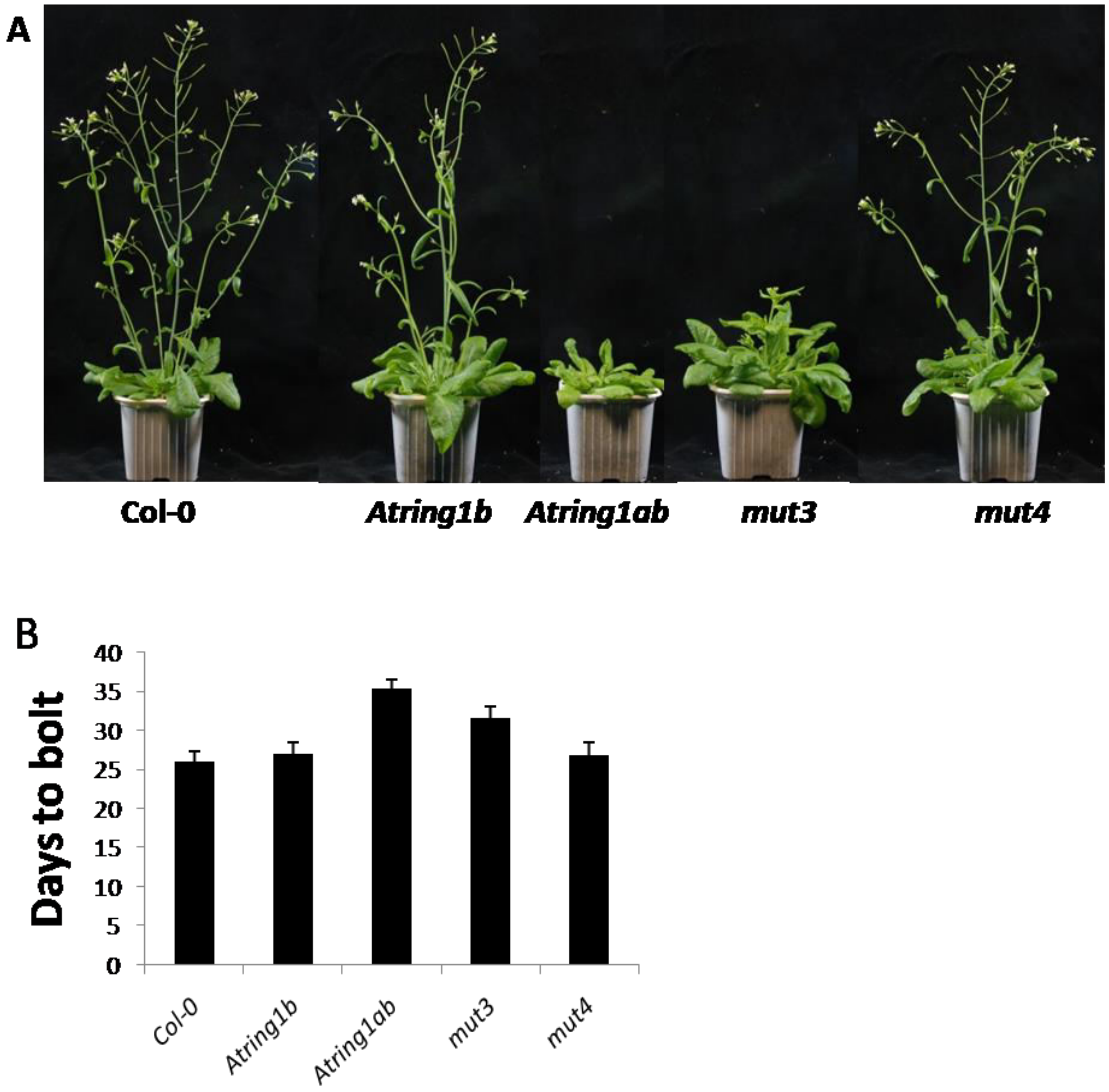

Figure II-17. The flowering phenotype of the wild-type Col-0 and different *Atring1* mutants.

Flowering time phenotype (**A**) and the measurement of the days to bolting (**B**) in Col-0 and *Atring1* mutants grown under LD conditions. At least 15 plants for each genotype were measured. Data was shown as mean ± SD.

AtRING1A, AtBMI1A/B and CLF-PRC2 repress *MAF4* and *MAF5* by affecting H3K27me3 deposition (Shen et al. 2014a; Pico et al. 2015). However, whether H2Aub1

mark is established on the floral regulators remain to be investigated.

Loss of function of AtRING1A and the double mutants *Atring1ab* shows late flowering (Shen et al. 2014a; Li et al. 2017). In terms of the indexes of days to bolting when floral shoot is about 0.5 cm under LD condition, *Atring1b* and *mut4* displayed normal flowering time but *mut3* showed comparable late-flowering phenotype to Col-0 but earlier than *Atring1ab* (**Figure II-17A, 12B**). It suggests that the disruption of the C terminal of AtRING1A interferes with the function of AtRING1A in regulating flowering time.

II.2.6.2. Expression of flowering-related genes

To identify the reason for the late flowering, I examined the temporal expression of several important flowering time regulators in 12-day-old seedlings of Col-0, *Atring1b*, *mut1*, *mut3* and *mut4* (**Figure II-18**). I found that there were slightly increase for the *FLC* expression in both *mut3* and *mut4* compared with Col, and *mut1* showed strongly increased expression. For *MAF4* and *MAF5*, *mut4* also showed mildly altered, whereas *mut1* and *mut3* had strongly raised expression. The expression level of both *FT* and *SOC1* were drastically reduced in *mut3*, and *mut1* had more severe impaired expression, while the decrease in *mut4* is tiny. *Atring1b* showed no misregulation. It suggests that AtRING1 is involved in the regulation of *FLC*, *MAF4* and *MAF5*, which in turn to influence the expression of *FT* and *SOC1*. Furthermore, the loss of RAWUL in AtRING1A retains partial activity of AtRING1A in regulating *FLC*, *FT* and *SOC1* but exhibits similarly to the totally loss-of–function AtRING1A (*mut1*) in *MAF4* and *MAF5* regulation. The L429 in AtRING1A play a marginal role in the repression role of AtRING1A.

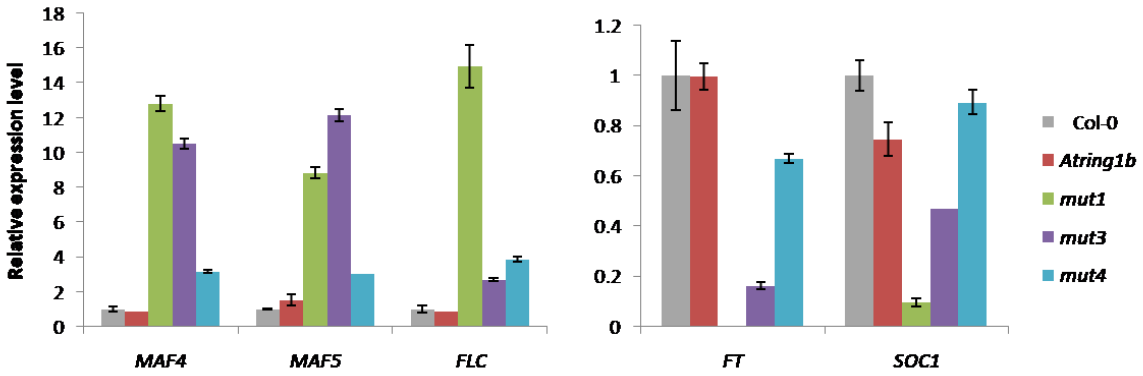

Figure II-18. Quantitative RT-PCR analysis of flowering related genes expression in different *Atring1* mutants as compared to wild-type Col-0.

Quantitative real-time PCR analysis of *MAF4*, *MAF5*, *FLC*, *FT*, *SOC1* in twelve-day-old seedlings. The expression levels were normalized to reference genes *GAPDH*, *EXP* and *Tip41* and relative to wild type. Data was shown as mean±SD. Similar results were obtained in three independent biological repeats.

II.2.6.3. Histone modification at flowering-related genes

To investigate further how AtRING1 regulates the expression of *MAF4*, *MAF5* and *FLC*, I firstly examined the H3K27me3 levels at these loci in 12-day-old wild type, *Atbmi1ab*, *Atring1ab*, *mut3* and *mut4* by ChIP assay (**Figure II-19C**). I found that the levels of H3K27me3 at *MAF4*, *MAF5* and *FLC* loci were decreased in *Atring1ab*, indicating that AtRING1 is involved in depositing H3K27me3 mark at *MAF4*, *MAF5* and *FLC*. It is noteworthy that, in *mut3*, the level of H3K27me3 at *FLC* was not altered but dramatically decreased at *MAF4* and *MAF5*. It indicates the loss of RAWUL domain in AtRING1A affects the H3K27me3 deposition at *MAF4* and *MAF5* loci but not at *FLC* loci. In addition, the mutation in *mut4* didn't significantly change the level of H3K27me3 at these loci. Since AtRING1 and AtBMI1 are involved in the H2Aub1 deposition, I investigated the level of H2Aub1 at these 3 genes (**Figure II-19B**). I found that the level of this mark at *MAF4*, *MAF5* and *FLC* were dramatically reduced in *Atbmi1ab*, *Atring1ab* and *mut3* with the exception of *mut4* that showed only slight decrease.

The mildly decreased level of H2Aub1 and H3K27me3 at *FLC*, *MAF4* and *MAF5* in *mut4* was in agreement with the only slightly increased gene expression levels. Similarly, the drastically decreased deposition of both H2Aub1 and H3K27me3 at *MAF4* and

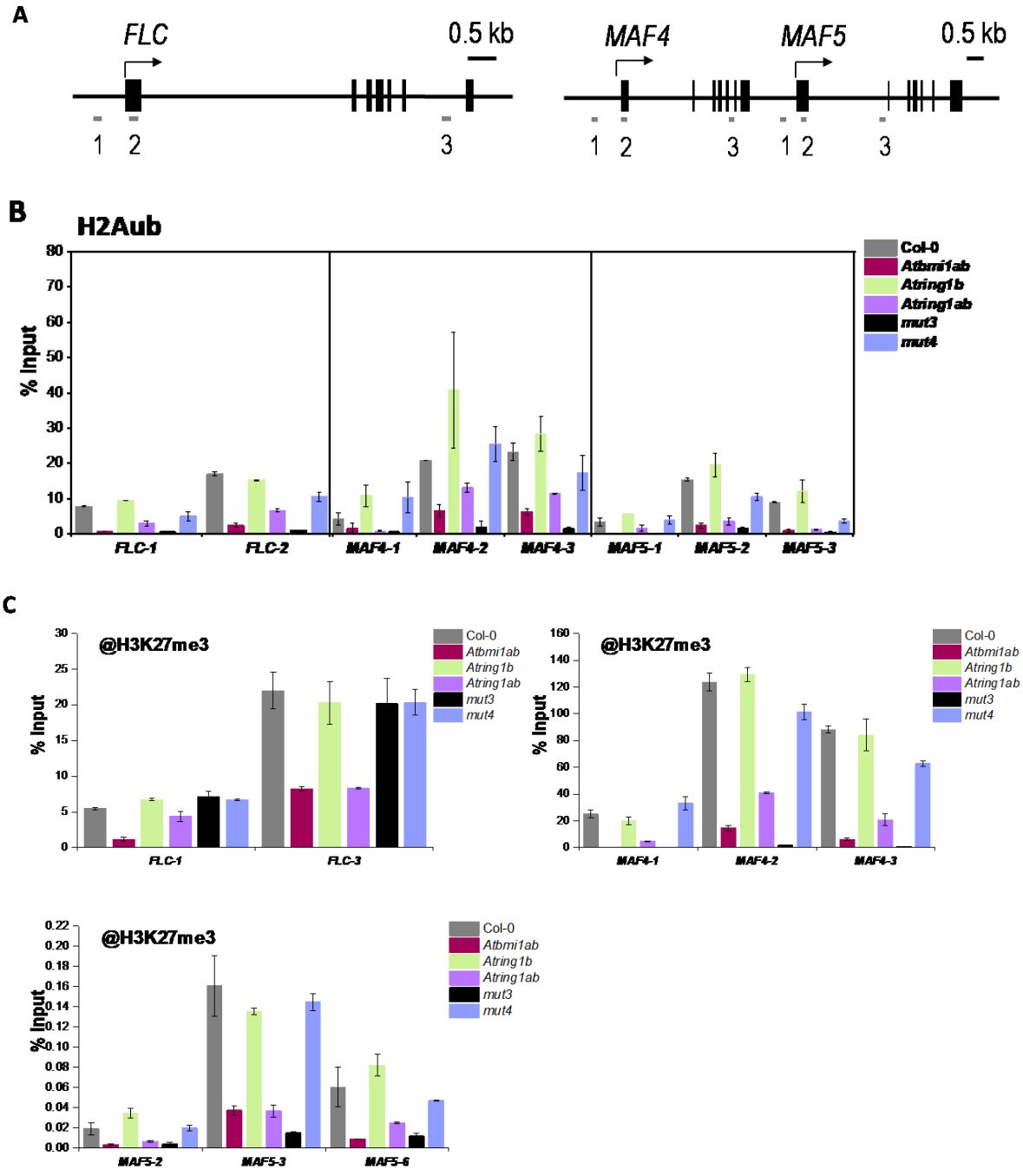

Figure II-19. ChIP analysis of H2Aub1 and H3K27me3 levels at specific regions of flowering genes in different *Atring1* mutants and wild type Col-0.

(**A**) Gene structures of *FLC*, *MAF4* and *MAF5* are schematically represented by wide

boxes for exons, black lines for promoters and introns, arrow for transcription start site. DNA regions analyzed by ChIP assay are indicated by the grey lines beneath the gene structure. Scale bar represents 0.5kb.

(**B-C**) ChIP analyses of H2Aub1 (**B**) and H3K27me3 (**C**) enrichment at *FLC*, *MAF4* and *MAF5* in wild type Col-0 and *Atring1* mutants. Chromatin was prepared from twelve-day-old seedlings grown under LD condition. Data was normalized to input and shown as mean ±SD. Similar results were obtained in three independent biological repeats.

MAF5 in *mut3* is consistent with largely increased expression of *MAF4* and *MAF5*. In summary, AtBMI1 and AtRING1 are pivotal for both the H2Aub1 and H3K27me3 mark on the *FLC*, *MAF4* and *MAF5*. It challenges again the hierarchical recruitment model of PRC1 and PRC2 to chromatin. Furthermore, the RAWUL domain of AtRING1A is required for the H2Aub1 marking *FLC*, *MAF4* and *MAF5* and H3K27me3 marking *MAF4* and *MAF5*, but not *FLC*.

II.3. Discussion

II.3.1. RAWUL domain is involved in multiple plant development programs

The PRC1 RING finger proteins are characterized by the conserved N-terminal RING domain and C-terminal RAWUL domain. AtRING1, the RING finger protein in Arabidopsis, plays an essential role in regulating plant growth and development, such as cell differentiation (Xu and Shen 2008; Chen et al. 2010), germination (Molitor and Shen 2013), vegetative transition and floral timing (Li et al. 2017; Shen et al. 2014a). All the previous studies of AtRING1 function are based on the mutants created by T-DNA insertions (Xu and Shen 2008), which make the insight about protein domain function impossible. In my study, CRISPR/Cas9 was used to mutagenize specific regions of AtRING1.

The *mut1* mutant generated from the sgRNA1 construction has a stop codon upstream of RING-domain of AtRING1A and exhibited callus-like phenotype, which is similar to the phenotype of *Atbmi1abc* and to that of the PRC2 mutants *clf/swn* and *emf2/vrn2* (Bouyer et al. 2011; Chanvivattana et al. 2004; Chen et al. 2010; Bratzel et al. 2010). It represents the strongest loss-of-function mutant allele of *Atring1a*, and its phenotype further confirms key functions of PcGs in cell differentiation.

The *mut2* or *mut3* mutant each has a premature stop codon preceding RAWUL-domain. Phenotype analyses of these mutants showed that they display similar and mild growth defects including inhibition of leaf width expansion; increased variability of seedlings phenotype, flower organ number and increased seed production; precocious vegetative transition. These mutants have capacity to produce truncated AtRING1 proteins lacking the C-terminal RAWUL, pointing to a function of the RAWUL domain during plant

growth and development.

II.3.2. RAWUL domain is important for the E3 ligase activity of PRC1 *in vivo*

In animals, paired RING finger motifs formed by RING1A/B and PCGFs function through conferring the E3 ligase activity (Wang et al. 2004). In contrast, AtRING1A/B and AtBMI1A/B/C in Arabidopsis showed E3 ligase activity *in vitro* individually, while interactions between AtRING1A/B and AtBMI1A/B/C were detected (Xu and Shen 2008; Bratzel et al. 2010; Chen et al. 2010; Wang and Shen 2018). How the E3 ligase module forms in Arabidopsis remains unclear. In my further experiments of the immunobloting analysis on the nuclear protein and histone extracts with the antibody anti-H2Aub1, *mut1*, *mut2*/3/4 showed totally undetected or significantly decreased level of H2Aub1, respectively. Therefore, the loss of C terminal containing RAWUL domain impaired but not totally abolish the function of AtRING1 H2A monoubiquitination.

In animal, the RAWUL domain is mainly reported as binding platforms for the other PRC1 components. The binding specificity of RAWUL contributes to the mammalian functionally different PRC1s assembly (Wang et al. 2010; Blackledge et al. 2015; Junco et al. 2013; Alkema et al. 1997; Gunster et al. 1997; Bezsonova et al. 2009). In addition, RAWUL is also reported to serve as the platform for interaction between RING finger protein and with other proteins, such as KDM2B, PHCs, to mediate H2Aub1 (Wong et al. 2016; Gray et al. 2016). Therefore, it is the hypothesis that H2Aub1 in Arabidopsis is realized by multiple-protein complex, which is assembled by RAWUL (**Figure II-20.A**). Losing RAWUL domain of AtRING1A would largely impair the E3 ligase activity of the module (**Figure II-20.B**). How RAWUL domain of AtRING1A function in H2Aub1 in Arabidopsis and more interacting factors need to be identified in the future.

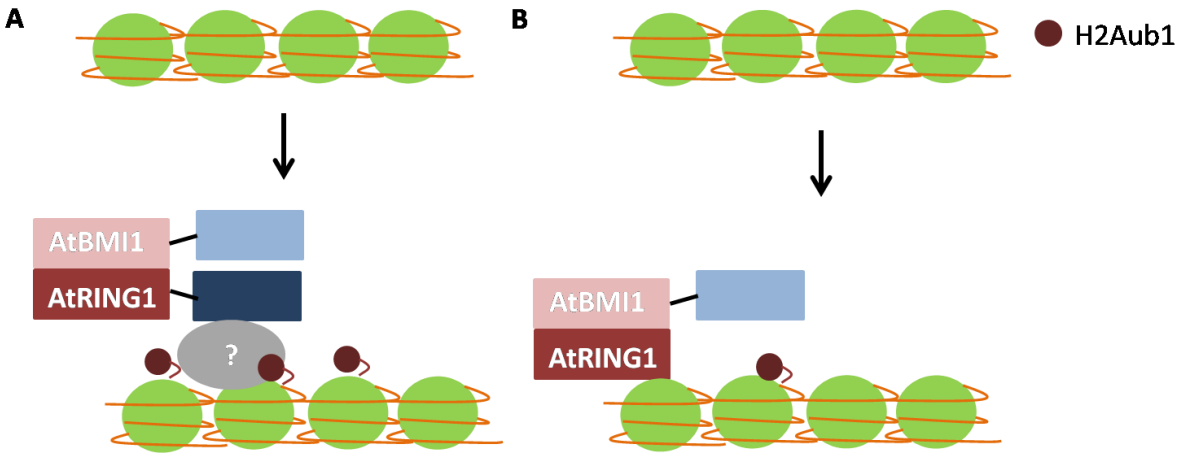

Figure II-20. Hypothesis of a RAWUL-domain function in H2Aub1 deposition.

(**A**) AtBMI1 and AtRING1 interact with each other by their RING domain (depicted with pink and red rectangle, respectively). The paired RING finger proteins interact with some unknown protein (grey circle with question mark inside) by RAWUL (dark blue rectangle) of AtRING1A to form the E3 ligase module in Arabidopsis. Red circle represents H2Aub1 mark.

(**B**) Losing RAWUL domain of AtRING1 severely impairs the E3 ligase activity of the module.

II.3.3. Function of AtRING1 in vegetative transition

The vegetative transition links juvenile vegetative phase to the adult vegetative phase. miR156/157-SPL pathway is the primary regulator for the transition (Wu et al. 2009). As the seedlings grow, the expression of miR156/157 decreases gradually, while *SPL* genes show the opposite trend (Wu and Poethig 2006; Wang et al. 2009) (**Figure I-8**).

PRC1 core components are involved in regulating the juvenile-to-adult transition. With the 10-day-old seedlings grown under LDs, AtBMI1 was proved to repress *MIR156* by catalyzing the H2Aub1 and H3K27me3 mark at the chromatin of *MIR156A/MIR156C* so as to prolong juvenile phase (Pico et al. 2015). Conversely, in 7-day-old seedlings grown under SDs, AtRING1-PRC1 is reported to establish H2Aub1 at *SPL3/9/10* to shorten juvenile phase (Li et al. 2017). The opposite function of the PRC1 components in regulating vegetative transition is really interesting, which requires further investigation.

In our study, *Atring1* and *mut3* showed earlier vegetative transition under both LDs and SDs. The transcription analysis of *SPL3* was performed in the 12-day-old *mut1*, *mut3*, *Atring1*, *Atbmi1ab* and Col-0 grown under LD conditions. In all mutants of *Atring1*, *SPL3* was found decreased, which is in line with the increased miR156 in 14-day-old *Atring1ab*. However, it is in contrast to the increased transcription activity of *SPL3* in 7-day-old *Atring1* under SDs. Therefore, I hypothesized that the regulation of *SPL* could be divided into two stages (**Figure II-21**). In young seedlings, such as 7 day old, the repression of *SPL* genes is mainly performed by H2Aub1 deposited by AtRING1, which ensure the low expression of *SPL* genes. The identical transcription repression of *SPL* genes and the increased miR156 in both *Atring1* and *Atbmi1* suggest that AtRING1 and AtBMI1 might coordinate to repress miR156 and in turn to increase the expression of

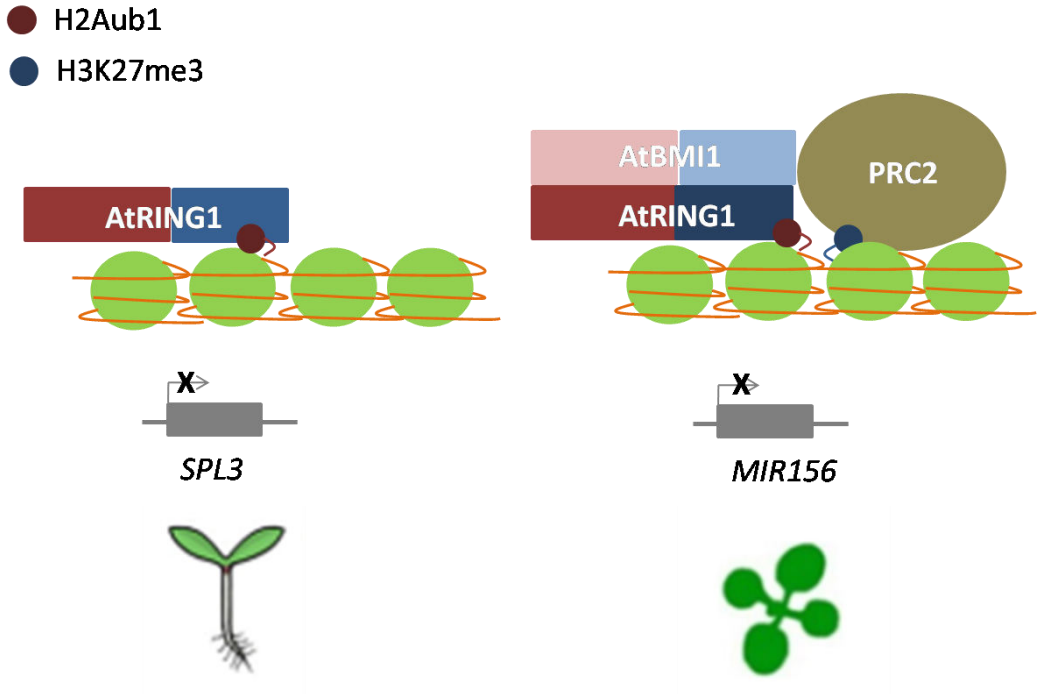

Figure II-21. Hypothesis of a PcG function in vegetative transition regulation.

The RING domains of AtBMI1 and AtRING1 are represented by pink and red rectangle, while the RAWUL domains are depicted by light and dark rectangle, respectively. The red and blue circles represent H2Aub1 and H3K27me3 mark, respectively. The cross above the gene structure means transcriptional repression.

SPL3 in older seedlings, such as older than 10 days under LDs. Therefore, as the seedlings grow, the repression of *SPL*s is changed to be conducted by miR156, which is mediated by H3K27me3 and the H2Aub1 catalyzed by AtRING1, AtBMI1 and PRC2. This indirect repression make sure the continuously and slowly accumulation of *SPL*s. More evidence should be provided in the future to check the hypothesized model.

II.3.4. Function of AtRING1 in cell differentiation

PcG proteins have been shown to play critical roles in cell differentiation and maintaining cell identity. The loss-of-function mutants of AtRING1, AtBMI1 showed derepression of embryonic traits. Similarly, the PRC2 mutants *clf*/*swn* and *emf*2/*vrn2* grow to be embryo-like structure. During floral development, *Atring1* and *Atbmi1ab* also showed perturbation in determining cell fate (Bouyer et al. 2011; Chanvivattana et al. 2004; Chen et al. 2010; Bratzel et al. 2010). Class I *KNOX* genes and *CUC* genes play important roles in determining cell fate and establishing organ boundaries.

The PRC2 mediated H3K27me3 was detected at the Class I *KNOX* genes (Katz et al. 2004; Schubert et al. 2006; Xu and Shen 2008), while the level of H3K27me3 at Class I *KNOX* genes is not affected by loss of AtRING1 (Xu and Shen 2008). The plants with totally abolished AtRING1 (*mut1*) showed increased expression of Class I *KNOX* and *CUC* genes, and the plants with RAWUL domain impaired (*mut3*) showed mild increase at *KNAT2*, *CUC1*, *CUC2* but not at *STM*, *KNAT6* and *CUC3*, which indicates that AtRING1 proteins are required for the Class I *KNOX* and *CUC* repression and RAWUL is involved but only in the repression of part of these genes: *KNAT2*, *CUC1*, *CUC2*. The enrichment of H2Aub1 at *KNAT2*, *CUC1*, *CUC2* in *Atring1*, *mut3* and *Atbmi1ab* dramatically decreased, which suggest that AtRING1 and AtBMI1 are required for the H2Aub1 marking at *KNAT2*, *CUC1*, *CUC2*, and RAWUL domain is important for H2Aub1 deposition. Further, although AtRING1 does not participate in establishing H3K27me3 at Class I *KNOX* genes, the H3K27me at *CUC1* and *CUC2* are affected by

AtRING1 and AtBMI1. Notably, RAWUL domain is crucial for the H3K27me3 at *CUC1* but not at *CUC2*.

II.3.5. Function of AtRING1 in germination

PcG proteins play important roles in silencing the seed developmental genes to regulate germination and postembryonic development (Mozgova et al. 2015; Wang and Shen 2018). Two related model were reported before. In one case, PRC1 RING finger protein AtRING1A/B and AtBMI1A/B were recruited by AL proteins, the reader of the active marker H3K4me3, to seed developmental genes, such as *ABI3* and *DOG1*, which subsequently recruit PRC2 to deposit H3K27me3 either by the interaction between AtRING1A with CLF or by LHP1 (Molitor and Shen 2013). In the other model, the VAL-AtBMI1 establishes H2Aub1 at seed maturation genes to initiate the repression, which is maintained by H3K27me3 mediated by PRC2. Both of the models placed the PRC1 upstream of PRC2 (Yang et al. 2013a). However, although AtRING1 was referred in the first model, how AtRING1 contributes to the gene repression during germination is unknown.

In my study, the slightly retard germination of *mut2* and *mut3* and the enhanced delayed germination phenotype of *mut1* firstly suggest that AtRING1 participates in promoting seed germination and RAWUL domain is also involved in it. The regulation is further evidenced by the derepression of *ABI3*, *DOG1*, *CRU1* and *CRU3* in *mut3* and more severe misregulation in *mut1*, which also accounts for the discrepancy of the germination rate between *mut1* and *mut3*. Furthermore, the ChIP assay with the 12-day-old seedlings showed that the enrichment of both H2Aub1 and H3K27me3 mark at *ABI3* and *DOG1* significantly were reduced in *Atbmi1ab*, *Atring1ab* and *mut3* compared to that of Col-0, placing PRC1 prior to PRC2, which provides further evidence for the published models.

II.3.6. Function of AtRING1 in flowering

The PcG proteins play key roles in repressing the floral integrators. H3K27me3 deposited by PRC2 was detected at the flowering regulators, such as *FLC*, *MAF4*, *MAF5*, *FT* (Mozgova et al. 2015). Consistently, the PRC1 components were reported to participate in regulating flowering. The overexpression line of AtBMI1C showed earlier flowering with the unchanged H3K27me3 enrichment at *FLC*. The EMF1c-PRC1 complex targeted directly to *FT* to silencing the expression (Li et al. 2011). The AtRING1A functions additively with CLF-PRC2 in regulating flowering by repressing *MAF4* and *MAF5* through establishing the H3K27me3 (Shen et al. 2014a). The distribution of H2Aub1 at the flowering genes mediated by AtRING1 is still unclear.

Since the observation that *Atring1* and *mut3* showed late flowering based on the index of days to bolting confirm the role of AtRING1 in floral transition, the expression level of key flowering related genes were detected in *mut1*, *mut3*, *mut4* and Col. The *mut1* and *mut3* showed derepression of *MAF4*, *MAF5* and *FLC*, which caused the repression of downstream activators genes *FT* and *SOC1*. The detected misregulation in *FLC*, *FT* and *SOC1* in *mut1* is more severe than that in *mut3*, indication the partial role of RAWUL domain in these genes regulation. However, the expression levels of *MAF4* and *MAF5* in *mut1* and *mut3* are similar, which suggests the important role of RAWUL in regulating *MAF4* and *MAF5*. Furthermore, it indicates the different mechanism of AtRING1 in promoting flowering through repressing different floral repressors.

To investigate the regulating mechanism of AtRING1 in silencing the floral repressors, the H2Aub1 and H3K27me3 enrichment on *FLC*, *MAF4* and *MAF5* in 12-day-old *Atbmi1ab*, *Atring1*, *mut3*, *mut4* and Col-0 was detected. In wild type, three analyzed loci (*FLC*, *MAF4* and *MAF5*) were enriched in H2Aub1 and H3K27me3. However, both of the H2Aub1 and H3K27me3 at three loci in *Atbmi1ab*, *Atring1* and *mut3* except the H3K27me3 at *FLC* in *mut3* dramatically decreased. Furthermore, EMF1 was previously

reported to repress *FLC*, *MAF4* and *MAF5* (Shen et al. 2014a; Pico et al. 2015). Thus, AtRING1 and AtBMI1 are hypothesized to function with EMF1, all of which form PRC1 to silence *FLC*, *MAF4* and *MAF5* by regulating the enrichment of H2Aub1 and H3K27me3. Furthermore, the RAWUL domain of AtRING1A is important for the modifications. More evidence should be provided for this hypothesized silencing mechanism.

Chapter III

RESULTS – Part II

Arabidopsis ZUOTIN RELATED FACTOR1 Chromatin Regulators Are Required for Proper Embryonic and Post-Embryonic Root Development

Donghong Chen, Qiannan Wang, Jing Feng, Ying Ruan, Wen-Hui Shen

III.1. Introduction

The Arabidopsis root has a well-organized structure with simple longitudinal organization and few well-defined cell lineages, providing an excellent model system to investigate asymmetric cell division and cell fate determinacy. Root development relies on the RAM, which not only maintains stem cell self-renewal but also provides different types of daughter cells, which subsequently undergo expansion to form elongation zone and then differentiation to form root hair zone (maturation zone). The balance between cell division and cell differentiation determines RAM size. The RAM consists of the proliferation domain with high dividing-cell content and the transition domain with low dividing-cell content along the longitudinal axis (Ivanov and Dubrovsky 2013). In Arabidopsis root proliferation domain, four types of initial stem cells surrounding approximately four quiescent center (QC) cells (Scheres et al. 1994), together constitute the stem cell niche (SCN). At the distal region, columella cells are generated from anticlinal divisions of thecolumella stem cell initials, and epidermal cell and lateral root cap are derived from sequentially anticlinal and periclinal divisions of their common epidermal/lateral root cap initials. At the proximal region, cortex and endodermis are derived from the periclinal division of their common ground tissue initials, and stele is formed from the stele stem cell initials. Within the root SCN, QC cells with slowly mitotic activity provide a reservoir for maintenance and replenishment of the surrounding initial stem cells, which exhibit high frequency of cell divisions (Heyman et al. 2013). These ascribed basic RAM cell pattern has been originally established during embryogenesis and maintained during postembryonic primary root growth (Dolan et al. 1993; Scheres et al. 1994).

Transcription factors and phytohormone auxin play critical roles in regulating RAM maintenance and stem cell homeostasis (Drisch and Stahl 2015). ETHYLENE RESPONSE FACTOR115 (ERF115) as a rate-limiting factor of QC divisions is

expressed in dividing QC cells, but it is usually restrained through proteolysis by the APC/$C^{CCS52A2}$ ubiquitin ligase in normal condition (Heyman et al. 2013). WUSCHEL-RELATED HOMEOBOX 5 (WOX5) as one of the most important root stem cell regulatory factor is specifically expressed in QC cells, necessary for the maintenance of undifferentiated state of surrounding stem cells (Sarkar et al. 2007). The CLAVATA3/EMBRYO SURROUNDING REGION (CLE) peptide CLE40 from columella cells is perceived *via* its receptors ARABIDOPSIS CRINKLY4 (ACR4) and CLAVATA1 (CLV1) to modulate the expression level and positioning of *WOX5* (CLE-WOX5 feedback loop), consequently regulating columella stem cell fates (Stahl et al. 2013; Stahl et al. 2009). It is known that auxin signal and distribution are widely involved in root patterning and polarity, SCN maintenance, and distal stem cell identity (Ding and Friml 2010; Friml et al. 2002; Sabatini et al. 1999). In fact, auxin signal and transcriptional factor usually function in a coordinate way. For instance, WOX5 action is balanced through the activity of indole-3-acetic acid 17 (IAA17) auxin response repressor, together forming WOX5–IAA17 feedback circuit, essential for the maintenance of auxin gradient in RAM and the auxin-mediated columella stem cell differentiation (Tian et al. 2014; Tian et al. 2013).

In Arabidopsis, PcG proteins play essential roles in root development. PRC2 components CLF, SWN, EMF2, VRN2, and FIE are involved in root meristem development and vascular cell proliferation in the maturation zone (Aichinger et al. 2011; de Lucas et al. 2016). CLF also associates with EMF2 to repress founder cell establishment during lateral root initiation associated with down-regulation of root auxin maxima (Gu et al. 2014). Additionally, PRC2 deficiency gives rise to mitotic reactivation and somatic embryogenesis in terminally differentiated root hairs (Ikeuchi et al. 2015). Consistently, the PRC1 subunits AtRING1A/B andAtBMI1A/B/C inhibit the formation of *pkl*-type root-phenotype displaying embryonic traits in primary root mainly through preventing an ectopic expression of embryonic master regulators (Chen

et al. 2010; Bratzel et al. 2010). The AtBMI1-interacting factors VAL1/2 also have a similar function (Hoppmann et al. 2011; Yang et al. 2013a).

The ZUOTIN-RELATED FACTOR (ZRF) proteins in eukaryotes constitute a novel clade of HSP40 family, which in general serves as co-chaperone of HSP70s to assist protein translation, folding, unfolding, translocation and degradation (Chen et al. 2014). However, the human ZRF1 was found to compete with and replace PRC1 RING1B from chromatin *via* competitively binding H2Aub1 mark, and to favor H2Aub1 removal *via* recruiting the specific deubiquitinase USP21, consequently leading to repressive-to-active chromatin state switch (Richly et al. 2010). In Arabidopsis, two ZRF1 homologs, AtZRF1A and AtZRF1B, showed redundant functions. AtZRF1B can bind ubiquitin *in vitro* and pull-down H2Aub1 and H2A from plant protein extracts (Feng et al. 2016), which is in agreement with the human ZRF1 acting as a H2Aub1 reader. The *AtZRF1A/B* genes display broad expression pattern, but with higher levels in the dividing cell-enriched tissues, *e.g.* meristem, floral bud and developing embryo. Loss-of-function of *AtZRF1A/B* causes pleiotropic abnormalities including delayed seed germination, plant dwarfism, formation of multiple ectopic meristems, and defects in flower development and gametophyte transmission as well as embryogenesis (Feng et al. 2016; Guzman-Lopez et al. 2016). The *atzrf1ab* (hereinafter referred as *atzrf1a;b*) mutant displays severely disrupted root developmental phenotype; yet, the underlying mechanism is far from clear.

III.2. Results

III.2.1. Loss of AtZRF1A/B causes primary root growth arrest

The *atzrf1a;b* double mutant displayed a drastically reduced root growth rate as compared to the wild-type (WT) control (**Figure III-1A**), leading to an extremely short-root phenotype, *e.g.* only ~2mm in length for the mutant roots as compared to ~20 mm for the WT roots at7 days after stratification (DAS). The mutant root displayed mature zone characteristically covered by root hairs that arise in close proximity to the root tip (**Figure III-1B**), indicating a drastic reduction of the meristem and elongation zone as well as developmentally advanced cell differentiation. The mutant primary roots ceased to grow as early as at 14 DAS (**Figure III-1D**), whereas the WT primary roots continuously grew and produced lateral roots (**Figure III-1C**). Later on, the mutant plants produced many adventitious roots (**Figure III-1E-1G**), which sustain plant growth in water and nutrition acquisition.

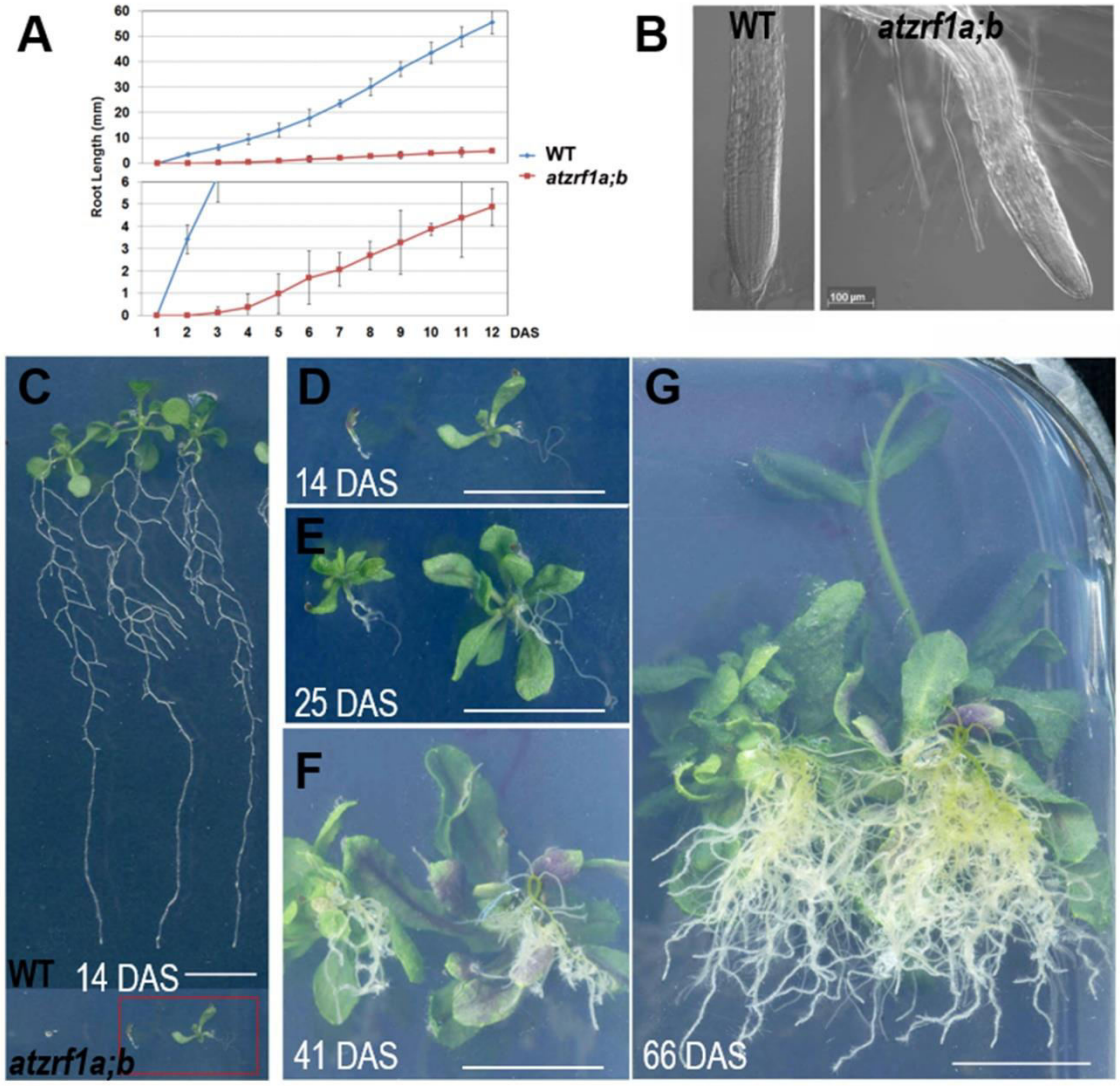

Figure III-1. Defective primary root development in the *atzrf1a;b* mutant.

(**A**) Comparison of primary root growth between the wild type (WT) and the *atzrf1a;b* mutant plants during 12 days after stratification (DAS). Histogram at the bottom shows a magnification of the Y-axe scale to better view the time course of the *atzrf1a;b* mutant growth.

(**B**) Representative images of the WT root tip and the *atzrf1a;b* mutant root tip at 5 DAS. (**C**) Representative WT seedlings showing continuous primary root growth and proliferation of lateral roots at 14 DAS.

(**D**-**G**) Representative seedlings of *atzrf1a;b* showing primary root growth arrest and adventitious root development at 14, 25, 41, 66 DAS.

Bars=50 µm in (**B**), and 1 cm in (**C**) to (**G**).

III.2.2. The *atzrf1a;b* mutant root exhibits cell division arrest and precocious cell differentiation

Hereinafter we focused on primary roots to investigate *AtZRF1A/B* function. Root growth largely depends on the RAM activity in which cells undergo mitotic cell division, cell expansion and cell differentiation. RAM size is relatively fixed in WT and constantly maintained by the dynamic balance between cell proliferation and cell differentiation. We found that RAM including proliferation domain and transition domain in *atzrf1a;b* is significantly shorter than that in the WT control (**Figure III-2A** and 2C). Sometimes, the cell arrangement was largely disorganized in *atzrf1a;b* RAM, so that it was hardly distinguished among different cell types (**Figure III-2C**). The root diameters in mutant became evidently narrow mainly due to thinner stele (**Figure III-2B** and 2C). Moreover, the average height-width ratio of the RAM cortical cells in mutant (1.3, n=30) was higher than that in WT (0.7, n=30). These results indicated that RAM cells in mutant were undergoing premature differentiation.

In order to investigate the underlying mechanism, we introgressed into the *atzrf1a;b* mutant the *CYCB1;1::Dbox-GUS* reporter which mark the cells at the G2-to-M transition of the cell cycle (Colon-Carmona et al. 1999). Compared to WT, the mutant RAM had reduced GUS staining (**Figure III-2D**), which indicates attenuated mitotic activity. On the other hand, we investigated the level of root endopolyploidy, which is associated with cell differentiation. In line with the reduced mitotic activity, endoreduplication index in *atzrf1a;b* was significantly increased, mainly due to the greatly elevated proportion of 8C and to a less degree of 16C cells (**Figure III-2E**), indicating an early mitosis-to-endocycle transition. Taken together, our data suggest that the decreased mitotic cell division capacity and the advanced onset of endoreduplication lead to reduced RAM size in the *atzrf1a;b* mutant.

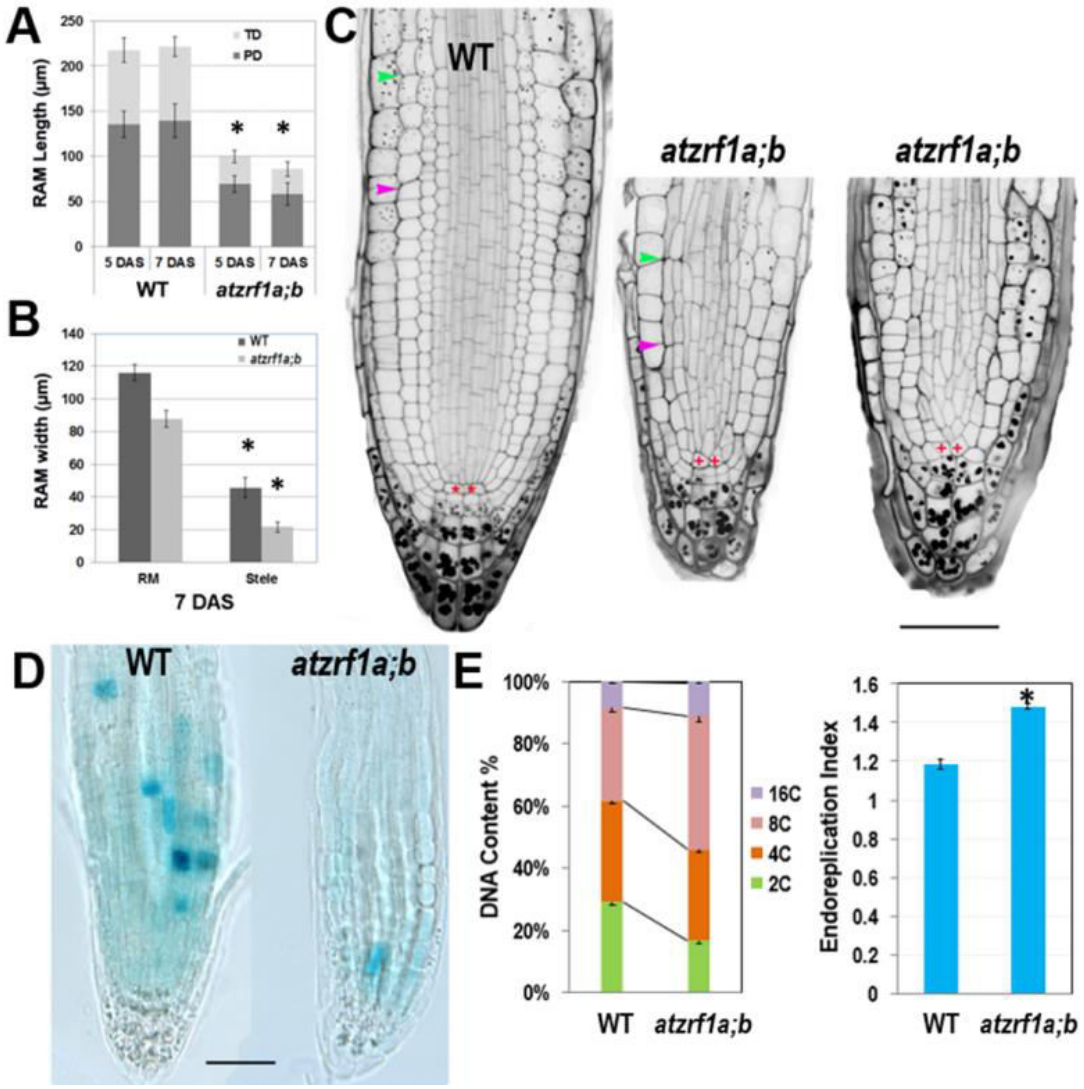

Figure III-2. Defective root development is associated with cell division arrest and precocious cell differentiation in the *atzrf1a;b* mutant.

(**A**-**B**) Comparison of meristem size between the wild-type (WT) control and the *atzrf1a;b* mutant at 5 or 7 days after stratification (DAS). The length of RAM including proliferation domain (PD) and transition domain (TD) indicates the vertical distance from QC to PD distal border, and finally to TD distal border. RAM width indicates the diameter at TD distal position.

(**C**) 5-day-old RAM in WT and *atzrf1a;b* after mPS-PI staining. Starch granule is visible in dark and accumulates in the root cap. Pink and green arrowheads indicate the distal borders of PD and TD, respectively. Asterisk indicates position of QC cells. Bar = 50 µm.
(**D**) GUS activity of *CYCB1;1::Dbox-GUS* reporter in 5-day-old WT and *atzrf1a;b* mutant. Blue staining indicates for positive GUS activity. Bar = 50 µm.

(**E**) Ploidy analysis in 7-day-old WT and *atzrf1a;b* mutant roots. Percentages of 2C, 4C, 8C, and 16C DNA content nuclei are shown. Data show means ± SE from three biological repeats. Asterisk indicates student's *t*-test statistically significant differences

at $P < 0.001$.

III.2.3. AtZRF1A/B are required for organization and maintenance of root stem cell niche

To gain insight about cell fate determinacy, root cell-type specific markers were introgressed into the *atzrf1a;b* mutant. Consistent with previous report (Blilou et al. 2005), *WOX5::erGFP* showed specifically expression in QC cells in WT (**Figure III-3A**). In contrast, it was found expressed in QC often with aberrant morphology as well as in adjacent cortex/endodermis initial cells in the *atzrf1a;b* mutant (**Figure III-3B-3D**). The abnormal pattern observed in the mutant might provide inappropriate position cues to surrounding stem cells, as reflected by irregular SCN formation in the mutant (**Figure III-2C**). The *J2341* enhancer trap marker carrying ER-tethered GFP (Kim et al. 2005a) was found expressed in approximately four columella initials in WT (**Figure III-3E**), but was found only expressed in one cell below the QC in the *atzrf1a;b* mutant (**Figure III-3F**), indicating weakened columella initial stem cell activity in the mutant. The *SCR::SCR-YFP* endodermis marker (Heidstra et al. 2004)was found expressed in endodermis, cortex/endodermis initials and QC in both WT (**Figure III-3G**) and the *atzrf1a;b* mutant (**Figure III-3H**). Remarkably, in the mutant, additionally *SCR::SCR-YFP* showed weak but significant expression in cells normally corresponding to the cortex cells (**Figure III-3H**). To further verify this mutant defect, we examined expression pattern of *CO2::H2B-YFP*, a marker specific for cortex cells (Heidstra et al. 2004). As expected, *CO2::H2B-YFP* was found expressed specifically in cortex layer cells in WT (**Figure III-3I**). In the *atzrf1a;b* mutant, however, only a few cells from the cortex layer showed roughly normal level of *CO2::H2B-YFP* expression whereas the other cells showed low or absence of *CO2::H2B-YFP* expression (**Figure III-3J**). These observations using both *SCR::SCR-YFP* and *CO2::H2B-YFP* indicate that the *atzrf1a;b* mutant is impeded in establishment and maintenance of the cortex cell fate during root

development. The *J1092* enhancer trap line (Blilou et al. 2002) displayed strong GFP signal in the lateral root cap initial cells and to a lesser extent in the columella root cap initial cells in WT (**Figure III-3K**), but showed rather uniform expression level throughout the root cap initial cells in the *atzrf1a;b* mutant (**Figure III-3L**), implying a weakened distinction between the two types of root cap initial cells in the mutant. Taken together, our analyses using cell fate markers indicate that *AtZRF1A/B* are required for whole SCN architecture, including QC localization, columella stem cell maintenance, separation between cortex and endodermis identities as well as stable maintenance of cortex cell fate, and distinction between the columella and lateral root cap initials.

Next, we performed quantitative RT-PCR (qRT-PCR) to compare the *atzrf1a;b* mutant and the WT control for relative expression levels of some of the above described genes as well as others genes known in previous publications as important regulators of root development. As shown in **Figure III-3M**, the expression of *WOX5* was upregulated whereas that of *CO2* was drastically downregulated in the *atzrf1a;b* mutant roots. This is in agreement with the *WOX5::erGFP* and *CO2::H2B-YFP*expression pattern described above. Consistent with the *CLE-WOX5* feedback repressive pathway, the expression levels of several CLE-reception component genes, i.e. *ACR4*, *CLV1*, *CLV2* and *CORYNE* (*CRN*) (Meng and Feldman 2010; Stahl et al. 2013; Stahl et al. 2009; Miwa et al. 2008), were downregulated albeit *CLE40* itself was upregulated in the *atzrf1a;b* mutant roots (**Figure III-3M**). In addition, expression of *ERF115*, which is associated with dividing QC cells (Heyman et al. 2013), was found drastically upregulated in *atzrf1a;b*, further indicating defects of QC regulation in the mutant. We then examined expression of several cell cycle regulatory genes known as being involved in root development, including the G1-phase D-type cyclins (*CYCD1;1*, *CYCD3;3*and *CYCD6;1*), the G1-Stransition inhibitor *RETINOBLASTOMA-RELATED* (*RBR*), the S-phase A-type cyclin *CYCA2;3*, and the endocycle switch regulators *CCS52A1*/*FZR2* and *CCS52A2*/*FZR1* (Cruz-Ramirez et al. 2012; Forzani et al. 2014; Sozzani et al. 2010;

Vanstraelen et al. 2009). It was found that *CYCD1;1*, *CCS52A2*/*FZR1* and to a less degree *CYCA2;3* were downregulated whereas *CCS52A1*/*FZR2* was upregulated and the other ones remained unchanged in the *atzrf1a;b* mutant roots (**Figure III-3M**). The downregulation of *CYCD1;1* correlates with the high level of *WOX5* in *atzrf1a;b*, which is in agreement with *CYCD1;1* being repressed by WOX5 (Forzani et al., 2014). Lastly, we checked expression of several root-patterning transcription factor genes, including *PLETHORA1* (*PLT1*) and *PLT2* involved in auxin-dependent axial patterning (Aida et al. 2004), *FEZ* and *SOMBRERO* (*SMB*) that antagonistically regulate asymmetric cell division of epidermal and lateral cap initials as well as columella stem cells (Bennett et al. 2014; Willemsen et al. 2008), *SCHIZORIZA* (*SCZ*) that is required for the specification of cortex identity and the separation of cell fates in surrounding RAM layers (Pernas et al. 2010; ten Hove et al. 2010), and *UPBEAT1* (*UPB1*) that functions in the maintenance of cell proliferation-differentiation balance by controlling ROS production (Tsukagoshi et al. 2010). It was found that *UPB1* and to a less degree *PLT2* were upregulated whereas *FEZ* and *SMB* were downregulated in *atzrf1a;b* (**Figure III-3M**), implying defects in the regulation of cell fate determinacy and homeostasis between cell proliferation and cell differentiation in the mutant. Taken together, our data indicate that loss of *AtZRF1A/B* perturbs expression of multiple sets of genes involved in diverse pathways in the regulation of postembryonic root development.

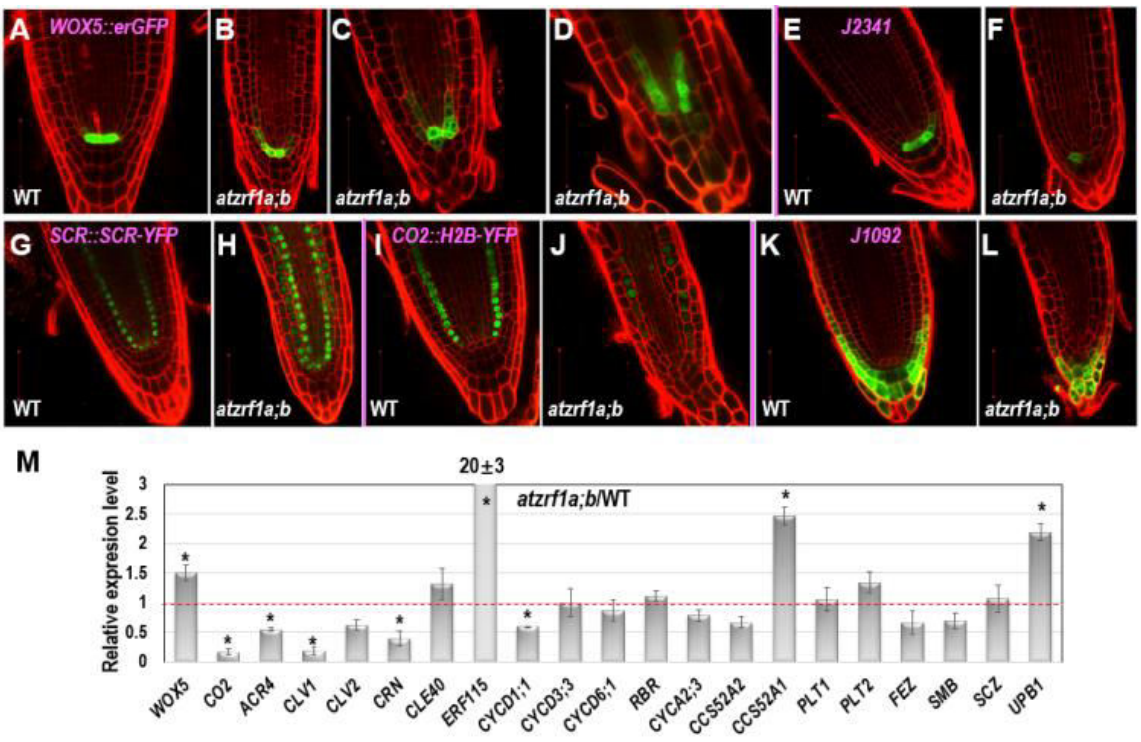

Figure III-3. The expression patterns of RAM specific markers in WT and *atzrf1a;b* roots.

5-day-old root was counterstained with propidium iodide (PI) and observed with confocal microscopy.

(**A**-**D**) *WOX5::erGFP* markers in WT and *atzrf1a;b*.

(**E**-**F**) *J2341* markers.

(**G**-**H**) *SCR::SCR-YFP* markers.

(**I**-**J**) *CO2::H2B-YFP* markers. Inset indicates the relative expression level of *CO2* in 7-day-old root of *atzrf1a;b* compared with that of WT.

(**K**-**L**) *J1092* markers.

(**M**) Relatively expression levels of some RAM-regulating genes in *atzrf1a;b* compared with WT (set as 1) examined by qRT-PCR. Asterisk indicates student's *t*-test statistically significant differences at $P < 0.001$.

Bars =50 μm.

III.2.4. AtZRF1A/B are required for proper auxin regulation of root development

Generation and maintenance of auxin gradients and regional maxima in root tip is crucial for normal root development (reviewed in (Overvoorde et al. 2010)). To survey whether the *atzrf1a;b* mutant abnormal root development is related to any impaired auxin regulation, we first tested plant growth sensitivity to auxin treatment. We found that the root growth of both WT and mutant was seriously inhibited by exogenous 1-naphthalene acetic acid (NAA) increasingly with higher concentrations (**Figure III-4A**). The mutant root growth became most completely blocked at the presence of 0.5 mg L^{-1} NAA. When grown at 1mg L^{-1} NAA for 3 weeks, all the mutant roots and about 10% (N=50) of whole seedlings developed into callus-like structures with root hairs appeared on the surface whereas WT seedlings barely showed callus formation (**Figure III-4B**). These data indicate that the *atzrf1a;b* mutant is more sensitive to auxin treatment as compared to WT.

To investigate whether auxin distribution is disturbed in the *atzrf1a;b* mutant RAM, we introgressed into the mutant the auxin-response reporter *DR5rev::GFP* (Friml et al. 2003). In WT, *DR5rev::GFP* was expressed in QC, columella stem cells and columella, displaying auxin gradient maxima in QC and distal columella cells (**Figure III-4C**). In the *atzrf1a;b* mutant, the number of cells expressing *DR5rev::GFP* was reduced at varied degrees in individual roots and the auxin gradient maxima at both QC and distal columella cells were lost or weakened (**Figure III-4D**). Furthermore, we carried out qRT-PCR to analyze the expression levels of auxin-responsive genes (*IAA14*, *IAA16*, *IAA19*, *IAA28-IAA30*, *IAA34*) and polar auxin transporter genes (*PIN1*, *PIN2*, *PIN4*, *PIN7*), which play important roles in root development (Blilou et al. 2005; Overvoorde et al. 2010). It was found that expression of *IAA14*, *IAA19* and *PIN2* was increased whereas that of *IAA28*, *IAA29*, *PIN4* and *PIN7* was decreased in the *atzrf1a;b* mutant roots (**Figure III-4E**). Collectively, our data indicate that defects in auxin signaling, transport and/or cell type-specific distribution contribute partly to explain the *atzrf1a;b* mutant root phenotype.

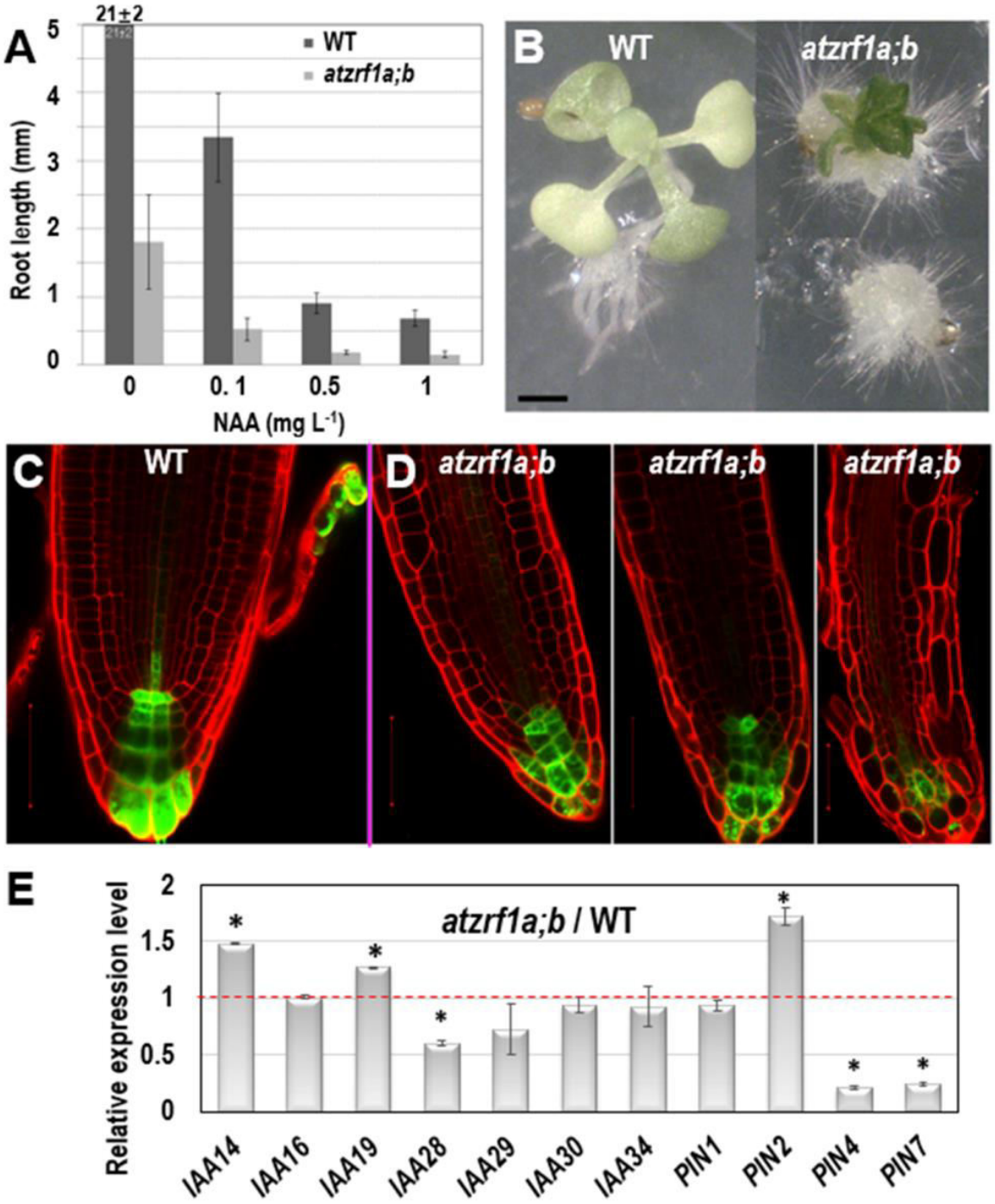

Figure III-4. Effect of auxin treatment on *atzrf1a;b* double mutant.

(**A**) Effects of exogenous NAA on root growth of WT and *atzrf1a;b* seedlings. Seeds were sown on MS medium containing the indicated concentration of NAA for 1 week. (**B**) WT and *atzrf1a;b* plants grown on the plate containing 1 mg L-1 NAA in 3 weeks.

(**C**-**D**) DR5rev::GFP markers in 5-day-old seedlings of WT (C) and *atzrf1a;b* (D). PI was used to stain the cell wall.

(**E**) Expression level of auxin-responsive genes in 7-day-old *atzrf1a;b* compared with WT.

Asterisk indicates student's t-test statistically significant differences at $P < 0.001$.

Bars = 1mm in (**B**), 50 μm in (**C**) and (**D**).

III.2.5. AtZRF1A/B regulate cell division and cell patterning in embryonic root

To trace the embryonic origin of defective RAM formation in the *atzrf1a;b* mutant, embryos at different developmental stages were analyzed using the cell-wall fluorescent dye SR2200, which had been previously demonstrated to be powerful for investigation of early stages of embryogenesis (Musielak et al. 2015). In globular stage, the extra-pro embryo-derived hypophysis located at the uppermost suspensor cell underwent an asymmetric division to produce an upper lens-shaped QC cell and a lower columella initial in both WT and *atzrf1a;b* without showing significant difference. In triangle stage, ground tissue initial in WT performed atypical anticlinal division to maintain self-renewal and at the same time create a new ground tissue initial daughter cell which subsequently underwent a periclinal asymmetric division (first formative division) to generate a cortical initial and an endodermis initial (**Figure III-5A**). However, the potential ground tissue initial in *atzrf1a;b* seemingly bypassed the former anticlinal division and directly underwent the first periclinal division to give rise to the presumptive cortex and endodermis (**Figure III-5B**) and absence of obvious ground tissue initial after this division (**Figure III-5D-5I**). In late heart stage, an additional cortical layer arises from the secondary formative divisions of endodermal cells in WT (**Figure III-5A**), demarcating the boundary between root and hypocotyl (Bougourd et al. 2000). Similarly, another periclinal division in mutant also happened in the inner ground tissue cell (**Figure III-5F**). In the early torpedo stage, the lowest of the protoderm cells in WT formally served as epidermal/lateral root cap initials characterized by the

emergence of lateral root cap due to the periclinal division (**Figure III-5A**) (Scheres et al. 1994). However, the corresponding protoderm cells in mutant lacking the hallmarking periclinal division failed to achieve the cell fate transition and to generate lateral root cap (**Figure III-5F-5I**). These indicate *AtZRF1A/B* are necessary for the formative cell division giving rise to epidermal/lateral root cap initials and lateral root cap. QC cells in WT are mitotically quiescent and were transversely aligned in the center of embryonic RAM throughout the whole embryogenesis (**Figure III-5A**). In comparison, QC cells in mutant were also easily recognized prior to the heart stage even their morphology gradually growing abnormal from trapezoid to triangle, and then inclined to become atypical in later stages due to their active and irregular divisions giving rise to ill-organized patterning (**Figure III-5G-5I**). Consistently, the columella cell and columella initial derived from QC exhibited anatomic defects to a different extent in *atzrf1a;b* mutant (**Figure III-5H-5I**). In mutant mature embryo, columella initial and columella cell in *atzrf1a;b* mutant displayed distorted and reduced number of cell layers, with 82% of mutants owning 3 layers instead of 4 in WT (**Figure III-5A**, **5I-5J**). Consistently, 3-day-old *atzrf1a;b* seedlings still have 3 layers of columella cells, less than WT with 5 layers (**Figure III-5K**). Additionally, the embryonic radicle length in *atzrf1a;b* mutant (~10 μm) was only about one seventh of that in WT during mature embryo stage, giving rise to a round end phenotype (**Figure III-5I**, **5L**). Correspondingly, the mutant radicle had only ~2 cells in a longitudinal cortex file, much fewer than WT with ~10 (**Figure III-5M**), indicating that AtZRF1A/B promote cell division during embryonic root morphogenesis. Suspensor is comprised of a single file of about seven cells, bridges the embryo proper to surrounding endosperm tissues, and transports nutrients and growth regulators to the embryo (Kawashima and Goldberg 2010). As embryo grows up, suspensor gradually degenerates till to disappear. But in mutant, suspensor cells were usually arranged into two files at the basal part (**Figure III-5B**), and sometimes proliferated into a cell mass. Even in mature embryos, 32%

(n=50) of suspensors were still visible. In summary, *AtZRF1A/B* participate in the proper radicle cell patterning, maintenance of QC and surrounding stem cell identity, promotion of cell division, and normal degradation of suspensor cell during embryonic radicle formation.

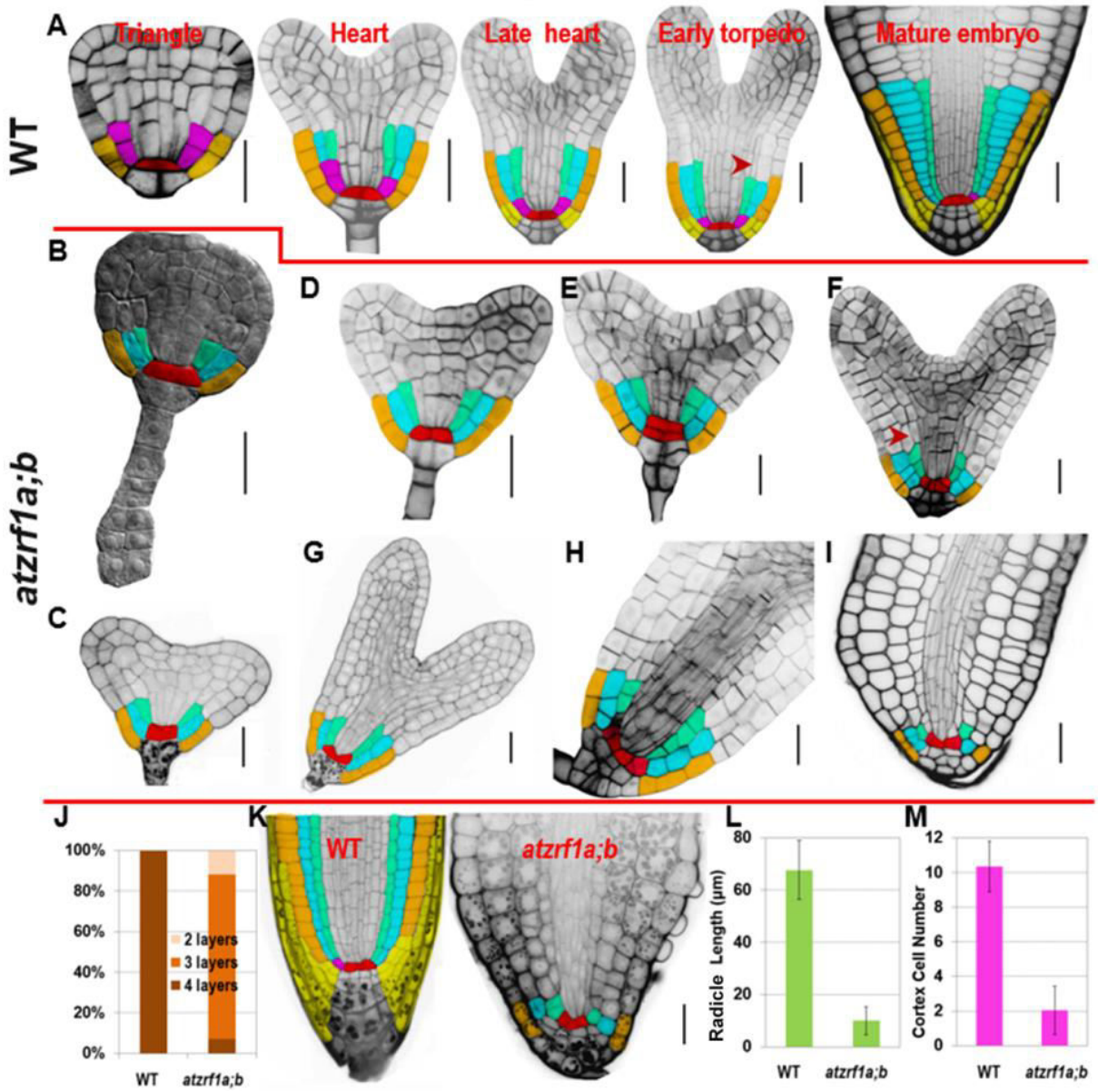

Figure III-5. Defective embryogenesis in *atzrf1a;b* mutant.

(**A**) Representative embryogenetic stages in WT according to previously reported (Scheres et al. 1994).

(**B-I**) Embryogenesis in *atzrf1a;b* (**B**) in triangle stage, (**C-E**) in different heart-stages, (**F-H**) in torpedo stages, and (I) in mature embryo stage.(**J**) Columella cell layers of

mature embryos in WT and *atzrf1a;b*.

(**K**) 3-day-old RAM in WT and *atzrf1a;b* mutant observed *via* mPS-PI method.

(**L**) Length of mature embryonic roots in WT and *atzrf1a;b*.

(**M**) Cell numbers in a single file of cortex of mature embryos in WT and *atzrf1a;b*.

Red, QC; pink, ground tissue initial; cyan, cortex; green, endodermis; brown, epidermis; yellow, lateral root cap and its initials. Arrowhead, the 2nd formative cell division giving rise to the 2nd cortex file.

Asterisk indicates student's *t*-test statistically significant differences at $P < 0.001$.

Bars = 20 µm.

III.2.6. AtZRF1A/B are required for embryonic root cell fate establishment

To gain insight into the embryonic root cell identity in *atzrf1a;b*, some aforementioned marker lines were investigated during embryogenesis. QC-specific marker *WOX5::erGFP* also displayed significantly diffused expression in adjacent initials from torpedo stage onward in mutant embryo (**Figure III-6A-C** and **6G-I**), consistent with the *WOX5* performance in the postembryonic root. *SCR::SCR-YFP* marked QC, ground tissue initial, and endodermis in embryo as it is in seedling stage in WT. In mutant, *SCR* signal firstly appeared in the inner ground tissue layer from the first unusual periclinal division of ground tissue initial in triangle-stage mutant embryo, confirming the ground tissue inner layer adapted the endodermis cell fate. Subsequently, signal was also observed in the fourth layer from the second periclinal division in mutant embryo, corresponding to the same endodermis layer in WT hypocotyl (**Figure III-6D-6F** and **6J-6L**). *CO2::H2B-YFP* marker was firstly observed in the cortex cells in the upper part of torpedo-stage WT embryo but excluding embryonic root region, and subsequently in all the cortex cells in later stages (**Figure III-6M-6N**). However, in *atzrf1a;b* mutant, YFP signal was not detected in torpedo-stage, but later was sporadically found in some cortex cells excluding embryonic root region (**Figure III-6S-6T**), indicating *AtZRF1A/B*

are required for determination of cortex cell identity in embryonic root. *J1092* marker specified root cap in the embryos of WT and *atzrf1a;b* mutant, though mutant had no lateral root cap or significantly reduced lateral root cap region in later stage (**Figure III-6O-6P** and **6U-6V**). *DR5rev::GFP* marker had the strongest expression in the nearest suspensor cell attaching to embryo proper in WT and mutant, and subsequently auxin distribution gradients were established from columella cells to QC in WT, but absent in mutant (**Figure III-6Q-6R** and **6W-6X**). These data suggested *AtZRF1A/B* are necessary for cell identity maintenance of QC and different initials and the formation of auxin gradients during embryogenesis.

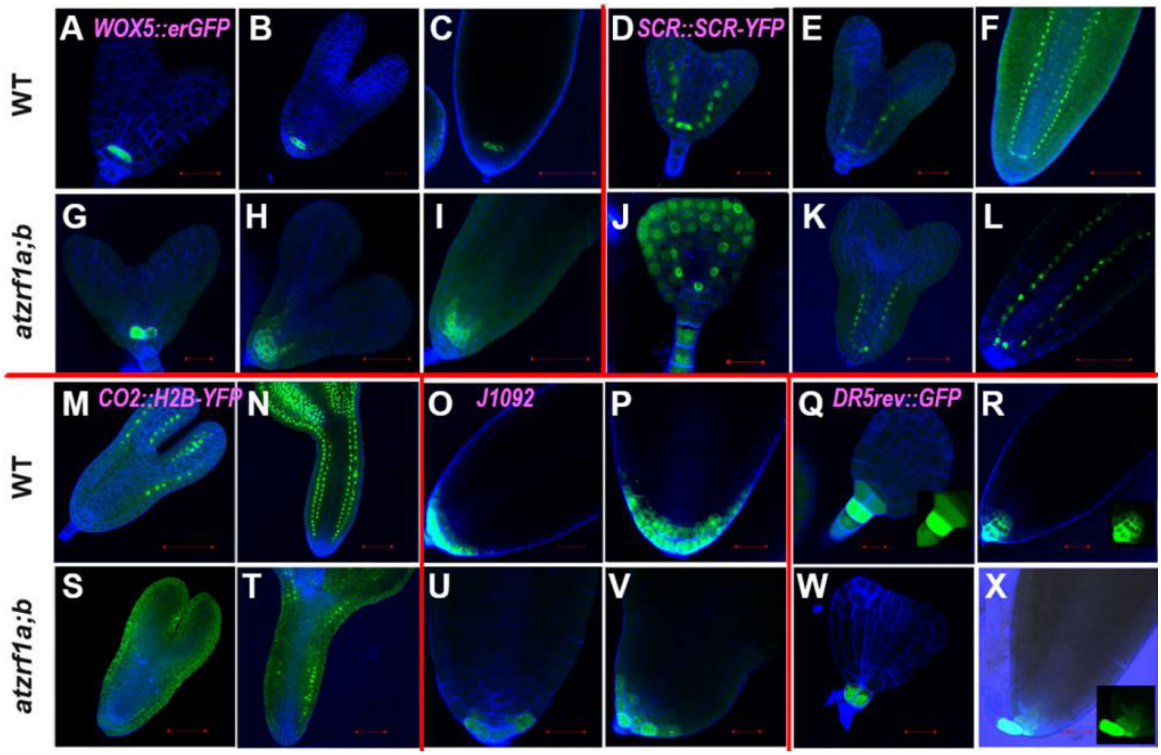

Figure III-6. The expression of RAM-specific markers in *atzrf1a;b* embryos.

Different stages of embryos were hand-dissected, counterstained with SR2200 and observed under confocal.

(**A**-**C**) and (**G**-**I**) *WOX5::erGFP* markers in WT and *atzrf1a;b*.

(**D**-**F**) and (**J**-**L**) *SCR::SCR-YFP* markers.

(**M**-**N**) and (**S**-**T**) *CO2::H2B-YFP* markers.

(**O**-**P**) and (**U**-**V**) *J1092* markers.

(**Q-R**) and (**W**-**X**) *DR5rev::GFP* markers.

Bars = 20 µm, except 50 µm in (**C**), (**F**), (**H**), (**I**), (**L**), (**M**), and (**S**).

III.3. Discussion

In this study, we provide important insights about the roles of the H2A/UBIQUITIN-binding chromatin regulator genes *AtZRF1A/B* in embryonic and post-embryonic root development. In the loss-of-function *atzrf1a;b* mutant, the primary root growth ceased early during seedling growth because RAM became shortened and exhausted due to spoiled balance between cell proliferation and differentiation. The *atzrf1a;b* RAM displayed low mitotic activities, which was consistent with the very slow root growth. Elevated polyploid levels were detected, indicating an advanced onset of endoreduplication in the mutant roots. In a previous study, endoreduplication levels were also found increased in true leaves of the *atzrf1a;b* mutant plants (Feng et al. 2016). It thus appears that *AtZRF1A/B* repress the mitosis-to-endocycle transition in a general rather than an organ-specific manner.

Proper RAM structure organization is crucial in maintaining continuous post-embryonic root development. Our study showed that *AtZRF1A/B* are crucial in establishment and maintenance of cell fate of various cell types within RAM. The hardly recognizable QC cells together with expanding zone of *WOX5::erGFP* expression outside QC position indicated that the QC cell fate was drastically impacted in the *atzrf1a;b* mutant. In addition, the cell identities of surrounding initials and their corresponding descendants were also altered to different extents in the mutant. Columella root cap was frequently found disorganized, correspondingly, columella initial marker *J2341* displayed reduced activity in the mutant. Lateral root cap was clearly separated from columella root cap in WT, but seemingly became undistinguished from columella root capor absent in the *atzrf1a;b* mutant. Ground tissues including cortex and endodermis partially lost their cell identities, which was reflected by diffused *SCR::SCR-YFP* expression and reduced *CO2::H2B-YFP* signal in the mutant.

RAM defects in *atzrf1a;b* could be traced back to early embryogenesis. The first major

defect in *atzrf1a;b* happened in triangle-stage embryo where potential ground tissue initial skipped the first anticlinal division (proliferative division) which was substituted by a periclinal division. The inner ground tissue layer had the endodermis cell identity confirmed by *SCR::SCR-YFP* marker, which was different from that in seedling, whereas the outer ground tissue layer seemed to loss partial cortex cell identity reflected by *CO2::H2B-YFP* marker. The second major defect occurred in late heart-stage embryo, in which the potential epidermal/lateral root cap initial failed to perform the periclinal division (formative division), leading to no lateral root cap formation in late stages. Accordingly, *J1092* marking root cap has reduced expression domains in mutant. So, the *atzrf1a;b* root cap mainly results from columella cell cap but not lateral root cap. In fact, the both major defects above mentioned in mutant were characterized by transformation of cell division orientation (anticlinal-to-periclinal or vice versa). So, *AtZRF1A/B* regulate the conversion between proliferative division and formative division rather than specific proliferative or formative division. Additionally, embryonic QC was conspicuous at the beginning, and subsequently conducted a few more divisions even in oblique direction to generate some offspring with similar size and irregular organization, leading to hardly distinguishing from surrounding stem cells in most cases. It seems that *AtZRF1A/B* are required for repression of cell divisions and maintenance of precise division orientation within QC. *WOX5::erGFP* also displayed expanded expression during the late embryogenesis, similar to its performance in seedling root.

The phytohormone auxin plays key roles in root development. In WT, local auxin maximum as the prerequisite for QC establishment determines the position of the QC, and the auxin gradient is crucial for maintaining columella initial identity (Sabatini et al. 1999; Tian et al. 2014). In the *atzrf1a;b* mutant, the auxin maximum and/or gradient were perturbed in postembryonic and embryonic roots, where the cell patterning of QC and columella cell was mostly impaired. Accordingly, several *IAA* genes as auxin signal pathway repressors (De Rybel et al. 2010; Fukaki et al. 2002) and *PIN* genes as auxin

transporters (Blilou et al. 2005)were misregulated in the mutant roots. Exogenous auxin treatment also showed that *atzrf1a;b* was more sensitive, with enhanced facilities of ectopic callus formation. Future genetic interaction studies may precisely investigate the role and regulatory pathways of auxin in the *AtZRF1*-regulated root development.

In addition to *IAA* and *PIN* genes, several other genes were found deregulated, which likely contributes to the *atzrf1a;b* mutant root developmental defects. Firstly, *AtZRF1A/B* may regulate the balance between cell division and differentiation in RAM partially through CCS52A-activating APC/C ubiquitin ligase. *CCS52A* has two isoforms with antagonistic functions; *CCS52A1* expressed in the root elongation zone promotes endocycle onset and mitotic exit through destruction of A2-type cyclin CYCA2;3 (Boudolf et al. 2009), whereas *CCS52A2* expressed in the RAM distal region controls QC identity and stem cell maintenance (Vanstraelen et al. 2009) through proteolysis of QC division marker ERF115 (Heyman et al. 2013). In *atzrf1a;b*, upregulation of *CCS52A1* coupled with downregulation of *CYCA2;3* was associated with downregulation of *CCS52A2* coupled with upregulation of *ERF115*, which was in line with *ccs52a2* mutant root phenotype displaying the consumed and disorganized RAM (Vanstraelen et al. 2009). Secondly, upregulation of *UPB1* in *atzrf1a;b* was consistent with reduced root length and RAM size in *UPB1* overexpression line (Tsukagoshi et al. 2010). Lastly, CLE peptide ligands in differentiated columella cells regulate *WOX5* expression and columella initial fate through the receptor-like kinases *ACR4*,*CLV1*, *CRN* and *CLV2* (Meng and Feldman 2010; Stahl et al. 2013; Stahl et al. 2009; Miwa et al. 2008). *AtZRF1A/B* also regulated RAM organization dependent on *CLE-WOX5* pathway inferred from uniformly downregulated expression of *CLE* receptors in mutant. Correspondingly, *ACR4* has an important role in formative cell division and columella cell organization in the root apex (De Smet et al. 2008).

In multicellular organisms, stem cells can maintain self-renewal and produce the new daughter cells with distinct fates by asymmetric cell divisions or formative divisions,

which are coordinated by extrinsic and intrinsic cues (Kajala et al. 2014). Asymmetric cell division can be considered as the evolutionary engine, leading to cell differentiation necessary for the innovation of novel organ and the emergence of higher life form. Our study demonstrates that the Arabidopsis *AtZRF1A/B* are required for formative division giving rise to lateral root cap during embryogenesis, though their more precise role mainly in the alteration of cell division orientation. Likely, *ZRF1* orthologs have an evolutionarily conserved function in asymmetric cell division. For instance, in the classic animal model *Caenorhabditis elegans*, *DNJ11* is involved in the asymmetric division of the neuroblast *via* regulating the orientation of the mitotic spindle (Hatzold and Conradt 2008). In green algae *Volvox carteri*, *Gonidialess A* (*GlsA*) is necessary for separation of germ and somatic cell fate during gonidium formation (Miller and Kirk 1999).

AtZRF1A and *AtZRF1B* have similar and broad expression in almost all the young plant organs including root tips, shoot tips, developing leaves, inflorescences, floral buds and embryos; their expression intensity is positively correlated to dividing activities of the organs (Guzman-Lopez et al. 2016). Consistently, loss of *AtZRF1* function results in morphological defects in almost all the developmental phases related to dividing cells and meristematic tissues (Feng et al. 2016; Guzman-Lopez et al. 2016). Recently *AtZRF1A/B* have been reported to perform both PRC1-related and independent functions in regulating plant growth and development (Feng et al. 2016). Consistently, PRC1 RING-finger proteins functioning as H2Aub1 writers and AtZRF1 as H2Aub1 reader share a set of target genes and partial regulatory pathways (Feng et al. 2016). In addition, PRC1 RING-finger proteins display the similar expression pattern and tendency with ubiquitously organic distribution but high levels in dividing cells (Chen et al. 2010; Chen et al. 2016; Qin et al. 2008). Furthermore, *AtRING1A/b* and *AtBMI1a/b* are also widely involved in regulating multiple developmental processes. On the other hand, according to the working model of human *ZRF1* (Richly et al. 2010), *AtZRF1A/B* might

also act as a chromatin state switch to remove PRC1 function in the specific developmental context. Future studies are necessary to investigate these different aspects of interplay between *AtZRF1A/B* and PRC1 complexes the regulation of gene transcription in the root and other plant organ development.

Chapter IV

CONCLUSIONS and PERSPECTIVES

The results of my PhD work have significantly advanced our understanding of the roles and the molecular mechanisms of AtRING1 and AtZRF1 in transcription and regulation of plant development.

Firstly, by using the genome editing tool CRISPR/Cas9 to mutagenize different regions of AtRING1A, 4 novel *Atring1* mutants were screened. The morphological and molecular analysis of the *Atring1* mutants confirmed the essential function of AtRING1 in cell differentiation. It also demonstrated the marginal effects of RAWUL on regulating plant development (plant vegetative growth, floral organ formation and seed production) and phase transition (germination, vegetative and floral transition) as well as its important role in H2A *in vivo* monoubiquitination. The mutation L429F in RAWUL domain has no effect on plant growth and development, but impaires H2Aub1. The E3 ligase module in Arabidopsis is hypothesized to be realized by RING-finger protein containing multiple-protein complex, which is assembled by RAWUL (**Figure II-20**). Whether more components are involved in the E3 ligase module remains to be investigated.

It has long been accepted that PRC2 functions followed by PRC1 in PcG working paradigm, which is questioned constantly in recent years (Yang et al. 2017b). In Arabidopsis, the distribution of H2Aub1 usually colocalizes with H3K27me3 (Zhou et al. 2017a). The further molecular analysis in this work showed that AtRING1 and AtBMI1 are responsible for regulating the key genes of the programs described above by mediating the enrichment of both H2Aub1 and H3K27me3. Moreover, RAWUL domain is important for the H2Aub1 deposition at all loci detected but showed targets specificity on H3K27me3 marking. Taken together, PRC1 is proposed to be upstream of PRC2 at the loci examined and the recruitment of PRC2 is in either RAWUL-dependent or –independent manner.

Secondly, *Atzrf1* showed short root phenotype and prematurely differentiated RAM stem

cells. By introducing multiple reporter genes, it is characterized that the root growth defects of *Atzrf1* are due to the impaired mitotic capacity, endoreduplication as well as auxin signaling, transport and/or cell-specific distribution. Furthermore, the transcriptional analysis indicates that several important regulators of root development are deregulated in the mutant. As a whole, it uncovered that AtZRF1 plays a crucial role in maintaining stem cell activity, cell identity, and spatial organization of cells during embryonic and post-embryonic plant development.

The *Atzrf1*, *Atring1* and *Atbmi1* shared several developmental defects and a set of target genes regulatory pathways and AtZRF1 serves as the H2Aub1 reader (Feng et al. 2016). Moreover, AtZRF1 was involved in depositing H2Aub1 and H3K27me3 at *ABI3*, the mechanism of recruiting PRC2 is biased towards by AtZRF1 (Feng et al. 2016). Future investigation on whether ZRF1 interacts with PRC2 may provide a mechanism for PRC2 reading of H2Aub1 after PRC1 deposition (**Figure IV-1A**).

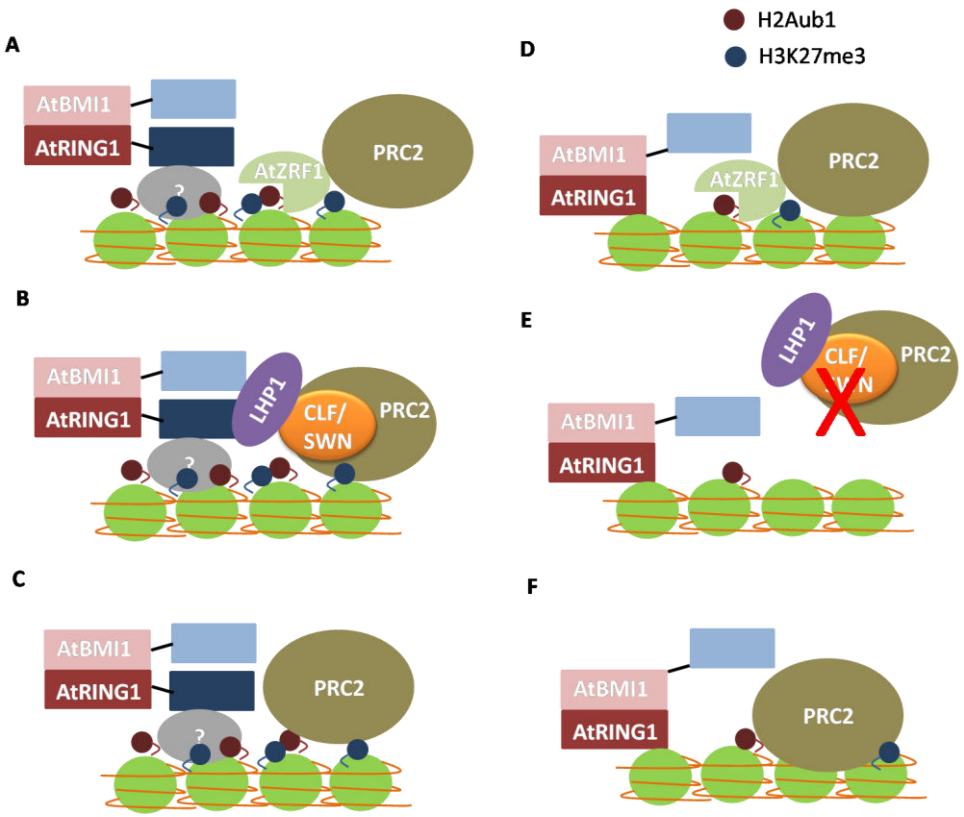

Figure IV-1. The hypothesis for PcG mediated gene repression in Arabidopsis.

The interaction between AtRING1A and AtBMI1, LHP1, CLF; LHP1 and EMF2, MSI1 and VRN2 has been reported previously. A simple hypothesis could be that PRC2 complex is recruited to establish H3K27me3 on target genes by the direct or indirect interaction with RAWUL domain of AtRING1A (**Figure IV-1B**).

In addition, *in vitro* reconstituted PRC2 complexes are able to bind the H2Aub1-enriched nucleosomes in mammalian cells (Kalb et al. 2014). I hypothesized that directly binding H2Aub1 could be another mechanism of PRC2 recruitment (**Figure IV-1C**).

The loss of RAWUL domain weakened the E3 ligase activity and disturbed the recruitment of PRC2 at specific loci, which led to the decrease of the enrichment of H2Aub1 and H3K27me3 at specific target genes (**Figure IV-1D, E, F**).

The detailed recruitment for PRC2 need to be clarified in the future investigation. Furthermore, with the largely decreased enrichment of H2Aub1 and H3K27me3, and the derepression of *CUC1*, *ABI3*, *DOG1*, *MAF4* and *MAF5*, *mut3* only showed mildly growth defects. It suggests the complexity of the regulation network of plant development. More evidence should be provided in the future research.

However, the H3K27me3 level at *CUC2* and *FLC* loci in *mut3* remains unchanged, which suggest that the establishment of H3K27me3 at *CUC2*, *FLC* is independent of AtRING1 RAWUL domain. The silencing mechanism of different genes seems to follow the distinct mechanism.

The mutant lines generated during my thesis will elucidate by the further genomic/epigenomic approaches the global role of H2Aub1 in the regulation of genome transcription. In the future, a characterization of AtRING1-associated proteins *in vivo* could provide a better understanding of the function and biochemical composition of the PRC1 complex, as well as the molecular basis of the targeting mechanism of AtRING1

at specific chromatin sites within the genome.

Chapter V

MATERIALS and METHODS

V.1. Materials

V.1.1. Plant materials and growth conditions

Mutants *Atring1a* (AL_945948), *Atring1b* (SALK_117958), a*tbmi1a* (WiscDsLox437G06), *Atbmi1b* (SALK_145041), the enhancer trap *GFP* lines J1092 (N9147) and J2341 (N9118) were obtained from the Arabidopsis Biological Resource Center (ABRC, http://www.Arabidopsis.org) or the European Arabidopsis Stock Centre (NASC, http://www.arabidopsis.org.uk). The double mutants *Atring1ab*, *Atbmi1ab* and *Atzrf1a;Atzrf1b*; and the marker lines *CYCB1;1:Dbox-GUS* (Colon-Carmona et al. 1999), *WOX5*::*erGFP* (Blilou et al. 2005), *SCR::SCR-YFP* (Heidstra et al. 2004), *CO2*::*H2B-YFP* (Heidstra et al. 2004), *DR5rev*::*GFP* (Friml et al. 2003) have been previously described (Feng et al. 2016; Xu and Shen 2008; Chen et al. 2010). *mut1*, *mut2*, *mut3* and *mut4* were generated by mutating a specific region of the *AtRING1A* gene in the *Atring1b* background through CRISPR/Cas9 system.

Seeds were sown either in soil or on 1/2 strength Murashige and Skoog (1/2 MS) medium (0.8% agar, 1% sucrose, pH5.8). After stratification at 4 °C for 3 days in the dark, they were transferred to a growth chamber at 18~21°C under LD (16hours light/8 hours dark) or SD (8 hours light/16 hours dark) conditions. The transformants generated through *Agrobacterium tumefaciens*-mediated transformation (Zhang et al. 2006) were selected on 1/2 MS supplemented with 35 mg/L hygromycin and 200 mg/L carbenicillin.

V.1.2. Bacterial strains

DH5α was used for heat shock transformation and GV3101 was used for *Agrobacterium tumefaciens*-mediated plant transformation.

V.1.3. Vectors

Vectors used in this thesis are listed below and all constructs were created by restriction enzyme digestion and ligation (**Table V-1**).

Vector	Experiment	Resistance
AtU6-26-sgRNA-SK	CRISPR/Cas9	Ampicillin
pCAMBIA1300-pYAO:Cas9	CRISPR/Cas9	Kanamycin (bacteria); Hygromycin (plant)

V.1.4. Antibodies and beads

Antibodies and beads used in this thesis are listed below (**Table V-2**).

Name	Company	Product code	Purpose
Ubiquityl-Histone H2A (Lys119)	Cell signaling	D27C4	WB, ChIP
Anti-Histone H3 (tri methyl K27)	Abcam	Ab6002	WB, ChIP
Anti-Histone H3	Abcam	Ab1790	ChIP
Protein A magnetic beads	Millipore	16-661	ChIP

V.1.5. SgRNA

All sgRNAs used for *AtRING1A* gene editing were designed using the tool on the https://www.genome.arizona.edu/crispr/ and their sequences are listed below (**Table V-3**).

sgRNA	Target sequences
sgRNA1	CAAGAATAATAGCTTCTCGTCGG GTCGGCTGAGATTCCCGATGTGG
sgRNA2	CCGATGTGGCAGACCAACCACGC
sgRNA3	GTGCAGTGTCCAATATGCCTAGG CCACAGGTTCTGCCGGGAATGTA
sgRNA4	CAGGTATTATAAAGAAAACAAGG
sgRNA5	AATGTCTCCACAGGTTCTGCCGG
sgRNA6	CCACAGGTTCTGCCGGGAATGTA
sgRNA7	CATGGGAATAATACTTCTGGAGG GAGGTAGTAGTAAGAGTGTAAGG

sgRNA8	CCACAGCCATATCTCTGTTGCCG
sgRNA9	CCATATCTCTGTTGCCGACCCAC

V.1.6. Primers

Table V-4. List of primers used for sgRNA cloning in the thesis:

Name	sequences
Primers for sgRNA cloning in CRISPR/Cas9 system	
sgRNA1-1-F	5'-ATTGCAAGAATAATAGCTTCTCGT-3'
sgRNA1-1-R	5'-AAACACGAGAAGCTATTATTCTTG-3'
sgRNA1-2-F	5'-ATTGGTCGGCTGAGATTCCCGATG-3'
sgRNA1-2-R	5'-AAACCATCGGGAATCTCAGCCGAC-3'
sgRNA2-F	5'-ATTGGCGTGGTTGGTCTGCCACAT-3'
sgRNA2-R	5'-AAACATGTGGCAGACCAACCACGC-3'
sgRNA3-1-F	5'-ATTGGTGCAGTGTCCAATATGCCT-3'
sgRNA3-1-R	5'-AAACAGGCATATTGGACACTGCAC-3'
sgRNA3-2-F	5'-ATTGTACATTCCCGGCAGAACCTG-3'
sgRNA3-2-R	5'-AAACCAGGTTCTGCCGGGAATGTA-3'
sgRNA4-F	5'-ATTGCAGGTATTATAAAGAAAACA-3'
sgRNA4-R	5'-AAACTGTTTTCTTTATAATACCTG-3'
sgRNA5-F	5'-ATTGAATGTCTCCACAGGTTCTGC-3'
sgRNA5-R	5'-AAACGCAGAACCTGTGGAGACATT-3'
sgRNA6-F	5'-ATTGTACATTCCCGGCAGAACCTG-3'
sgRNA6-R	5'-AAACCAGGTTCTGCCGGGAATGTA-3'
sgRNA7-1-F	5'-ATTGGAGGTAGTAGTAAGAGTGTA-3'
sgRNA7-1-R	5'-AAACTACACTCTTACTACTACCTC-3'
sgRNA7-2-F	5'-ATTGCATGGGAATAATACTTCTGG-3'
sgRNA7-2-R	5'-AAACCCAGAAGTATTATTCCCATG-3'
sgRNA8-F	5'-ATTGGTGGGTCGGCAACAGAGATA-3'
sgRNA8-R	5'-AAACTATCTCTGTTGCCGACCCAC-3'
sgRNA9-F	5'-ATTGCGGCAACAGAGATATGGCTG-3'
sgRNA9-R	5'-AAACCAGCCATATCTCTGTTGCCG-3'
SK-gRNA-F	5’-CTCACTATAGGGCGAATTGG-3’
1300-gRNA-F	CCAGTCACGACGTTGTAAAAC
1300-gRNA-R	CAATGAATTTCCCATCGTCGAG

Table V-5. Primers used for identifying CRISPR/Cas9 edited plants (genomic PCR and sequencing)

Name	Sequence	For target
Genomic PCR primers		
AtRING1A-GENOMIC-F1	5'-CGATTTTATGTTTTTTAAGTTTT-3'	sgRNA1-2
AtRING1A-GENOMIC-R1	5'-ATGAACAAACACAAAACACTCTC-3'	sgRNA1-2
AtRING1A-GENOMIC-F2	5'-GCGGCCATTACTGGAAGTT-3'	sgRNA3-6
AtRING1A-GENOMIC-R2	5'-GCTTGCACAATGCTTCCTG-3'	sgRNA3-6
AtRING1A-GENOMIC-F3	5'-TAACAACAGAGGAAGAGACAAAGAT-3'	sgRNA7-9
AtRING1A-GENOMIC-R3	5'-TATCTGAAGTGCAACGAACTGTAC-3'	sgRNA7-9
Cas9-F	5'-CCGAAGAGGTCGTGAAGAAG-3'	
Cas9-R	5'-TCGCTTTCCAGCTTAGGGTA-3'	
cDNA PCR primers (ATG =+1~+3)		
AtRING1A-(-140)-F	5'-ATATCGGCACCGAACCAA-3'	
AtRING1A-(+370)-F	5'-GAAATTGATCTAGGGGAAATCCGT-3'	
AtRING1A-(+1638)-R	5'-AACGGATAAACAAAACAAGCCC-3'	
Sequencing primers		
AtRING1A-GENOMIC seq-F1	5'-AAATTCTCACTTTTTTCTTCGACC-3'	sgRNA1-2
AtRING1A-GENOMIC seq-R1 (AtRING1A-GENOMIC-R1)	5'-ATGAACAAACACAAAACACTCTC-3'	sgRNA1-2
AtRING1A-GENOMIC seq-F2	5'-AGAACTTTTGCTAAAGCTCGAAAG-3'	sgRNA3-6
AtRING1A-GENOMIC seq-R2 (AtRING1A-GENOMIC-R2)	5'-GCTTGCACAATGCTTCCTG-3'	sgRNA3-6
AtRING1A-GENOMIC seq-F3	5'-ATGAGCGTGGTACAGAAGTCC-3'	sgRNA7
AtRING1A-GENOMIC seq-R3	5'-AATCGAAATCCAAACTAACTGCA-3'	sgRNA7
AtRING1A-GENOMIC seq-F4	5'-GAGTGTAAGGAATGCCCGTG-3'	sgRNA8-9
AtRING1A-GENOMIC seq-R4 (AtRING1A-GENOMIC-R3)	5'-TATCTGAAGTGCAACGAACTGTAC-3'	sgRNA8-9
AtRING1A-cDNA seq-F1	5'-GAAGAATAGAGAGAGACGTAGAGAGAG-3'	
AtRING1A-cDNA seq-F2	5'-CGAATGTCCTGCTTGCAG-3'	
AtRING1A-cDNA seq-F3	5'-GGAACAACAAAACGCATCAG-3'	
AtRING1A-cDNA seq-F4	5'-AAGGCATGGGAATAATACTTCTG-3'	

Table V-6. Primers used for RT-qPCR

Name	Sequence
AtRING1A-qPCR-F	5'-ATCTCTGTTGCCGACCCACT-3'
AtRING1A-qPCR-R	5'-GCCGCATCTTCTCCTACTCT-3'
AtRING1B-qPCR-F	5'-TGAGAGGCAACGAAAAAAGC-3'
AtRING1B-qPCR-R	5'-AGTTCCACACAAGCACAGGT-3'
STM-qPCR-F	5'-GCAACACATCCTCACCATTACTTCA -3'
STM-qPCR-R	5'-ATCAAAGCATGGTGGAGGAGA-3'
KNAT2-qPCR-F	5'-AAACGCCATTGGAAGCCT-3'
KNAT2-qPCR-R	5'-ACAATGCACAATTTCATGTCTCTCT-3'

KNAT6-qPCR-F	5'-CCAAGAGAAGCAAGACAAGCTC-3'
KNAT6-qPCR-R	5'-CAGCTAATGCTATCTTATCTCCTTCAG-3'
CUC1-qPCR-F	5'-ACATTCCTTCCCGCTCCACC-3'
CUC1-qPCR-R	5'-AACTGACCAAACGCCACGCC-3'
CUC2-qPCR-F	5'-GAGCAACTGTGAGCGTAAGC-3'
CUC2-qPCR-R	5'-GGAGTGAGACGGAGGAAGGA-3'
CUC3-qPCR-F	5'-GGAACAACAACAACGACGAAG-3'
CUC3-qPCR-R	5'-AGACGAAAAACCCAACAGACC-3'
WOX5-qPCR-F	5'-CCAAGGTGGACAAAATGAGAG-3'
WOX5-qPCR-R	5'-ATGATGAGTATGGAGAAAACG-3'
ABI3-qPCR-F	5'-ATGTATCTCCTCGAGAACAC-3'
ABI3-qPCR-R	5'-CCCTCGTATCAAATATTTGCC-3'
DOG1-qPCR-F	5'-TAGGCTCGTTTATGCTTTGTGTGG-3'
DOG1-qPCR-R	5'-CGCACTTAAGTCGCTAAGTGATGC-3'
CRU1-qPCR-F	5'-CCGTGGATCTATCCGTCAAA-3'
CRU1-qPCR-R	5'-CAAACACTCTGTTACCATTGTCG-3'
CRU3-qPCR-F	5'-TGGCGTTCTCCAGGGTAAT-3'
CRU3-qPCR-R	5'-TGACCACTTGGATCCTTCCT-3'
SPL3-qPCR-F	5'-CTTAGCTGGACACAACGAGAGAAGGC-3'
SPL3-qPCR-R	5'-GAGAAACAGACAGAGACACAGAGGA-3'
MAF4-qPCR-F	5′-TGGCCAAGATCCTCAGTCGTTATGA-3′
MAF4-qPCR-R	5′-GCTGCTCTTCCAGGGACTTTAGACA-3′
MAF5-qPCR-F	5′-GATGGAGCTTGTGAAGAACCTTCAGG-3′
MAF5-qPCR-R	5′-CAGCCGTTGATGATTGGTGGTTACTTG-3′
FLC-qPCR-F	5'-CTAGCCAGATGGAGAATAATCATCATG-3'
FLC-qPCR-R	5'-TTAAGGTGGCTAATTAAGTAGTGGGAG-3'
FT-qPCR-F	5'-CTTGGCAGGCAAACAGTGTATGCAC-3'
FT-qPCR-R	5'-GCCACTCTCCCTCTGACAATTGTAGA-3'
SOC1-qPCR-F	5'-AGCTGCAGAAAACGAGAAGCTCTCTG-3'
SOC1-qPCR-R	5'-GGGCTACTCTCTTCATCACCTCTTCC-3'
EXP-qPCR-F	5'-GAGCTGAAGTGGCTTCAATGA-3'
EXP-qPCR-R	5'-GGTCCGACATACCCATGATCC-3'
Tip41-qPCR-F	5'-GTGAAAACTGTTGGAGAGAAGCAA-3'
Tip41-qPCR-R	5'-TCAACTGGATACCCTTTCGCA-3'
GAPDH-qPCR-F	5'-TTGGTGACAACAGGTCAAGCA-3'
GAPDH-qPCR-R	5'-AAACTTGTCGCTCAATGCAATC-3'

Table V-7. Primers used for ChIP-qPCR

Name	**Sequence**
STM-1F	5'-TTCCTGGTCTCTCTTCTGCTGCTT-3'
STM-1R	5'-AAGTGGTCTCCCGGGATTTATGCT-3'

STM-2F	5'-ATGGGACCAACAGGATGTCTAGGT-3'
STM-2R	5'-ACTCGACACGTTGAAGGAAGACCA-3'
KNAT2-1F	5'-CCTCAACTTGGCCAGTCTATCT-3'
KNAT2-1R	5'-AGCGGAAACCACACATTCTATC-3'
KNAT2-2F	5'-CTCGATTGGTGGAATGTTCATA-3'
KNAT2-2R	5'-AAACCTGTTTCTTCAGCCAGAG-3'
CUC1-1F	5'-GTGCCGACAATGGATGTTGATGTG-3'
CUC1-1R	5'-AACCCAGGTGGCATAAGGGATTC-3'
CUC1-2F	5'-GATGGCGTGGCGTTTGGT-3'
CUC1-2R	5'-CGTGGGAGGCAGAGAAGGTAGA-3'
CUC2-1F	5'-ACCACTGCACTTTTTCTCATGCACG-3'
CUC2-1R	5'-AAGAAACGAGGAATGGGCTCTTGT-3'
CUC2-2F	5'-GACAGCCAATATCTTCCACCGGG-3'
CUC2-2R	5'-GAGAAGCAACCGTCGAGGACT-3'
ABI3-1F	5'-GTTTAAGAACCACCGCTTGG-3'
ABI3-1R	5'-CTCCTCGTGCCGCTAGTATC-3'
ABI3-2F	5'-TCGGATCTTTTCATATGCTTTG-3'
ABI3-2R	5'-GAGATTCAAAAAGAACTCTTGATAAGG-3'
DOG1-1F	5'-TGGAACAACAACTCGCACTC-3'
DOG1-1R	5'-GTGCTTTCCGAGCAAATAAAA-3'
DOG1-2F	5'-TCTCGAGTGGATGAGTTTGC-3'
DOG1-2R	5'-TCTTCATCACCGTGAGATCG-3'
MAF3-F	5'-GTCTAGCCCAAAAGAAGAAGATAGAAACG-3'
MAF3-R	5'-GGAGGCAGAGTCGTAGAGTTTTCC-3'
MAF4-1F	5'-CCATAATTTAAATATGGTGGCCCA-3'
MAR4-1R	5'-AGCCGAACCAAATTTCAAACC-3'
MAF4-2F	5'-CGGCGAGTTATGCAGACATCACA-3'
MAR4-2R	5'-GTGGCAGAGATGATGATAAGAGCGA-3'
MAF4-3F	5'-ATTCTTGAATCCTCTGAAACTCCG-3'
MAR4-3R	5'-TGGACACCATCACAACTTTATTCAG-3'
MAF5-1F	5'-GTTTCTCATACAGCCCAATACATGC-3'
MAR5-1R	5'-GATTGGATTTAGTTCATTCCACCG-3'
MAF5-2F	5'-CAGGATCTCCGACCAGTTTATACAGAC-3'
MAR5-2R	5'-GAGGAGTTGTAGAGTTTGCCGGT-3'
MAF5-3F	5'-GAAAGAGAAAATTGTGTCCTGGAAA-3'
MAR5-3R	5'-CTCTATTGAATTGTTAGTTGTTCCGC-3'
FLC-1F	5'-ATTTAGCAACGAAAGTGAAAACTAAGG-3'
FLC-1R	5'-GCCACGTGTACCGCATGAC-3'
FLC-2F	5'-AGAAATCAAGCGAATTGAGAACAA-3'
FLC-2R	5'-CGTTGCGACGTTTGGAGAA-3'
FLC-3F	5'-CATCATGTGGGAGCAGAAGCT-3'

FLC-3R	5'-CGGAAGATTGTCGGAGATTTG-3'
ACT7-F	5'-CGTTTCGCTTTCCTTAGTGTTAGCT-3'
ACT7-R	5'-AGCGAACGGATCTAGAGACTCACCTTG-3'
TA3-F	5'-CGAAGACAGTTCCGCTTACC-3'
TA3-R	5'-GCTTGTTCCGATTGTTCGAT-3'
TUB2-F	5'-GACATCCCACCTACTGGTCTGAA-3'
TUB2-R	5'-CTCGCCTGAACATCTCTTGGA-3'

V.2. Methods

V.2.1. Plant methods

V.2.1.1. Seed sterilization

Seeds from transgenic T0 Arabidopsis plants transformed by CRIPSR/Cas9-sgRNA systems were surface sterilized with 70% ethanol for 40 minutes. Seeds used for the other experiments were sterilized successively by 70% and 95% ethanol for 10 min.

V.2.1.2. Germination test

The sterilized seeds were sown on 1/2 MS medium and stratified at 4°C for 3 days. Then the seeds were transferred to growth chamber at 22°C under LDs (16 hours light/8 hours dark). Germination rate was recorded daily for 8 days following stratification. Seeds with radicle protruded beyond the testa were considered to have germinated. Germination test comprised 3 replications of roughly 100 seeds on each plate.

V.2.1.3. Arabidopsis transformation

The binary vectors were introduced to *Agrobacterium tumefaciens* GV3101, and all the resulting strains were used for transforming Arabidopsis plants by the floral-dip method. The protocol was similar to the one previously described (Zhang et al. 2006).

After harvesting Agrobacterium cells by centrifugation, the pellet was washed once by

floral dip inoculation medium without Silwet L-77. Then the bacteria were resuspended by the floral dip inoculation medium (same volume with cell culture). After 2 to 3 hours, plants were submerged in the bacteria solution for 30 seconds and the dipping was repeated after 15 minutes. The same manipulation was performed again after one week.

Inoculation medium: 1/2 MS medium, 5% sucrose, 0.02% Silwet L-77, pH5.8

V.2.1.4. Fat red staining

Whole seedlings were incubated in saturated Fat red solution [Fat red 7B (Sigma-Aldrich) powder dissolved with 70% Ethanol] for 2 hours and then washed 3 times with water.

V.2.1.5. Plant growth analysis

To analyze leaf development, twenty 35-day-old plants grown under LDs were evaluated: Rosette width was measured as the maximum diameter of rosette in one plant; leaf length was the maximum vertical diameter from leaf tip to the center of the rosette; leaf width was the cross diameter of the widest leave; petiole length was the length of the longest petiole. Flowering time was measured from the sowing day to the day when the floral shoot was longer than 0.5 cm.

For root length comparison, mutant and control plants were grown side by side on a same plate. Root length was measured from the root tip to the root/hypocotyl border of vertically grown seedlings *via* ImageJ software. The lengths of RAM, proliferation domain and transition domain were measured according to the defined criteria (Napsucialy-Mendivil et al. 2014). In mature embryo, the number of cortex cells was counted in a cell file extending from QC to hypocotyl rootward border; the maximum number of columella cell layers was counted in the columella cell cap including initials. All the above experiments were repeated three times (mean ± SE), each repeat

containing at least 15 plants.

V.2.1.6. Histology and microscopy

GUS staining assay was performed as described (Chen et al. 2010). Briefly, whole seedlings were sequentially treated by fixative cold acetone for 30 min, and GUS staining buffer at 37℃ in the dark for 4 h. Samples were cleared overnight in 90% lactic acid and were photographed with a differential interference contrast (DIC) microscope (Leica). For whole-mount visualization, the roots were directly cleared in choral hydrate solution. For starch granule staining, roots were stained with Lugol solution (Chen et al, 2010). For florescent microscope observation, the roots were counterstained with 20 μg/ml of propidium iodide (PI). Mature embryos and root tips were stained *via* the mPS-PI method (Truernit et al. 2008), or mature embryos were also stained with Aniline-blue as previously described (Bougourd et al. 2000).

For young embryo observation, embryos at different stages were dissected from developing seeds with tweezers and fine syringe needles, and were stained with newly-developed cell-wall dye SCRI Renaissance 2200 (SR2200) as described (Musielak et al. 2015).

GUS staining buffer: 100 mM phosphate buffer, pH 7.4, 2 mM ferricyanide, and 0.5 mM ferrocyanide, and 4 mM X-Gluc

Choral hydrate solution: chloral hydrate/ glycerol/H_2O, 8/2/1, m/v/v

V.2.1.7. Flow cytometry

Nuclei were prepared from roots of 1-week-old plants and analyzed on an Attune™ Acoustic Focusing Cytometer (Applied Biosystems, USA). Typically, 10,000 nuclei per sample from at least 100 WT roots and 200 mutant roots were analyzed. Three replicates were performed for each sample. Endoreduplication index (EI) which represents the

average number of endocycles undergone by a typical nucleus (EI = [0 · n2C + 1 · n4C + 2 · n8C + 3 · n16C] / [n2C + n4C + n8C + n16C]) was calculated as published (Vanstraelen et al. 2009; Barow and Meister 2003).

V.2.2. Bacterial methods

V.2.2.1. Preparation of competent cells for heat shock transformation

A single bacterial colony was inoculated in 1 ml LB medium and incubated with shaking at 37 °C overnight. The culture was used to inoculate 100 ml LB (1: 100) and incubated by shaking at 37 °C until OD_{600} value reaches 0.3-0.5. The cell culture was chilled in ice for 10 minutes and harvested by centrifugation at 3000 g for 10 minutes at 4 °C. After pouring off the supernatant, the pellet was resuspended gently in 10 ml of ice-cold 0.05 M $CaCl_2$ solution and placed on ice for 30 minutes. After centrifugation at 3000 g for 10 minutes at 4 °C, the supernatant was discarded and cells were resuspended gently in 4 ml of ice-cold 0.05 M $CaCl_2$ (15% glycerol) on ice. The competent cells were then dispensed into 50 µl aliquots, frozen in liquid nitrogen and stored in -80 °C.

LB medium: 10 g/ L Tryptone; 5 g/ L Yeast extract; 10 g/ L NaCl

V.2.2.2. Preparation of *Agrobacterium* competent cells for electroporation

A single colony of the *Agrobacterium* strain was inoculated in 2 ml LB (rifampicin 40 mg/L, gentamycin 50mg/L) and incubated with shaking at 30 °C overnight. The fresh culture was used to inoculate 400 ml fresh SOB medium and incubated by shaking at 30 °C until OD_{600} value reaches 0.5 to 1.0. Cells were harvested in chilled flask by spinning at 3600 rpm for 10 minutes at 4 °C and resuspended twice in 40 ml ice-cold 10% glycerol and one time in 18 ml of ice-cold 10% glycerol. After centrifugation at 3600 rpm for 10 minutes at 4 °C, supernatant was poured off and cells were resuspended gently in 1 ml ice-cold 10% glycerol. The competent cells were then dispensed into 50

μl aliquots and quick-frozen in liquid nitrogen and stored at -80 °C.

SOB medium: Trypton 20 g/L, Yeast extract 5 g/L, NaCl 0.5 g/L

V.2.2.3. Heat shock transformation

After a short incubation in ice, a mixture of DNA and 50 μl chemically competent bacteria was placed at 42 °C for 45 seconds and then placed back in ice for 2 to 5 minutes. Added LB media and incubated the transformed cells at 37 °C for 1 hour with agitation. Centrifuged the cell culture at 4000 to 5000 rpm for 1 minute; removed the supernatant with 100 μl left. Resuspended the cell culture and evenly spread on LB medium containing antibiotics. The inverted plates were incubated at 37 °C for 12-16 hours.

V.2.2.4. Transformation of *Agrobacterium via* electroporation

Agrobacterium GV3101 competent cells were thawed in ice and mixed with 0.5 μl (6-10 ng/μl) DNA gently. The mixture was transferred to the chilled electroporation cuvette, and 2.5 V was applied using the Gene Pulse (Bio red). Following the pulse, the cells were removed to polypropylene tube and mixed with LB medium. The transformed cells were incubated at 28 °C for 2 hours. 300 μl cell culture was spread on LB medium supplied with gentamicin, rifampicin and other corresponding antibiotics. The inverted plates were incubated at 28 °C for 2 days.

V.2.3. Nucleic acid techniques

V.2.3.1. Plant DNA analysis

1. Collected plant materials (one leaf disk, 0.5 cm in diameter) and put it in 96-well plate for tissue lyser filled with metal beads.

2. Added 500 µl of Edwards buffer in each well and crashed the tissue with machine (2x 1 minute, 25 fpm).

3. Spun the plate at 3700 rpm for 10 minutes at room temperature.

4. Filled each well of 96-well PCR plate with isopopanol. Transferred 100 µl of supernatant into the PCR plant and mixed supernatant with isopropanol. Centrifuged the plate at 3700 rpm for 15 min.

5. Removed the supernatant and dried the plate for 2 hours. Resuspended the DNA with water and stored the plate in 4°C overnight. The DNA was ready to be used for PCR.

Edwards buffer: 200 mM Tris-HCl (pH 7.5), 250 mM NaCl, 25 mM EDTA, 0.5% SDS

V.2.3.2. RNA isolation and reverse transcription

For the 12-day-old seedlings, total RNA was isolated using TRI Reagent (Molecular research center, https://www.mrcgene.com/) according to the manufacturer's instruction.

For the 7-day-old roots, total RNA was isolated from 7-day-old roots using the NucleoSpin RNA Plant kit (Macherey-Nagel, Germany).

For the seeds/seedlings at 0, 24 and 72 HAS, total RNA was extracted as previously described (Ramakers et al. 2003). After treatment with DNAase (Promega, http://www.promega.com), complementary DNA was synthesized using a reverse transcription kit (Promega) according to the manufacturer's recommendation.

V.2.3.3. Gene expression analysis

Quantitative RT-PCR was performed in triplicate with LightCycler® 480 SYBR Green I Master (Roche) in a light cycler 480II (Roche), according to the manufacturer's instructions. Reaction volumes were scaled to 10 µl comprising 5 µl of SYBR Green PCR master mix, 2 µl of primer mix, 2µl H_2O and 1 µl of template. The expressions of

GAPDH, *EXP*, *Tip41* (for chapter II) and *PP2A* (for chapter III) were used as internal control. For Semi-quantitative RT-PCR analyses, *ACTIN2* was used as endogenous control.

V.2.4. Protein techniques

V.2.4.1. Nuclear protein extraction

12-day-old Arabidopsis seedlings grown under LD were harvested in liquid nitrogen to a quantity of about 3 ml. Then nuclear protein extraction steps are as listed below.

1. Ground the tissues to a fine powder in liquid nitrogen

2. Added 40 ml cold Lysis buffer to homogenize the power by vortex and placed on a rotation wheel for 20 minutes at 4 °C.

3. Filtered the solution through a 100 µm nylon mesh.

4. Centrifuged the filtered homogenate at 4000 rpm at 4 °C for 20 minutes to pellet the nuclei and discarded the supernatant as completely as possible.

5. Washed the pellet in 2 ml Lysis Buffer and transferred it to a 2 ml tube.

6. Centrifuged the solution at 4000 rpm at 4 °C for 20 minutes and removed the supernatant.

7. Resuspended the pellet in 150 µl 1 x SDS loading buffer by vortexing.

8. Added DTT and incubated at 95 °C for 10 min.

9. Spun the sample at 12000 rpm at 25 °C for 5 min.

10. Removed the supernatant to a new tube. Dispensed aliquots of 20 µl and stored at -20 °C.

Reagent:

Low salt wash buffer (200 ml): 0.05 M HEPES pH 7.5, 0.15 M NaCl, 0.25 mM EDTA

Lysis Buffer (50 ml): 45 ml low salt wash buffer, 500 µl Triton X-100, 5 ml glycerol, 50 µl EDTA-free Protease Inhibitor Cocktail, 20 µl β-mercaptoethanol

TE buffer: 10 mM Tris-HCl pH 8.0, 1 mM EDTA pH 8.0

1 x SDS loading buffer: 62.5 mM Tris-HCl pH 6.8, 3% SDS, 10% glycerol, 0.1% Bromophenol blue, 5 mM DTT (add before use)

V.2.4.2. Histone extraction

Samples of approximately 1g of Arabidopsis leaves from 12-day-old seedlings grown under LDs were ground to be fine powder in liquid nitrogen and homogenized in solution A. The resulting slurry was incubated at 4 °C by rotating for 30 min. Then filtered the slurry through 3 layers of 100 µm nylon meshes. The filtrate was centrifuged at 4000 rpm for 20 minutes at 4 °C. The pellet was washed by resuspending in solution B and centrifuging at 13000 rpm for 10 minutes. Following this wash, the pelleted chromatin was homogenized in solution C and centrifuged at 13000rpm for 1 hour. Resuspended the pellet with 0.4 M H_2SO_4, sonicated 5 minutes (30 seconds ON and 30 seconds OFF at high power) with a Bioruptor (Diagenode) and incubated on wheel at 4 °C overnight. Spun 5 minutes at 13000 rpm, kept the supernatant and treated the pellet with 0.4 M H_2SO_4 again. Combined the supernatant and precipitated the protein with 33% TCA overnight. The precipitated proteins were washed once by acetone, air-dried and resuspended with 4 M urea.

solution A: 0.4 M sucrose, 10 mM Tris-HC1 pH 8, 10 mM $MgC1_2$, 5mM β-mercaptoethanol, 1mM PMSF

solution B: 0.25 M sucrose, 10 mM Tris-HCl pH 8, 10 mM $MgCl_2$, 1% Triton X-100, 5mM β-mercaptoethanol, 1mM PMSF

solution C: 1.7 M sucrose, 10 mM Tris-HCl pH 8, 0.15% Triton X-100, 2 mM $MgC1_2$, 5mM β-mercaptoethanol, 1mM PMSF

V.2.4.3. Western Blot analysis

Extracted proteins (in 1×SDS loading buffer) were boiled at 95°C for 10 min. The lysate was then centrifuged at 13200 rpm at room temperature for 15 minutes to remove debris. Then equal amount of protein samples were separated on 15% SDS/PAGE gels, transferred to a PVDF membrane (Roche) and probed with anti-H2Aub1, -H3K27me3 or -H3. The dilutions of antibody are listed below. The visualization was realized by ECL (Milipore) chemiluminesence detection system (Bio-Rad).

Table V-8. The dilution of antibodies used in this thesis.

Antibody	Dilution of primary antibody	Dilution of secondary antibody
H2Aub1	1:2000(BSA)	1:5000(BSA)
H3K27me3	1:1000(milk)	1:2000(milk)
H3	1:10000(milk)	1:20000(milk)

V.2.4.4. Chromatin ImmunoPrecipitation (ChIP)

ChIP assay was performed according to a previously described method (Saleh et al. 2008) with modifications.

Cross-linking

1. 1 g 12-day-old Arabidopsis seedlings grown in 1/2 MS medium under LD were harvested in 100 ml Fixation buffer. Applied vacuum for 8 minutes twice at room temperature for cross-linking.

2. Stopped the cross-linking reaction by adding 10 ml of 2.6 M glycine.

Chromatin isolation and sonication

3. Washed plant tissues five times in deionized water, removed the water as much as

possible by blotting the tissues between paper towels and quick-freezed in liquid nitrogen.

4. Ground the tissue to a fine powder in liquid nitrogen and ensured that the samples do not thaw during grinding.

5. Resuspended each sample in 40 ml of cold Extraction buffer I.

6. Vortexed violently to mix and put the samples on wheel at 4°C until complete homogenization was achieved (15 min).

7. Filtered the homogenized slurry through three layers of cheesecloth and centrifuged the filtrate at 2800g for 20 min.

8. Discarded the supernatants and resuspended the pellet (nuclei) in 1 ml of cold Extraction buffer II; centrifuged at 12000g for 10 min.

9. Discarded the supernatants and resuspended the pellet (nuclei) in 300 µl fresh prepared sonication buffer. Sheared the DNA into ~200 bp fragments by sonicating with a Bioruptor (Diagenode) for four times of 5 minutes (30s/30s) at power 6. Put ice to chill the sonicator at each interval.

10. To test the sonication efficiency, mixed 10 µl of the samples with 10µl phenol:chloroform. Vortexed and spun the mixture at 12000 rpm for 3 minutes at 4°C.

11. Checked the size of the DNA fragment by agarose gel electrophoresis. A smear from 200 to 1000 bp, but concentrated 200 bp should be observed in the sonicated samples.

12. Centrifuged samples for 5 minutes at 16000 g at 4°C and kept the supernatant. Repeated the manipulation for another time.

Immunoprecipitation

13. Washed the Protein A magnetic beads for three times with antibody binding buffer (40 µl beads: 1 ml buffer). Incubated 2 µl antibody with beads in 180 µl antibody

binding buffer on wheel at 4°C for 1 hour. An additional aliquot of the same sample was included to be treated in the same way but without antibody to serve as negative control.

14. Took a 20 µl aliquot from the sonicated chromatin sample (from Step 13) and added to mixture prepared in 13. Incubated on wheel at 4°C overnight.

15. The beads were pelleted using a Magana GrIP racks (Millipore) and washed successively with 1ml of low salt wash buffer, high salt wash buffer, LiCl wash buffer and TE buffer under rotation at 4 °C for 5 min, then removed TE buffer as much as possible.

Reverse cross-linking and protein digestion

16. The beads-antibody chromatin complex and 10 µl sonicated chromatin (from Step 12, serve as an input) were eluted in freshly prepared 100 µl elution buffer with 1 µl of protease K and incubated at 62 °C overnight under agitation (950rpm).

17. The beads were pelleted by the Magna GrIP rack and the supernatant was transferred to a new 1.5 ml tube. DNA was recovered by NucleoSpin® Gel and PCR Cleanup kit (MACHEREY-NAGEL, Germany) and was then used for quantitative real-time PCR analysis.

Fixation buffer: 0.4 M sucrose; 10 mM Tris-HCl pH 8.0; 5 mM EDTA pH 8.0; 3% Formaldehyde; 5 mM β-mercaptoethanol; 1mM PMSF

Extraction buffer I: 0.4 M sucrose; 10 mM Tris-HCl pH 8.0; 5 mM β-mercaptoethanol; 10 mM $MgCl_2$; 1 mM PMSF

Extraction buffer II: 0.25 M sucrose; 10 mM Tris-HCl pH 8.0; 5 mM β-mercaptoethanol; 10mM $MgCl_2$; 1% Triton X-100; Protease Inhibitor Cocktail (1 tablet in 50ml)

Sonication buffer: 25 mM Tris-HCl pH 8.0; 5 mM EDTA; 0.5% SDS; Protease Inhibitor Cocktail, without EDTA (cOmplete; Roche) (1 tablet in 50 ml)

Antibody binding buffer: 50 mM Tris-HCl pH 8.0; 1 mM EDTA pH 8.0; 150 mM NaCl; 0.1% Triton X-100

Low salt wash buffer: 150 mM NaCl; 0.1% SDS; 1% Triton X-100; 2 mM EDTA pH 8.0; 20 mM Tris-HCl pH 8.0

High salt wash buffer: 500 mM NaCl; 0.1% SDS; 1% Triton X-100; 2 mM EDTA pH 8.0; 20 mM Tris-HCl pH 8.0

LiCl wash buffer: 0.25 M LiCl; 1% NP-40; Sodium desoxycholate 1%; 20 mM Tris-HCl pH 8.0; 1 mM EDTA pH 8.0

TE buffer: 1 mM Tris-HCl pH 8.0; 10 mM EDTA pH 8.0

Elution buffer: 1% SDS; 0.1 M $NaHCO_3$； 100 mM NaCl

V.2.5. Generation of Arabidopsis transgenic plants using CRISPR/Cas9 system

V.2.5.1. Plasmid construction and plant transformation

Plasmid constructions of AtU6-26-target-sgRNA and p*YAO*:hSpCas9-target-sgRNA was performed as previously published (Yan et al. 2015b). The double-target site sgRNAs (sgRNA1, sgRNA3, sgRNA7) were designed as follows: individual targeting sequence was inserted to the AtU6-26-target-sgRNA, and then their sgRNA expression cassettes were combined to p*YAO*:hSpCas9-target-sgRNA successively.

The binary vectors were transformed into *Agrobacterium* strain GV3101 using electroporation method. Transformation of Arabidopsis was performed by the floral dip method.

V.2.5.2. Screen of T1 transgenic plants for edited mutation

The T1 seeds were screened on 1/2 MS medium supplied with 200 mg/L carbenicillin

and 35 mg/L hygromycin. To screen for the genome-edited plants, DNA of all the T1 transgenic plants was isolated by Edward buffer. PCR was performed using goTag G2 flex DNA polymerase (Promega) with primers located at around 350 bp of the target. The PCR products were delivered to be sequenced (2 μl PCR product, 2 μl H_2O, 1 μl primer). The sequencing primers were designed to be 150 bp around the target sequence. The sequencing results were analyzed by the software Chromas.

V.2.5.3. Screen of T2/3 transgenic plants for genome edited homozygotes

Seeds of 5 T2 lines for each construct were selected by hygromycin. The lines with one insertion loci of CRISPR Cas9, which exhibited the expected 3:1 Mendelian segregation pattern (live: dead~3:1), were selected. 48 T2 plants per line were cultured, extracted DNA, and Cas9 amplification. The target regions of all Cas9-free plants were amplified and sequenced. The same manipulation was repeated for the progeny of T2 homozygotes to confirm the heritability of the mutations.

V.2.5.4. Sequencing of AtRING1A

Total RNA was isolated from the 12-day-old plants grown under LDs. After the treatment with DNAase I and synthesis of complementary DNA, *AtRING1A* was amplified from 140 bp upsteam of start codon to 91 bp downsteam of stop codon with primer AtRING1A-(-140)-F and AtRING1A-(+1638)-R. The PCR product was sequenced directly using primers AtRING1A-cDNAseq-F1 to F4 listed in table 1.

Chapter VI

REFERENCES

Abe M, Kobayashi Y, Yamamoto S, Daimon Y, Yamaguchi A, Ikeda Y, Ichinoki H, Notaguchi M, Goto K, Araki T (2005) FD, a bZIP protein mediating signals from the floral pathway integrator FT at the shoot apex. Science 309 (5737):1052-1056. doi:10.1126/science.1115983

Abou-Elwafa SF, Buttner B, Chia T, Schulze-Buxloh G, Hohmann U, Mutasa-Gottgens E, Jung C, Muller AE (2011) Conservation and divergence of autonomous pathway genes in the flowering regulatory network of Beta vulgaris. J Exp Bot 62 (10):3359-3374. doi:10.1093/jxb/erq321

Adenot X, Elmayan T, Lauressergues D, Boutet S, Bouche N, Gasciolli V, Vaucheret H (2006) DRB4-dependent TAS3 trans-acting siRNAs control leaf morphology through AGO7. Curr Biol 16 (9):927-932. doi:10.1016/j.cub.2006.03.035

Adli M (2018) The CRISPR tool kit for genome editing and beyond. Nat Commun 9 (1):1911. doi:10.1038/s41467-018-04252-2

Aichinger E, Villar CB, Di Mambro R, Sabatini S, Kohler C (2011) The CHD3 chromatin remodeler PICKLE and polycomb group proteins antagonistically regulate meristem activity in the Arabidopsis root. Plant Cell 23 (3):1047-1060. doi:10.1105/tpc.111.083352

Aida M, Beis D, Heidstra R, Willemsen V, Blilou I, Galinha C, Nussaume L, Noh YS, Amasino R, Scheres B (2004) The PLETHORA genes mediate patterning of the Arabidopsis root stem cell niche. Cell 119 (1):109-120. doi:10.1016/j.cell.2004.09.018

Aida M, Ishida T, Fukaki H, Fujisawa H, Tasaka M (1997) Genes involved in organ separation in Arabidopsis: an analysis of the cup-shaped cotyledon mutant. Plant Cell 9 (6):841-857. doi:10.1105/tpc.9.6.841

Ali I, Conrad RJ, Verdin E, Ott M (2018) Lysine Acetylation Goes Global: From Epigenetics to Metabolism and Therapeutics. Chem Rev 118 (3):1216-1252. doi:10.1021/acs.chemrev.7b00181

Alkema MJ, Bronk M, Verhoeven E, Otte A, van 't Veer LJ, Berns A, van Lohuizen M (1997) Identification of Bmi1-interacting proteins as constituents of a multimeric mammalian polycomb complex. Genes Dev 11 (2):226-240

Allen E, Xie Z, Gustafson AM, Carrington JC (2005) microRNA-directed phasing during trans-acting siRNA biogenesis in plants. Cell 121 (2):207-221. doi:10.1016/j.cell.2005.04.004

An H, Roussot C, Suarez-Lopez P, Corbesier L, Vincent C, Pineiro M, Hepworth S, Mouradov A, Justin S, Turnbull C, Coupland G (2004) CONSTANS acts in the phloem to regulate a systemic signal that induces photoperiodic flowering of Arabidopsis. Development 131 (15):3615-3626. doi:10.1242/dev.01231

Ariel F, Jegu T, Latrasse D, Romero-Barrios N, Christ A, Benhamed M, Crespi M (2014) Noncoding transcription by alternative RNA polymerases dynamically regulates an auxin-driven chromatin loop. Mol Cell 55 (3):383-396. doi:10.1016/j.molcel.2014.06.011

Ashtiyani RK, Moghaddam AM, Schubert V, Rutten T, Fuchs J, Demidov D, Blattner FR, Houben A (2011) AtHaspin phosphorylates histone H3 at threonine 3 during mitosis and contributes to embryonic patterning in Arabidopsis. Plant J 68 (3):443-454. doi:10.1111/j.1365-313X.2011.04699.x

Aukerman MJ, Sakai H (2003) Regulation of flowering time and floral organ identity by a MicroRNA and its APETALA2-like target genes. Plant Cell 15 (11):2730-2741. doi:10.1105/tpc.016238

Bajusz I, Kovács G, Pirity M (2018) From Flies to Mice: The Emerging Role of Non-Canonical PRC1 Members in Mammalian Development. Epigenomes 2 (1):4. doi:10.3390/epigenomes2010004

Bannister AJ, Kouzarides T (2011) Regulation of chromatin by histone modifications. Cell Res 21 (3):381-395. doi:10.1038/cr.2011.22

Bao Y, Shen X (2011) SnapShot: Chromatin remodeling: INO80 and SWR1. Cell 144 (1):158-158 e152. doi:10.1016/j.cell.2010.12.024

Barow M, Meister A (2003) Endopolyploidy in seed plants is differently correlated to systematics, organ, life strategy and genome size. Plant, Cell & Environment 26 (4):571–584. doi:10.1046/j.1365-3040.2003.00988.x

Barrero JM, Gonzalez-Bayon R, del Pozo JC, Ponce MR, Micol JL (2007) INCURVATA2 encodes the catalytic subunit of DNA Polymerase alpha and interacts with genes involved in chromatin-mediated cellular memory in Arabidopsis thaliana. Plant Cell 19 (9):2822-2838. doi:10.1105/tpc.107.054130

Bartholomew B (2014) Regulating the chromatin landscape: structural and mechanistic perspectives. Annu Rev Biochem 83:671-696. doi:10.1146/annurev-biochem-051810-093157

Beh LY, Colwell LJ, Francis NJ (2012) A core subunit of Polycomb repressive complex 1 is broadly conserved in function but not primary sequence. Proc Natl Acad Sci U S A 109 (18):E1063-1071. doi:10.1073/pnas.1118678109

Belotserkovskaya R, Oh S, Bondarenko VA, Orphanides G, Studitsky VM, Reinberg D (2003) FACT facilitates transcription-dependent nucleosome alteration. Science 301 (5636):1090-1093. doi:10.1126/science.1085703

Bennett T, van den Toorn A, Willemsen V, Scheres B (2014) Precise control of plant stem cell activity through parallel regulatory inputs. Development 141 (21):4055-4064. doi:10.1242/dev.110148

Berger SL (2007) The complex language of chromatin regulation during transcription. Nature 447 (7143):407-412. doi:10.1038/nature05915

Berke L, Snel B (2015) The plant Polycomb repressive complex 1 (PRC1) existed in the ancestor of seed plants and has a complex duplication history. BMC Evol Biol 15:44. doi:10.1186/s12862-015-0319-z

Berry S, Rosa S, Howard M, Buhler M, Dean C (2017) Disruption of an RNA-binding hinge region abolishes LHP1-mediated epigenetic repression. Genes Dev 31 (21):2115-2120. doi:10.1101/gad.305227.117

Bezsonova I, Walker JR, Bacik JP, Duan S, Dhe-Paganon S, Arrowsmith CH (2009) Ring1B contains a ubiquitin-like docking module for interaction with Cbx proteins. Biochemistry-Us 48 (44):10542-10548. doi:10.1021/bi901131u

Black JC, Van Rechem C, Whetstine JR (2012) Histone lysine methylation dynamics: establishment, regulation, and biological impact. Mol Cell 48 (4):491-507. doi:10.1016/j.molcel.2012.11.006

Blackledge NP, Rose NR, Klose RJ (2015) Targeting Polycomb systems to regulate gene expression: modifications to a complex story. Nat Rev Mol Cell Biol 16 (11):643-649. doi:10.1038/nrm4067

Blilou I, Frugier F, Folmer S, Serralbo O, Willemsen V, Wolkenfelt H, Eloy NB, Ferreira PC, Weisbeek P, Scheres B (2002) The Arabidopsis HOBBIT gene encodes a CDC27 homolog that links the plant cell cycle to progression of cell differentiation. Genes Dev 16 (19):2566-2575. doi:10.1101/gad.237302

Blilou I, Xu J, Wildwater M, Willemsen V, Paponov I, Friml J, Heidstra R, Aida M, Palme K, Scheres B (2005) The PIN auxin efflux facilitator network controls growth and patterning in Arabidopsis roots. Nature 433 (7021):39-44. doi:10.1038/nature03184

Bloomer RH, Dean C (2017) Fine-tuning timing: natural variation informs the mechanistic basis of the switch to flowering in Arabidopsis thaliana. J Exp Bot 68 (20):5439-5452. doi:10.1093/jxb/erx270

Boss PK, Bastow RM, Mylne JS, Dean C (2004) Multiple pathways in the decision to flower: enabling, promoting, and resetting. Plant Cell 16 Suppl:S18-31. doi:10.1105/tpc.015958

Boudolf V, Lammens T, Boruc J, Van Leene J, Van Den Daele H, Maes S, Van Isterdael G, Russinova E, Kondorosi E, Witters E, De Jaeger G, Inze D, De Veylder L (2009) CDKB1;1 forms a functional complex with CYCA2;3 to suppress endocycle onset. Plant Physiol 150 (3):1482-1493. doi:10.1104/pp.109.140269

Bougourd S, Marrison J, Haseloff J (2000) Technical advance: an aniline blue staining procedure for confocal microscopy and 3D imaging of normal and perturbed

cellular phenotypes in mature Arabidopsis embryos. Plant J 24 (4):543-550

Boukarabila H, Saurin AJ, Batsche E, Mossadegh N, van Lohuizen M, Otte AP, Pradel J, Muchardt C, Sieweke M, Duprez E (2009) The PRC1 Polycomb group complex interacts with PLZF/RARA to mediate leukemic transformation. Genes Dev 23 (10):1195-1206. doi:10.1101/gad.512009

Boureau L, How-Kit A, Teyssier E, Drevensek S, Rainieri M, Joubes J, Stammitti L, Pribat A, Bowler C, Hong Y, Gallusci P (2016) A CURLY LEAF homologue controls both vegetative and reproductive development of tomato plants. Plant Mol Biol 90 (4-5):485-501. doi:10.1007/s11103-016-0436-0

Bouyer D, Roudier F, Heese M, Andersen ED, Gey D, Nowack MK, Goodrich J, Renou JP, Grini PE, Colot V, Schnittger A (2011) Polycomb repressive complex 2 controls the embryo-to-seedling phase transition. PLoS Genet 7 (3):e1002014. doi:10.1371/journal.pgen.1002014

Bowman GD, Poirier MG (2015) Post-Translational Modifications of Histones That Influence Nucleosome Dynamics. Chem Rev 115 (6):2274-2295. doi:10.1021/cr500350x

Boycheva I, Vassileva V, Iantcheva A (2014) Histone acetyltransferases in plant development and plasticity. Curr Genomics 15 (1):28-37. doi:10.2174/1389202915011403061127 42

Brahma S, Udugama MI, Kim J, Hada A, Bhardwaj SK, Hailu SG, Lee TH, Bartholomew B (2017) INO80 exchanges H2A.Z for H2A by translocating on DNA proximal to histone dimers. Nat Commun 8:15616. doi:10.1038/ncomms15616

Bratzel F, Lopez-Torrejon G, Koch M, Del Pozo JC, Calonje M (2010) Keeping cell identity in Arabidopsis requires PRC1 RING-finger homologs that catalyze H2A monoubiquitination. Curr Biol 20 (20):1853-1859. doi:10.1016/j.cub.2010.09.046

Bratzel F, Yang C, Angelova A, Lopez-Torrejon G, Koch M, del Pozo JC, Calonje M (2012) Regulation of the new Arabidopsis imprinted gene AtBMI1C requires the interplay of different epigenetic mechanisms. Molecular plant 5 (1):260-269. doi:10.1093/mp/ssr078

Bu ZY, Yu Y, Li ZP, Liu YC, Jiang W, Huang Y, Dong AW (2014) Regulation of Arabidopsis Flowering by the Histone Mark Readers MRG1/2 via Interaction with CONSTANS to Modulate FT Expression. Plos Genetics 10 (9). doi:ARTN e1004617

10.1371/journal.pgen.1004617

Bungard D, Fuerth BJ, Zeng PY, Faubert B, Maas NL, Viollet B, Carling D, Thompson

CB, Jones RG, Berger SL (2010) Signaling kinase AMPK activates stress-promoted transcription via histone H2B phosphorylation. Science 329 (5996):1201-1205. doi:10.1126/science.1191241

Butenko Y, Ohad N (2011) Polycomb-group mediated epigenetic mechanisms through plant evolution. Biochim Biophys Acta 1809 (8):395-406. doi:10.1016/j.bbagrm.2011.05.013

Calonje M, Sanchez R, Chen L, Sung ZR (2008) EMBRYONIC FLOWER1 participates in polycomb group-mediated AG gene silencing in Arabidopsis. Plant Cell 20 (2):277-291. doi:10.1105/tpc.106.049957

Carles CC, Fletcher JC (2009) The SAND domain protein ULTRAPETALA1 acts as a trithorax group factor to regulate cell fate in plants. Genes Dev 23 (23):2723-2728. doi:10.1101/gad.1812609

Cartagena JA, Matsunaga S, Seki M, Kurihara D, Yokoyama M, Shinozaki K, Fujimoto S, Azumi Y, Uchiyama S, Fukui K (2008) The Arabidopsis SDG4 contributes to the regulation of pollen tube growth by methylation of histone H3 lysines 4 and 36 in mature pollen. Dev Biol 315 (2):355-368. doi:10.1016/j.ydbio.2007.12.016

Chadee DN, Hendzel MJ, Tylipski CP, Allis CD, Bazett-Jones DP, Wright JA, Davie JR (1999) Increased Ser-10 phosphorylation of histone H3 in mitogen-stimulated and oncogene-transformed mouse fibroblasts. J Biol Chem 274 (35):24914-24920

Chagraoui J, Niessen SL, Lessard J, Girard S, Coulombe P, Sauvageau M, Meloche S, Sauvageau G (2006) E4F1: a novel candidate factor for mediating BMI1 function in primitive hematopoietic cells. Genes Dev 20 (15):2110-2120. doi:10.1101/gad.1453406

Chanvivattana Y, Bishopp A, Schubert D, Stock C, Moon YH, Sung ZR, Goodrich J (2004) Interaction of Polycomb-group proteins controlling flowering in Arabidopsis. Development 131 (21):5263-5276. doi:10.1242/dev.01400

Chaudhury AM, Ming L, Miller C, Craig S, Dennis ES, Peacock WJ (1997) Fertilization-independent seed development in Arabidopsis thaliana. Proc Natl Acad Sci U S A 94 (8):4223-4228

Chen D, Molitor A, Liu C, Shen WH (2010) The Arabidopsis PRC1-like ring-finger proteins are necessary for repression of embryonic traits during vegetative growth. Cell Res 20 (12):1332-1344. doi:10.1038/cr.2010.151

Chen D, Molitor AM, Xu L, Shen WH (2016) Arabidopsis PRC1 core component AtRING1 regulates stem cell-determining carpel development mainly through repression of class I KNOX genes. BMC Biol 14 (1):112. doi:10.1186/s12915-016-0336-4

Chen DH, Huang Y, Liu C, Ruan Y, Shen WH (2014) Functional conservation and divergence of J-domain-containing ZUO1/ZRF orthologs throughout evolution. Planta 239 (6):1159-1173. doi:10.1007/s00425-014-2058-6

Chen LJ, Diao ZY, Specht C, Sung ZR (2009) Molecular evolution of VEF-domain-containing PcG genes in plants. Molecular plant 2 (4):738-754. doi:10.1093/mp/ssp032

Chen Z, Tan JL, Ingouff M, Sundaresan V, Berger F (2008) Chromatin assembly factor 1 regulates the cell cycle but not cell fate during male gametogenesis in Arabidopsis thaliana. Development 135 (1):65-73. doi:10.1242/dev.010108

Chen ZJ, Tian L (2007) Roles of dynamic and reversible histone acetylation in plant development and polyploidy. Biochim Biophys Acta 1769 (5-6):295-307. doi:10.1016/j.bbaexp.2007.04.007

Cheng JZ, Zhou YP, Lv TX, Xie CP, Tian CE (2017) Research progress on the autonomous flowering time pathway in Arabidopsis. Physiol Mol Biol Plants 23 (3):477-485. doi:10.1007/s12298-017-0458-3

Cheung P, Tanner KG, Cheung WL, Sassone-Corsi P, Denu JM, Allis CD (2000) Synergistic coupling of histone H3 phosphorylation and acetylation in response to epidermal growth factor stimulation. Mol Cell 5 (6):905-915

Cheutin T, Cavalli G (2018) Loss of PRC1 induces higher-order opening of Hox loci independently of transcription during Drosophila embryogenesis. Nat Commun 9 (1):3898. doi:10.1038/s41467-018-05945-4

Chiang GC, Bartsch M, Barua D, Nakabayashi K, Debieu M, Kronholm I, Koornneef M, Soppe WJ, Donohue K, De Meaux J (2011) DOG1 expression is predicted by the seed-maturation environment and contributes to geographical variation in germination in Arabidopsis thaliana. Mol Ecol 20 (16):3336-3349. doi:10.1111/j.1365-294X.2011.05181.x

Choi HS, Choi BY, Cho YY, Mizuno H, Kang BS, Bode AM, Dong Z (2005) Phosphorylation of histone H3 at serine 10 is indispensable for neoplastic cell transformation. Cancer Res 65 (13):5818-5827. doi:10.1158/0008-5472.CAN-05-0197

Choi K, Kim J, Hwang HJ, Kim S, Park C, Kim SY, Lee I (2011) The FRIGIDA complex activates transcription of FLC, a strong flowering repressor in Arabidopsis, by recruiting chromatin modification factors. Plant Cell 23 (1):289-303. doi:10.1105/tpc.110.075911

Choi K, Zhao X, Kelly KA, Venn O, Higgins JD, Yelina NE, Hardcastle TJ, Ziolkowski PA, Copenhaver GP, Franklin FC, McVean G, Henderson IR (2013) Arabidopsis meiotic crossover hot spots overlap with H2A.Z nucleosomes at gene promoters.

Nat Genet 45 (11):1327-1336. doi:10.1038/ng.2766

Chopra VS, Hendrix DA, Core LJ, Tsui C, Lis JT, Levine M (2011) The polycomb group mutant esc leads to augmented levels of paused Pol II in the Drosophila embryo. Mol Cell 42 (6):837-844. doi:10.1016/j.molcel.2011.05.009

Clapier CR, Iwasa J, Cairns BR, Peterson CL (2017) Mechanisms of action and regulation of ATP-dependent chromatin-remodelling complexes. Nat Rev Mol Cell Biol 18 (7):407-422. doi:10.1038/nrm.2017.26

Clayton AL, Rose S, Barratt MJ, Mahadevan LC (2000) Phosphoacetylation of histone H3 on c-fos- and c-jun-associated nucleosomes upon gene activation. EMBO J 19 (14):3714-3726. doi:10.1093/emboj/19.14.3714

Colon-Carmona A, You R, Haimovitch-Gal T, Doerner P (1999) Technical advance: spatio-temporal analysis of mitotic activity with a labile cyclin-GUS fusion protein. Plant J 20 (4):503-508

Connelly KE, Dykhuizen EC (2017) Compositional and functional diversity of canonical PRC1 complexes in mammals. Biochim Biophys Acta 1860 (2):233-245. doi:10.1016/j.bbagrm.2016.12.006

Corbesier L, Vincent C, Jang S, Fornara F, Fan Q, Searle I, Giakountis A, Farrona S, Gissot L, Turnbull C, Coupland G (2007) FT protein movement contributes to long-distance signaling in floral induction of Arabidopsis. Science 316 (5827):1030-1033. doi:10.1126/science.1141752

Cosgrove MS, Boeke JD, Wolberger C (2004) Regulated nucleosome mobility and the histone code. Nat Struct Mol Biol 11 (11):1037-1043. doi:10.1038/nsmb851

Cosgrove MS, Wolberger C (2005) How does the histone code work? Biochem Cell Biol 83 (4):468-476. doi:10.1139/o05-137

Crevillen P, Yang HC, Cui X, Greeff C, Trick M, Qiu Q, Cao XF, Dean C (2014) Epigenetic reprogramming that prevents transgenerational inheritance of the vernalized state. Nature 515 (7528):587-+. doi:10.1038/nature13722

Cruz-Ramirez A, Diaz-Trivino S, Blilou I, Grieneisen VA, Sozzani R, Zamioudis C, Miskolczi P, Nieuwland J, Benjamins R, Dhonukshe P, Caballero-Perez J, Horvath B, Long Y, Mahonen AP, Zhang H, Xu J, Murray JA, Benfey PN, Bako L, Maree AF, Scheres B (2012) A bistable circuit involving SCARECROW-RETINOBLASTOMA integrates cues to inform asymmetric stem cell division. Cell 150 (5):1002-1015. doi:10.1016/j.cell.2012.07.017

Cui H, Benfey PN (2009) Interplay between SCARECROW, GA and LIKE HETEROCHROMATIN PROTEIN 1 in ground tissue patterning in the Arabidopsis root. The Plant Journal 58 (6):1016-1027. doi:10.1111/j.1365-313X.2009.03839.x

Dahlin JL, Chen X, Walters MA, Zhang Z (2015) Histone-modifying enzymes, histone modifications and histone chaperones in nucleosome assembly: Lessons learned from Rtt109 histone acetyltransferases. Crit Rev Biochem Mol Biol 50 (1):31-53. doi:10.3109/10409238.2014.978975

Dawson MA, Bannister AJ, Gottgens B, Foster SD, Bartke T, Green AR, Kouzarides T (2009) JAK2 phosphorylates histone H3Y41 and excludes HP1alpha from chromatin. Nature 461 (7265):819-822. doi:10.1038/nature08448

de la Paz Sanchez M, Aceves-Garcia P, Petrone E, Steckenborn S, Vega-Leon R, Alvarez-Buylla ER, Garay-Arroyo A, Garcia-Ponce B (2015) The impact of Polycomb group (PcG) and Trithorax group (TrxG) epigenetic factors in plant plasticity. New Phytol 208 (3):684-694. doi:10.1111/nph.13486

de Lucas M, Pu L, Turco G, Gaudinier A, Morao AK, Harashima H, Kim D, Ron M, Sugimoto K, Roudier F, Brady SM (2016) Transcriptional Regulation of Arabidopsis Polycomb Repressive Complex 2 Coordinates Cell-Type Proliferation and Differentiation. Plant Cell 28 (10):2616-2631. doi:10.1105/tpc.15.00744

De Lucia F, Crevillen P, Jones AM, Greb T, Dean C (2008) A PHD-polycomb repressive complex 2 triggers the epigenetic silencing of FLC during vernalization. Proc Natl Acad Sci U S A 105 (44):16831-16836. doi:10.1073/pnas.0808687105

De Rybel B, Vassileva V, Parizot B, Demeulenaere M, Grunewald W, Audenaert D, Van Campenhout J, Overvoorde P, Jansen L, Vanneste S, Moller B, Wilson M, Holman T, Van Isterdael G, Brunoud G, Vuylsteke M, Vernoux T, De Veylder L, Inze D, Weijers D, Bennett MJ, Beeckman T (2010) A novel aux/IAA28 signaling cascade activates GATA23-dependent specification of lateral root founder cell identity. Curr Biol 20 (19):1697-1706. doi:10.1016/j.cub.2010.09.007

De Smet I, Vassileva V, De Rybel B, Levesque MP, Grunewald W, Van Damme D, Van Noorden G, Naudts M, Van Isterdael G, De Clercq R, Wang JY, Meuli N, Vanneste S, Friml J, Hilson P, Jurgens G, Ingram GC, Inze D, Benfey PN, Beeckman T (2008) Receptor-like kinase ACR4 restricts formative cell divisions in the Arabidopsis root. Science 322 (5901):594-597. doi:10.1126/science.1160158

Dean Rider S, Jr., Henderson JT, Jerome RE, Edenberg HJ, Romero-Severson J, Ogas J (2003) Coordinate repression of regulators of embryonic identity by PICKLE during germination in Arabidopsis. Plant J 35 (1):33-43

del Olmo I, Lopez-Gonzalez L, Martin-Trillo MM, Martinez-Zapater JM, Pineiro M, Jarillo JA (2010) EARLY IN SHORT DAYS 7 (ESD7) encodes the catalytic subunit of DNA polymerase epsilon and is required for flowering repression

through a mechanism involving epigenetic gene silencing. Plant J 61 (4):623-636. doi:10.1111/j.1365-313X.2009.04093.x

Demidov D, Van Damme D, Geelen D, Blattner FR, Houben A (2005) Identification and dynamics of two classes of aurora-like kinases in Arabidopsis and other plants. Plant Cell 17 (3):836-848. doi:10.1105/tpc.104.029710

Deng X, Qiu Q, He K, Cao X (2018) The seekers: how epigenetic modifying enzymes find their hidden genomic targets in Arabidopsis. Curr Opin Plant Biol 45 (Pt A):75-81. doi:10.1016/j.pbi.2018.05.006

Derkacheva M, Liu S, Figueiredo DD, Gentry M, Mozgova I, Nanni P, Tang M, Mannervik M, Kohler C, Hennig L (2016) H2A deubiquitinases UBP12/13 are part of the Arabidopsis polycomb group protein system. Nat Plants 2:16126. doi:10.1038/nplants.2016.126

Derkacheva M, Steinbach Y, Wildhaber T, Mozgova I, Mahrez W, Nanni P, Bischof S, Gruissem W, Hennig L (2013) Arabidopsis MSI1 connects LHP1 to PRC2 complexes. EMBO J 32 (14):2073-2085. doi:10.1038/emboj.2013.145

Dhalluin C, Carlson JE, Zeng L, He C, Aggarwal AK, Zhou MM (1999) Structure and ligand of a histone acetyltransferase bromodomain. Nature 399 (6735):491-496. doi:10.1038/20974

Dillon SC, Zhang X, Trievel RC, Cheng X (2005) The SET-domain protein superfamily: protein lysine methyltransferases. Genome Biol 6 (8):227. doi:10.1186/gb-2005-6-8-227

Ding Z, Friml J (2010) Auxin regulates distal stem cell differentiation in Arabidopsis roots. Proc Natl Acad Sci U S A 107 (26):12046-12051. doi:10.1073/pnas.1000672107

Dolan L, Janmaat K, Willemsen V, Linstead P, Poethig S, Roberts K, Scheres B (1993) Cellular organisation of the Arabidopsis thaliana root. Development 119 (1):71-84

Drisch RC, Stahl Y (2015) Function and regulation of transcription factors involved in root apical meristem and stem cell maintenance. Front Plant Sci 6:505. doi:10.3389/fpls.2015.00505

Driscoll R, Hudson A, Jackson SP (2007) Yeast Rtt109 promotes genome stability by acetylating histone H3 on lysine 56. Science 315 (5812):649-652. doi:10.1126/science.1135862

Dronamraju R, Ramachandran S, Jha DK, Adams AT, DiFiore JV, Parra MA, Dokholyan NV, Strahl BD (2017) Redundant Functions for Nap1 and Chz1 in H2A.Z Deposition. Sci Rep 7 (1):10791. doi:10.1038/s41598-017-11003-8

Duc C, Benoit M, Detourne G, Simon L, Poulet A, Jung M, Veluchamy A, Latrasse D, Le Goff S, Cotterell S, Tatout C, Benhamed M, Probst AV (2017) Arabidopsis ATRX Modulates H3.3 Occupancy and Fine-Tunes Gene Expression. Plant Cell 29 (7):1773-1793. doi:10.1105/tpc.16.00877

Duc C, Benoit M, Le Goff S, Simon L, Poulet A, Cotterell S, Tatout C, Probst AV (2015) The histone chaperone complex HIR maintains nucleosome occupancy and counterbalances impaired histone deposition in CAF-1 complex mutants. Plant J 81 (5):707-722. doi:10.1111/tpj.12758

Emre NC, Ingvarsdottir K, Wyce A, Wood A, Krogan NJ, Henry KW, Li K, Marmorstein R, Greenblatt JF, Shilatifard A, Berger SL (2005) Maintenance of low histone ubiquitylation by Ubp10 correlates with telomere-proximal Sir2 association and gene silencing. Mol Cell 17 (4):585-594. doi:10.1016/j.molcel.2005.01.007

English CM, Adkins MW, Carson JJ, Churchill ME, Tyler JK (2006) Structural basis for the histone chaperone activity of Asf1. Cell 127 (3):495-508. doi:10.1016/j.cell.2006.08.047

Eshed Y, Baum SF, Bowman JL (1999) Distinct mechanisms promote polarity establishment in carpels of Arabidopsis. Cell 99 (2):199-209

Eskeland R, Leeb M, Grimes GR, Kress C, Boyle S, Sproul D, Gilbert N, Fan Y, Skoultchi AI, Wutz A, Bickmore WA (2010) Ring1B compacts chromatin structure and represses gene expression independent of histone ubiquitination. Mol Cell 38 (3):452-464. doi:10.1016/j.molcel.2010.02.032

Eustermann S, Schall K, Kostrewa D, Lakomek K, Strauss M, Moldt M, Hopfner KP (2018) Structural basis for ATP-dependent chromatin remodelling by the INO80 complex. Nature 556 (7701):386-390. doi:10.1038/s41586-018-0029-y

Exner V, Aichinger E, Shu H, Wildhaber T, Alfarano P, Caflisch A, Gruissem W, Kohler C, Hennig L (2009) The chromodomain of LIKE HETEROCHROMATIN PROTEIN 1 is essential for H3K27me3 binding and function during Arabidopsis development. PLoS One 4 (4):e5335. doi:10.1371/journal.pone.0005335

Fahlgren N, Montgomery TA, Howell MD, Allen E, Dvorak SK, Alexander AL, Carrington JC (2006) Regulation of AUXIN RESPONSE FACTOR3 by TAS3 ta-siRNA affects developmental timing and patterning in Arabidopsis. Curr Biol 16 (9):939-944. doi:10.1016/j.cub.2006.03.065

Farcas AM, Blackledge NP, Sudbery I, Long HK, McGouran JF, Rose NR, Lee S, Sims D, Cerase A, Sheahan TW, Koseki H, Brockdorff N, Ponting CP, Kessler BM, Klose RJ (2012) KDM2B links the Polycomb Repressive Complex 1 (PRC1) to recognition of CpG islands. Elife 1:e00205. doi:10.7554/eLife.00205

Feng J, Chen D, Berr A, Shen WH (2016) ZRF1 Chromatin Regulators Have Polycomb

Silencing and Independent Roles in Development. Plant Physiol 172 (3):1746-1759. doi:10.1104/pp.16.00193

Feng J, Shen WH (2014) Dynamic regulation and function of histone monoubiquitination in plants. Front Plant Sci 5:83. doi:10.3389/fpls.2014.00083

Feng Q, Wang H, Ng HH, Erdjument-Bromage H, Tempst P, Struhl K, Zhang Y (2002) Methylation of H3-lysine 79 is mediated by a new family of HMTases without a SET domain. Curr Biol 12 (12):1052-1058

Fletcher JC (2017) State of the Art: trxG Factor Regulation of Post-embryonic Plant Development. Front Plant Sci 8:1925. doi:10.3389/fpls.2017.01925

Foltman M, Evrin C, De Piccoli G, Jones RC, Edmondson RD, Katou Y, Nakato R, Shirahige K, Labib K (2013) Eukaryotic replisome components cooperate to process histones during chromosome replication. Cell Rep 3 (3):892-904. doi:10.1016/j.celrep.2013.02.028

Fornara F, Panigrahi KC, Gissot L, Sauerbrunn N, Ruhl M, Jarillo JA, Coupland G (2009) Arabidopsis DOF transcription factors act redundantly to reduce CONSTANS expression and are essential for a photoperiodic flowering response. Dev Cell 17 (1):75-86. doi:10.1016/j.devcel.2009.06.015

Forzani C, Aichinger E, Sornay E, Willemsen V, Laux T, Dewitte W, Murray JA (2014) WOX5 suppresses CYCLIN D activity to establish quiescence at the center of the root stem cell niche. Curr Biol 24 (16):1939-1944. doi:10.1016/j.cub.2014.07.019

Francis NJ, Saurin AJ, Shao Z, Kingston RE (2001) Reconstitution of a functional core polycomb repressive complex. Mol Cell 8 (3):545-556

Friml J, Benkova E, Blilou I, Wisniewska J, Hamann T, Ljung K, Woody S, Sandberg G, Scheres B, Jurgens G, Palme K (2002) AtPIN4 mediates sink-driven auxin gradients and root patterning in Arabidopsis. Cell 108 (5):661-673

Friml J, Vieten A, Sauer M, Weijers D, Schwarz H, Hamann T, Offringa R, Jurgens G (2003) Efflux-dependent auxin gradients establish the apical-basal axis of Arabidopsis. Nature 426 (6963):147-153. doi:10.1038/nature02085

Fritsch O, Benvenuto G, Bowler C, Molinier J, Hohn B (2004a) The INO80 protein controls homologous recombination in Arabidopsis thaliana. Mol Cell 16 (3):479-485

Fritsch O, Benvenuto G, Bowler C, Molinier J, Hohn B (2004b) The INO80 protein controls homologous recombination in Arabidopsis thaliana. Mol Cell 16 (3):479-485. doi:10.1016/j.molcel.2004.09.034

Fuchs G, Oren M (2014) Writing and reading H2B monoubiquitylation. Biochim

Biophys Acta 1839 (8):694-701. doi:10.1016/j.bbagrm.2014.01.002

Fukaki H, Tameda S, Masuda H, Tasaka M (2002) Lateral root formation is blocked by a gain-of-function mutation in the SOLITARY-ROOT/IAA14 gene of Arabidopsis. Plant J 29 (2):153-168

Fyodorov DV, Zhou BR, Skoultchi AI, Bai Y (2018) Emerging roles of linker histones in regulating chromatin structure and function. Nat Rev Mol Cell Biol 19 (3):192-206. doi:10.1038/nrm.2017.94

Gambus A, Jones RC, Sanchez-Diaz A, Kanemaki M, van Deursen F, Edmondson RD, Labib K (2006) GINS maintains association of Cdc45 with MCM in replisome progression complexes at eukaryotic DNA replication forks. Nat Cell Biol 8 (4):358-366. doi:10.1038/ncb1382

Gan ES, Xu YF, Wong JY, Goh JG, Sun B, Wee WY, Huang JB, Ito T (2014) Jumonji demethylases moderate precocious flowering at elevated temperature via regulation of FLC in Arabidopsis. Nature Communications 5. doi:ARTN 5098

10.1038/ncomms6098

Gangaraju VK, Bartholomew B (2007) Dependency of ISW1a chromatin remodeling on extranucleosomal DNA. Mol Cell Biol 27 (8):3217-3225. doi:10.1128/MCB.01731-06

Gaudin V, Libault M, Pouteau S, Juul T, Zhao G, Lefebvre D, Grandjean O (2001) Mutations in LIKE HETEROCHROMATIN PROTEIN 1 affect flowering time and plant architecture in Arabidopsis. Development 128 (23):4847-4858

Gehani SS, Agrawal-Singh S, Dietrich N, Christophersen NS, Helin K, Hansen K (2010) Polycomb group protein displacement and gene activation through MSK-dependent H3K27me3S28 phosphorylation. Mol Cell 39 (6):886-900. doi:10.1016/j.molcel.2010.08.020

Gendall AR, Levy YY, Wilson A, Dean C (2001) The VERNALIZATION 2 gene mediates the epigenetic regulation of vernalization in Arabidopsis. Cell 107 (4):525-535

Glickman MH, Ciechanover A (2002) The ubiquitin-proteasome proteolytic pathway: destruction for the sake of construction. Physiol Rev 82 (2):373-428. doi:10.1152/physrev.00027.2001

Goldstein G, Scheid M, Hammerling U, Schlesinger DH, Niall HD, Boyse EA (1975) Isolation of a polypeptide that has lymphocyte-differentiating properties and is probably represented universally in living cells. Proc Natl Acad Sci U S A 72 (1):11-15

Goodrich J, Puangsomlee P, Martin M, Long D, Meyerowitz EM, Coupland G (1997) A

Polycomb-group gene regulates homeotic gene expression in Arabidopsis. Nature 386 (6620):44-51. doi:10.1038/386044a0

Grau DJ, Chapman BA, Garlick JD, Borowsky M, Francis NJ, Kingston RE (2011) Compaction of chromatin by diverse Polycomb group proteins requires localized regions of high charge. Genes Dev 25 (20):2210-2221. doi:10.1101/gad.17288211

Gray F, Cho HJ, Shukla S, He S, Harris A, Boytsov B, Jaremko L, Jaremko M, Demeler B, Lawlor ER, Grembecka J, Cierpicki T (2016) BMI1 regulates PRC1 architecture and activity through homo- and hetero-oligomerization. Nat Commun 7:13343. doi:10.1038/ncomms13343

Grossniklaus U, Vielle-Calzada JP, Hoeppner MA, Gagliano WB (1998) Maternal control of embryogenesis by MEDEA, a polycomb group gene in Arabidopsis. Science 280 (5362):446-450

Grune T, Brzeski J, Eberharter A, Clapier CR, Corona DF, Becker PB, Muller CW (2003) Crystal structure and functional analysis of a nucleosome recognition module of the remodeling factor ISWI. Mol Cell 12 (2):449-460

Gu X, Le C, Wang Y, Li Z, Jiang D, Wang Y, He Y (2013) Arabidopsis FLC clade members form flowering-repressor complexes coordinating responses to endogenous and environmental cues. Nat Commun 4:1947. doi:10.1038/ncomms2947

Gu X, Xu T, He Y (2014) A histone H3 lysine-27 methyltransferase complex represses lateral root formation in Arabidopsis thaliana. Molecular plant 7 (6):977-988. doi:10.1093/mp/ssu035

Gunster MJ, Satijn DP, Hamer KM, den Blaauwen JL, de Bruijn D, Alkema MJ, van Lohuizen M, van Driel R, Otte AP (1997) Identification and characterization of interactions between the vertebrate polycomb-group protein BMI1 and human homologs of polyhomeotic. Mol Cell Biol 17 (4):2326-2335

Guo L, Cao X, Liu Y, Li J, Li Y, Li D, Zhang K, Gao C, Dong A, Liu X (2018) A Chromatin Loop Represses WUSCHEL Expression in Arabidopsis. Plant J. doi:10.1111/tpj.13921

Gutierrez L, Van Wuytswinkel O, Castelain M, Bellini C (2007) Combined networks regulating seed maturation. Trends Plant Sci 12 (7):294-300. doi:10.1016/j.tplants.2007.06.003

Guzman-Lopez JA, Abraham-Juarez MJ, Lozano-Sotomayor P, de Folter S, Simpson J (2016) Arabidopsis thaliana gonidialess A/Zuotin related factors (GlsA/ZRF) are essential for maintenance of meristem integrity. Plant Mol Biol 91 (1-2):37-51. doi:10.1007/s11103-016-0439-x

Hammond CM, Stromme CB, Huang H, Patel DJ, Groth A (2017) Histone chaperone networks shaping chromatin function. Nat Rev Mol Cell Biol 18 (3):141-158. doi:10.1038/nrm.2016.159

Han J, Zhang H, Zhang H, Wang Z, Zhou H, Zhang Z (2013) A Cul4 E3 ubiquitin ligase regulates histone hand-off during nucleosome assembly. Cell 155 (4):817-829. doi:10.1016/j.cell.2013.10.014

Han SK, Wu MF, Cui S, Wagner D (2015) Roles and activities of chromatin remodeling ATPases in plants. Plant J 83 (1):62-77. doi:10.1111/tpj.12877

Hansen KH, Bracken AP, Pasini D, Dietrich N, Gehani SS, Monrad A, Rappsilber J, Lerdrup M, Helin K (2008) A model for transmission of the H3K27me3 epigenetic mark. Nat Cell Biol 10 (11):1291-1300. doi:10.1038/ncb1787

Hatzold J, Conradt B (2008) Control of apoptosis by asymmetric cell division. Plos Biol 6 (4):e84. doi:10.1371/journal.pbio.0060084

Hauer MH, Gasser SM (2017) Chromatin and nucleosome dynamics in DNA damage and repair. Genes Dev 31 (22):2204-2221. doi:10.1101/gad.307702.117

He Y, Michaels SD, Amasino RM (2003) Regulation of flowering time by histone acetylation in Arabidopsis. Science 302 (5651):1751-1754. doi:10.1126/science.1091109

Hecker A, Brand LH, Peter S, Simoncello N, Kilian J, Harter K, Gaudin V, Wanke D (2015) The Arabidopsis GAGA-Binding Factor BASIC PENTACYSTEINE6 Recruits the POLYCOMB-REPRESSIVE COMPLEX1 Component LIKE HETEROCHROMATIN PROTEIN1 to GAGA DNA Motifs. Plant Physiol 168 (3):1013-1024. doi:10.1104/pp.15.00409

Heidstra R, Welch D, Scheres B (2004) Mosaic analyses using marked activation and deletion clones dissect Arabidopsis SCARECROW action in asymmetric cell division. Genes Dev 18 (16):1964-1969. doi:10.1101/gad.305504

Hennig L, Bouveret R, Gruissem W (2005) MSI1-like proteins: an escort service for chromatin assembly and remodeling complexes. Trends Cell Biol 15 (6):295-302. doi:10.1016/j.tcb.2005.04.004

Henry KW, Wyce A, Lo WS, Duggan LJ, Emre NC, Kao CF, Pillus L, Shilatifard A, Osley MA, Berger SL (2003) Transcriptional activation via sequential histone H2B ubiquitylation and deubiquitylation, mediated by SAGA-associated Ubp8. Genes Dev 17 (21):2648-2663. doi:10.1101/gad.1144003

Heo JB, Sung S (2011) Vernalization-mediated epigenetic silencing by a long intronic noncoding RNA. Science 331 (6013):76-79. doi:10.1126/science.1197349

Heyman J, Cools T, Vandenbussche F, Heyndrickx KS, Van Leene J, Vercauteren I,

Vanderauwera S, Vandepoele K, De Jaeger G, Van Der Straeten D, De Veylder L (2013) ERF115 controls root quiescent center cell division and stem cell replenishment. Science 342 (6160):860-863. doi:10.1126/science.1240667

Hibara K, Takada S, Tasaka M (2003) CUC1 gene activates the expression of SAM-related genes to induce adventitious shoot formation. Plant J 36 (5):687-696

Hohenstatt ML, Mikulski P, Komarynets O, Klose C, Kycia I, Jeltsch A, Farrona S, Schubert D (2018) PWWP-DOMAIN INTERACTOR OF POLYCOMBS1 Interacts with Polycomb-Group Proteins and Histones and Regulates Arabidopsis Flowering and Development. Plant Cell 30 (1):117-133. doi:10.1105/tpc.17.00117

Hohmann AF, Vakoc CR (2014) A rationale to target the SWI/SNF complex for cancer therapy. Trends Genet 30 (8):356-363. doi:10.1016/j.tig.2014.05.001

Hojfeldt JW, Laugesen A, Willumsen BM, Damhofer H, Hedehus L, Tvardovskiy A, Mohammad F, Jensen ON, Helin K (2018) Accurate H3K27 methylation can be established de novo by SUZ12-directed PRC2. Nat Struct Mol Biol 25 (3):225-232. doi:10.1038/s41594-018-0036-6

Holdsworth MJ, Bentsink L, Soppe WJ (2008) Molecular networks regulating Arabidopsis seed maturation, after-ripening, dormancy and germination. New Phytol 179 (1):33-54. doi:10.1111/j.1469-8137.2008.02437.x

Hollender C, Liu Z (2008) Histone deacetylase genes in Arabidopsis development. J Integr Plant Biol 50 (7):875-885. doi:10.1111/j.1744-7909.2008.00704.x

Hoppmann V, Thorstensen T, Kristiansen PE, Veiseth SV, Rahman MA, Finne K, Aalen RB, Aasland R (2011) The CW domain, a new histone recognition module in chromatin proteins. EMBO J 30 (10):1939-1952. doi:10.1038/emboj.2011.108

How Kit A, Boureau L, Stammitti-Bert L, Rolin D, Teyssier E, Gallusci P (2010) Functional analysis of SlEZ1 a tomato enhancer of zeste (E(z)) gene demonstrates a role in flower development. Plant Mol Biol 74 (3):201-213. doi:10.1007/s11103-010-9657-9

Huang X, Lu Z, Wang X, Ouyang Y, Chen W, Xie K, Wang D, Luo M, Luo J, Yao J (2016) Imprinted gene OsFIE1 modulates rice seed development by influencing nutrient metabolism and modifying genome H3K27me3. Plant J 87 (3):305-317. doi:10.1111/tpj.13202

Huang Y, Chen DH, Liu BY, Shen WH, Ruan Y (2017) Conservation and diversification of polycomb repressive complex 2 (PRC2) proteins in the green lineage. Brief Funct Genomics 16 (2):106-119. doi:10.1093/bfgp/elw007

Hunter C, Sun H, Poethig RS (2003) The Arabidopsis heterochronic gene ZIPPY is an

ARGONAUTE family member. Curr Biol 13 (19):1734-1739

Hunter C, Willmann MR, Wu G, Yoshikawa M, de la Luz Gutierrez-Nava M, Poethig SR (2006) Trans-acting siRNA-mediated repression of ETTIN and ARF4 regulates heteroblasty in Arabidopsis. Development 133 (15):2973-2981. doi:10.1242/dev.02491

Huo YQ, Yan ZQ, Zhang BS, Wang XX (2016) Recruitment of Polycomb Repressive Complex 2 is Essential to Suppress the Target Chromatin in Arabidopsis. Crit Rev Plant Sci 35 (3):131-145. doi:10.1080/07352689.2016.1245055

Ikeuchi M, Iwase A, Rymen B, Harashima H, Shibata M, Ohnuma M, Breuer C, Morao AK, de Lucas M, De Veylder L, Goodrich J, Brady SM, Roudier F, Sugimoto K (2015) PRC2 represses dedifferentiation of mature somatic cells in Arabidopsis. Nat Plants 1:15089. doi:10.1038/nplants.2015.89

Imaizumi T, Schultz TF, Harmon FG, Ho LA, Kay SA (2005) FKF1 F-box protein mediates cyclic degradation of a repressor of CONSTANS in Arabidopsis. Science 309 (5732):293-297. doi:10.1126/science.1110586

Ivanov VB, Dubrovsky JG (2013) Longitudinal zonation pattern in plant roots: conflicts and solutions. Trends Plant Sci 18 (5):237-243. doi:10.1016/j.tplants.2012.10.002

Jackson V (1987) Deposition of newly synthesized histones: misinterpretations due to cross-linking density-labeled proteins with Lomant's reagent. Biochemistry-Us 26 (8):2325-2334

Jaeger KE, Wigge PA (2007) FT protein acts as a long-range signal in Arabidopsis. Curr Biol 17 (12):1050-1054. doi:10.1016/j.cub.2007.05.008

Jenuwein T (2006) The epigenetic magic of histone lysine methylation. FEBS J 273 (14):3121-3135. doi:10.1111/j.1742-4658.2006.05343.x

Jenuwein T, Laible G, Dorn R, Reuter G (1998) SET domain proteins modulate chromatin domains in eu- and heterochromatin. Cell Mol Life Sci 54 (1):80-93

Jia H, Suzuki M, McCarty DR (2014) Regulation of the seed to seedling developmental phase transition by the LAFL and VAL transcription factor networks. Wiley Interdiscip Rev Dev Biol 3 (1):135-145. doi:10.1002/wdev.126

Jiang D, Berger F (2017) DNA replication-coupled histone modification maintains Polycomb gene silencing in plants. Science 357 (6356):1146-1149. doi:10.1126/science.aan4965

Jiang D, Yang W, He Y, Amasino RM (2007) Arabidopsis relatives of the human lysine-specific demethylase1 repress the expression of FWA and FLOWERING LOCUS C and thus promote the floral transition. Plant Cell 19 (10):2975-2987.

doi:10.1105/tpc.107.052373

Jiang DH, Gu XF, He YH (2009) Establishment of the Winter-Annual Growth Habit via FRIGIDA-Mediated Histone Methylation at FLOWERING LOCUS C in Arabidopsis. Plant Cell 21 (6):1733-1746. doi:10.1105/tpc.109.067967

Johnson L, Mollah S, Garcia BA, Muratore TL, Shabanowitz J, Hunt DF, Jacobsen SE (2004) Mass spectrometry analysis of Arabidopsis histone H3 reveals distinct combinations of post-translational modifications. Nucleic Acids Res 32 (22):6511-6518. doi:10.1093/nar/gkh992

Junco SE, Wang R, Gaipa JC, Taylor AB, Schirf V, Gearhart MD, Bardwell VJ, Demeler B, Hart PJ, Kim CA (2013) Structure of the polycomb group protein PCGF1 in complex with BCOR reveals basis for binding selectivity of PCGF homologs. Structure 21 (4):665-671. doi:10.1016/j.str.2013.02.013

Jurgens G (1985) A Group of Genes-Controlling the Spatial Expression of the Bithorax Complex in Drosophila. Nature 316 (6024):153-155. doi:DOI 10.1038/316153a0

Kajala K, Ramakrishna P, Fisher A, Bergmann DC, De Smet I, Sozzani R, Weijers D, Brady SM (2014) Omics and modelling approaches for understanding regulation of asymmetric cell divisions in arabidopsis and other angiosperm plants. Annals of botany 113 (7):1083-1105. doi:10.1093/aob/mcu065

Kalb R, Latwiel S, Baymaz HI, Jansen PW, Muller CW, Vermeulen M, Muller J (2014) Histone H2A monoubiquitination promotes histone H3 methylation in Polycomb repression. Nat Struct Mol Biol 21 (6):569-571. doi:10.1038/nsmb.2833

Kandasamy MK, McKinney EC, Deal RB, Smith AP, Meagher RB (2009) Arabidopsis actin-related protein ARP5 in multicellular development and DNA repair. Dev Biol 335 (1):22-32. doi:10.1016/j.ydbio.2009.08.006

Karssen CM, Brinkhorst-van der Swan DL, Breekland AE, Koornneef M (1983) Induction of dormancy during seed development by endogenous abscisic acid: studies on abscisic acid deficient genotypes of Arabidopsis thaliana (L.) Heynh. Planta 157 (2):158-165. doi:10.1007/BF00393650

Kassis JA, Kennison JA, Tamkun JW (2017) Polycomb and Trithorax Group Genes in Drosophila. Genetics 206 (4):1699-1725. doi:10.1534/genetics.115.185116

Katz A, Oliva M, Mosquna A, Hakim O, Ohad N (2004) FIE and CURLY LEAF polycomb proteins interact in the regulation of homeobox gene expression during sporophyte development. Plant J 37 (5):707-719

Kaufman PD, Kobayashi R, Kessler N, Stillman B (1995) The p150 and p60 subunits of chromatin assembly factor I: a molecular link between newly synthesized histones and DNA replication. Cell 81 (7):1105-1114

Kawashima T, Goldberg RB (2010) The suspensor: not just suspending the embryo. Trends Plant Sci 15 (1):23-30. doi:10.1016/j.tplants.2009.11.002

Keith K, Kraml M, Dengler NG, McCourt P (1994) fusca3: A Heterochronic Mutation Affecting Late Embryo Development in Arabidopsis. Plant Cell 6 (5):589-600. doi:10.1105/tpc.6.5.589

Kendall SL, Hellwege A, Marriot P, Whalley C, Graham IA, Penfield S (2011) Induction of dormancy in Arabidopsis summer annuals requires parallel regulation of DOG1 and hormone metabolism by low temperature and CBF transcription factors. Plant Cell 23 (7):2568-2580. doi:10.1105/tpc.111.087643

Kerstetter RA, Poethig RS (1998) The specification of leaf identity during shoot development. Annu Rev Cell Dev Biol 14:373-398. doi:10.1146/annurev.cellbio.14.1.373

Khan MRG, Ai XY, Zhang JZ (2014) Genetic regulation of flowering time in annual and perennial plants. Wires Rna 5 (3):347-359. doi:10.1002/wrna.1215

Kim DH, Sung S (2017) Vernalization-Triggered Intragenic Chromatin Loop Formation by Long Noncoding RNAs. Dev Cell 40 (3):302-312 e304. doi:10.1016/j.devcel.2016.12.021

Kim DH, Xi Y, Sung S (2017) Modular function of long noncoding RNA, COLDAIR, in the vernalization response. PLoS Genet 13 (7):e1006939. doi:10.1371/journal.pgen.1006939

Kim I, Cho E, Crawford K, Hempel FD, Zambryski PC (2005a) Cell-to-cell movement of GFP during embryogenesis and early seedling development in Arabidopsis. Proc Natl Acad Sci U S A 102 (6):2227-2231. doi:10.1073/pnas.0409193102

Kim SY, He Y, Jacob Y, Noh YS, Michaels S, Amasino R (2005b) Establishment of the vernalization-responsive, winter-annual habit in Arabidopsis requires a putative histone H3 methyl transferase. Plant Cell 17 (12):3301-3310. doi:10.1105/tpc.105.034645

Kim SY, Lee J, Eshed-Williams L, Zilberman D, Sung ZR (2012) EMF1 and PRC2 cooperate to repress key regulators of Arabidopsis development. PLoS Genet 8 (3):e1002512. doi:10.1371/journal.pgen.1002512

Kim SY, Zhu T, Sung ZR (2010) Epigenetic regulation of gene programs by EMF1 and EMF2 in Arabidopsis. Plant Physiol 152 (2):516-528. doi:10.1104/pp.109.143495

Kimura H, Cook PR (2001) Kinetics of core histones in living human cells: little exchange of H3 and H4 and some rapid exchange of H2B. J Cell Biol 153 (7):1341-1353

King HW, Fursova NA, Blackledge NP, Klose RJ (2018) Polycomb repressive complex 1 shapes the nucleosome landscape but not accessibility at target genes. Genome Res 28 (10):1494-1507. doi:10.1101/gr.237180.118

King IF, Francis NJ, Kingston RE (2002) Native and recombinant polycomb group complexes establish a selective block to template accessibility to repress transcription in vitro. Mol Cell Biol 22 (22):7919-7928

Klose RJ, Kallin EM, Zhang Y (2006) JmjC-domain-containing proteins and histone demethylation. Nat Rev Genet 7 (9):715-727. doi:10.1038/nrg1945

Kobayashi Y, Weigel D (2007) Move on up, it's time for change--mobile signals controlling photoperiod-dependent flowering. Genes Dev 21 (19):2371-2384. doi:10.1101/gad.1589007

Kohler C, Hennig L, Bouveret R, Gheyselinck J, Grossniklaus U, Gruissem W (2003) Arabidopsis MSI1 is a component of the MEA/FIE Polycomb group complex and required for seed development. EMBO J 22 (18):4804-4814. doi:10.1093/emboj/cdg444

Komander D, Rape M (2012) The ubiquitin code. Annu Rev Biochem 81:203-229. doi:10.1146/annurev-biochem-060310-170328

Konev AY, Tribus M, Park SY, Podhraski V, Lim CY, Emelyanov AV, Vershilova E, Pirrotta V, Kadonaga JT, Lusser A, Fyodorov DV (2007) CHD1 motor protein is required for deposition of histone variant H3.3 into chromatin in vivo. Science 317 (5841):1087-1090. doi:10.1126/science.1145339

Krietenstein N, Wal M, Watanabe S, Park B, Peterson CL, Pugh BF, Korber P (2016) Genomic Nucleosome Organization Reconstituted with Pure Proteins. Cell 167 (3):709-721 e712. doi:10.1016/j.cell.2016.09.045

Kroj T, Savino G, Valon C, Giraudat J, Parcy F (2003) Regulation of storage protein gene expression in Arabidopsis. Development 130 (24):6065-6073. doi:10.1242/dev.00814

Kundu S, Ji F, Sunwoo H, Jain G, Lee JT, Sadreyev RI, Dekker J, Kingston RE (2017) Polycomb Repressive Complex 1 Generates Discrete Compacted Domains that Change during Differentiation. Mol Cell 65 (3):432-446 e435. doi:10.1016/j.molcel.2017.01.009

Kurihara D, Matsunaga S, Omura T, Higashiyama T, Fukui K (2011) Identification and characterization of plant Haspin kinase as a histone H3 threonine kinase. BMC Plant Biol 11:73. doi:10.1186/1471-2229-11-73

Kwon CS, Hibara K, Pfluger J, Bezhani S, Metha H, Aida M, Tasaka M, Wagner D (2006) A role for chromatin remodeling in regulation of CUC gene expression in the Arabidopsis cotyledon boundary. Development 133 (16):3223-3230.

doi:10.1242/dev.02508

Lafos M, Kroll P, Hohenstatt ML, Thorpe FL, Clarenz O, Schubert D (2011) Dynamic regulation of H3K27 trimethylation during Arabidopsis differentiation. PLoS Genet 7 (4):e1002040. doi:10.1371/journal.pgen.1002040

Lagarou A, Mohd-Sarip A, Moshkin YM, Chalkley GE, Bezstarosti K, Demmers JA, Verrijzer CP (2008) dKDM2 couples histone H2A ubiquitylation to histone H3 demethylation during Polycomb group silencing. Genes Dev 22 (20):2799-2810. doi:10.1101/gad.484208

Lanzuolo C, Orlando V (2012) Memories from the polycomb group proteins. Annu Rev Genet 46:561-589. doi:10.1146/annurev-genet-110711-155603

Latrasse D, Benhamed M, Bergounioux C, Raynaud C, Delarue M (2016) Plant programmed cell death from a chromatin point of view. J Exp Bot 67 (20):5887-5900. doi:10.1093/jxb/erw329

Latrasse D, Germann S, Houba-Herin N, Dubois E, Bui-Prodhomme D, Hourcade D, Juul-Jensen T, Le Roux C, Majira A, Simoncello N, Granier F, Taconnat L, Renou JP, Gaudin V (2011) Control of flowering and cell fate by LIF2, an RNA binding partner of the polycomb complex component LHP1. PLoS One 6 (1):e16592. doi:10.1371/journal.pone.0016592

Lau AT, Lee SY, Xu YM, Zheng D, Cho YY, Zhu F, Kim HG, Li SQ, Zhang Z, Bode AM, Dong Z (2011) Phosphorylation of histone H2B serine 32 is linked to cell transformation. J Biol Chem 286 (30):26628-26637. doi:10.1074/jbc.M110.215590

Lau MS, Schwartz MG, Kundu S, Savol AJ, Wang PI, Marr SK, Grau DJ, Schorderet P, Sadreyev RI, Tabin CJ, Kingston RE (2017) Mutation of a nucleosome compaction region disrupts Polycomb-mediated axial patterning. Science 355 (6329):1081-1084. doi:10.1126/science.aah5403

Lau PN, Cheung P (2011) Histone code pathway involving H3 S28 phosphorylation and K27 acetylation activates transcription and antagonizes polycomb silencing. Proc Natl Acad Sci U S A 108 (7):2801-2806. doi:10.1073/pnas.1012798108

Laux T (2003) The stem cell concept in plants: a matter of debate. Cell 113 (3):281-283

Lee HB, Noh H, Seo JY, Yu MR, Ha H (2007) Histone deacetylase inhibitors: a novel class of therapeutic agents in diabetic nephropathy. Kidney Int Suppl (106):S61-66. doi:10.1038/sj.ki.5002388

Lee WY, Lee D, Chung WI, Kwon CS (2009) Arabidopsis ING and Alfin1-like protein families localize to the nucleus and bind to H3K4me3/2 via plant homeodomain fingers. Plant Journal 58 (3):511-524. doi:10.1111/j.1365-313X.2009.03795.x

Lewis EB (1978) A gene complex controlling segmentation in Drosophila. Nature 276 (5688):565-570

Li B, Carey M, Workman JL (2007) The role of chromatin during transcription. Cell 128 (4):707-719. doi:10.1016/j.cell.2007.01.015

Li H, Luan S (2011) The cyclophilin AtCYP71 interacts with CAF-1 and LHP1 and functions in multiple chromatin remodeling processes. Molecular plant 4 (4):748-758. doi:10.1093/mp/ssr036

Li J, Wang Z, Hu Y, Cao Y, Ma L (2017) Polycomb Group Proteins RING1A and RING1B Regulate the Vegetative Phase Transition in Arabidopsis. Front Plant Sci 8:867. doi:10.3389/fpls.2017.00867

Li S, Zhou B, Peng X, Kuang Q, Huang X, Yao J, Du B, Sun MX (2014) OsFIE2 plays an essential role in the regulation of rice vegetative and reproductive development. New Phytol 201 (1):66-79. doi:10.1111/nph.12472

Li W, Wang Z, Li J, Yang H, Cui S, Wang X, Ma L (2011) Overexpression of AtBMI1C, a polycomb group protein gene, accelerates flowering in Arabidopsis. PLoS One 6 (6):e21364. doi:10.1371/journal.pone.0021364

Li Z, Li B, Liu J, Guo Z, Liu Y, Li Y, Shen WH, Huang Y, Huang H, Zhang Y, Dong A (2016) Transcription factors AS1 and AS2 interact with LHP1 to repress KNOX genes in Arabidopsis. J Integr Plant Biol 58 (12):959-970. doi:10.1111/jipb.12485

Li ZC, Fu X, Wang YZ, Liu RY, He YH (2018) Polycomb-mediated gene silencing by the BAH-EMF1 complex in plants. Nature Genetics 50 (9):1254-+. doi:10.1038/s41588-018-0190-0

Libault M, Tessadori F, Germann S, Snijder B, Fransz P, Gaudin V (2005) The Arabidopsis LHP1 protein is a component of euchromatin. Planta 222 (5):910-925. doi:10.1007/s00425-005-0129-4

Lin MK, Belanger H, Lee YJ, Varkonyi-Gasic E, Taoka K, Miura E, Xoconostle-Cazares B, Gendler K, Jorgensen RA, Phinney B, Lough TJ, Lucas WJ (2007) FLOWERING LOCUS T protein may act as the long-distance florigenic signal in the cucurbits. Plant Cell 19 (5):1488-1506. doi:10.1105/tpc.107.051920

Liu C, Lu F, Cui X, Cao X (2010) Histone methylation in higher plants. Annu Rev Plant Biol 61:395-420. doi:10.1146/annurev.arplant.043008.091939

Liu C, Xi W, Shen L, Tan C, Yu H (2009) Regulation of floral patterning by flowering time genes. Dev Cell 16 (5):711-722. doi:10.1016/j.devcel.2009.03.011

Liu DD, Zhou LJ, Fang MJ, Dong QL, An XH, You CX, Hao YJ (2016a) Polycomb-group protein SlMSI1 represses the expression of fruit-ripening genes

to prolong shelf life in tomato. Sci Rep 6:31806. doi:10.1038/srep31806

Liu J, Deng S, Wang H, Ye J, Wu HW, Sun HX, Chua NH (2016b) CURLY LEAF Regulates Gene Sets Coordinating Seed Size and Lipid Biosynthesis. Plant Physiol 171 (1):424-436. doi:10.1104/pp.15.01335

Liu L, Liu C, Hou X, Xi W, Shen L, Tao Z, Wang Y, Yu H (2012) FTIP1 is an essential regulator required for florigen transport. Plos Biol 10 (4):e1001313. doi:10.1371/journal.pbio.1001313

Liu X, Kim YJ, Muller R, Yumul RE, Liu C, Pan Y, Cao X, Goodrich J, Chen X (2011) AGAMOUS terminates floral stem cell maintenance in Arabidopsis by directly repressing WUSCHEL through recruitment of Polycomb Group proteins. Plant Cell 23 (10):3654-3670. doi:10.1105/tpc.111.091538

Liu X, Wei X, Sheng Z, Jiao G, Tang S, Luo J, Hu P (2016c) Polycomb Protein OsFIE2 Affects Plant Height and Grain Yield in Rice. PLoS One 11 (10):e0164748. doi:10.1371/journal.pone.0164748

Liu X, Yang S, Zhao M, Luo M, Yu CW, Chen CY, Tai R, Wu K (2014a) Transcriptional repression by histone deacetylases in plants. Molecular plant 7 (5):764-772. doi:10.1093/mp/ssu033

Liu X, Zhou C, Zhao Y, Zhou S, Wang W, Zhou DX (2014b) The rice enhancer of zeste [E(z)] genes SDG711 and SDG718 are respectively involved in long day and short day signaling to mediate the accurate photoperiod control of flowering time. Front Plant Sci 5:591. doi:10.3389/fpls.2014.00591

Lo WS, Trievel RC, Rojas JR, Duggan L, Hsu JY, Allis CD, Marmorstein R, Berger SL (2000) Phosphorylation of serine 10 in histone H3 is functionally linked in vitro and in vivo to Gcn5-mediated acetylation at lysine 14. Mol Cell 5 (6):917-926

Lodha M, Marco CF, Timmermans MC (2013) The ASYMMETRIC LEAVES complex maintains repression of KNOX homeobox genes via direct recruitment of Polycomb-repressive complex2. Genes Dev 27 (6):596-601. doi:10.1101/gad.211425.112

Lolas IB, Himanen K, Gronlund JT, Lynggaard C, Houben A, Melzer M, Van Lijsebettens M, Grasser KD (2010) The transcript elongation factor FACT affects Arabidopsis vegetative and reproductive development and genetically interacts with HUB1/2. Plant J 61 (4):686-697. doi:10.1111/j.1365-313X.2009.04096.x

Lotan T, Ohto M, Yee KM, West MA, Lo R, Kwong RW, Yamagishi K, Fischer RL, Goldberg RB, Harada JJ (1998) Arabidopsis LEAFY COTYLEDON1 is sufficient to induce embryo development in vegetative cells. Cell 93 (7):1195-1205

Lu FL, Cui X, Zhang SB, Jenuwein T, Cao XF (2011) Arabidopsis REF6 is a histone H3 lysine 27 demethylase. Nature Genetics 43 (7):715-U144. doi:10.1038/ng.854

Lu FL, Cui X, Zhang SB, Liu CY, Cao XF (2010) JMJ14 is an H3K4 demethylase regulating flowering time in Arabidopsis. Cell Research 20 (3):387-390. doi:10.1038/cr.2010.27

Lu FL, Li GL, Cui X, Liu CY, Wang XJ, Cao XF (2008) Comparative analysis of JmjC domain-containing proteins reveals the potential histone demethylases in Arabidopsis and rice. Journal of Integrative Plant Biology 50 (7):886-896. doi:10.1111/j.1744-7909.2008.00692.x

Luerssen H, Kirik V, Herrmann P, Misera S (1998) FUSCA3 encodes a protein with a conserved VP1/AB13-like B3 domain which is of functional importance for the regulation of seed maturation in Arabidopsis thaliana. Plant J 15 (6):755-764

Luger K, Mader AW, Richmond RK, Sargent DF, Richmond TJ (1997) Crystal structure of the nucleosome core particle at 2.8 A resolution. Nature 389 (6648):251-260. doi:10.1038/38444

Lukas J, Lukas C, Bartek J (2011) More than just a focus: The chromatin response to DNA damage and its role in genome integrity maintenance. Nat Cell Biol 13 (10):1161-1169. doi:10.1038/ncb2344

Luo M, Bilodeau P, Koltunow A, Dennis ES, Peacock WJ, Chaudhury AM (1999) Genes controlling fertilization-independent seed development in Arabidopsis thaliana. Proc Natl Acad Sci U S A 96 (1):296-301

Luo M, Platten D, Chaudhury A, Peacock WJ, Dennis ES (2009) Expression, imprinting, and evolution of rice homologs of the polycomb group genes. Molecular plant 2 (4):711-723. doi:10.1093/mp/ssp036

Lusser A, Urwin DL, Kadonaga JT (2005) Distinct activities of CHD1 and ACF in ATP-dependent chromatin assembly. Nat Struct Mol Biol 12 (2):160-166. doi:10.1038/nsmb884

Mahajan K, Fang B, Koomen JM, Mahajan NP (2012) H2B Tyr37 phosphorylation suppresses expression of replication-dependent core histone genes. Nat Struct Mol Biol 19 (9):930-937. doi:10.1038/nsmb.2356

Makarevich G, Leroy O, Akinci U, Schubert D, Clarenz O, Goodrich J, Grossniklaus U, Kohler C (2006) Different Polycomb group complexes regulate common target genes in Arabidopsis. EMBO Rep 7 (9):947-952. doi:10.1038/sj.embor.7400760

Manzanero S, Rutten T, Kotseruba V, Houben A (2002) Alterations in the distribution of histone H3 phosphorylation in mitotic plant chromosomes in response to cold treatment and the protein phosphatase inhibitor cantharidin. Chromosome Res 10 (6):467-476

March-Diaz R, Garcia-Dominguez M, Lozano-Juste J, Leon J, Florencio FJ, Reyes JC (2008) Histone H2A.Z and homologues of components of the SWR1 complex are required to control immunity in Arabidopsis. Plant J 53 (3):475-487

March-Diaz R, Reyes JC (2009) The beauty of being a variant: H2A.Z and the SWR1 complex in plants. Molecular plant 2 (4):565-577

Margueron R, Justin N, Ohno K, Sharpe ML, Son J, Drury WJ, 3rd, Voigt P, Martin SR, Taylor WR, De Marco V, Pirrotta V, Reinberg D, Gamblin SJ (2009) Role of the polycomb protein EED in the propagation of repressive histone marks. Nature 461 (7265):762-767. doi:10.1038/nature08398

Martin C, Zhang Y (2005) The diverse functions of histone lysine methylation. Nat Rev Mol Cell Biol 6 (11):838-849. doi:10.1038/nrm1761

Masumoto H, Hawke D, Kobayashi R, Verreault A (2005) A role for cell-cycle-regulated histone H3 lysine 56 acetylation in the DNA damage response. Nature 436 (7048):294-298. doi:10.1038/nature03714

Mathieu J, Warthmann N, Kuttner F, Schmid M (2007) Export of FT protein from phloem companion cells is sufficient for floral induction in Arabidopsis. Curr Biol 17 (12):1055-1060. doi:10.1016/j.cub.2007.05.009

Mathieu J, Yant LJ, Murdter F, Kuttner F, Schmid M (2009) Repression of flowering by the miR172 target SMZ. Plos Biol 7 (7):e1000148. doi:10.1371/journal.pbio.1000148

Matsoukas IG, Massiah AJ, Thomas B (2013) Starch metabolism and antiflorigenic signals modulate the juvenile-to-adult phase transition in Arabidopsis. Plant Cell Environ 36 (10):1802-1811. doi:10.1111/pce.12088

Mattiroli F, D'Arcy S, Luger K (2015) The right place at the right time: chaperoning core histone variants. EMBO Rep 16 (11):1454-1466. doi:10.15252/embr.201540840

Mayer KF, Schoof H, Haecker A, Lenhard M, Jurgens G, Laux T (1998) Role of WUSCHEL in regulating stem cell fate in the Arabidopsis shoot meristem. Cell 95 (6):805-815

McDowell GS, Philpott A (2013) Non-canonical ubiquitylation: mechanisms and consequences. Int J Biochem Cell Biol 45 (8):1833-1842. doi:10.1016/j.biocel.2013.05.026

McKnight SL, Miller OL, Jr. (1977) Electron microscopic analysis of chromatin replication in the cellular blastoderm Drosophila melanogaster embryo. Cell 12 (3):795-804

Meinke DW (1992) A Homoeotic Mutant of Arabidopsis thaliana with Leafy Cotyledons. Science 258 (5088):1647-1650. doi:10.1126/science.258.5088.1647

Meinke DW, Franzmann LH, Nickle TC, Yeung EC (1994) Leafy Cotyledon Mutants of Arabidopsis. Plant Cell 6 (8):1049-1064. doi:10.1105/tpc.6.8.1049

Meng L, Feldman LJ (2010) CLE14/CLE20 peptides may interact with CLAVATA2/CORYNE receptor-like kinases to irreversibly inhibit cell division in the root meristem of Arabidopsis. Planta 232 (5):1061-1074. doi:10.1007/s00425-010-1236-4

Merini W, Calonje M (2015) PRC1 is taking the lead in PcG repression. Plant J 83 (1):110-120. doi:10.1111/tpj.12818

Merini W, Romero-Campero FJ, Gomez-Zambrano A, Zhou Y, Turck F, Calonje M (2017) The Arabidopsis Polycomb Repressive Complex 1 (PRC1) Components AtBMI1A, B, and C Impact Gene Networks throughout All Stages of Plant Development. Plant Physiol 173 (1):627-641. doi:10.1104/pp.16.01259

Michaels SD (2009) Flowering time regulation produces much fruit. Curr Opin Plant Biol 12 (1):75-80. doi:10.1016/j.pbi.2008.09.005

Miller SM, Kirk DL (1999) glsA, a Volvox gene required for asymmetric division and germ cell specification, encodes a chaperone-like protein. Development 126 (4):649-658

Misteli T (2007) Beyond the sequence: cellular organization of genome function. Cell 128 (4):787-800. doi:10.1016/j.cell.2007.01.028

Miwa H, Betsuyaku S, Iwamoto K, Kinoshita A, Fukuda H, Sawa S (2008) The receptor-like kinase SOL2 mediates CLE signaling in Arabidopsis. Plant Cell Physiol 49 (11):1752-1757. doi:10.1093/pcp/pcn148

Molitor A, Latrasse D, Zytnicki M, Andrey P, Houba-Herin N, Hachet M, Battail C, Del Prete S, Alberti A, Quesneville H, Gaudin V (2016) The Arabidopsis hnRNP-Q Protein LIF2 and the PRC1 subunit LHP1 function in concert to regulate the transcription of stress-responsive genes. Plant Cell. doi:10.1105/tpc.16.00244

Molitor A, Shen WH (2013) The polycomb complex PRC1: composition and function in plants. J Genet Genomics 40 (5):231-238. doi:10.1016/j.jgg.2012.12.005

Molitor AM, Bu Z, Yu Y, Shen WH (2014) Arabidopsis AL PHD-PRC1 complexes promote seed germination through H3K4me3-to-H3K27me3 chromatin state switch in repression of seed developmental genes. PLoS Genet 10 (1):e1004091. doi:10.1371/journal.pgen.1004091

Monke G, Seifert M, Keilwagen J, Mohr M, Grosse I, Hahnel U, Junker A, Weisshaar B, Conrad U, Baumlein H, Altschmied L (2012) Toward the identification and regulation of the Arabidopsis thaliana ABI3 regulon. Nucleic Acids Res 40 (17):8240-8254. doi:10.1093/nar/gks594

Moon J, Suh SS, Lee H, Choi KR, Hong CB, Paek NC, Kim SG, Lee I (2003a) The SOC1 MADS-box gene integrates vernalization and gibberellin signals for flowering in Arabidopsis. Plant J 35 (5):613-623

Moon YH, Chen L, Pan RL, Chang HS, Zhu T, Maffeo DM, Sung ZR (2003b) EMF genes maintain vegetative development by repressing the flower program in Arabidopsis. Plant Cell 15 (3):681-693

Moreno-Mateos MA, Vejnar CE, Beaudoin JD, Fernandez JP, Mis EK, Khokha MK, Giraldez AJ (2015) CRISPRscan: designing highly efficient sgRNAs for CRISPR-Cas9 targeting in vivo. Nat Methods 12 (10):982-988. doi:10.1038/nmeth.3543

Morrison AJ, Shen X (2009) Chromatin remodelling beyond transcription: the INO80 and SWR1 complexes. Nat Rev Mol Cell Biol 10 (6):373-384. doi:10.1038/nrm2693

Mosquna A, Katz A, Decker EL, Rensing SA, Reski R, Ohad N (2009) Regulation of stem cell maintenance by the Polycomb protein FIE has been conserved during land plant evolution. Development 136 (14):2433-2444. doi:10.1242/dev.035048

Mozgova I, Hennig L (2015) The polycomb group protein regulatory network. Annu Rev Plant Biol 66:269-296. doi:10.1146/annurev-arplant-043014-115627

Mozgova I, Kohler C, Hennig L (2015) Keeping the gate closed: functions of the polycomb repressive complex PRC2 in development. Plant J 83 (1):121-132. doi:10.1111/tpj.12828

Mukherjee S, P. Khurana J (2018) Developmental Defects in Pusa Basmati 1 Transgenic Rice Plants Harboring Antisense OsiEZ1 Gene. International Journal of Current Research in Biosciences and Plant Biology 5 (7):53-69. doi:10.20546/ijcrbp.2018.507.008

Muller-Xing R, Clarenz O, Pokorny L, Goodrich J, Schubert D (2014) Polycomb-Group Proteins and FLOWERING LOCUS T Maintain Commitment to Flowering in Arabidopsis thaliana. Plant Cell 26 (6):2457-2471. doi:10.1105/tpc.114.123323

Murawska M, Brehm A (2011) CHD chromatin remodelers and the transcription cycle. Transcription 2 (6):244-253. doi:10.4161/trns.2.6.17840

Musielak TJ, Schenkel L, Kolb M, Henschen A, Bayer M (2015) A simple and versatile cell wall staining protocol to study plant reproduction. Plant reproduction 28 (3-4):161-169. doi:10.1007/s00497-015-0267-1

Nakabayashi K, Bartsch M, Xiang Y, Miatton E, Pellengahr S, Yano R, Seo M, Soppe WJ (2012) The time required for dormancy release in Arabidopsis is determined by DELAY OF GERMINATION1 protein levels in freshly harvested seeds. Plant Cell 24 (7):2826-2838. doi:10.1105/tpc.112.100214

Nakagawa T, Kajitani T, Togo S, Masuko N, Ohdan H, Hishikawa Y, Koji T, Matsuyama T, Ikura T, Muramatsu M, Ito T (2008) Deubiquitylation of histone H2A activates transcriptional initiation via trans-histone cross-talk with H3K4 di- and trimethylation. Genes Dev 22 (1):37-49. doi:10.1101/gad.1609708

Nakagawa T, Nakayama K (2015) Protein monoubiquitylation: targets and diverse functions. Genes Cells 20 (7):543-562. doi:10.1111/gtc.12250

Nallamilli BR, Zhang J, Mujahid H, Malone BM, Bridges SM, Peng Z (2013) Polycomb group gene OsFIE2 regulates rice (Oryza sativa) seed development and grain filling via a mechanism distinct from Arabidopsis. PLoS Genet 9 (3):e1003322. doi:10.1371/journal.pgen.1003322

Napsucialy-Mendivil S, Alvarez-Venegas R, Shishkova S, Dubrovsky JG (2014) Arabidopsis homolog of trithorax1 (ATX1) is required for cell production, patterning, and morphogenesis in root development. J Exp Bot 65 (22):6373-6384. doi:10.1093/jxb/eru355

Nassrallah A, Rougee M, Bourbousse C, Drevensek S, Fonseca S, Iniesto E, Ait-Mohamed O, Deton-Cabanillas AF, Zabulon G, Ahmed I, Stroebel D, Masson V, Lombard B, Eeckhout D, Gevaert K, Loew D, Genovesio A, Breyton C, de Jaeger G, Bowler C, Rubio V, Barneche F (2018) DET1-mediated degradation of a SAGA-like deubiquitination module controls H2Bub homeostasis. Elife 7. doi:10.7554/eLife.37892

Negishi M, Saraya A, Mochizuki S, Helin K, Koseki H, Iwama A (2010) A novel zinc finger protein Zfp277 mediates transcriptional repression of the Ink4a/arf locus through polycomb repressive complex 1. PLoS One 5 (8):e12373. doi:10.1371/journal.pone.0012373

Noh B, Lee SH, Kim HJ, Yi G, Shin EA, Lee M, Jung KJ, Doyle MR, Amasino RM, Noh YS (2004) Divergent roles of a pair of homologous jumonji/zinc-finger-class transcription factor proteins in the regulation of Arabidopsis flowering time. Plant Cell 16 (10):2601-2613. doi:10.1105/tpc.104.025353

Ogas J, Kaufmann S, Henderson J, Somerville C (1999) PICKLE is a CHD3 chromatin-remodeling factor that regulates the transition from embryonic to vegetative development in Arabidopsis. Proc Natl Acad Sci U S A 96 (24):13839-13844

Ohad N, Yadegari R, Margossian L, Hannon M, Michaeli D, Harada JJ, Goldberg RB, Fischer RL (1999) Mutations in FIE, a WD polycomb group gene, allow endosperm development without fertilization. Plant Cell 11 (3):407-416

Okano Y, Aono N, Hiwatashi Y, Murata T, Nishiyama T, Ishikawa T, Kubo M, Hasebe M

(2009) A polycomb repressive complex 2 gene regulates apogamy and gives evolutionary insights into early land plant evolution. Proc Natl Acad Sci U S A 106 (38):16321-16326. doi:10.1073/pnas.0906997106

Ooms J, Leon-Kloosterziel KM, Bartels D, Koornneef M, Karssen CM (1993) Acquisition of Desiccation Tolerance and Longevity in Seeds of Arabidopsis thaliana (A Comparative Study Using Abscisic Acid-Insensitive abi3 Mutants). Plant Physiol 102 (4):1185-1191

Overvoorde P, Fukaki H, Beeckman T (2010) Auxin control of root development. Cold Spring Harbor perspectives in biology 2 (6):a001537. doi:10.1101/cshperspect.a001537

Pandey R, Muller A, Napoli CA, Selinger DA, Pikaard CS, Richards EJ, Bender J, Mount DW, Jorgensen RA (2002) Analysis of histone acetyltransferase and histone deacetylase families of Arabidopsis thaliana suggests functional diversification of chromatin modification among multicellular eukaryotes. Nucleic Acids Res 30 (23):5036-5055

Papamichos-Chronakis M, Watanabe S, Rando OJ, Peterson CL (2011) Global regulation of H2A.Z localization by the INO80 chromatin-remodeling enzyme is essential for genome integrity. Cell 144 (2):200-213. doi:10.1016/j.cell.2010.12.021

Parcy F, Valon C, Kohara A, Misera S, Giraudat J (1997) The ABSCISIC ACID-INSENSITIVE3, FUSCA3, and LEAFY COTYLEDON1 loci act in concert to control multiple aspects of Arabidopsis seed development. Plant Cell 9 (8):1265-1277. doi:10.1105/tpc.9.8.1265

Parcy F, Valon C, Raynal M, Gaubier-Comella P, Delseny M, Giraudat J (1994) Regulation of gene expression programs during Arabidopsis seed development: roles of the ABI3 locus and of endogenous abscisic acid. Plant Cell 6 (11):1567-1582. doi:10.1105/tpc.6.11.1567

Pazhouhandeh M, Molinier J, Berr A, Genschik P (2011) MSI4/FVE interacts with CUL4-DDB1 and a PRC2-like complex to control epigenetic regulation of flowering time in Arabidopsis. Proc Natl Acad Sci U S A 108 (8):3430-3435. doi:10.1073/pnas.1018242108

Peng L, Wang L, Zhang Y, Dong A, Shen WH, Huang Y (2018) Structural Analysis of the Arabidopsis AL2-PAL and PRC1 Complex Provides Mechanistic Insight into Active-to-Repressive Chromatin State Switch. J Mol Biol 430 (21):4245-4259. doi:10.1016/j.jmb.2018.08.021

Peragine A, Yoshikawa M, Wu G, Albrecht HL, Poethig RS (2004) SGS3 and SGS2/SDE1/RDR6 are required for juvenile development and the production of

trans-acting siRNAs in Arabidopsis. Genes Dev 18 (19):2368-2379. doi:10.1101/gad.1231804

Pereman I, Mosquna A, Katz A, Wiedemann G, Lang D, Decker EL, Tamada Y, Ishikawa T, Nishiyama T, Hasebe M, Reski R, Ohad N (2016) The Polycomb group protein CLF emerges as a specific tri-methylase of H3K27 regulating gene expression and development in Physcomitrella patens. Biochim Biophys Acta 1859 (7):860-870. doi:10.1016/j.bbagrm.2016.05.004

Pernas M, Ryan E, Dolan L (2010) SCHIZORIZA controls tissue system complexity in plants. Curr Biol 20 (9):818-823. doi:10.1016/j.cub.2010.02.062

Phillips DM (1963) The presence of acetyl groups of histones. Biochem J 87:258-263

Pickart CM, Eddins MJ (2004) Ubiquitin: structures, functions, mechanisms. Biochim Biophys Acta 1695 (1-3):55-72. doi:10.1016/j.bbamcr.2004.09.019

Pico S, Ortiz-Marchena MI, Merini W, Calonje M (2015) Deciphering the Role of POLYCOMB REPRESSIVE COMPLEX1 Variants in Regulating the Acquisition of Flowering Competence in Arabidopsis. Plant Physiol 168 (4):1286-1297. doi:10.1104/pp.15.00073

Piquet S, Le Parc F, Bai SK, Chevallier O, Adam S, Polo SE (2018) The Histone Chaperone FACT Coordinates H2A.X-Dependent Signaling and Repair of DNA Damage. Mol Cell. doi:10.1016/j.molcel.2018.09.010

Poethig RS (1990) Phase change and the regulation of shoot morphogenesis in plants. Science 250 (4983):923-930. doi:10.1126/science.250.4983.923

Preston JC, Hileman LC (2013) Functional Evolution in the Plant SQUAMOSA-PROMOTER BINDING PROTEIN-LIKE (SPL) Gene Family. Front Plant Sci 4:80. doi:10.3389/fpls.2013.00080

Prior CP, Cantor CR, Johnson EM, Allfrey VG (1980) Incorporation of exogenous pyrene-labeled histone into Physarum chromatin: a system for studying changes in nucleosomes assembled in vivo. Cell 20 (3):597-608

Pu L, Sung ZR (2015) PcG and trxG in plants - friends or foes. Trends in Genetics 31 (5):252-262. doi:10.1016/j.tig.2015.03.004

Putterill J, Robson F, Lee K, Simon R, Coupland G (1995) The CONSTANS gene of Arabidopsis promotes flowering and encodes a protein showing similarities to zinc finger transcription factors. Cell 80 (6):847-857

Qin F, Sakuma Y, Tran LS, Maruyama K, Kidokoro S, Fujita Y, Fujita M, Umezawa T, Sawano Y, Miyazono K, Tanokura M, Shinozaki K, Yamaguchi-Shinozaki K (2008) Arabidopsis DREB2A-interacting proteins function as RING E3 ligases and negatively regulate plant drought stress-responsive gene expression. Plant

Cell 20 (6):1693-1707. doi:10.1105/tpc.107.057380

Ramakers C, Ruijter JM, Deprez RH, Moorman AF (2003) Assumption-free analysis of quantitative real-time polymerase chain reaction (PCR) data. Neurosci Lett 339 (1):62-66

Ramirez-Prado JS, Piquerez SJM, Bendahmane A, Hirt H, Raynaud C, Benhamed M (2018) Modify the Histone to Win the Battle: Chromatin Dynamics in Plant-Pathogen Interactions. Front Plant Sci 9:355. doi:10.3389/fpls.2018.00355

Ratcliffe OJ, Nadzan GC, Reuber TL, Riechmann JL (2001) Regulation of flowering in Arabidopsis by an FLC homologue. Plant Physiol 126 (1):122-132

Raz V, Bergervoet JH, Koornneef M (2001) Sequential steps for developmental arrest in Arabidopsis seeds. Development 128 (2):243-252

Ream TS, Woods DP, Amasino RM (2012) The molecular basis of vernalization in different plant groups. Cold Spring Harb Symp Quant Biol 77:105-115. doi:10.1101/sqb.2013.77.014449

Richly H, Rocha-Viegas L, Ribeiro JD, Demajo S, Gundem G, Lopez-Bigas N, Nakagawa T, Rospert S, Ito T, Di Croce L (2010) Transcriptional activation of polycomb-repressed genes by ZRF1. Nature 468 (7327):1124-1128. doi:10.1038/nature09574

Riese M, Hohmann S, Saedler H, Munster T, Huijser P (2007) Comparative analysis of the SBP-box gene families in P. patens and seed plants. Gene 401 (1-2):28-37. doi:10.1016/j.gene.2007.06.018

Robzyk K, Recht L, Osley MA (2000) Rad6-dependent ubiquitination of histone H2B in yeast. Science 287 (5452):501-504. doi:DOI 10.1126/science.287.5452.501

Rosa M, Von Harder M, Cigliano RA, Schlogelhofer P, Mittelsten Scheid O (2013) The Arabidopsis SWR1 chromatin-remodeling complex is important for DNA repair, somatic recombination, and meiosis. Plant Cell 25 (6):1990-2001. doi:10.1105/tpc.112.104067

Rosa S, Duncan S, Dean C (2016) Mutually exclusive sense-antisense transcription at FLC facilitates environmentally induced gene repression. Nat Commun 7:13031. doi:10.1038/ncomms13031

Rossetto D, Avvakumov N, Cote J (2012) Histone phosphorylation: a chromatin modification involved in diverse nuclear events. Epigenetics 7 (10):1098-1108. doi:10.4161/epi.21975

Rossetto D, Truman AW, Kron SJ, Cote J (2010) Epigenetic modifications in double-strand break DNA damage signaling and repair. Clin Cancer Res 16 (18):4543-4552. doi:10.1158/1078-0432.CCR-10-0513

Ruthenburg AJ, Allis CD, Wysocka J (2007) Methylation of lysine 4 on histone H3: Intricacy of writing and reading a single epigenetic mark. Mol Cell 25 (1):15-30. doi:10.1016/j.molcel.2006.12.014

Sabatini S, Beis D, Wolkenfelt H, Murfett J, Guilfoyle T, Malamy J, Benfey P, Leyser O, Bechtold N, Weisbeek P, Scheres B (1999) An auxin-dependent distal organizer of pattern and polarity in the Arabidopsis root. Cell 99 (5):463-472

Saleh A, Al-Abdallat A, Ndamukong I, Alvarez-Venegas R, Avramova Z (2007) The Arabidopsis homologs of trithorax (ATX1) and enhancer of zeste (CLF) establish 'bivalent chromatin marks' at the silent AGAMOUS locus. Nucleic Acids Res 35 (18):6290-6296. doi:10.1093/nar/gkm464

Saleh A, Alvarez-Venegas R, Avramova Z (2008) An efficient chromatin immunoprecipitation (ChIP) protocol for studying histone modifications in Arabidopsis plants. Nat Protoc 3 (6):1018-1025. doi:10.1038/nprot.2008.66

Sanchez MD, Aceves-Garcia P, Petrone E, Steckenborn S, Vega-Leon R, Alvarez-Buylla ER, Garay-Arroyo A, Garcia-Ponce B (2015) The impact of Polycomb group (PcG) and Trithorax group (TrxG) epigenetic factors in plant plasticity. New Phytol 208 (3):684-694. doi:10.1111/nph.13486

Sanchez MD, Gutierrez C (2009) Arabidopsis ORC1 is a PHD-containing H3K4me3 effector that regulates transcription. P Natl Acad Sci USA 106 (6):2065-2070. doi:10.1073/pnas.0811093106

Sander JD, Joung JK (2014) CRISPR-Cas systems for editing, regulating and targeting genomes. Nat Biotechnol 32 (4):347-355. doi:10.1038/nbt.2842

Sarkar AK, Luijten M, Miyashima S, Lenhard M, Hashimoto T, Nakajima K, Scheres B, Heidstra R, Laux T (2007) Conserved factors regulate signalling in Arabidopsis thaliana shoot and root stem cell organizers. Nature 446 (7137):811-814. doi:10.1038/nature05703

Sawa M, Nusinow DA, Kay SA, Imaizumi T (2007) FKF1 and GIGANTEA complex formation is required for day-length measurement in Arabidopsis. Science 318 (5848):261-265. doi:10.1126/science.1146994

Scheres BJG, Wolkenfelt H, Willemsen V, Terlouw M, Lawson E, Dean C, Weisbeek P (1994) Embryonic origin of the Arabidopsis primary root and root meristem initials. Development 120 (9):13

Schmitz RJ, Tamada Y, Doyle MR, Zhang X, Amasino RM (2009) Histone H2B deubiquitination is required for transcriptional activation of FLOWERING LOCUS C and for proper control of flowering in Arabidopsis. Plant Physiol 149 (2):1196-1204. doi:10.1104/pp.108.131508

Schubert D, Primavesi L, Bishopp A, Roberts G, Doonan J, Jenuwein T, Goodrich J

(2006) Silencing by plant Polycomb-group genes requires dispersed trimethylation of histone H3 at lysine 27. EMBO J 25 (19):4638-4649. doi:10.1038/sj.emboj.7601311

Schuettengruber B, Bourbon HM, Di Croce L, Cavalli G (2017) Genome Regulation by Polycomb and Trithorax: 70 Years and Counting. Cell 171 (1):34-57. doi:10.1016/j.cell.2017.08.002

Scortecci K, Michaels SD, Amasino RM (2003) Genetic interactions between FLM and other flowering-time genes in Arabidopsis thaliana. Plant Mol Biol 52 (5):915-922

Shafiq S, Berr A, Shen WH (2014a) Combinatorial functions of diverse histone methylations in Arabidopsis thaliana flowering time regulation. New Phytol 201 (1):312-322. doi:10.1111/nph.12493

Shafiq S, Berr A, Shen WH (2014b) Combinatorial functions of diverse histone methylations in Arabidopsis thaliana flowering time regulation. New Phytol 201 (1):312-322. doi:10.1111/nph.12493

Shahbazian MD, Grunstein M (2007) Functions of site-specific histone acetylation and deacetylation. Annu Rev Biochem 76:75-100. doi:10.1146/annurev.biochem.76.052705.162114

Sharif J, Koseki H (2017) No Winter Lasts Forever: Polycomb Complexes Convert Epigenetic Memory of Cold into Flowering. Dev Cell 42 (6):563-564. doi:10.1016/j.devcel.2017.09.004

Shaver S, Casas-Mollano JA, Cerny RL, Cerutti H (2010) Origin of the polycomb repressive complex 2 and gene silencing by an E(z) homolog in the unicellular alga Chlamydomonas. Epigenetics 5 (4):301-312

Shen L, Thong Z, Gong X, Shen Q, Gan Y, Yu H (2014a) The putative PRC1 RING-finger protein AtRING1A regulates flowering through repressing MADS AFFECTING FLOWERING genes in Arabidopsis. Development 141 (6):1303-1312. doi:10.1242/dev.104513

Shen Y, Silva NCE, Audonnet L, Servet C, Wei W, Zhou DX (2014b) Over-expression of histone H3K4 demethylase gene JMJ15 enhances salt tolerance in Arabidopsis. Frontiers in Plant Science 5. doi:ARTN 290

10.3389/fpls.2014.00290

Shi Y, Lan F, Matson C, Mulligan P, Whetstine JR, Cole PA, Casero RA, Shi Y (2004) Histone demethylation mediated by the nuclear amine oxidase homolog LSD1. Cell 119 (7):941-953. doi:10.1016/j.cell.2004.12.012

Simon AC, Zhou JC, Perera RL, van Deursen F, Evrin C, Ivanova ME, Kilkenny ML,

Renault L, Kjaer S, Matak-Vinkovic D, Labib K, Costa A, Pellegrini L (2014) A Ctf4 trimer couples the CMG helicase to DNA polymerase alpha in the eukaryotic replisome. Nature 510 (7504):293-297. doi:10.1038/nature13234

Singer MS, Kahana A, Wolf AJ, Meisinger LL, Peterson SE, Goggin C, Mahowald M, Gottschling DE (1998) Identification of high-copy disruptors of telomeric silencing in Saccharomyces cerevisiae. Genetics 150 (2):613-632

Sobhian B, Shao G, Lilli DR, Culhane AC, Moreau LA, Xia B, Livingston DM, Greenberg RA (2007) RAP80 targets BRCA1 to specific ubiquitin structures at DNA damage sites. Science 316 (5828):1198-1202. doi:10.1126/science.1139516

Sogo JM, Stahl H, Koller T, Knippers R (1986) Structure of replicating simian virus 40 minichromosomes. The replication fork, core histone segregation and terminal structures. J Mol Biol 189 (1):189-204

Song YH, Smith RW, To BJ, Millar AJ, Imaizumi T (2012) FKF1 conveys timing information for CONSTANS stabilization in photoperiodic flowering. Science 336 (6084):1045-1049. doi:10.1126/science.1219644

Sorensen MB, Chaudhury AM, Robert H, Bancharel E, Berger F (2001) Polycomb group genes control pattern formation in plant seed. Curr Biol 11 (4):277-281

Sozzani R, Cui H, Moreno-Risueno MA, Busch W, Van Norman JM, Vernoux T, Brady SM, Dewitte W, Murray JA, Benfey PN (2010) Spatiotemporal regulation of cell-cycle genes by SHORTROOT links patterning and growth. Nature 466 (7302):128-132. doi:10.1038/nature09143

Spedaletti V, Polticelli F, Capodaglio V, Schinina ME, Stano P, Federico R, Tavladoraki P (2008) Characterization of a lysine-specific histone demethylase from Arabidopsis thaliana. Biochemistry-Us 47 (17):4936-4947. doi:10.1021/bi701969k

Stahl Y, Grabowski S, Bleckmann A, Kuhnemuth R, Weidtkamp-Peters S, Pinto KG, Kirschner GK, Schmid JB, Wink RH, Hulsewede A, Felekyan S, Seidel CA, Simon R (2013) Moderation of Arabidopsis root stemness by CLAVATA1 and ARABIDOPSIS CRINKLY4 receptor kinase complexes. Curr Biol 23 (5):362-371. doi:10.1016/j.cub.2013.01.045

Stahl Y, Wink RH, Ingram GC, Simon R (2009) A signaling module controlling the stem cell niche in Arabidopsis root meristems. Curr Biol 19 (11):909-914. doi:10.1016/j.cub.2009.03.060

Stock JK, Giadrossi S, Casanova M, Brookes E, Vidal M, Koseki H, Brockdorff N, Fisher AG, Pombo A (2007) Ring1-mediated ubiquitination of H2A restrains poised RNA polymerase II at bivalent genes in mouse ES cells. Nat Cell Biol 9 (12):1428-1435. doi:10.1038/ncb1663

Stone SL, Kwong LW, Yee KM, Pelletier J, Lepiniec L, Fischer RL, Goldberg RB, Harada JJ (2001) LEAFY COTYLEDON2 encodes a B3 domain transcription factor that induces embryo development. Proc Natl Acad Sci U S A 98 (20):11806-11811. doi:10.1073/pnas.201413498

Su D, Hu Q, Li Q, Thompson JR, Cui G, Fazly A, Davies BA, Botuyan MV, Zhang Z, Mer G (2012) Structural basis for recognition of H3K56-acetylated histone H3-H4 by the chaperone Rtt106. Nature 483 (7387):104-107. doi:10.1038/nature10861

Sun B, Looi LS, Guo S, He Z, Gan ES, Huang J, Xu Y, Wee WY, Ito T (2014) Timing mechanism dependent on cell division is invoked by Polycomb eviction in plant stem cells. Science 343 (6170):1248559. doi:10.1126/science.1248559

Sun B, Xu Y, Ng KH, Ito T (2009) A timing mechanism for stem cell maintenance and differentiation in the Arabidopsis floral meristem. Genes Dev 23 (15):1791-1804. doi:10.1101/gad.1800409

Suzuki M, McCarty DR (2008) Functional symmetry of the B3 network controlling seed development. Curr Opin Plant Biol 11 (5):548-553. doi:10.1016/j.pbi.2008.06.015

Suzuki M, Wang HH, McCarty DR (2007) Repression of the LEAFY COTYLEDON 1/B3 regulatory network in plant embryo development by VP1/ABSCISIC ACID INSENSITIVE 3-LIKE B3 genes. Plant Physiol 143 (2):902-911. doi:10.1104/pp.106.092320

Takada S, Hibara K, Ishida T, Tasaka M (2001) The CUP-SHAPED COTYLEDON1 gene of Arabidopsis regulates shoot apical meristem formation. Development 128 (7):1127-1135

Tan BC, Chien CT, Hirose S, Lee SC (2006) Functional cooperation between FACT and MCM helicase facilitates initiation of chromatin DNA replication. EMBO J 25 (17):3975-3985. doi:10.1038/sj.emboj.7601271

Tang X, Lim MH, Pelletier J, Tang M, Nguyen V, Keller WA, Tsang EW, Wang A, Rothstein SJ, Harada JJ, Cui Y (2012) Synergistic repression of the embryonic programme by SET DOMAIN GROUP 8 and EMBRYONIC FLOWER 2 in Arabidopsis seedlings. J Exp Bot 63 (3):1391-1404. doi:10.1093/jxb/err383

Taverna SD, Li H, Ruthenburg AJ, Allis CD, Patel DJ (2007) How chromatin-binding modules interpret histone modifications: lessons from professional pocket pickers. Nature Structural & Molecular Biology 14 (11):1025-1040. doi:10.1038/nsmb1338

Telfer A, Bollman KM, Poethig RS (1997) Phase change and the regulation of trichome distribution in Arabidopsis thaliana. Development 124 (3):645-654

ten Hove CA, Willemsen V, de Vries WJ, van Dijken A, Scheres B, Heidstra R (2010) SCHIZORIZA encodes a nuclear factor regulating asymmetry of stem cell divisions in the Arabidopsis root. Curr Biol 20 (5):452-457. doi:10.1016/j.cub.2010.01.018

Tessarz P, Kouzarides T (2014) Histone core modifications regulating nucleosome structure and dynamics. Nat Rev Mol Cell Biol 15 (11):703-708. doi:10.1038/nrm3890

Thiriet C, Hayes JJ (2005) Chromatin in need of a fix: phosphorylation of H2AX connects chromatin to DNA repair. Mol Cell 18 (6):617-622. doi:10.1016/j.molcel.2005.05.008

Thorstensen T, Grini PE, Aalen RB (2011) SET domain proteins in plant development. Biochim Biophys Acta 1809 (8):407-420. doi:10.1016/j.bbagrm.2011.05.008

Thorstensen T, Grini PE, Mercy IS, Alm V, Erdal S, Aasland R, Aalen RB (2008) The Arabidopsis SET-domain protein ASHR3 is involved in stamen development and interacts with the bHLH transcription factor ABORTED MICROSPORES (AMS). Plant Mol Biol 66 (1-2):47-59. doi:10.1007/s11103-007-9251-y

Tian H, Niu T, Yu Q, Quan T, Ding Z (2013) Auxin gradient is crucial for the maintenance of root distal stem cell identity in Arabidopsis. Plant signaling & behavior 8 (12):e26429. doi:10.4161/psb.26429

Tian H, Wabnik K, Niu T, Li H, Yu Q, Pollmann S, Vanneste S, Govaerts W, Rolcik J, Geisler M, Friml J, Ding Z (2014) WOX5-IAA17 feedback circuit-mediated cellular auxin response is crucial for the patterning of root stem cell niches in Arabidopsis. Molecular plant 7 (2):277-289. doi:10.1093/mp/sst118

Tirosh I, Sigal N, Barkai N (2010) Widespread remodeling of mid-coding sequence nucleosomes by Isw1. Genome Biol 11 (5):R49. doi:10.1186/gb-2010-11-5-r49

Trejo-Arellano MS, Mahrez W, Nakamura M, Moreno-Romero J, Nanni P, Kohler C, Hennig L (2017) H3K23me1 is an evolutionarily conserved histone modification associated with CG DNA methylation in Arabidopsis. Plant J 90 (2):293-303. doi:10.1111/tpj.13489

Truernit E, Bauby H, Dubreucq B, Grandjean O, Runions J, Barthelemy J, Palauqui JC (2008) High-resolution whole-mount imaging of three-dimensional tissue organization and gene expression enables the study of Phloem development and structure in Arabidopsis. Plant Cell 20 (6):1494-1503. doi:10.1105/tpc.107.056069

Tsukada Y, Fang J, Erdjument-Bromage H, Warren ME, Borchers CH, Tempst P, Zhang Y (2006) Histone demethylation by a family of JmjC domain-containing proteins. Nature 439 (7078):811-816. doi:10.1038/nature04433

Tsukagoshi H, Busch W, Benfey PN (2010) Transcriptional regulation of ROS controls transition from proliferation to differentiation in the root. Cell 143 (4):606-616. doi:10.1016/j.cell.2010.10.020

Tsukaya H, Shoda K, Kim GT, Uchimiya H (2000) Heteroblasty in Arabidopsis thaliana (L.) Heynh. Planta 210 (4):536-542. doi:10.1007/s004250050042

Turck F, Roudier F, Farrona S, Martin-Magniette ML, Guillaume E, Buisine N, Gagnot S, Martienssen RA, Coupland G, Colot V (2007a) Arabidopsis TFL2/LHP1 specifically associates with genes marked by trimethylation of histone H3 lysine 27. PLoS Genet 3 (6):e86. doi:10.1371/journal.pgen.0030086

Turck F, Roudier F, Farrona S, Martin-Magniette ML, Guillaume E, Buisine N, Gagnot S, Martienssen RA, Coupland G, Colot V (2007b) Arabidopsis TFL2/LHP1 specifically associates with genes marked by trimethylation of histone H3 lysine 27. Plos Genetics 3 (6):855-866. doi:ARTN e86

10.1371/journal.pgen.0030086

Turinetto V, Giachino C (2015) Multiple facets of histone variant H2AX: a DNA double-strand-break marker with several biological functions. Nucleic Acids Res 43 (5):2489-2498. doi:10.1093/nar/gkv061

Tweedie-Cullen RY, Brunner AM, Grossmann J, Mohanna S, Sichau D, Nanni P, Panse C, Mansuy IM (2012) Identification of combinatorial patterns of post-translational modifications on individual histones in the mouse brain. PLoS One 7 (5):e36980. doi:10.1371/journal.pone.0036980

Udugama M, Sabri A, Bartholomew B (2011) The INO80 ATP-dependent chromatin remodeling complex is a nucleosome spacing factor. Mol Cell Biol 31 (4):662-673. doi:10.1128/MCB.01035-10

Usami T, Horiguchi G, Yano S, Tsukaya H (2009) The more and smaller cells mutants of Arabidopsis thaliana identify novel roles for SQUAMOSA PROMOTER BINDING PROTEIN-LIKE genes in the control of heteroblasty. Development 136 (6):955-964. doi:10.1242/dev.028613

Utley RT, Lacoste N, Jobin-Robitaille O, Allard S, Cote J (2005) Regulation of NuA4 histone acetyltransferase activity in transcription and DNA repair by phosphorylation of histone H4. Mol Cell Biol 25 (18):8179-8190. doi:10.1128/MCB.25.18.8179-8190.2005

van Attikum H, Gasser SM (2005) The histone code at DNA breaks: a guide to repair? Nat Rev Mol Cell Biol 6 (10):757-765. doi:10.1038/nrm1737

Vanstraelen M, Baloban M, Da Ines O, Cultrone A, Lammens T, Boudolf V, Brown SC, De Veylder L, Mergaert P, Kondorosi E (2009) APC/C-CCS52A complexes control meristem maintenance in the Arabidopsis root. Proc Natl Acad Sci U S A

106 (28):11806-11811. doi:10.1073/pnas.0901193106

Veluchamy A, Jegu T, Ariel F, Latrasse D, Mariappan KG, Kim SK, Crespi M, Hirt H, Bergounioux C, Raynaud C, Benhamed M (2016) LHP1 Regulates H3K27me3 Spreading and Shapes the Three-Dimensional Conformation of the Arabidopsis Genome. PLoS One 11 (7):e0158936. doi:10.1371/journal.pone.0158936

Vicient CM, Bies-Etheve N, Delseny M (2000) Changes in gene expression in the leafy cotyledon1 (lec1) and fusca3 (fus3) mutants of Arabidopsis thaliana L. J Exp Bot 51 (347):995-1003

Vroemen CW, Mordhorst AP, Albrecht C, Kwaaitaal MA, de Vries SC (2003) The CUP-SHAPED COTYLEDON3 gene is required for boundary and shoot meristem formation in Arabidopsis. Plant Cell 15 (7):1563-1577

Wang H, Liu C, Cheng J, Liu J, Zhang L, He C, Shen WH, Jin H, Xu L, Zhang Y (2016) Arabidopsis Flower and Embryo Developmental Genes are Repressed in Seedlings by Different Combinations of Polycomb Group Proteins in Association with Distinct Sets of Cis-regulatory Elements. PLoS Genet 12 (1):e1005771. doi:10.1371/journal.pgen.1005771

Wang H, Wang L, Erdjument-Bromage H, Vidal M, Tempst P, Jones RS, Zhang Y (2004) Role of histone H2A ubiquitination in Polycomb silencing. Nature 431 (7010):873-878. doi:10.1038/nature02985

Wang HF, Jiang DH, Axelsson E, Lorkovic ZJ, Montgomery S, Holec S, Pieters BJGE, Al Temimi AHK, Mecinovic J, Berger F (2018) LHP1 Interacts with ATRX through Plant-Specific Domains at Specific Loci Targeted by PRC2. Molecular plant 11 (8):1038-1052. doi:10.1016/j.molp.2018.05.004

Wang J, Tian C, Zhang C, Shi B, Cao X, Zhang TQ, Zhao Z, Wang JW, Jiao Y (2017) Cytokinin Signaling Activates WUSCHEL Expression during Axillary Meristem Initiation. Plant Cell 29 (6):1373-1387. doi:10.1105/tpc.16.00579

Wang JW, Czech B, Weigel D (2009) miR156-regulated SPL transcription factors define an endogenous flowering pathway in Arabidopsis thaliana. Cell 138 (4):738-749. doi:10.1016/j.cell.2009.06.014

Wang M, Tang D, Luo Q, Jin Y, Shen Y, Wang K, Cheng Z (2012) BRK1, a Bub1-related kinase, is essential for generating proper tension between homologous kinetochores at metaphase I of rice meiosis. Plant Cell 24 (12):4961-4973. doi:10.1105/tpc.112.105874

Wang Q, Shen WH (2018) Chromatin modulation and gene regulation in plants: insight about PRC1 function. Biochem Soc Trans 46 (4):957-966. doi:10.1042/BST20170576

Wang R, Taylor AB, Leal BZ, Chadwell LV, Ilangovan U, Robinson AK, Schirf V, Hart

PJ, Lafer EM, Demeler B, Hinck AP, McEwen DG, Kim CA (2010) Polycomb group targeting through different binding partners of RING1B C-terminal domain. Structure 18 (8):966-975. doi:10.1016/j.str.2010.04.013

Wang Y, Gu X, Yuan W, Schmitz RJ, He Y (2014) Photoperiodic control of the floral transition through a distinct polycomb repressive complex. Dev Cell 28 (6):727-736. doi:10.1016/j.devcel.2014.01.029

West M, Harada JJ (1993) Embryogenesis in Higher Plants: An Overview. Plant Cell 5 (10):1361-1369. doi:10.1105/tpc.5.10.1361

West M, Yee KM, Danao J, Zimmerman JL, Fischer RL, Goldberg RB, Harada JJ (1994) LEAFY COTYLEDON1 Is an Essential Regulator of Late Embryogenesis and Cotyledon Identity in Arabidopsis. Plant Cell 6 (12):1731-1745. doi:10.1105/tpc.6.12.1731

Whitehouse I, Tsukiyama T (2006) Antagonistic forces that position nucleosomes in vivo. Nat Struct Mol Biol 13 (7):633-640. doi:10.1038/nsmb1111

Widiez T, Symeonidi A, Luo C, Lam E, Lawton M, Rensing SA (2014) The chromatin landscape of the moss Physcomitrella patens and its dynamics during development and drought stress. Plant J 79 (1):67-81. doi:10.1111/tpj.12542

Wiest NE, Houghtaling S, Sanchez JC, Tomkinson AE, Osley MA (2017) The SWI/SNF ATP-dependent nucleosome remodeler promotes resection initiation at a DNA double-strand break in yeast. Nucleic Acids Res 45 (10):5887-5900. doi:10.1093/nar/gkx221

Wigge PA, Kim MC, Jaeger KE, Busch W, Schmid M, Lohmann JU, Weigel D (2005) Integration of spatial and temporal information during floral induction in Arabidopsis. Science 309 (5737):1056-1059. doi:10.1126/science.1114358

Willemsen V, Bauch M, Bennett T, Campilho A, Wolkenfelt H, Xu J, Haseloff J, Scheres B (2008) The NAC domain transcription factors FEZ and SOMBRERO control the orientation of cell division plane in Arabidopsis root stem cells. Dev Cell 15 (6):913-922. doi:10.1016/j.devcel.2008.09.019

Williams L, Carles CC, Osmont KS, Fletcher JC (2005) A database analysis method identifies an endogenous trans-acting short-interfering RNA that targets the Arabidopsis ARF2, ARF3, and ARF4 genes. Proc Natl Acad Sci U S A 102 (27):9703-9708. doi:10.1073/pnas.0504029102

Wong SJ, Gearhart MD, Taylor AB, Nanyes DR, Ha DJ, Robinson AK, Artigas JA, Lee OJ, Demeler B, Hart PJ, Bardwell VJ, Kim CA (2016) KDM2B Recruitment of the Polycomb Group Complex, PRC1.1, Requires Cooperation between PCGF1 and BCORL1. Structure 24 (10):1795-1801. doi:10.1016/j.str.2016.07.011

Wood A, Krogan NJ, Dover J, Schneider J, Heidt J, Boateng MA, Dean K, Golshani A,

Zhang Y, Greenblatt JF, Johnston M, Shilatifard A (2003) Bre1, an E3 ubiquitin ligase required for recruitment and substrate selection of Rad6 at a promoter. Mol Cell 11 (1):267-274. doi:Doi 10.1016/S1097-2765(02)00802-X

Wood CC, Robertson M, Tanner G, Peacock WJ, Dennis ES, Helliwell CA (2006) The Arabidopsis thaliana vernalization response requires a polycomb-like protein complex that also includes VERNALIZATION INSENSITIVE 3. Proc Natl Acad Sci U S A 103 (39):14631-14636. doi:10.1073/pnas.0606385103

Wu G, Park MY, Conway SR, Wang JW, Weigel D, Poethig RS (2009) The sequential action of miR156 and miR172 regulates developmental timing in Arabidopsis. Cell 138 (4):750-759. doi:10.1016/j.cell.2009.06.031

Wu G, Poethig RS (2006) Temporal regulation of shoot development in Arabidopsis thaliana by miR156 and its target SPL3. Development 133 (18):3539-3547. doi:10.1242/dev.02521

Wu K, Tian L, Malik K, Brown D, Miki B (2000) Functional analysis of HD2 histone deacetylase homologues in Arabidopsis thaliana. Plant J 22 (1):19-27

Wu X, Johansen JV, Helin K (2013) Fbxl10/Kdm2b recruits polycomb repressive complex 1 to CpG islands and regulates H2A ubiquitylation. Mol Cell 49 (6):1134-1146. doi:10.1016/j.molcel.2013.01.016

Xiao J, Jin R, Yu X, Shen M, Wagner JD, Pai A, Song C, Zhuang M, Klasfeld S, He C, Santos AM, Helliwell C, Pruneda-Paz JL, Kay SA, Lin X, Cui S, Garcia MF, Clarenz O, Goodrich J, Zhang X, Austin RS, Bonasio R, Wagner D (2017) Cis and trans determinants of epigenetic silencing by Polycomb repressive complex 2 in Arabidopsis. Nat Genet 49 (10):1546-1552. doi:10.1038/ng.3937

Xiao J, Lee US, Wagner D (2016) Tug of war: adding and removing histone lysine methylation in Arabidopsis. Curr Opin Plant Biol 34:41-53. doi:10.1016/j.pbi.2016.08.002

Xiao J, Wagner D (2015) Polycomb repression in the regulation of growth and development in Arabidopsis. Curr Opin Plant Biol 23:15-24. doi:10.1016/j.pbi.2014.10.003

Xie K, Wu C, Xiong L (2006) Genomic organization, differential expression, and interaction of SQUAMOSA promoter-binding-like transcription factors and microRNA156 in rice. Plant Physiol 142 (1):280-293. doi:10.1104/pp.106.084475

Xu C, Bian C, Yang W, Galka M, Ouyang H, Chen C, Qiu W, Liu H, Jones AE, MacKenzie F, Pan P, Li SS, Wang H, Min J (2010) Binding of different histone marks differentially regulates the activity and specificity of polycomb repressive complex 2 (PRC2). Proc Natl Acad Sci U S A 107 (45):19266-19271.

doi:10.1073/pnas.1008937107

Xu F, Kuo T, Rosli Y, Liu MS, Wu L, Chen LO, Fletcher JC, Sung ZR, Pu L (2018a) Trithorax Group Proteins Act Together with a Polycomb Group Protein to Maintain Chromatin Integrity for Epigenetic Silencing during Seed Germination in Arabidopsis. Molecular plant 11 (5):659-677. doi:10.1016/j.molp.2018.01.010

Xu F, Kuo T, Rosli Y, Liu MS, Wu L, Oliver Chen LF, Fletcher JC, Sung ZR, Pu L (2018b) Trithorax group proteins act together with a Polycomb group protein to maintain chromatin integrity for epigenetic silencing during seed germination in Arabidopsis. Molecular plant. doi:10.1016/j.molp.2018.01.010

Xu L, Shen WH (2008) Polycomb silencing of KNOX genes confines shoot stem cell niches in Arabidopsis. Curr Biol 18 (24):1966-1971. doi:10.1016/j.cub.2008.11.019

Xu L, Zhao Z, Dong A, Soubigou-Taconnat L, Renou JP, Steinmetz A, Shen WH (2008) Di- and tri- but not monomethylation on histone H3 lysine 36 marks active transcription of genes involved in flowering time regulation and other processes in Arabidopsis thaliana. Mol Cell Biol 28 (4):1348-1360. doi:10.1128/MCB.01607-07

Xu M, Hu T, Smith MR, Poethig RS (2016a) Epigenetic Regulation of Vegetative Phase Change in Arabidopsis. Plant Cell 28 (1):28-41. doi:10.1105/tpc.15.00854

Xu M, Hu T, Zhao J, Park MY, Earley KW, Wu G, Yang L, Poethig RS (2016b) Developmental Functions of miR156-Regulated SQUAMOSA PROMOTER BINDING PROTEIN-LIKE (SPL) Genes in Arabidopsis thaliana. PLoS Genet 12 (8):e1006263. doi:10.1371/journal.pgen.1006263

Xu Y, Guo C, Zhou B, Li C, Wang H, Zheng B, Ding H, Zhu Z, Peragine A, Cui Y, Poethig S, Wu G (2016c) Regulation of Vegetative Phase Change by SWI2/SNF2 Chromatin Remodeling ATPase BRAHMA. Plant Physiol 172 (4):2416-2428. doi:10.1104/pp.16.01588

Xu Y, Zhang L, Wu G (2018c) Epigenetic Regulation of Juvenile-to-Adult Transition in Plants. Front Plant Sci 9:1048. doi:10.3389/fpls.2018.01048

Xu YF, Gan ES, Zhou J, Wee WY, Zhang XY, Ito T (2014) Arabidopsis MRG domain proteins bridge two histone modifications to elevate expression of flowering genes. Nucleic Acids Research 42 (17):10960-10974. doi:10.1093/nar/gku781

Yamaguchi A, Wu MF, Yang L, Wu G, Poethig RS, Wagner D (2009) The microRNA-regulated SBP-Box transcription factor SPL3 is a direct upstream activator of LEAFY, FRUITFULL, and APETALA1. Dev Cell 17 (2):268-278. doi:10.1016/j.devcel.2009.06.007

Yan D, Zhang X, Zhang L, Ye S, Zeng L, Liu J, Li Q, He Z (2015a) Curved chimeric

palea 1 encoding an EMF1-like protein maintains epigenetic repression of OsMADS58 in rice palea development. Plant J 82 (1):12-24. doi:10.1111/tpj.12784

Yan L, Wei S, Wu Y, Hu R, Li H, Yang W, Xie Q (2015b) High-Efficiency Genome Editing in Arabidopsis Using YAO Promoter-Driven CRISPR/Cas9 System. Molecular plant 8 (12):1820-1823. doi:10.1016/j.molp.2015.10.004

Yan YY, Shen LS, Chen Y, Bao SJ, Thong ZH, Yu H (2014) A MYB-Domain Protein EFM Mediates Flowering Responses to Environmental Cues in Arabidopsis. Dev Cell 30 (4):437-448. doi:10.1016/j.devcel.2014.07.004

Yang C, Bratzel F, Hohmann N, Koch M, Turck F, Calonje M (2013a) VAL- and AtBMI1-mediated H2Aub initiate the switch from embryonic to postgerminative growth in Arabidopsis. Curr Biol 23 (14):1324-1329. doi:10.1016/j.cub.2013.05.050

Yang H, Berry S, Olsson TSG, Hartley M, Howard M, Dean C (2017a) Distinct phases of Polycomb silencing to hold epigenetic memory of cold in Arabidopsis. Science 357 (6356):1142-1145. doi:10.1126/science.aan1121

Yang H, Han Z, Cao Y, Fan D, Li H, Mo H, Feng Y, Liu L, Wang Z, Yue Y, Cui S, Chen S, Chai J, Ma L (2012a) A companion cell-dominant and developmentally regulated H3K4 demethylase controls flowering time in Arabidopsis via the repression of FLC expression. PLoS Genet 8 (4):e1002664. doi:10.1371/journal.pgen.1002664

Yang H, Howard M, Dean C (2014) Antagonistic roles for H3K36me3 and H3K27me3 in the cold-induced epigenetic switch at Arabidopsis FLC. Curr Biol 24 (15):1793-1797. doi:10.1016/j.cub.2014.06.047

Yang HC, Mo HX, Fan D, Cao Y, Cui SJ, Ma LG (2012b) Overexpression of a histone H3K4 demethylase, JMJ15, accelerates flowering time in Arabidopsis. Plant Cell Rep 31 (7):1297-1308. doi:10.1007/s00299-012-1249-5

Yang J, Lee S, Hang R, Kim SR, Lee YS, Cao X, Amasino R, An G (2013b) OsVIL2 functions with PRC2 to induce flowering by repressing OsLFL1 in rice. Plant J 73 (4):566-578. doi:10.1111/tpj.12057

Yang J, Zhang X, Feng J, Leng H, Li S, Xiao J, Liu S, Xu Z, Xu J, Li D, Wang Z, Wang J, Li Q (2016) The Histone Chaperone FACT Contributes to DNA Replication-Coupled Nucleosome Assembly. Cell Rep 14 (5):1128-1141. doi:10.1016/j.celrep.2015.12.096

Yang L, Xu M, Koo Y, He J, Poethig RS (2013c) Sugar promotes vegetative phase change in Arabidopsis thaliana by repressing the expression of MIR156A and MIR156C. Elife 2:e00260. doi:10.7554/eLife.00260

Yang X, Tong A, Yan B, Wang X (2017b) Governing the Silencing State of Chromatin: The Roles of Polycomb Repressive Complex 1 in Arabidopsis. Plant Cell Physiol 58 (2):198-206. doi:10.1093/pcp/pcw209

Yang XJ, Seto E (2007) HATs and HDACs: from structure, function and regulation to novel strategies for therapy and prevention. Oncogene 26 (37):5310-5318. doi:10.1038/sj.onc.1210599

Yang YJ, Wang Y, Li ZF, Gong Y, Zhang P, Hu WC, Sheng DH, Li YZ (2017c) Increasing on-target cleavage efficiency for CRISPR/Cas9-induced large fragment deletion in Myxococcus xanthus. Microb Cell Fact 16 (1):142. doi:10.1186/s12934-017-0758-x

Yelagandula R, Stroud H, Holec S, Zhou K, Feng S, Zhong X, Muthurajan UM, Nie X, Kawashima T, Groth M, Luger K, Jacobsen SE, Berger F (2014) The histone variant H2A.W defines heterochromatin and promotes chromatin condensation in Arabidopsis. Cell 158 (1):98-109. doi:10.1016/j.cell.2014.06.006

Yoshida N, Yanai Y, Chen L, Kato Y, Hiratsuka J, Miwa T, Sung ZR, Takahashi S (2001) EMBRYONIC FLOWER2, a novel polycomb group protein homolog, mediates shoot development and flowering in Arabidopsis. Plant Cell 13 (11):2471-2481

Yu S, Cao L, Zhou CM, Zhang TQ, Lian H, Sun Y, Wu J, Huang J, Wang G, Wang JW (2013) Sugar is an endogenous cue for juvenile-to-adult phase transition in plants. Elife 2:e00269. doi:10.7554/eLife.00269

Yu Y, Bu ZY, Shen WH, Dong AW (2009) An update on histone lysine methylation in plants. Prog Nat Sci-Mater 19 (4):407-413. doi:10.1016/j.pnsc.2008.07.015

Yu Y, Dong A, Shen WH (2004) Molecular characterization of the tobacco SET domain protein NtSET1 unravels its role in histone methylation, chromatin binding, and segregation. Plant J 40 (5):699-711. doi:10.1111/j.1365-313X.2004.02240.x

Yuan W, Luo X, Li Z, Yang W, Wang Y, Liu R, Du J, He Y (2016) A cis cold memory element and a trans epigenome reader mediate Polycomb silencing of FLC by vernalization in Arabidopsis. Nat Genet 48 (12):1527-1534. doi:10.1038/ng.3712

Yuan W, Wu T, Fu H, Dai C, Wu H, Liu N, Li X, Xu M, Zhang Z, Niu T, Han Z, Chai J, Zhou XJ, Gao S, Zhu B (2012) Dense chromatin activates Polycomb repressive complex 2 to regulate H3 lysine 27 methylation. Science 337 (6097):971-975. doi:10.1126/science.1225237

Yun M, Wu J, Workman JL, Li B (2011) Readers of histone modifications. Cell Res 21 (4):564-578. doi:10.1038/cr.2011.42

Zeng L, Zhang Q, Li S, Plotnikov AN, Walsh MJ, Zhou MM (2010) Mechanism and regulation of acetylated histone binding by the tandem PHD finger of DPF3b. Nature 466 (7303):258-262. doi:10.1038/nature09139

Zhang B, Dong Q, Su H, Birchler JA, Han F (2014) Histone phosphorylation: its role during cell cycle and centromere identity in plants. Cytogenet Genome Res 143 (1-3):144-149. doi:10.1159/000360435

Zhang C, Cao L, Rong L, An Z, Zhou W, Ma J, Shen WH, Zhu Y, Dong A (2015) The chromatin-remodeling factor AtINO80 plays crucial roles in genome stability maintenance and in plant development. Plant J 82 (4):655-668. doi:10.1111/tpj.12840

Zhang L, Eugeni EE, Parthun MR, Freitas MA (2003) Identification of novel histone post-translational modifications by peptide mass fingerprinting. Chromosoma 112 (2):77-86. doi:10.1007/s00412-003-0244-6

Zhang X, Clarenz O, Cokus S, Bernatavichute YV, Pellegrini M, Goodrich J, Jacobsen SE (2007a) Whole-genome analysis of histone H3 lysine 27 trimethylation in Arabidopsis. Plos Biol 5 (5):e129. doi:10.1371/journal.pbio.0050129

Zhang X, Germann S, Blus BJ, Khorasanizadeh S, Gaudin V, Jacobsen SE (2007b) The Arabidopsis LHP1 protein colocalizes with histone H3 Lys27 trimethylation. Nat Struct Mol Biol 14 (9):869-871. doi:10.1038/nsmb1283

Zhang X, Henriques R, Lin SS, Niu QW, Chua NH (2006) Agrobacterium-mediated transformation of Arabidopsis thaliana using the floral dip method. Nat Protoc 1 (2):641-646. doi:10.1038/nprot.2006.97

Zhang XY, Clarenz O, Cokus S, Bernatavichute YV, Pellegrini M, Goodrich J, Jacobsen SE (2007c) Whole-genome analysis of histone H3 lysine 27 trimethylation in Arabidopsis. Plos Biol 5 (5):1026-1035. doi:ARTN e129

10.1371/journal.pbio.0050129

Zhao ML, Yang SG, Liu XC, Wu KQ (2015) Arabidopsis histone demethylases LDL1 and LDL2 control primary seed dormancy by regulating DELAY OF GERMINATION 1 and ABA signaling-related genes. Frontiers in Plant Science 6. doi:ARTN 159

10.3389/fpls.2015.00159

Zhao Z, Yu Y, Meyer D, Wu CJ, Shen WH (2005) Prevention of early flowering by expression of FLOWERING LOCUS C requires methylation of histone H3K36. Nature Cell Biology 7 (12):1256-1260. doi:10.1038/ncb1329

Zhong J, Peng Z, Peng Q, Cai Q, Peng W, Chen M, Yao J (2018) Regulation of plant height in rice by the Polycomb group genes OsEMF2b, OsFIE2 and OsCLF. Plant Sci 267:157-167. doi:10.1016/j.plantsci.2017.11.007

Zhou JX, Liu ZW, Li YQ, Li L, Wang B, Chen S, He XJ (2018) Arabidopsis PWWP domain proteins mediate H3K27 trimethylation on FLC and regulate flowering

time. J Integr Plant Biol. doi:10.1111/jipb.12630

Zhou W, Gao J, Ma J, Cao L, Zhang C, Zhu Y, Dong A, Shen WH (2016a) Distinct roles of the histone chaperones NAP1 and NRP and the chromatin-remodeling factor INO80 in somatic homologous recombination in Arabidopsis thaliana. Plant J 88 (3):397-410. doi:10.1111/tpj.13256

Zhou W, Zhu P, Wang J, Pascual G, Ohgi KA, Lozach J, Glass CK, Rosenfeld MG (2008) Histone H2A monoubiquitination represses transcription by inhibiting RNA polymerase II transcriptional elongation. Mol Cell 29 (1):69-80. doi:10.1016/j.molcel.2007.11.002

Zhou W, Zhu Y, Dong A, Shen WH (2015) Histone H2A/H2B chaperones: from molecules to chromatin-based functions in plant growth and development. Plant J 83 (1):78-95. doi:10.1111/tpj.12830

Zhou Y, Hartwig B, James GV, Schneeberger K, Turck F (2016b) Complementary Activities of TELOMERE REPEAT BINDING Proteins and Polycomb Group Complexes in Transcriptional Regulation of Target Genes. Plant Cell 28 (1):87-101. doi:10.1105/tpc.15.00787

Zhou Y, Romero-Campero FJ, Gomez-Zambrano A, Turck F, Calonje M (2017a) H2A monoubiquitination in Arabidopsis thaliana is generally independent of LHP1 and PRC2 activity. Genome Biol 18 (1):69. doi:10.1186/s13059-017-1197-z

Zhou Y, Tergemina E, Cui H, Forderer A, Hartwig B, Velikkakam James G, Schneeberger K, Turck F (2017b) Ctf4-related protein recruits LHP1-PRC2 to maintain H3K27me3 levels in dividing cells in Arabidopsis thaliana. Proc Natl Acad Sci U S A 114 (18):4833-4838. doi:10.1073/pnas.1620955114

Zhu P, Li G (2016) Structural insights of nucleosome and the 30-nm chromatin fiber. Curr Opin Struct Biol 36:106-115. doi:10.1016/j.sbi.2016.01.013

Zhu Y, Dong A, Shen WH (2011a) Histone variants and chromatin assembly in plant abiotic stress responses. Biochim Biophys Acta 1819 (3-4):343-348. doi:10.1016/j.bbagrm.2011.07.012

Zhu Y, Weng M, Yang Y, Zhang C, Li Z, Shen WH, Dong A (2011b) Arabidopsis homologues of the histone chaperone ASF1 are crucial for chromatin replication and cell proliferation in plant development. Plant J 66 (3):443-455. doi:10.1111/j.1365-313X.2011.04504.x

Université de Strasbourg

Qiannan WANG

École Doctorale des Sciences de la Vie et de la Santé STRASBOURG

Investigation du mécanisme fonctionnel des gènes *AtRING1* et *AtZRF1* dans la régulation de la croissance et du développement chez les plantes

Résumé

Chez les plantes comme chez les animaux, les protéines du groupe Polycomb (PcG) jouent des rôles essentiels dans les processus développementaux par la répression de l'expression des gènes. Dans mes travaux de thèse, j'ai caractérisé AtRING1, un sous-unité essentiel du PcG, et AtZRF1, une protéine proposée comme lecteur del'histone H2A monoubiquitinée (H2Aub1) en aval du fonctionnement du PcG. Mes résultats montrent qu'une perte-de-fonction totale de AtRING1A, par 'CRISPR/Cas9 gene-editing', causes une létalité partielle embryonnaire et la dédifférenciation cellulaire de la plantule d'Arabidopsis. Les mutations du domaine RAWUL au C-terminal de AtRING1A sont plus tolérées mais induisent certains défauts sur la croissance végétative, la floraison, l'organogénèse, et la production des graines. Mes analyses moléculaires révèlent que ces mutations du domaine RAWUL réduisent H2Aub1 et augmentent l'expression de plusieurs gènes essentiels dans la régulation du développement de la plante. Ainsi, mes données ont permis à établir une fonction primordiale de AtRING1 et à attribuer un rôle de son domaine RAWUL dans la déposition de H2Aub1 et répression des gènes *in vivo*. Nos analyses sur AtZRF1 ont permis à détailler son rôle sur la division and différenciation cellulaire.

MOTS-CLÉS:

Chromatine regulateur; Épigénétique; H2Aub1; H3K27me3; Régulation de la transcription; Développement de la plante; AtRING1; RAWUL; AtZRF1

Summary

In plants as in animals, the Polycomb Group (PcG) proteins play key roles in diverse developmental processes by repressing the expression of genes. My thesis work focused on the characterization of AtRING1A, one of the PcG core subunits, and of AtZRF1, a protein proposed as a reader of the histone H2A-monoubiquitin (H2Aub1) downstream to the PcG function. My results show that a total loss-of-function of AtRING1A, by CRISPR/Cas9 gene editing, leads to partial embryonic lethal and callus-formation of seedlings in Arabidopsis. Several mutations within the RAWUL domain at the C-terminus of AtRING1A are better tolerated and induce several defects in plant vegetative growth, flowering time, floral organ formation and seed production. My molecular data indicate a role of the RAWUL domain in H2Aub1 deposition in vivo and suppression of several key developmental genes. Our characterization of loss-of-function of AtZRF1 provides important detailed information about its function in the regulation of cell division and cell differentiation.

KEYWORDS:

Chromatin regulator; Epigenetics; H2Aub1; H3K27me3; Transcription regulation; Plant development; AtRING1; RAWUL; AtZRF1